Contributions to Sliding Mode Control and Observation of Nonlinear Uncertain Systems

Von der Fakultät für Ingenieurwissenschaften,
Abteilung Maschinenbau und Verfahrenstechnik
der
Universität Duisburg-Essen
zur Erlangung des akademischen Grades
eines
Doktors der Ingenieurwissenschaften
Dr.-Ing.
genehmigte Dissertation

von

Mark Spiller
aus
Löbau, Deutschland

Gutachter: Univ.-Prof. Dr.-Ing. Dirk Söffker
Univ.-Prof. Dr.-Ing. Rolf Findeisen, TU Darmstadt

Tag der mündlichen Prüfung: 28. April 2022

Acknowledgments

My first thanks go to Univ.-Prof. Dr.-Ing. Dirk Söffker who supported me throughout my time at the Chair of Dynamics and Control. Thank you for your guidance and encouragement. Thank you for being able to work at Chair for the past five years. This helped me to improve in a lot of aspects. Thank you also for your support with a one year scholarship that allowed me to publish my first scientific contributions and also thank you for the possibility to work at the Chair as a student assistant during my study time. Many thanks go to my Ph.D. co-advisor Univ.-Prof. Dr.-Ing. Rolf Findeisen. Thank you for your advice, help, and suggestions. Thank you also for the insights and impressions I was able to grasp from the GAMM meetings. Thank you to Univ.-Prof. Dr. rer. nat. Burak Atakan for being the head of the examination committee and thank you to Univ.-Prof. Dr.-Ing. Wojciech Kowalczyk for your participation in the committee.

Special thanks go to all former and present members of the Chair of Dynamics and Control. I always appreciated the cultural diversity and the internationality of our team. Many thanks go also to the students that contributed to my work based on the discussions and projects that we had together.

My heartfelt thanks go to my family especially to my parents who always supported me. Thank you for all of the sacrifices that you have both made for me and for all of the love you haven given to me.

Oberhausen, May 2022 Mark Spiller

Kurzfassung

Bei den meisten regelungstechnischen Verfahren handelt es sich um modellbasierte Methoden, die eine präzise mathematische Beschreibung des betrachteten dynamischen Systems voraussetzen. Die modellbasierte Regelung erlaubt es steuerbare Eigenvorgänge im System so zu beeinflussen, dass ein gewünschtes, vorgegebenes Systemverhalten erzielt wird. Allerdings ist die Modellbildung der meisten technischen Systeme komplex und es ist schwierig und zeitaufwändig oder sogar unmöglich eine exakte Beschreibung vorzunehmen. Zu den Schwierigkeiten bei der Modellbildung zählen unter anderem: Systemparameter, die nicht genau identifiziert werden können oder zeitvariant sind; Systemvorgänge, die real existieren jedoch beim Modellbildungsprozess nicht berücksichtigt werden; Interaktionen mit der Umgebung, wie sie sich bei modernen regelungstechnischen Systemen wie bspw. Robotern ergeben und die zur Folge haben, dass unbekannte äußere Eingänge auf das zu beschreibende System wirken. Aufgrund der erläuterten Komplexität der Modellbildung existiert im Allgemeinen eine Diskrepanz zwischen der modellierten und der tatsächlichen Dynamik des Systems. Um die regelungstechnischen Ziele trotz vorhandener Modelldiskrepanz garantiert einhalten zu können wird vom Regler die Eigenschaft der Robustheit gefordert. Der Sliding-Mode-Regler ist eine regelungstechnische Methode, welche eine derartige Robustheit aufweist. Mittels des Sliding-Mode-Reglers kann eine Invarianz der Systemdynamik gegenüber Störungen im Eingangskanal erreicht werden. Als Folge wird trotz Modelldiskrepanz die gewünschte Systemdynamik garantiert erzielt. Jedoch besitzt der Sliding-Mode-Regler trotz seiner Robustheit einige Nachteile, die im Folgenden näher erläutert werden:

- Die konventionelle Sliding-Mode-Regelung führt zu einem hochfrequentem Schaltvorgang im Signal der Stellgröße, welcher als Rattern bezeichnet wird. Das Rattern kann eine Beschädigung des zu regelnden Systems zur Folge haben, woraus sich in praktischer Konsequenz die Nichtausführbarkeit des Reglers ergibt. Die Verwendung von Sliding-Mode-Reglern höherer Ordnung erlaubt eine effektive Abmilderung des Ratterns. Allerdings werden dazu typischerweise zusätzliche Zeitableitungen des Messsignals benötigt, welche die Sensitivität des regelungstechnischen Ansatzes gegenüber Messrauschen erhöhen. Adaptive Sliding-Mode-Regler eignen sich ebenfalls, um eine Dämpfung des Ratterns zu erzielen. Jedoch kann das Rattern nur bis zu einem gewissen Grad gedämpft werden, da andernfalls die regelungstechnischen Ziele nicht garantiert eingehalten werden können.

- Die Berücksichtigung von Nebenbedingungen im Rahmen der Sliding-Mode-Regelung ist komplex, da hierfür der Sliding-Mode-Regler an sich modifiziert werden muss. Die Nebenbedingungen können nicht durch Aufschalten bereits bekannter regelungstechnischer Ansätze wie bspw. dem Invarianz-Regler (Wolff and Buss, 2004) oder dem Reference-Governor Ansatz (Bemporad, 1998) erzwungen werden. Die genannten

Methoden versagen, da sie auf Systeme mit Modellunsicherheit, von der typischerweise bei der Sliding-Mode-Regelung ausgegangen wird, nicht angewandt werden können. Sliding-Mode-Regler, die eine Berücksichtigung von Nebenbedingungen erlauben, existieren zwar, allerdings wird üblicherweise von Nebenbedingung ausgegangen, die zeitlich unveränderlich sind. Als Folge ist das Anwendungsfeld dieser Regler limitiert. Ein weiteres Problem ist, dass die meisten sliding-mode-basierten Regler eine Berücksichtigung von Nebenbedingungen nur theoretisch zulassen. In der Praxis führt ein Großteil der entworfenen Verfahren zum Auftreten des Ratterns und ist deshalb unausführbar. Eine nachträgliche Approximation des Reglergesetzes erlaubt zwar eine Dämpfung des Ratterns, führt jedoch dazu, dass die Einhaltung der Nebenbedingungen nicht mehr garantiert werden kann.

Beobachterbasierte Verfahren finden vielfältig Anwendung im Rahmen der Überwachung und Regelung dynamischer Systeme. Typischerweise handelt es sich dabei um modellbasierte Methoden, welche eine exakte Modellbeschreibung voraussetzen. Die Gestaltungsprinzipien der Sliding-Mode-Regelung können auch zum Entwurf von Beobachtern verwendet werden. Die Robustheit der daraus resultierenden sogenannten Sliding-Mode-Beobachter ist jedoch bei weitem nicht so umfassend wie jene der Sliding-Mode-Regler. Entwurfsverfahren für Sliding-Mode-Beobachter, die eine Modellunsicherheit erlauben, existieren für spezielle Klassen von Systemen. Dies sind insbesondere spezielle lineare Systeme mit unbekannten Eingängen und nichtlineare Systeme in Regelungsnormalform. Darüber hinaus existieren Sliding-Mode-Beobachter für weitere Systemklassen, die meisten setzten jedoch eine exakte Modellbeschreibung voraus.

Auf Grundlage der zuvor beschriebenen Nachteile und Limitierungen der Sliding-Mode-Regelung und Beobachtung werden folgenden Thematiken innerhalb dieser Arbeit behandelt.

Betrachtet wird ein nichtlinearer Ansatz zur Zustandsschätzung, welcher unter dem Namen Smooth-Variable-Structure-Filter (SVSF) bekannt ist. Das SVSF basiert einerseits auf dem Prädiktor-Korrektor Schema des Kalman Filters und nutzt andererseits bekannte Gestaltungsprinzipien der Sliding-Mode-Regelung und Beobachtung. Das Filter ist anwendbar auf nichtlineare Systeme für die keine exakte Modellbeschreibung vorliegt. Die Genauigkeit der Zustandsschätzung hängt stark von der Wahl der Filterparameter ab, welche durch den Anwender vorgegeben werden. In dieser Arbeit wird das SVSF in eine neuartige, äquivalente Beschreibung überführt, die Aufschluss darüber gibt, wie das Verhalten des Filters über die Filterparameter beeinflusst werden kann. Anhand der äquivalenten Beschreibung wird eine Gleichung zur Berechnung der Schätzfehlerkovarianzmatrix hergeleitet. Die Berechnung der Schätzfehlerkovarianzmatrix erlaubt es eine neue Filter-Verstärkungsmatrix zu bestimmen, um den mittleren, quadratischen Schätzfehler zu minimieren. Wird die neue Verstärkungsmatrix auf auf das SVSF angewandt, ergibt sich ein Algorithmus der identisch zu dem des erweiterten Kalman Filters (EKF) ist. Um die Robustheit des SVSFs weitergehend zu untersuchen wird ein kombinierter Schätzansatz formuliert. Der kombinierte Schätzansatz basiert auf einer Gewichtung der Verstärkungsmatrizen des SVSFs und des EKFs. Zur Optimierung der eingeführten Gewichtungsfaktoren und der Filterparameter wird ein Optimierungsschema entworfen. Das Optimierungsschema bedarf weder Experimenten am realen System noch Kenntnis über eine exakte Modellbeschreibung. Darüber hinaus ist das vorgeschlagene Optimierungsschema nicht auf die betrachteten Filterverfahren beschränkt. Es kann grundsätzlich auf alle modellbasierten

Filterverfahren angewandt werden für die keine exakte Modellbeschreibung vorliegt. Um die Schätzgenauigkeit des kombinierten Ansatzes mit dem des SVSFs zu vergleichen, wird ein Anwendungsbeispiel mit einer nichtlinearen Dynamik betrachtet. Das exakte Verhalten des Systems wird als nicht bekannt angenommen. Zur Lösung der Schätzaufgabe steht lediglich ein nominelles Systemmodell zur Verfügung, das vom realen Systemverhalten abweicht. Die Filterparameter der beiden Schätzverfahren werden anhand des entworfenen Optimierungsschemas bestimmt. Für das bei der Untersuchung verwendete System zeigt sich, dass der kombinierte Ansatz dem SVSF hinsichtlich der Schätzgenauigkeit überlegen ist. Bei Betrachtung der optimierten Filterparameter zeigt sich, dass die Robustheit des kombinierten Ansatzes weitestgehend von der Verstärkungsmatrix des EKFs ausgeht. Als Folge verhält sich der kombinierte Ansatz strukturell ähnlich zum EKF. Er weist jedoch eine parametrierte Verstärkungsmatrix auf, die über das entwickelte Optimierungsschema angepasst wurde. Mittels dieser Anpassung wird eine gesteigerte Robustheit gegenüber der vorliegenden Modellunsicherheit erreicht, aus welcher sich die verbesserte Schätzleistung des Filters ergibt.

Ferner wird in dieser Arbeit ein modifizierter Ansatz zur adaptiven Sliding-Mode-Regelung entworfen. Der Ansatz hat zum Ziel den Effekt des Ratterns stärker abzumildern als dies bei konventionellen adaptiven Sliding-Mode-Verfahren der Fall ist. Dafür wird ein daten-basierter, adaptiver Sliding-Mode-Regler entwickelt. Dieser ist auf nichtlinearer Systeme mit hinreichend träger Dynamik anwendbar. Ein- und Ausgangsdaten des Systems werden verwendet, um ein lokales, lineares Abbild des Systems zu identifizieren. Das Systemabbild dient der Vorhersage zukünftigen Systemverhaltens. Die Systemidentifikation findet rekursiv mittels eines Kalman Filters statt. Dabei wird das lokale Abbild des Systems in jedem Zeitschritt, also online, über die empfangenen Daten aktualisiert. Basierend auf der Vorhersagefähigkeit des lokalen Systemabbildes wird ein Optimierungsproblem formuliert. Ziel der Optimierung ist es die quadratische Regelabweichung und die Stellgrößenenergie zu minimieren. Die sich aus dem Optimierungsproblem ergebene optimale Stellgröße wird nachfolgend als Optimalregler bezeichnet. Der Optimalregler wird mit einem adaptiven Sliding-Mode-Regler erster Ordnung kombiniert. Im Zusammenhang mit dem verwendeten Sliding-Mode-Regler wird eine Gleitebene definiert, auf welcher die Regelabweichung asymptotisch stabil konvergiert. Durch die Verwendung von Gewichtungsfunktionen wird sichergestellt, dass die Systemzustände immer wieder hinreichend genau an die Gleitebene herangeführt werden, falls sie den Bereich um die Gleitebene verlassen sollten. Daraus folgt, dass die Beschränktheit des Regelfehlers garantiert werden kann. In der direkten Umgebung um die Gleitebene wird die Reglerverstärkung des adaptiven Sliding-Mode-Reglers abgesenkt und der Optimalregler dominiert die Stellgröße. Als Folge davon kann das Rattern stark vermindert werden. Eine Sollwert-Regelung eines nichtlinearen Systems wird betrachtet, um den datenbasierten Ansatz mit einem konventionellen, adaptiven Sliding-Mode-Regler zu vergleichen. Im Gegensatz zum konventionellen Regler erreicht der daten-basierte Ansatz eine stationäre Sollwertfolge, ohne dass merkliches Rattern auftritt. Bezogen auf das betrachtete System lassen sich die genannten Ergebnisse ohne konkretes Wissen über die Systemparameter erzielen.

Abschließend beschäftigt sich diese Arbeit mit der Berücksichtigung von Nebenbedingungen im Rahmen der Sliding-Mode-Regelung. In diesem Zusammenhang wird ein Sliding-Mode-Regler entworfen, der sich zur Regelung spezieller nichtlinearer Systeme unter Nebenbedingungen eignet. Betrachtet wird die Klasse der nichtlinearen Systeme mit einem relativen Grad zwei. Die Nebenbedingungen sind bezüglich der ersten Zeitableitung

der Regelgröße formuliert. Erschwerend wird angenommen, dass sich die Nebenbedingungen im Laufe der Zeit verändern können. Der zur Lösung des Problems entworfene regelungstechnische Ansatz basiert auf einer Verknüpfung zweier untergeordneter Sliding-Mode-Regler. Im Gegensatz zu den bisher existierenden Verfahren wird der Schaltvorgang zwischen den beiden untergeordneten Reglern so gestaltet, dass keine Diskontinuitäten im Signal der Stellgröße auftreten. Darüber hinaus lässt sich mit dem entworfenen Regler eine Abmilderung des Ratterns erzielen, ohne dass es zu einer Verletzung der formulierten Nebenbedingungen kommt. Da es sich bei dem vorgestellten Ansatz um eine Sliding-Mode-Regelung handelt, ist keine exakte Modellbeschreibung erforderlich. Der entworfene Regler garantiert die Konvergenz des Regelfehlers. Die Regelabweichung erreicht innerhalb endlicher Zeit ein Fehlerintervall, in welchem der Regelfehler nach oben und unten beschränkt ist. Die Grenzwerte des Fehlerintervalls lassen sich über die gewählten Reglerparameter bestimmen. Zusätzlich kann die Konvergenz zeitlich quantifiziert werden. Es ist möglich anzugeben wie lange es maximal dauert bis sich der Regelfehler innerhalb des spezifizierten Fehlerintervalls befindet. Der entwickelte Ansatz eignet sich insbesondere für Anwendungen bei denen sich die Nebenbedingungen zur Laufzeit ändern. Aus diesem Grund wird eine Punkt zu Punkt Regelung eines Roboter Endeffektors betrachtet. Dabei ändern sich die erlaubten Winkelgeschwindigkeiten der Roboterarme zur Laufzeit. Erschwerend soll der Roboter eine Pick-and-Place Aufgabe lösen. Eine Traglast mit einer unbekannten Masse soll aufgenommen und zu einem anderen Wegpunkt transportiert werden. Die Traglast fungiert als Störung, die vom Regler ausgeregelt werden muss. Bevor die gestellte Aufgabe praktisch gelöst wird, kann das Verhalten des Reglers auf Basis der entwickelten Theorie vorhergesagt werden. So kann der auftretende stationäre Regelfehler vorab bestimmt werden und die maximale Zeitdauer kann angegeben werden, die der Regler zur Vollendung der gestellten Aufgabe benötigt. Die ermittelten theoretischen Ergebnisse lassen sich anhand einer Simulation validieren. Da sich der vorgestellte Regler gut für die Regelung von Robotern mit beschränkten Winkelgeschwindigkeiten eignet, wird ferner ein Konzept zur sicheren Mensch-Roboter-Kooperation entworfen. Dieses Konzept garantiert, dass die Geschwindigkeit des Roboters einen Sollwert nicht überschreitet, wenn der Mensch mit dem Roboter in Kontakt ist. Das vorgestellte Konzept zur Mensch-Roboter-Kooperation wird anhand eines entworfenen Szenarios getestet. Die theoretisch erreichbaren Ergebnisse werden über eine Simulation abgesichert.

Abstract

Most control approaches are model-based methods and require a precise mathematical description of the considered dynamical system. System modeling offers the advantage that the controllable system dynamics can be affected by control in such a way that some given desired dynamics is achieved. However, most technical systems are complex and it is difficult and time-consuming to describe them exactly or it may even be impossible. Challenges that arise in system modeling can be for instance: parameters that are not precisely known or that vary in time, dynamics that exist but are unmodeled, or especially for modern control systems interactions with the environment that lead to unknown exogenous inputs. Consequently, it is common that a discrepancy between the modeled dynamics and the true dynamics exists. The applied controller is required to be robust in the sense that the control goals are also guaranteed to be achieved in presence of the model discrepancy. Sliding mode control (SMC) is such a robust control method. It can make the system dynamics invariant to disturbances that appear in the input channel so that the desired dynamics are still achieved. However, besides its strong robustness properties sliding mode control also has some disadvantages:

- Conventional sliding mode control leads to a high frequent switching effect in the input signal denoted as chattering making the controller inapplicable in practice. Higher order SMC approaches may effectively mitigate the chattering but typically require higher order time derivatives of the measured signal. As a consequence, the whole approach becomes more sensitive to noise. Adaptive SMC approaches have been developed to reduce the chattering as well. However, chattering reduction can only be achieved to a certain extend as otherwise the control goals may not be achieved anymore.

- The handling of constraints in the context of sliding mode control is not straight forward as due to the model uncertainty standard add-on control approaches like the invariance control method (Wolff and Buss, 2004) or the reference governor approach (Bemporad, 1998) can not be applied directly. Constrained SMC approaches exist but they typically only consider box constraints with time-invariant bounds which limits the field of applications. Another problem is that most of the existing constrained SMC approaches only solve the constrained control problem in theory but are not applicable in practice due to chattering. Approximation techniques are required to be applied to mitigate the chattering. However, as the approximation techniques modify the original control laws it can not be guaranteed anymore that the constraints remain satisfied in general.

State estimation approaches are widely applied in the field of control and system monitoring. Typically, the estimation approaches are model-based methods and require a precise

system description to be known. Design principles of sliding mode control can also be applied to design state estimation approaches leading to the so-called sliding mode observers. However, in contrast to the SMCs the robustness of the sliding mode observers (SMOs) is much more restricted. General design concepts for SMO approaches that can handle model uncertainty only exist for specific classes of linear systems with unknown inputs and for nonlinear systems in companion form. There exist SMO approaches for other classes of systems as well, but most of them require a precise model description.

Based on the aforementioned limitations and problems of sliding mode control and observation the following topics are discussed within this thesis.

A nonlinear state estimation approach denoted as smooth variable structure filter (SVSF) is considered. The SVSF combines the predictor corrector scheme of the Kalman filter with design elements known from sliding mode control and observation. It is applicable to nonlinear systems and can handle model uncertainty. However, the estimation performance of the SVSF highly depends on the choice of some tuning parameters. In this thesis a reformulation of the SVSF is stated which gives an easy interpretation on how the tuning parameters affect the behavior of the filter. An equation to determine the error covariance of the reformulated filter is derived. Based on the error covariance a new filter gain is determined which minimizes the mean squared estimation error. If the new gain is applied to the reformulated filter it can be shown that the obtained estimation algorithm equals the one of the extended Kalman filter (EKF). To further investigate the robustness of the SVSF a combined estimation approach is formulated. The combined approach is equal to the reformulated SVSF but has a combined gain consisting of a weighted sum of the SVSF and the EKF gains. To optimize the filter parameters and weighting factors a parameter optimization scheme is proposed. The scheme neither requires any experiments on the real system to be conducted nor does it require the true system description to be known. The optimization scheme is generic in the sense that it can be applied to optimize any model-based state estimation approach that has to deal with an imprecise system description. The performance of the proposed combined estimation approach is compared with the one of the SVSF. A nonlinear system is simulated and the system description is assumed to be unknown. Both, the parameters of the combined approach and the ones of SVSF are optimized using the proposed scheme. For the considered system the combined approach outperforms the SVSF. Further, from the optimized parameters it can be seen that the robustness of the combined approach is mainly achieved by the EKF gain. That means that the combined approach behaves structural similar to the EKF but with a parameterized gain that is optimized by the proposed optimization scheme to handle model uncertainty.

Further, adaptive sliding mode control is considered in this thesis. The ability of adaptive sliding mode control to mitigate the chattering effect is improved. Therefore, a new data-driven adaptive SMC for nonlinear systems is designed. The system description is not necessarily required to be explicitly known but the dynamics are assumed to be sufficiently slow. Input- and output-data of the system is applied to train a linear local model that predicts the future system behavior. The local model is trained by a Kalman filter which allows to update the model at each time step based on the incoming data of the system. Using the prediction capabilities of the local model an optimization problem is formulated to minimize the squared control error and the input energy. The optimal control input is determined and combined with a first order adaptive sliding mode controller. Weighting functions are introduced to guarantee reaching of a subspace around the sliding manifold

from which follows that the tracking error is bounded. In the vicinity of the sliding surface the gain of the sliding mode controller is scaled down. As a consequence, the control law is dominated by the optimal control input and the chattering effect can be effectively mitigated. Set point tracking of a nonlinear system is considered to compare the proposed data-driven approach with a conventional first order adaptive SMC. In contrast to the conventional adaptive SMC the developed approach achieves stationary accurate tracking without noticeable chattering. For the considered specific system the control results of the proposed method are achieved even without concrete knowledge of the system parameters.

Finally, the development of a constrained sliding mode controller is considered in this thesis. The approach is applicable to nonlinear relative degree two systems and assumes the first time derivative of the control variable to be constrained. The bounds of the constraints may explicitly depend on time. The controller is designed based on a combination of two SMC sub-controllers. In contrast to the existing approaches a smooth transition between the sub-controllers is achieved and chattering mitigation is considered in such a way that it does not lead to constraint violation. As the developed method is based on sliding mode control design it can handle model uncertainty. The proposed approach guarantees convergence of the tracking error with respect to a domain that can be specified based on the controller parameters. In addition, a maximum time period can be stated after which convergence of the tracking error is guaranteed to be achieved. As the proposed controller allows to update the constraints online it is tested on a robotic system with time-dependent velocity constraints. The angular velocities change online dependent on the distance between the end effector and the waypoints. Moreover, the robot has to accomplish a pick and place problem in which an unknown payload is considered. The payload servers as a disturbance and is required to be rejected by the controller. Based on the developed theory about the proposed controller the tracking error bounds can be determined beforehand. The maximum time period that is required to accomplish the pick and place problem can also be stated in advance. The results have been successfully confirmed by simulation. As the proposed controller is well suited for velocity constraint control of robotic systems a safety concept for human-robot collaboration tasks is developed in addition. The proposed concept guarantees that the robot velocity is restricted to a desired value in the moment when the human and the robot are in contact with each other. A scenario of human robot interaction is considered to test the developed concept. The theoretical controller performance is confirmed by the simulation results.

Contents

List of Abbreviations

A-SMC	Adaptive sliding mode controller
CA	Combined estimation approach
CBF	Control barrier function
CLF	Control Lyapunov functions
CM-SMC	Chattering mitigated sliding mode controller
CSTR	Continuous stirred tank reactor
EKF	Extended Kalman filter
HOSMC	Higher order sliding mode control / Higher order sliding mode controller
HOSMD	Higher order sliding mode differentiator
ISMC	Integral sliding mode control / Integral sliding mode controller
KF	Kalman filter
LS	Least squares
LQR	Linear quadratic regulator
min-LS	Minimal Euclidean norm least squares solution (controller)
MPC	Model predictive control
MSE	Mean squared error
PC	Predictive controller
RMSE	Root mean squared error
RPI	Robust positive invariant
SMC	Sliding mode control / Sliding mode controller
SMO	Sliding mode observation / Sliding mode observer

SMRC	Sliding mode reference conditioning
SVD	Singular value decomposition
SVSF	Smooth variable structure filter
UKF	Unscented Kalman filter
WLS	Weighted least squares
WP	Waypoint

List of Mathematical Notations

Symbols

$\hat{a}$	Estimation of vector $a \in \mathbb{R}^n$
$f(\cdot)$	True system model
$\breve{f}(\cdot)$	Nominal system model (imprecise)
I_n	Identity matrix of $\mathbb{R}^{n \times n}$
$\mathbf{1}_n$	All-ones vector of dimension n
$z \in \mathbb{C}_-$	Negative conjugate complex plane i.e. z has negative real part

Operators

$\text{rank}\{A\}$	Rank of matrix $A \in \mathbb{R}^{n \times m}$
$\det\{A\}$	Determinant of matrix $A \in \mathbb{R}^{n \times n}$
$E\{\cdot\}$	Expectation value
$\text{tr}\{A\}$	Trace of matrix $A \in \mathbb{R}^{n \times n}$
a_{ij}	Element a_{ij} of matrix $A = (a_{ij}) \in \mathbb{R}^{n \times m}$
$\lvert a \rvert$	Absolute value applied element-wise on vector $a \in \mathbb{R}^n$
$\lambda_{min}\{A\}$	Minimal eigenvalue of matrix $A \in \mathbb{R}^{n \times n}$
$\lambda_{max}\{A\}$	Maximal eigenvalue of matrix $A \in \mathbb{R}^{n \times n}$
$A \times B$	Multiplication of $A \in \mathbb{R}^{n \times m}$ and $B \in \mathbb{R}^{m \times p}$ i. e. $A \times B = AB$
$a \circ b$	Schur product of vectors $a, b \in \mathbb{R}^n$
$A \otimes B$	Kronecker product of matrices $A \in \mathbb{R}^{n \times m}$, $B \in \mathbb{R}^{p \times r}$
$\lVert a \rVert$	Euclidean norm $\sqrt{a^T a}$ of vector $a \in \mathbb{R}^n$
$\lVert a \rVert_W$	Weighted Euclidean norm $\sqrt{a^T W a}$ of vector $a \in \mathbb{R}^n$, $W \succeq 0$
$\lVert A \rVert$	Frobenius norm of matrix $A \in \mathbb{R}^{n \times m}$

$\text{vec}\{A\}$	Concatenating matrix columns of $A \in \mathbb{R}^{n\times m}$ to form vector $a \in \mathbb{R}^{nm}$
$\text{vec}^{-1}\{a\}$	Form matrix $A \in \mathbb{R}^{n\times m}$ by applying inverse vector operator on vector $a \in \mathbb{R}^{nm}$
$\text{sgn}(a)$	Signum function applied element-wise on vector $a \in \mathbb{R}^n$
$\text{diag}\{a\}$	Build diagonal matrix $B = (b_{ij}) \in \mathbb{R}^{n\times n}$ from vector $a = (a_i) \in \mathbb{R}^n$ so that $b_{ii} = a_i$
$\text{row}_i\{A\}$	i-th row of matrix $A \in \mathbb{R}^{n\times n}$
$L_f h_i$	Lie derivative along f i. e. $L_f h_i = \frac{\partial h_i}{\partial x} f(x)$, where $\dot{x} = f(x)+g(x)u$ with $x \in \mathbb{R}^n$ and $h_i : \mathbb{R}^n \to \mathbb{R}$
$L_g h_i$	Lie derivative along g i. e. $L_g h_i = \frac{\partial h_i}{\partial x} g(x)$, where $\dot{x} = f(x)+g(x)u$ with $x \in \mathbb{R}^n$ and $h_i : \mathbb{R}^n \to \mathbb{R}$

Miscellaneous

$A \succ 0$	Positive definite matrix $A \in \mathbb{R}^{n\times n}$
$A \succeq 0$	Positive semi-definite matrix $A \in \mathbb{R}^{n\times n}$
$(a_0, a_1, \dots)$	Sequence
$\{a_0, a_1, \dots\}$	Set

1 Introduction

Most technical systems cannot be modeled perfectly. There may be discrepancies between the modeled and the actual system arising from e. g. parametric variations, unmodeled dynamics, or unknown disturbances. As the uncertainties cannot be quantified exactly it is typically stated that they arise within some known bounds. For this known bounds the controller is required to be robust meaning that the closed loop system should still be stable and the control goals should still be achieved. Sliding mode control (SMC) is a control method that exactly provides this kind of robustness. It is well established and can be applied to linear as well as nonlinear systems. Generally, the design of a sliding mode controller is characterized by two main steps.

First, a sliding manifold is designed within the state space. The sliding manifold defines a system mode "the sliding mode" in which desired dynamics such as state convergence are achieved. Consequently, in sliding mode the states slide on the manifold towards the origin of the state space. In addition, if the system is in sliding mode it is insensitive to so-called matched uncertainties leading to great robustness.

The second design step is the derivation of the reaching law. The reaching law defines the control input and guarantees that the sliding manifold is reached within finite-time. The time period of reaching is denoted as reaching phase. In conventional SMC design the reaching law is discontinuous and SMC can be regarded as a special type of variable structure control. The discontinuity of the reaching law leads to a high frequent switching of the control input denoted as chattering. The chattering is the major drawback of conventional sliding mode control. However, chattering can be effectively attenuated without the loss of control accuracy by means of higher order sliding mode control (HOSMC). Higher order SMC may be interpreted as the design of several sliding manifolds. The sliding mode is then defined by the intersection of these manifolds and the reaching law forces the states towards the intersection so that the sliding mode becomes active in finite-time. Based on HOSMC design convergence of the system states or tracking error can also be achieved in finite-time for any well-defined relative degree of the system. In conventional SMC design this can only be achieved for relative degree one systems without the use of nonlinear sliding manifolds. However, application of HOSMC approaches requires higher order time derivatives of the so-called sliding variable to be known. In theory the higher order time derivatives can be perfectly determined by means of sliding mode differentiators but only if the measured signal is noise-free.

For many control methods such as for state feedback controllers or exact input-output linearization approaches the system states are required to be known. Also for sliding mode controllers knowledge of the system states may be required or advantageous. For example for the sliding mode controller design of linear systems the system states are required to be known to achieve state stability as the sliding variable has to be defined with respect to the system states. In addition, for uncertain systems the bounds of the uncertainty

can be reduced if the system dynamics is partially known including knowledge of the states. To avoid measuring of all the states an observer is typically applied to estimate the system states. As SMC is a robust control approach the observer has to be robust too meaning that the states are required to be estimated without exact knowledge of the system dynamics. This can be achieved by sliding mode observation (SMO) approaches at least for some classes of systems. Typically, SMO approaches do not consider effects of measurement or process noise and are described with respect to deterministic systems. A problem of SMO approaches is that their robustness against model uncertainty is much more restricted as it is the case for the SMC approaches. Sliding mode observers that can handle model uncertainty exist for specific linear systems with unknown inputs. In this case the SMO has a structure similar to the Luenberger observer but with an additional discontinuous feedback of the output estimation error. This kind of SMO approaches also allows to estimate the unknown input itself making it attractive for fault detection, localization, and monitoring. For nonlinear systems robust SMO methods also only exist for special system classes e. g. for nonlinear systems in companion form. There exist SMO approaches for other types of systems as well but most of them require a precise model description.

1.1 Motivation and Problem Statement

This thesis considers contributions to sliding mode control and observation. In particular three main topics are discussed.

The first topic is about a sliding mode observation approach for nonlinear uncertain systems known as the smooth variable structure filter (SVSF). The SVSF approach can be considered as a sliding mode observer formulated with respect to discrete-time stochastic systems. The filter makes use of the boundary layer concept known from sliding mode control. The boundary layer is introduced to reduce the negative impact of measurement noise on the estimation performance of the SVSF. From the literature it is known that the SVSF has the ability to achieve improved estimation performance in comparison to the Kalman filter if the system description is imprecise. However, the improved performance can only be achieved if some filter parameters of the SVSF approach are properly tuned. In contrast to the Kalman filter the SVSF approach does not propagate the error covariance. An attempt to analytically minimize the SVSFs mean squared error (MSE) with respect to the filter parameters has been undertaken in Gadsden *et al.* (2011*b*). Therefore, a model to propagate the error covariance of the SVSF is proposed in Gadsden and Habibi (2010) which is then used to find the filter parameters that minimize the MSE. The approach cannot be considered to be consistent. The propagation of the error covariance as proposed in Gadsden and Habibi (2010) assumes the system dynamics to be linear and precisely known which clearly contradicts the claim of the SVSF to be a robust estimation approach for nonlinear systems. In addition, the gain of the SVSF is stochastic as it feeds back the output estimation error which is a stochastic process. However, the estimation error model proposed in Gadsden and Habibi (2010) is only mathematically correct if the gain is assumed to be deterministic. In contrast to the aforementioned parametric optimization a structural optimization of the SVSF approach is proposed by Gadsden *et al.* (2011*a*). The formulated strategy considers a simple switching between the SVSF and the Kalman filter gain. The Kalman filter gain is applied when the assumed system model fits well to the true system dynamics. In this case the Kalman filter is known to achieve a

minimization of the MSE. However, if there is a discrepancy between the assumed model and the true system behavior the SVSF gain is applied because it is considered to be more robust. The switching of the gains is induced by a condition that is formulated with respect to the optimized SVSF parameters. As a result the switching is also affected by the inconsistencies of the SVSF parameter optimization approach of Gadsden and Habibi (2010).

However, from a principal point of view it makes sense to optimize the SVSF parameters as the filter has not been derived based on a minimization of the MSE. Consequently, the following goals are formulated with respect to this thesis:

- Investigation of the effects of the SVSF parameters on the filters estimation performance
- Derivation of an error model for the SVSF that is applicable to nonlinear systems with imprecise model description
- Development of a parameter optimization process for the SVSF that does not require the true estimation error to be known

The second topic discussed in this thesis is related to chattering attenuation. As already mentioned higher order sliding mode control can be applied to effectively mitigate chattering. However, HOSMC approaches require higher order time derivatives of the sliding variable to be known. Typically, control approaches that rely on higher order time derivatives are undesired because the estimation of the related time derivatives may be very sensitive to measurement noise. First order conventional SMC does not rely on any time derivatives of the sliding variable. With regards to these conventional SMC approaches several adaptive gain methods have been proposed in the past fifteen years (e. g. Plestan *et al.*, 2010; Edwards and Shtessel, 2016). The goal of the adaptation strategies is to adjust the controller gain online making it large enough to guarantee reaching of the sliding surface but not too large to keep the chattering effect small. The main problem of the adaptive gain approaches is that in the moment when the sliding manifold is reached and the chattering occurs the SMC gain cannot be reduced to a value close to zero. This cannot be achieved because the gain has at least to be chosen sufficient large to keep the system on the sliding manifold. As a consequence the chattering effect cannot be effectively mitigated by the existing adaptation strategies. This motivates the idea to combine adaptive SMC with another control method able to take over control in the vicinity of the sliding manifold so that the chattering can be avoided entirely. Adaptive SMC has the advantage that it does not require a precise model description. Only the relative degree of the system and the sign of the appearing Lie derivatives have to be known. In addition, the so-called uncertainty bounds must be assumed to be finite. As adaptive SMC does not require a complete system description it makes sense to combine it with another control method for which the same holds true. This is obviously the case for model-free control approaches. Commonly, two types of model-free controllers exist. Those with given structure of the controller and those which formulate a generic controller based on a local system description. The local system description allows to predict the future system behavior. As a consequence, predictive control approaches can be formulated leading to minimization of the squared control error and the control input energy. In the literature, combination of MPC and SMC have already been considered. But to the best knowledge

of the author MPC has not been combined with adaptive SMC approaches before. This thesis especially focuses on a combined model-free predictive control and adaptive SMC approach that requires a minimal amount of system knowledge and allows mitigation of the chattering effect. Therefore, the following goals are formulated with respect to this thesis:

- Development of a data-driven control approach that in combination with an adaptive SMC allows control of nonlinear systems and mitigation of the chattering effect
- Establishment of a local system description that is capable to predict the future behavior of a class of nonlinear uncertain systems
- Formulation of a framework that combines predictive control and adaptive SMC
- Guarantee of tracking error boundedness for the proposed control approach

The third and last topic considered in this thesis is about constrained sliding mode control. Generally, the most frequently used constrained control method is MPC. Even if the system description is not precisely known robust MPC approaches such as tube MPC (Langson *et al.*, 2004) or min-max MPC (Raimondo *et al.*, 2009) can be applied. However, MPC relies on a prediction of the system behavior which might not fit well to every kind of application. For instance, in scenarios in which human and robot interact with each other it is not only required to predict the future behavior of the robot but also the future behavior of the human. This interacting scenarios are safety critical meaning that the correctness of the prediction of the human behavior must be guaranteed. As this is hard to achieve in practice MPC might be considered to be unsuited. In contrast to that sliding mode control does not rely on a prediction of the system behavior. In addition, the inherent robustness property of SMC guarantees the constraints to be satisfied even in case of model uncertainties. In comparison to MPC constrained SMC is typically less computationally expensive as it is not the solution of any optimization problem. Consequently, SMC may be considered to be of particular interest especially for constrained control of safety critical systems that involve the behavior of humans. In the literature a wide variety of constrained SMC approaches can be found. There exist approaches based on e. g. combined controllers (Richter, 2011; Incremona *et al.*, 2016; Song *et al.*, 2016; Jaskuła and Leśniewski, 2020), parameter selection strategies (Bartoszewicz and Nowacka-Leverton, 2010; Pietrala *et al.*, 2018; Pietrala and Jaskuła, 2019), positively robust invariant sets (Richter *et al.*, 2007), reference governor control strategies (Garelli *et al.*, 2011), and prescribed performance functions (Liu and Yang, 2017). Except for the reference governor approach of Garelli *et al.* (2011) all aforementioned control strategies lead to discontinuous control laws that generate chattering making the approaches inapplicable in practice. Smoothing of the control laws based on the introduction of a smoothing boundary layer may be considered. However, approximating the control laws may lead to constraint violations as stated in e. g. Incremona *et al.* (2016). In addition, most constrained SMC approaches are restricted to box constraints with constant bounds. However, constant bounds are undesired and limit the filed of applications. For instance, in human-robot interaction it is important to limit the robot velocity online dependent on the distance between the human and the robot. In summary, the following goals are formulated with respect to this thesis:

- Development of a constrained sliding mode control approach for nonlinear systems such as robots

- Achievement of constrained control under the influence of disturbances and model uncertainties
- Achievement of chattering mitigation without constraint violation
- Guarantee of control error convergence and analysis of control error dynamics and control error bounds

1.2 Thesis Organization

This thesis is organized as follows.

In Chapter 2 the fundamentals of sliding mode control and observation are explained. The requirements and design principles for conventional sliding mode control are discussed for both, linear and nonlinear systems. The concept of integral sliding mode control is introduced. Explanation is given about how integral sliding mode control servers as a framework to combine SMC with other control methods. The chattering effect is discussed and basic techniques for chattering mitigation are explained. Higher order SMC approaches are described with their ability to achieve finite-time convergence for systems with generic relative degree. In addition, their application with respect to chattering mitigation is explained. Nonlinear sliding manifolds are introduced to achieve fast finite-time convergence for conventional SMC approaches. Adaptive SMC methods are considered as a relatively new approach for chattering mitigation. The basic theory of sliding mode observers is introduced as well. Design principles for linear and nonlinear systems are considered. In addition, differentiation based on sliding mode differentiators is discussed.

In Chapter 3 an estimation approach for nonlinear uncertain systems is described. The approach is based on a combination of the smooth variable structure filter and the Kalman filter. First, the SVSF is introduced. A reformulation of the SVSF is stated and it is analyzed how the tuning parameters affect the behavior of the filter. The error covariance matrix of the reformulated filter is determined and serves to calculate a new filter gain that minimizes the MSE. Applying the new gain to the reformulated filter gives a connection between the SVSF and the Kalman filter. A combined filtering approach is formulated using elements from both, the SVSF and the Kalman filter. An optimization scheme is proposed to optimize the tuning parameters of the considered filters. A nonlinear chemical plant is considered to compare the estimation performance of the combined approach with the one of the SVSF and the Kalman filter.

In Chapter 4 an approach for chattering mitigated control of uncertain nonlinear systems with slow dynamics is discussed. First, a data driven model-free controller is designed. Therefore, local system dynamics are recursively identified based on a Kalman filter. The identified dynamics is used to design a model-free predictive controller. The obtained predictive controller is tested on an uncertain nonlinear multi-input multi-output three-tank water system to solve both, an unconstrained and a constrained set-point tracking problem. Subsequently, the predictive controller is combined with an adaptive SMC. Therefore, additional assumptions are formulated. The chattering mitigated control approach is formulated and its properties are studied. Finally, set-point tracking of a nonlinear uncertain chemical plant is considered to compare the control performance of the proposed method with the one of a conventional adaptive SMC.

In Chapter 5 a constrained SMC for uncertain nonlinear relative degree two systems is developed. First, a literature review about constrained SMC is given. A well-known

recent approach from the literature is studied. The controller is able to handle box constraints but it is inapplicable in practice due to chattering. After the literature review the constrained control problem that is considered in this thesis is specified. Assumptions are made required for the design of the proposed constrained controller. Possible implementation issues such as chattering or switching effects are avoided during the design process of the controller. The mathematical properties of the developed SMC are analyzed. The dynamics of the tracking error are studied and error bounds are given. Admissible values for the controller parameters are stated guaranteeing the constraints to be satisfied and the chattering to be mitigated. The proposed approach is applied to a multi-input multi-output nonlinear robotic system. A pick and place problem with an unknown payload and velocity constraints is considered. The constrained control problem can be solved by the developed controller. In addition to the control method a safety concept for human-robot collaborations tasks is proposed. The concept is described and its properties are mathematically analyzed. In particular, safety margins with reduced angular velocities are designed to guarantee the robot velocity to be restricted when human and robot are in contact with each other. The developed concept and its theory are validated by simulation.

In Chapter 6 a summary of the developed methods is given. The main design steps of the approaches are described. Scientific results are highlighted and remaining limitations are discussed. In addition, explanation about possible future works is given.

2 Theoretical Background of Sliding Mode Control and Observation

In this chapter the fundamentals of sliding mode control (SMC) and sliding mode observation (SMO) are introduced. A general review about the most important controller and observer design methods is given. Linear systems as well as nonlinear systems are considered. Bounded but unknown uncertainties are assumed to be present. Design principles are introduced to achieve finite-time convergence of tracking or estimation errors in presence of disturbances.

2.1 Sliding Mode Control

In the following the design of sliding mode controllers for linear and nonlinear systems is discussed. The control task can be divided into two main design steps. First, the sliding surface which characterizes the sliding mode is required to be designed. In the following approaches are introduced to design linear sliding surfaces with asymptotic convergence or nonlinear sliding surfaces with finite-time convergence. The second part of the controller design defines the control law. The control law is designed in such a way that it guarantees the sliding surface to be reached after a finite period of time called the reaching phase. As a consequence, after the reaching phase the sliding mode is guaranteed to become active. Related to the reaching of the sliding surface two main design principles are introduced known as the unit vector and the relay control approaches. These two control methods are conventional first order design approaches which are characterized by a discontinuous control law. Both control methods guarantee the sliding surface to be reached in finite-time but generate a high frequent switching effect in the input signal known as chattering. To make the controller applicable the chattering is required to be attenuated. Therefore, approximation techniques, adaptive control approaches as well as higher order sliding mode controllers are introduced with their ability to mitigate the chattering.

Further, additional design methods of sliding mode control are considered. In particular, integral sliding mode control is applied to eliminate the reaching phase so that the sliding mode is active from the beginning. Integral SMC is also shown to offer a suitable framework to combine SMC with other control methods.

2.1.1 Linear Systems

A brief introduction to sliding mode control of linear systems is given as follows. A linear time-invariant system

$$\dot{x} = Ax + Bu + B\xi, \tag{2.1}$$

with states $x \in \mathbb{R}^n$, inputs $u \in \mathbb{R}^m$, and uncertainties $\xi \in \mathbb{R}^m$ is considered. The state x is assumed as known. The unknown uncertainties may comprise e. g. unmodeled dynamics, nonlinear terms, or unknown inputs. As ξ acts in the same input channel as u it is called a matched uncertainty. Let

$$\sigma = Sx = 0 \tag{2.2}$$

define a sliding mode of system (2.1) where $S \in \mathbb{R}^{m \times n}$ describes a set of hyperplanes. If (2.2) holds then x evolves on the intersection of the hyperplanes and system (2.1) is said to be in a sliding mode. The intersection of hyperplanes defined by (2.2) is also denoted as the sliding surface. The goal is to design the sliding surface in such a way that x converges to zero i. e. x slides towards the origin of the state space if it moves along the intersection of the hyperplanes. When the system is in sliding mode the behavior of x is characterized by the so-called sliding dynamics.

In the following it is assumed that (2.2) holds i. e. the system is assumed to be in sliding mode. According to Shtessel *et al.* (2014, Chap. 2.2.1) the design of the sliding surface which defines the sliding dynamics is discussed. The desired sliding dynamics can be achieved by a proper choice of the matrix S. Consider a state transformation

$$z = Tx, \tag{2.3}$$

where $T \in \mathbb{R}^{n \times n}$ solves

$$TB = \begin{bmatrix} 0 \\ \bar{B}_2 \end{bmatrix}, \tag{2.4}$$

with $\bar{B}_2 \in \mathbb{R}^{m \times m}$ being nonsingular. The transformation matrix T is assumed to be obtained from a QL decomposition which is described as follows. As B is a n by m matrix with $n \geq m$ its QL decomposition is given by

$$B = Q \begin{bmatrix} 0 \\ L \end{bmatrix}, \tag{2.5}$$

with $Q \in \mathbb{R}^{n \times n}$ being an orthogonal matrix and $L \in \mathbb{R}^{m \times m}$ being a lower triangular matrix. Consequently, if $\bar{B}_2$ of (2.4) is chosen lower triangular then an orthogonal transformation matrix $T = Q^T$ can be obtained from the QL decomposition of B. Based on (2.4) the system can be transformed as

$$\underbrace{\begin{bmatrix} \dot{z}_1 \\ \dot{z}_2 \end{bmatrix}}_{\dot{z}} = \underbrace{\begin{bmatrix} \bar{A}_{11} & \bar{A}_{12} \\ \bar{A}_{21} & \bar{A}_{22} \end{bmatrix}}_{\bar{A}} \underbrace{\begin{bmatrix} z_1 \\ z_2 \end{bmatrix}}_{z} + \underbrace{\begin{bmatrix} 0 \\ \bar{B}_2 \end{bmatrix}}_{\bar{B}} u + \underbrace{\begin{bmatrix} 0 \\ \bar{B}_2 \end{bmatrix}}_{\bar{B}} \xi, \tag{2.6}$$

with

$$\bar{A} = TAT^T, \qquad \bar{B} = TB, \tag{2.7}$$

and partitions $z_1 \in \mathbb{R}^{(n-m)}$ and $z_2 \in \mathbb{R}^m$. A system with an input matrix of the form of $\bar{B}$ is said to be in regular form. Applying the state transformation on (2.2) yields

$$\sigma = ST^T z = \bar{S}z = \begin{bmatrix} \bar{S}_1 & \bar{S}_2 \end{bmatrix} \begin{bmatrix} z_1^T & z_2^T \end{bmatrix}^T = 0, \tag{2.8}$$

with $\bar{S}_1 \in \mathbb{R}^{m\times(n-m)}$ and $\bar{S}_2 \in \mathbb{R}^{m\times m}$. Matrix S and its submatrices $\bar{S}_1$, $\bar{S}_2$ which characterize the sliding mode are yet undefined. Let $\bar{S}_2$ be chosen nonsingular then

$$z_2 = -Mz_1, \qquad M = \bar{S}_2^{-1}\bar{S}_1 \tag{2.9}$$

can be obtained from (2.8). Substituting (2.9) in (2.6) yields the sliding dynamics

$$\dot{z}_1 = (\bar{A}_{11} - \bar{A}_{12}M)z_1. \tag{2.10}$$

Equations (2.9) and (2.10) describe the dynamics when system (2.1) is in sliding mode. These dynamics are of reduced order as (2.9) has no dynamics and (2.10) has dynamics of order $n - m$ which is less then n. From (2.9) and (2.10) it can be detected that the matched uncertainty ξ does not affect the reduced order system. This holds true in general as long as the uncertainty is a matched uncertainty. The invariance of the reduced order system with respect to the matched uncertainty is the main robustness feature of SMC and often denoted as invariance property.

To achieve convergence of the transformed states the reduced order system must be made asymptotically stable based on the choice of matrix M. It can be shown that the matrix pair ($\bar{A}_{11}$, $\bar{A}_{12}$) is fully controllable if and only if ($\bar{A}$, $\bar{B}$) is fully controllable (Edwards and Spurgeon, 1998, Proposition 3.3). As the transformation between (2.1) and (2.6) preserves controllability it follows that ($\bar{A}_{11}$, $\bar{A}_{12}$) is fully controllable if and only if (A, B) is fully controllable. Using pole placement a matrix M can be determined to make the dynamics of (2.10) asymptotically stable. It follows that z_1 converges to zero and from (2.9) it follows that z_2 also converges to zero. Consequently, from transformation (2.3) with nonsingular T it follows that the original states x converge to zero. According to (2.9) submatrix $\bar{S}_1$ can be obtained from M and any nonsingular matrix $\bar{S}_2$. Consequently, S and thus the sliding mode (2.2) is completely defined. Regarding the choice of the desired eigenvalues it may be required to make the dynamics of (2.10) not only asymptotically stable but also to achieve desired locations of the eigenvalues that are least sensitive to parameter perturbations $\Delta\bar{A}_{11}$, $\Delta\bar{A}_{12}$ of matrices $\bar{A}_{11}$ and $\bar{A}_{12}$. This design goal can be realized by choosing orthogonal eigenvectors denoted as eigenstructure assignment. For details see e. g. Edwards and Spurgeon (1998, Chap. 4.2.1). Classic LQR approaches can also be applied to design the sliding manifold. It is shown in Shtessel *et al.* (2014, Chap. 2.2.3) that the minimization problem

$$J = \frac{1}{2}\int_{t_s}^{\infty} x^T Q x \, dt, \qquad Q \succ 0, \qquad Q = Q^T \tag{2.11}$$

related to the original states x can be reformulated as a standard LQR design problem

$$J = \frac{1}{2}\int_{t_s}^{\infty} z_1^T \grave{Q} z_1 + v^T \bar{Q}_{22} v \, dt, \qquad \grave{Q} = \bar{Q}_{11} - \bar{Q}_{12}\bar{Q}_{22}^{-1}\bar{Q}_{12}^T, \tag{2.12}$$

with virtual control input

$$v = z_2 + \bar{Q}_{22}^{-1}\bar{Q}_{12}^T z_1, \tag{2.13}$$

subject to the dynamics

$$\dot{z}_1 = \grave{A} z_1 + \bar{A}_{12} v, \qquad \grave{A} = \bar{A}_{11} - \bar{A}_{12}\bar{Q}_{22}^{-1}\bar{Q}_{12}^T. \tag{2.14}$$

The time instant t_s denotes the time when the sliding surface is reached and the transformed weighting matrix and its submatrices are given by

$$TQT^T = \bar{Q} = \begin{bmatrix} \bar{Q}_{11} & \bar{Q}_{12} \\ \bar{Q}_{21} & \bar{Q}_{22} \end{bmatrix}. \tag{2.15}$$

The solution of this standard LQR problem is

$$v = -\bar{Q}_{22}^{-1}\bar{A}_{12}^T P z_1, \tag{2.16}$$

where P is obtained from the Ricatti equation. Substituting (2.16) in (2.13) and comparing the resulting equation with (2.9) determines M and finally the sliding mode. The LQR design requires $(\grave{A},\ \bar{A}_{12})$ to be completely controllable (Edwards and Spurgeon, 1998, Chap. 4.2.2). Based on Edwards and Spurgeon (1998, Proposition 3.3) it can be shown that the matrix pair $(\grave{A},\ \bar{A}_{12})$ is completely controllable if and only if $(A,\ B)$ is completely controllable.

So far it has been assumed that (2.2) holds and system (2.1) is in sliding mode. In the following a control law is derived that forces the system to be in sliding mode and to remain in there. From a geometrical point of view the states x are forced to move towards the sliding surface based on a suitable control law u. Following Shtessel *et al.* (2014, Chap. 2.4.1) a control law

$$u = u_l + u_{nl} \tag{2.17}$$

comprised by linear and nonlinear terms is studied. The linear term is given by state feedback

$$u_l = -(SB)^{-1}(SA - \Upsilon S)x, \tag{2.18}$$

and requires SB to be nonsingular. From transformation (2.3) it is known that

$$SB = ST^T TB = \bar{S}\bar{B} = \bar{S}_2\bar{B}_2 \tag{2.19}$$

holds. As $\bar{B}_2$ is the lower triangular matrix of the QL decomposition and $\bar{S}_2$ was required to be chosen nonsingular it follows

$$\det\{SB\} = \det\{\bar{S}_2\bar{B}_2\} = \det\{\bar{S}_2\}\det\{\bar{B}_2\} \neq 0. \tag{2.20}$$

Matrix $\Upsilon \in \mathbb{R}^{m\times m}$ of (2.18) can be any stable matrix i. e. the real part of any eigenvalue of Υ is less than zero. The effect of control input (2.18) can be further understood by considering the dynamics of σ. Derivating (2.1) with respected to time and substituting (2.2) yields

$$\dot{\sigma} = S\dot{x} = SAx + SBu + SB\xi. \tag{2.21}$$

Substituting (2.17) in (2.21) leads to

$$\dot{\sigma} = S\dot{x} = \Upsilon Sx + SBu_{nl} + SB\xi = \Upsilon\sigma + SBu_{nl} + SB\xi. \tag{2.22}$$

Consequently, if the uncertainty ξ and the nonlinear term u_{nl} are assumed zero then the linear part of the control law drives the states towards the sliding manifold with dynamics

dependent on the chosen eigenvalues of Υ. The rejection of the uncertainty is achieved by the nonlinear term u_{nl} of the control law which is given as

$$u_{nl} = -(SB)^{-1} k_s \phi(P_2, \sigma), \tag{2.23}$$

with

$$\phi(P, \sigma) = \begin{cases} \frac{P\sigma}{\|P\sigma\|} & \text{if } \|P\sigma\| \neq 0, \\ 0 & \text{else.} \end{cases} \tag{2.24}$$

The static gain k_s is chosen as

$$k_s \geq \|SB\| \xi_M + \gamma, \tag{2.25}$$

with $\gamma > 0$ being a controller parameter and ξ_M being an upper bound of the uncertainty ξ according to

$$\|\xi\| \leq \xi_M. \tag{2.26}$$

Matrix $P_2 \in \mathbb{R}^{m \times m}$ is obtained from the Lyapunov equation

$$\Upsilon P_2 + P_2 \Upsilon^T = -I_m, \tag{2.27}$$

and is symmetric as well as positive definite. Due to the definition (2.24) the controller (2.23) is denoted as unit vector approach and was first published by Ryan and Corless (1984). Referring to Edwards and Spurgeon (1998, Chap. 3.6.1) it will be shown that the control law (2.17) guarantees finite-time stability of σ. Let

$$V = \sigma^T P_2 \sigma, \tag{2.28}$$

be a Lyapunov function candidate. Derivating (2.28) with respect to time leads to

$$\dot{V} = \dot{\sigma}^T P_2 \sigma + \sigma^T P_2 \dot{\sigma}. \tag{2.29}$$

Substituting (2.23) in (2.22) gives

$$\dot{\sigma} = \Upsilon \sigma - k_s \phi(P_2, \sigma) + SB\xi, \tag{2.30}$$

and substituting (2.30) in (2.29) yields

$$\dot{V} = \sigma^T (\Upsilon^T P_2 + P_2 \Upsilon) \sigma + 2\sigma^T P_2 SB\xi - 2k_s \frac{\sigma^T P_2^2 \sigma}{\|P_2 \sigma\|}, \tag{2.31}$$

for $\sigma \neq 0$. Based on the Euclidean norm

$$\sigma^T P_2^2 \sigma = \sigma^T P_2^T P_2 \sigma = \|P_2 \sigma\|^2, \tag{2.32}$$

and equation (2.27) expression (2.29) can be rewritten as

$$\dot{V} = -\sigma^T \sigma + 2\sigma^T P_2 SB\xi - 2k_s \|P_2 \sigma\|. \tag{2.33}$$

Applying the submultiplicative Frobenius norm leads to

$$\begin{aligned}\dot{V} &\leq -\sigma^T\sigma + 2\|\sigma^T P_2\|\|SB\|\xi_M - 2k_s\|P_2\sigma\|, \\ &= -\sigma^T\sigma + 2\|P_2\sigma\|(\|SB\|\xi_M - k_s),\end{aligned} \tag{2.34}$$

and substituting (2.25) in (2.34) yields

$$\dot{V} \leq -\sigma^T\sigma - 2\|P_2\sigma\|\gamma = -\sigma^T\sigma - 2\gamma\sqrt{(P_2^{1/2}\sigma)^T P_2 (P_2^{1/2}\sigma)}, \tag{2.35}$$

where $P_2^{1/2}$ is defined as

$$P_2 = P_2^{1/2} P_2^{1/2}. \tag{2.36}$$

As P_2 is symmetric the statement

$$\sqrt{\lambda_{min}\{P_2\}(P_2^{1/2}\sigma)^T(P_2^{1/2}\sigma)} \leq \sqrt{(P_2^{1/2}\sigma)^T P_2 (P_2^{1/2}\sigma)} \tag{2.37}$$

holds which in combination with (2.35) leads to

$$\dot{V} \leq -2\gamma\sqrt{\lambda_{min}\{P_2\}(P_2^{1/2}\sigma)^T(P_2^{1/2}\sigma)} = -2\gamma\sqrt{\lambda_{min}\{P_2\}}\sqrt{V}. \tag{2.38}$$

Integrating (2.38) gives

$$-\frac{1}{\gamma\sqrt{\lambda_{min}\{P_2\}}}\Big(V(t)^{1/2} - V(t_0)^{1/2}\Big) = t - t_0, \tag{2.39}$$

which shows that σ is finite-time stable with respect to zero.

Up until now state stability of system (2.1) has been considered. It was shown how the states x can be made asymptotically stable even in presence of an uncertainty. In the following reference tracking is considered. A common way to achieve reference tracking is to apply integral control. Following Edwards and Spurgeon (1998, Chap. 4.4.2) the linear time-invariant system (2.1) with m inputs $u \in \mathbb{R}^m$ is assumed to have m control variables $y_r \in \mathbb{R}^m$ according to

$$y_r = C_r x. \tag{2.40}$$

System (2.1), (2.40) is transformed into regular form leading to

$$\underbrace{\begin{bmatrix}\dot{z}_1 \\ \dot{z}_2\end{bmatrix}}_{\dot{z}} = \underbrace{\begin{bmatrix}\bar{A}_{11} & \bar{A}_{12} \\ \bar{A}_{21} & \bar{A}_{22}\end{bmatrix}}_{\bar{A}}\underbrace{\begin{bmatrix}z_1 \\ z_2\end{bmatrix}}_{z} + \underbrace{\begin{bmatrix}0 \\ \bar{B}_2\end{bmatrix}}_{\bar{B}} u + \underbrace{\begin{bmatrix}0 \\ \bar{B}_2\end{bmatrix}}_{\bar{B}} \xi, \tag{2.41}$$

$$y_r = \bar{C}_r z, \tag{2.42}$$

with

$$\bar{A} = TAT^T, \qquad \bar{B} = TB, \qquad \bar{C}_r = C_r T^T, \tag{2.43}$$

and states $z_1 \in \mathbb{R}^{(n-m)}$, $z_2 \in \mathbb{R}^m$, and $z \in \mathbb{R}^n$. Let $w \in \mathbb{R}^m$ be the reference variable which is assumed to converge to a desired constant set-point $w_c \in \mathbb{R}^m$. Signal w can be generated based on

$$\dot{w} = \Phi w - \Phi w_c, \tag{2.44}$$

with design matrix Φ chosen asymptotically stable so that the error dynamics

$$\dot{w} - \dot{w}_c = \Phi(w - w_c), \tag{2.45}$$

converge to zero asymptotically. An integral state $\mu \in \mathbb{R}^m$ is introduced as

$$\mu = \int w - y_r, \tag{2.46}$$

and system (2.41)–(2.42) is augmented according to

$$\underbrace{\begin{bmatrix}\dot{\mu}\\ \dot{z}\end{bmatrix}}_{\dot{\zeta}} = \underbrace{\begin{bmatrix}0 & -\bar{C}_r\\ 0 & \bar{A}\end{bmatrix}}_{\overset{*}{A}} \underbrace{\begin{bmatrix}\mu\\ z\end{bmatrix}}_{\zeta} + \underbrace{\begin{bmatrix}0\\ \bar{B}\end{bmatrix}}_{\overset{*}{B}} u + \underbrace{\begin{bmatrix}0\\ \bar{B}\end{bmatrix}}_{\overset{*}{B}} \xi + \underbrace{\begin{bmatrix}I\\ 0\end{bmatrix}}_{N} w, \tag{2.47}$$

where $\zeta \in \mathbb{R}^{(m+n)}$ denotes the augmented state being defined as

$$\zeta = \begin{bmatrix}\mu\\ z\end{bmatrix}. \tag{2.48}$$

The augmented system (2.47) is partitioned as

$$\begin{bmatrix}\dot{\zeta}_1\\ \dot{\zeta}_2\end{bmatrix} = \begin{bmatrix}\overset{*}{A}_{11} & \overset{*}{A}_{12}\\ \overset{*}{A}_{21} & \overset{*}{A}_{22}\end{bmatrix} \begin{bmatrix}\zeta_1\\ \zeta_2\end{bmatrix} + \begin{bmatrix}\overset{*}{B}_1\\ \overset{*}{B}_2\end{bmatrix} u + \begin{bmatrix}\overset{*}{B}_1\\ \overset{*}{B}_2\end{bmatrix} \xi + \begin{bmatrix}N_1\\ N_2\end{bmatrix} w, \tag{2.49}$$

with $\zeta_1 \in \mathbb{R}^n$ and $\zeta_2 \in \mathbb{R}^m$ defined as

$$\zeta_1 = \begin{bmatrix}\mu\\ z_1\end{bmatrix}, \qquad \zeta_2 = z_2. \tag{2.50}$$

Comparing (2.49) with (2.41) and (2.47) yields the identities

$$\left[\begin{array}{c|c}\overset{*}{A}_{11} & \overset{*}{A}_{12}\\ \hline \overset{*}{A}_{21} & \overset{*}{A}_{22}\end{array}\right] = \left[\begin{array}{cc|c}0 & -\bar{C}_{r,1} & -\bar{C}_{r,2}\\ 0 & \bar{A}_{11} & \bar{A}_{12}\\ \hline 0 & \bar{A}_{21} & \bar{A}_{22}\end{array}\right], \quad \left[\begin{array}{c}\overset{*}{B}_1\\ \hline \overset{*}{B}_2\end{array}\right] = \left[\begin{array}{c}0\\ 0\\ \hline \bar{B}_2\end{array}\right], \quad \left[\begin{array}{c}N_1\\ \hline N_2\end{array}\right] = \left[\begin{array}{c}I\\ 0\\ \hline 0\end{array}\right], \tag{2.51}$$

where $\bar{C}_{r,1}$ and $\bar{C}_{r,2}$ are defined by

$$\bar{C}_r z = \begin{bmatrix}\bar{C}_{r,1} & \bar{C}_{r,2}\end{bmatrix} \begin{bmatrix}z_1\\ z_2\end{bmatrix}. \tag{2.52}$$

Let

$$\sigma = S\zeta = \begin{bmatrix}S_1 & S_2\end{bmatrix} \begin{bmatrix}\zeta_1\\ \zeta_2\end{bmatrix} = 0, \tag{2.53}$$

with $S \in \mathbb{R}^{m\times(n+m)}$ define a sliding mode of the augmented system (2.49), where $S_2 \in \mathbb{R}^{m\times m}$ is chosen nonsingular. It is assumed that the system is in sliding mode so that

$$\zeta_2 = -M\zeta_1, \qquad M = S_2^{-1}S_1, \tag{2.54}$$

holds. Substituting (2.54) in (2.49) and considering the identities (2.51) yields the dynamics of ζ_1 according to

$$\dot{\zeta}_1 = (\overset{*}{A}_{11} - \overset{*}{A}_{12}M)\zeta_1 + N_1 w. \tag{2.55}$$

It can be shown (Edwards and Spurgeon, 1998, Lemma 4.1) that the matrix pair $(\overset{*}{A}_{11}, \overset{*}{A}_{12})$ is fully controllable if system (2.41) has no invariant zeros at the origin and its matrix pair $(\bar{A}, \bar{B})$ is fully controllable. Regarding invariance of the state transformation it follows that the matrix pair $(\overset{*}{A}_{11}, \overset{*}{A}_{12})$ is fully controllable if system (2.1), (2.40) has no invariant zeros at the origin and (A, B) is fully controllable. Based on e. g. pole placement the dynamics of (2.55) are made asymptotically stable which defines M and according to (2.54) the yet undefined matrix S_1. From (2.45) it is known that $\lim_{t\to\infty} w(t) = w_c$ holds. Consequently, as the dynamics of (2.55) are asymptotically stable it is $\lim_{t\to\infty} \dot{\zeta}_1(t) = 0$ and from (2.54) it follows that $\lim_{t\to\infty} \dot{\zeta}_2(t) = 0$ holds. As ζ_1 and ζ_2 define the augmented state ζ it can be concluded that $\lim_{t\to\infty} \dot{\zeta}(t) = 0$ holds. Considering (2.47) with $\lim_{t\to\infty} \dot{\zeta}(t) = 0$ shows that $\lim_{t\to\infty} y_r(t) = w_c$ must hold true. Consequently, set-point tracking is achieved and the state z is stable as well as its pendant x. To reach the designed sliding mode the control law

$$u = -(S_2\bar{B}_2)^{-1}\left(S\overset{*}{A}\zeta - \Upsilon\sigma + S_1N_1w + k_s\phi(P_2, \sigma)\right), \tag{2.56}$$

is proposed based on the unit vector approach. The quantities $\phi(\cdot)$, Υ, and P_2 are defined as before. The sliding variable σ is defined based on (2.53) and the static gain is chosen as

$$k_s \geq \|S_2\bar{B}_2\|\zeta_M + \gamma, \tag{2.57}$$

with $\gamma > 0$ being a controller parameter. Derivating (2.53) with respect to time yields

$$\dot{\sigma} = S\dot{\zeta} = S\overset{*}{A}\zeta + S\overset{*}{B}u + S\overset{*}{B}\xi + SNw, \qquad S\overset{*}{B} = S_2\bar{B}_2, \qquad SN = S_1N_1. \tag{2.58}$$

Substituting (2.56) in (2.58) leads to

$$\dot{\sigma} = \Upsilon\sigma - k_s\phi(P_2, \sigma) + S_2\bar{B}_2\xi. \tag{2.59}$$

As (2.30) and (2.59) only differ by $SB\zeta$ and $S_2\bar{B}_2\zeta$ it is straight forward to show that control law (2.56) guarantees finite-time stability of σ.

So far it has been assumed that the state vector x of the dynamical system (2.1) is known. Under certain conditions it is also possible to achieve stabilization of system (2.1) based on output feedback control. Instead of x the outputs

$$y = Cx, \tag{2.60}$$

with $y \in \mathbb{R}^p$ are required to be known and are feed back to the system. From classic output feedback control $u = -Ky$ it is known that if system (2.1), (2.60) is completely controllable and observable and if it satisfies the dimensional requirement

$$m + p + 1 \geq n, \tag{2.61}$$

then the eigenvalues of the closed loop system matrix $A - BKC$ can be placed arbitrarily (Edwards and Spurgeon, 1998, Chap. 2). Similar restrictions have to be made to design a sliding mode

$$\sigma = SCx = Sy, \tag{2.62}$$

based on the outputs y so that it induces arbitrary desired dynamics of x (Edwards and Spurgeon, 1998, Chap. 5.3 & 5.4). The strategy suggested in Edwards and Spurgeon (1998) to design the sliding surface and the related control law involves two state transformations. For details see e. g. Edwards and Spurgeon (1998). Instead of measuring all states of x it is also possible to estimate the states by an observer. However, the states are required to be estimated in presence of the uncertainty ξ. Sliding mode observers can be applied to solve such kind of estimation problems. If the linear system equals a chain of integrators high-gain observers can also be applied to estimate the states in presence of uncertainties (Khalil, 2002, Chap. 14.5). In addition, applications of PI-observers can be found in e. g. Hu *et al.* (2013); Söffker *et al.* (1995) to estimate the states as well as uncertainties.

Up to now the disturbance ξ has been assumed to be a matched uncertainty. Consider a linear time-invariant system

$$\dot{x} = Ax + Bu + f, \tag{2.63}$$

with states $x \in \mathbb{R}^n$, inputs $u \in \mathbb{R}^m$, and an uncertainty term $f \in \mathbb{R}^n$. Following Shtessel *et al.* (2014, Chap. 2.4.2) system (2.63) can be transformed into regular form which yields the dynamics

$$\dot{z}_1 = \bar{A}_{11} z_1 + \bar{A}_{12} z_2 + \bar{f}_u, \tag{2.64}$$

$$\dot{z}_2 = \bar{A}_{21} z_1 + \bar{A}_{22} z_2 + \bar{B}_2 u + \bar{f}_m, \tag{2.65}$$

in transformed and partitioned coordinates z. The transformed uncertainty $\bar{f} = Tf$ can be partitioned into the two terms $\bar{f}_u$ and $\bar{f}_m$. If the system is in sliding mode it follows from (2.8) and (2.9) that the dynamics are

$$\dot{z}_1 = (\bar{A}_{11} - \bar{A}_{12} M) z_1 + \bar{f}_u, \tag{2.66}$$

$$z_2 = -M z_1, \tag{2.67}$$

where (2.66) denotes the reduced order dynamics. The unmatched uncertainty $\bar{f}_u$ is the input of the reduced order system whereas the matched uncertainty $\bar{f}_m$ does not appear at all. The effect of $\bar{f}_u$ on z_1 depends on the design of the matrix $\bar{A}_{11} - \bar{A}_{12} M$. Even in presence of the unmatched uncertainty the stability of z_1 can still be guaranteed. Therefore, the uncertainty $\bar{f}_u$ has to satisfy several conditions and the matrix M is required to be suitably designed. For details see e. g. Shtessel *et al.* (2014, Chap. 2.4.2).

2.1.2 Nonlinear Systems

Consider a nonlinear input-affine square system of the form

$$\dot{x} = f(x) + \sum_{i=1}^{m} g_i(x) u_i = f(x) + g(x) u, \tag{2.68}$$

$$\underbrace{\begin{bmatrix} y_{r,1} \\ y_{r,2} \\ \vdots \\ y_{r,m} \end{bmatrix}}_{y_r} = \underbrace{\begin{bmatrix} h_1(x) \\ h_2(x) \\ \vdots \\ h_m(x) \end{bmatrix}}_{h(x)}, \tag{2.69}$$

with states $x \in \mathbb{R}^n$, inputs $u \in \mathbb{R}^m$, and control variables $y_r \in \mathbb{R}^m$. According to the definition of Isidori *et al.* (1995, Chap. 5.1) system (2.68)–(2.69) is assumed to have a well-defined vector of relative degree $(r_1, \ldots, r_m)$. Further, the total relative degree r is assumed to satisfy $r = r_1 + \cdots + r_m < n$. Based on the made assumptions it is stated by Isidori *et al.* (1995, Proposition 5.1.2) that a diffeomorphism

$$\Phi \colon x \to \begin{bmatrix} \zeta \\ \eta \end{bmatrix}, \tag{2.70}$$

is guaranteed to exist that transforms system (2.68)–(2.69) into the form

$$\begin{bmatrix} y_{r,1} \\ y_{r,2} \\ \vdots \\ y_{r,m} \end{bmatrix} = \begin{bmatrix} \zeta_1^1 \\ \zeta_1^2 \\ \vdots \\ \zeta_1^m \end{bmatrix}, \quad \begin{bmatrix} \dot{\zeta}_1^1 \\ \dot{\zeta}_1^2 \\ \vdots \\ \dot{\zeta}_1^m \end{bmatrix} = \begin{bmatrix} \zeta_2^1 \\ \zeta_2^2 \\ \vdots \\ \zeta_2^m \end{bmatrix}, \quad \begin{bmatrix} \dot{\zeta}_2^1 \\ \dot{\zeta}_2^2 \\ \vdots \\ \dot{\zeta}_2^m \end{bmatrix} = \begin{bmatrix} \zeta_3^1 \\ \zeta_3^2 \\ \vdots \\ \zeta_3^m \end{bmatrix} \quad \cdots \quad \begin{bmatrix} \dot{\zeta}_{r_1-1}^1 \\ \dot{\zeta}_{r_2-1}^2 \\ \vdots \\ \dot{\zeta}_{r_m-1}^m \end{bmatrix} = \begin{bmatrix} \zeta_{r_1}^1 \\ \zeta_{r_2}^2 \\ \vdots \\ \zeta_{r_m}^m \end{bmatrix}, \tag{2.71}$$

$$\begin{bmatrix} \dot{\zeta}_{r_1}^1 \\ \dot{\zeta}_{r_2}^2 \\ \vdots \\ \dot{\zeta}_{r_m}^m \end{bmatrix} = a(\zeta, \eta) + B(\zeta, \eta)u, \tag{2.72}$$

$$\eta = q(\zeta, \eta) + p(\zeta, \eta)u, \tag{2.73}$$

with the transformed states η and ζ. Here state ζ is specified by

$$\zeta = \begin{bmatrix} \zeta^1 \\ \zeta^2 \\ \vdots \\ \zeta^m \end{bmatrix}, \qquad \zeta^i = \begin{bmatrix} \zeta_1^i \\ \zeta_2^i \\ \vdots \\ \zeta_{r_i}^i \end{bmatrix}, \tag{2.74}$$

and vector $a(\zeta, \eta)$ and matrix $B(\zeta, \eta)$ are defined based on the Lie derivatives of the system according to

$$a = \begin{bmatrix} L_f^{r_1} h_1 \\ L_f^{r_2} h_2 \\ \vdots \\ L_f^{r_m} h_m \end{bmatrix}, \qquad B = \begin{bmatrix} L_{g_1} L_f^{r_1-1} h_1 & L_{g_2} L_f^{r_1-1} h_1 & \ldots & L_{g_m} L_f^{r_1-1} h_1 \\ L_{g_1} L_f^{r_2-1} h_2 & L_{g_2} L_f^{r_2-1} h_2 & \ldots & L_{g_m} L_f^{r_2-1} h_2 \\ \vdots & \vdots & \ddots & \vdots \\ L_{g_1} L_f^{r_m-1} h_m & L_{g_2} L_f^{r_m-1} h_m & \ldots & L_{g_m} L_f^{r_m-1} h_m \end{bmatrix}. \tag{2.75}$$

The assumption of the vector of relative degree to be well-defined implies that matrix $B(\zeta, \eta)$ is invertible (Isidori *et al.*, 1995, Chap. 5.1). Following Slotine and Li (1991,

Chap. 7.4) a vector

$$\sigma = \begin{bmatrix} \sigma_1 \\ \sigma_2 \\ \vdots \\ \sigma_m \end{bmatrix}, \tag{2.76}$$

of sliding variables is defined based on the polynomials

$$\sigma_i = (\frac{d}{dt} + \lambda_i)^{r_i - 1} e_i, \qquad \lambda_i > 0, \quad 1 \leq i \leq m. \tag{2.77}$$

In (2.77) quantity e_i denotes the tracking error

$$e_i = y_{r,i} - w_i, \tag{2.78}$$

of control variable $y_{r,i}$ related to a reference $w_i(t)$ that may depend on time. Choosing λ_i as $\lambda_i > 0$ makes the polynomial in (2.77) Hurwitz. Derivating σ of (2.77) with respect to time yields

$$\dot{\sigma}_i = \frac{\partial^{r_i} y_{r,i}}{\partial t^{r_i}} + \varrho_i(e_i) = \dot{\zeta}_{r_i}^i + \varrho_i(e_i), \tag{2.79}$$

so that due to $\dot{\zeta}_{r_i}^i$ from (2.72) the input u appears in $\dot{\sigma}_i$. The term $\varrho_i(e_i)$ is assumed as known as it only depends on the known design parameter λ_i and the time derivatives of e_i. The time derivatives of e_i can be determined based on high-gain observers or sliding mode differentiators. The sliding mode of the nonlinear system is defined as

$$\sigma = \begin{bmatrix} \sigma_1 \\ \sigma_2 \\ \vdots \\ \sigma_m \end{bmatrix} = 0. \tag{2.80}$$

Consequently, if the system is in sliding mode $\sigma_i = 0$ holds and due to the Hurwitz polynomial asymptotic convergence of the tracking error is achieved. Stabilization can be enforced by choosing the reference values and its time derivatives as $w_i(t) = 0$, $\dot{w}_i(t) = 0$, $\ddot{w}_i(t) = 0, \cdots$. To force the system on the sliding surface a Lyapunov function candidate $V_i = 0.5\sigma_i^2$ is considered. If

$$\dot{\sigma}_i \sigma_i \leq -\frac{\mu_i}{\sqrt{2}} |\sigma_i|, \qquad \mu_i > 0, \tag{2.81}$$

holds for $\sigma_i \neq 0$ then V_i is a Lyapunov function. Condition (2.81) is also referred to as reachability condition (Shtessel *et al.*, 2014, Chap. 1). Dividing (2.81) by $|\sigma_i| \neq 0$ leads to an equivalent expression of the reachability according to

$$\operatorname{sgn}(\sigma_i)\dot{\sigma}_i \leq -\frac{\mu_i}{\sqrt{2}}, \qquad \mu_i > 0. \tag{2.82}$$

In the following it is shown that finite-time convergence of the sliding variable can be guaranteed if the reachability condition is satisfied. Integrating (2.81) leads to

$$|\sigma_i(t_f)| - |\sigma_i(t)| = -\frac{\mu_i}{\sqrt{2}}(t_f - t), \qquad t_f \geq t, \tag{2.83}$$

so that the sliding surface can be reached in finite-time i. e. $|\sigma_i(t_f)|$ equals zero after the finite time interval

$$t_f - t = \frac{|\sigma_i(t)|\sqrt{2}}{\mu_i}. \tag{2.84}$$

Following Slotine and Li (1991, Chap. 7.4) it is assumed that the system is not accurately known. In particular, the true values of a and B are unknown. Instead known quantities $\breve{a}$ and $\breve{B}$ are introduced which describe the nominal system behavior. Uncertainty bounds are defined according to

$$|a_i - \breve{a}_i| \leq a_{i,M}, \tag{2.85}$$

$$B = (I_m + \Delta)\breve{B}, \tag{2.86}$$

where $\Delta = (\Delta_{ij}) \in \mathbb{R}^{m\times m}$ is a m by m matrix with elements Δ_{ij} being bounded as

$$|\Delta_{ij}| < D_{ij}, \qquad D_{ii} < 1. \tag{2.87}$$

The matrix $D = (D_{ij}) \in \mathbb{R}^{m\times m}$ defined by the elements D_{ij} is assumed to have a maximum eigenvalue less than one i. e.

$$\lambda_{max}\{D\} < 1. \tag{2.88}$$

In addition, it is assumed that $\breve{B}$ is invertible and $a_{i,M}$ is finite. Consider a control law of the form

$$u = -\breve{B}^{-1}(\breve{a} + \varrho + \vartheta(k,\sigma)), \tag{2.89}$$

where

$$\varrho = \begin{bmatrix}\varrho_1(e_1) & \varrho_2(e_2) & \dots & \varrho_m(e_m)\end{bmatrix}^T, \tag{2.90}$$

is known and $\vartheta(k,\sigma)$ is defined as

$$\vartheta(k,\sigma) = \begin{bmatrix}k_1\mathrm{sgn}(\sigma_1) & k_2\mathrm{sgn}(\sigma_2) & \dots & k_m\mathrm{sgn}(\sigma_m)\end{bmatrix}^T, \tag{2.91}$$

based on a set of controller gains $k_j \in \mathbb{R}$ with $j = 1 \dots m$. As (2.91) defines a vector of switching functions controller (2.89) is denoted as relay control approach. It is an alternative sliding mode control approach to the already introduced unit vector method. Substituting (2.89) in (2.72) yields

$$\begin{bmatrix}\dot{\zeta}^1_{r_1}\\ \dot{\zeta}^2_{r_2}\\ \vdots\\ \dot{\zeta}^m_{r_m}\end{bmatrix} = a - (I_m + \Delta) \times (\breve{a} + \varrho + \vartheta(k,\sigma)), \tag{2.92}$$

and substituting (2.92) in (2.79) leads to

$$\dot{\sigma}_i = a_i - \breve{a}_i - k_i(1 + \Delta_{ii})\mathrm{sgn}(\sigma_i) - \sum_{j=1}^{m}\Delta_{ij}(\breve{a}_j + \varrho_j) - \sum_{\substack{j=1,\\ j\neq i}}^{m} k_j\Delta_{ij}\mathrm{sgn}(\sigma_j). \tag{2.93}$$

Substituting (2.93) in the reachability condition (2.82) and rearranging gives

$$(1+\Delta_{ii})k_i \geq \operatorname{sgn}(\sigma_i)(a_i - \breve{a}_i) - \sum_{j=1}^{m} \Delta_{ij}(\breve{a}_j + \varrho_j)\operatorname{sgn}(\sigma_i) - \sum_{\substack{j=1,\\ j\neq i}}^{m} k_j \Delta_{ij}\operatorname{sgn}(\sigma_j)\operatorname{sgn}(\sigma_i) + \frac{\mu_i}{\sqrt{2}}. \tag{2.94}$$

A lower bound of the left side of (2.94) and an upper bound of the right side of (2.94) can be obtained according to

$$(1-D_{ii})k_i \geq a_{i,M} + \sum_{j=1}^{m} D_{ij}|\breve{a}_j + \varrho_j| + \sum_{\substack{j=1,\\ j\neq i}}^{m} k_j D_{ij} + \frac{\mu_i}{\sqrt{2}}, \qquad 1 \leq i \leq m, \tag{2.95}$$

where $0 \leq |\Delta_{ii}| < D_{ii} < 1$ from (2.87) has been used to obtain the bound on the left side and the controller gains k_j have been assumed to be non-negative. The m equations of (2.95) can also be written as

$$(I_m - D)k = z, \tag{2.96}$$

with $k \in \mathbb{R}^m$ being the vector of controller gains and $z \in \mathbb{R}^m$ being defined by the entries

$$z_i = a_{i,M} + \sum_{j=1}^{m} D_{ij}|\breve{a}_j + \varrho_j| + \frac{\mu_i}{\sqrt{2}}, \qquad 1 \leq i \leq m. \tag{2.97}$$

According to the Frobenius-Perron Theorem (see Slotine and Li, 1991) equation (2.96) has a solution with non-negative elements of k if the entries of z are non-negative (which is the case) and the largest eigenvalue of matrix D is less than one (which is also the case by assumption). Consequently, the previously made assumption about the non-negative gains k_j is indeed true.

As the sliding surface is reached in finite-time and the sliding dynamics are asymptotically stable due to the Hurwitz polynomials it follows stability of the transformed state ζ. If internal dynamics according to (2.73) exist it is required to prove stability of the transformed state η in addition.

So far the considered nonlinear system has been assumed to be input-affine. Consider a nonlinear non-input-affine system

$$\dot{x} = f(x,u), \tag{2.98}$$
$$y_r = h(x), \tag{2.99}$$

with states $x \in \mathbb{R}^n$, inputs $u \in \mathbb{R}^m$, and control variables $y_r \in \mathbb{R}^m$. According to e. g. Bartolini and Punta (2012, 2010) system (2.98) can be made input-affine by introducing the augmented state

$$x_a = \begin{bmatrix} x^T & u^T \end{bmatrix}^T, \tag{2.100}$$

and a virtual control input $v = \dot{u}$. In terms of the augmented state the dynamics of the nonlinear system can be written as

$$\underbrace{\begin{bmatrix}\dot{x}\\ \dot{u}\end{bmatrix}}_{\dot{x}_a} = \underbrace{\begin{bmatrix}f(x,u)\\ 0\end{bmatrix}}_{\bar{f}(x_a)} + \underbrace{\begin{bmatrix}0\\ I_m\end{bmatrix}}_{\bar{g}} v, \tag{2.101}$$

$$y_r = \bar{h}(x_a), \tag{2.102}$$

which is an input-affine system with respect to the virtual control input $v \in \mathbb{R}^m$. Consequently, v can be determined based on the design principles of input-affine systems. Finally, the control input u is obtained by solving the differential equation

$$\dot{u} = v. \tag{2.103}$$

Choosing the relay control approach

$$v = -\breve{B}^{-1}(\breve{a} + \varrho + \vartheta(k,\sigma)), \tag{2.104}$$

with ϑ being defined by (2.91) shows that the right hand side of (2.103) will be discontinuous as it depends on the signum function. An ordinary differential equation with discontinuous right hand side can not be interpreted in the classical way as Lipschitz continuity is not satisfied which guarantees existence and uniqueness of the solution. A common way in the field of SMC to treat that kind of problems is to apply the method of Fillipov (Filippov, 2013) which defines an average solution at the point of discontinuity. Alternatively, the signum function can be approximated by a saturation function which makes the right hand side of the differential equation continuous.

2.1.3 Integral Sliding Mode Control

Integral sliding mode control (ISMC) is a control approach that offers a framework to combine SMC with other control methods such as state feedback, optimal control, MPC etc. In addition ISMC has the ability to eliminate the reaching phase i. e. the phase in which the sliding surface is reached is eliminated so that the system is in sliding mode from the beginning. Elimination of the reaching phase is relevant as the dynamics of the system are invariant to matched uncertainties in sliding mode but not in the reaching phase. The concept of ISMC was first proposed by Utkin and Shi (1996). In the following explanation is given based on Utkin and Shi (1996); Shtessel *et al.* (2014). Consider a nonlinear input-affine system

$$\dot{x} = f(x) + g(x)u + g(x)\xi, \tag{2.105}$$

with states $x \in \mathbb{R}^n$, inputs $u \in \mathbb{R}^m$, and matched uncertainties $\xi \in \mathbb{R}^m$. Assume some nominal control input u_0 to be given that leads to desired dynamics of (2.105) in absence of the uncertainties. In case of nonlinear systems u_0 may be a feedback linearization or backstepping approach that is designed to achieve desired closed loop dynamics

$$\dot{x}_0 = f(x_0) + g(x_0)u_0, \tag{2.106}$$

of the nonlinear system. As the desired dynamics (2.106) are only achieved in absence of the uncertainty a SMC control input u_{SMC} is introduced to compensate the effect of ξ. A combined control input

$$u = u_0 + u_{SMC}, \tag{2.107}$$

is considered where u_{SMC} is yet undefined. In addition a sliding mode

$$\sigma(t) = G(x(t) - x(t_0)) + Gz(t) = 0, \tag{2.108}$$

$$z(t) = -\int_{t_0}^{t} f(x) + g(x)u_0 \, d\tau, \tag{2.109}$$

with sliding variable $\sigma \in \mathbb{R}^m$ and a design matrix $G \in \mathbb{R}^{m \times n}$ is defined. According to (2.108) the initial state $x(t_0)$ of the system is required to be known to appropriately define σ. In the context of ISMC the sliding mode (2.108) does not define the desired system dynamics. The sliding mode is only required to compensate the effect of the uncertainty. This compensation can be achieved by any matrix G for which $Gg(x)$ is nonsingular. Let

$$u_{SMC} = (Gg(x))^{-1}(\Upsilon\sigma - k_s\phi(P_2, \sigma)), \tag{2.110}$$

with

$$\phi(\sigma) = \begin{cases} \frac{P_2\sigma}{\|P_2\sigma\|} & \text{if } \|P_2\sigma\| \neq 0, \\ 0 & \text{else,} \end{cases} \tag{2.111}$$

define the unit vector control input. Matrix P_2 is obtained from the Lyapunov equation

$$\Upsilon P_2 + P_2\Upsilon^T = -I_m, \tag{2.112}$$

where $\Upsilon \in \mathbb{R}^{m \times m}$ is an asymptotically stable matrix. The scalar gain k_s is assumed to satisfy

$$k_s \geq \|Gg(x)\|\|\xi\| + \gamma, \qquad \gamma > 0. \tag{2.113}$$

Similarly to the proof of Section 2.1.1 it can be shown that finite-time stability of σ can be achieved based on the combined control law

$$u = u_0 + u_{SMC}. \tag{2.114}$$

However, from the definition of the sliding mode according to (2.108) it can be seen that no reaching phase exists as $\sigma(t_0) = 0$ holds. It follows that the states are on the sliding surface at the beginning. As control input (2.114) provides convergence of σ with respect to the origin the states remain exactly on the sliding surface thereafter. Consequently, control input (2.114) can be thought to be an input for which

$$\dot{\sigma}(t) = 0, \tag{2.115}$$

holds. Substituting (2.105) in the time derivative of (2.108) leads to

$$\begin{aligned} \dot{\sigma} &= G\Big(f(x) + g(x)(u_0 + u_{SMC} + \xi)\Big) - G\Big(f(x) + g(x)u_0\Big), \\ &= Gg(x)(u_{SMC} + \xi) = 0. \end{aligned} \tag{2.116}$$

As $Gg(x)$ is nonsingular by assumption it follows $u_{SMC}(t) = -\xi(t)$. Consequently, by applying control law (2.107) the desired dynamics (2.106) are achieved because the SMC cancel out the uncertainty term.

2.1.4 Chattering

The previously introduced unit vector and relay SMC approaches guarantee finite-time convergence of the sliding variable σ with respect to zero. Consequently, the states reach the sliding surface in finite-time and remain on it. However, in practice stability of σ can only be achieved with respect to a domain but not with respect to zero. The main reason for that is the sampling of the input signal when the SMC law is implemented on a microcontroller. The input will in general not be reduced at the moment when the state trajectory reaches the sliding surface. Instead, the input will be applied too long so that the states are pushed beyond the surface. As a consequence a high frequent zigzag motion across the sliding surface is induced. In particular, the sliding variable σ switches across the sliding surface with a high frequency. The resulting problem is that the control law which directly depends on σ induces discontinuous switchings in the signal of the control inputs. This effect of high frequent switching in the input signal is denoted as chattering. Chattering is undesired because it may lead to e. g. wear, material stress or damage, excitation of unwanted dynamics, heat losses in electric power converters, etc. (Utkin, 2011). A common way to mitigate chattering is to approximate the control law by some smooth approximation that makes the control input continuous. Let

$$u = -k_s \phi(P_2, \sigma), \qquad \phi(P, \sigma) = \begin{cases} \frac{P_2\sigma}{\|P_2\sigma\|} & \text{if } \|P_2\sigma\| \neq 0, \\ 0 & \text{else,} \end{cases} \tag{2.117}$$

be a controller designed based on the unit vector approach, where $k_s > 0$ denotes some static controller gain, $\sigma \in \mathbb{R}^m$ is the sliding variable and $P_2 \in \mathbb{R}^{m \times m}$ is a symmetric positive definite matrix. Following (Edwards and Spurgeon, 1998, Chap. 3.7) a so-called smoothing boundary layer

$$\mathcal{B} = \left\{ x \in \mathbb{R}^n \colon \sigma(x)^T P_2 \sigma(x) < \frac{\delta^2}{2} \right\}, \tag{2.118}$$

with size $\delta > 0$ is introduced, where the sliding variable $\sigma(x)$ is naturally defined in terms of the states $x \in \mathbb{R}^n$. Within the layer the control input is scaled down linearly according to

$$u = -k_s \frac{P_2\sigma}{\delta}, \qquad \|P_2\sigma\| < \delta, \tag{2.119}$$

whereas the control input

$$u = -k_s \frac{P_2\sigma}{\|P_2\sigma\|}, \qquad \|P_2\sigma\| \geq \delta, \tag{2.120}$$

is applied as usual if the states are outside of the layer. From the approximation (2.119), (2.120) it follows that finite-time stability of σ can still be achieved but with respect to the domain $\mathcal{B}$ of the boundary layer. By scaling down the control input it is intended to avoid that the states cross the sliding surface which would induce a switch of the control input. A very similar approximation can be formulated for the relay SMC approach. For details see e. g. Slotine and Li (1991).

2.1.5 Higher Order Sliding Mode Control

The aforementioned unit vector and relay SMC approaches are first order sliding mode controllers. That means that the control input appears in the first time derivative of the sliding variable. For instance consider a nonlinear SISO system

$$\begin{aligned} \dot{x} &= f(x) + g(x)u, \\ y_r &= h(x), \end{aligned} \tag{2.121}$$

with $x \in \mathbb{R}^n$, $u \in \mathbb{R}$, $y_r \in \mathbb{R}$ and well defined relative degree two i. e. $r = 2$. Considering first order SMC design the sliding variable $\sigma \in \mathbb{R}$ is defined as

$$\sigma = \dot{e} + \lambda e, \qquad \lambda > 0, \tag{2.122}$$

according to (2.77), where $e = y_r - w$ denotes the tracking error with respect to reference w. As the system has relative degree two it follows that the input appears in the first time derivative of σ if σ is defined as in (2.122). By first order SMC design σ can be driven to zero in finite-time. It follows that the tracking error e converges asymptotically to zero as defined by the Hurwitz polynomial of (2.122). However, it would be more advanced to define a sliding variable according to

$$\sigma = e, \tag{2.123}$$

so that by enforcing $\sigma = 0$ convergence of the tracking error can even be achieved in finite-time. As the system has relative degree two it follows that the input appears in the second time derivative of σ if σ is defined as in (2.123). Derivating (2.123) two times with respect to time yields

$$\ddot{\sigma} = L_f^2 h(x) - \ddot{w} + L_g L_f h(x) u = \Psi(x, w) + \Gamma(x) u. \tag{2.124}$$

Assume the bounds

$$|\Psi(x, w)| \leq \Psi_M, \qquad 0 < \Gamma_m \leq \Gamma(x) \leq \Gamma_M, \tag{2.125}$$

to be finite. A control law that enforces $\sigma = 0$ and $\dot{\sigma} = 0$ in finite-time is called a second order sliding mode controller. As shown in Levant (2003) it is always possible to formulate a second order SMC based on (2.124). More generally, a controller that ensures $\sigma = \dot{\sigma} = \ddot{\sigma} = \cdots = \delta^{r-1}\sigma / \delta t^{r-1} = 0$ in finite-time is named r-th order sliding mode controller. Based on

$$\frac{\delta^r \sigma}{\delta t^r} = L_f^r h(x) - \frac{d^r w}{dt^r} + L_g L_f^{r-1} h(x) u = \Psi(x, w) + \Gamma(x) u, \tag{2.126}$$

with finite uncertainty bounds

$$|\Psi(x, w)| \leq \Psi_M, \qquad 0 < \Gamma_m \leq \Gamma(x) \leq \Gamma_M, \tag{2.127}$$

it is always possible to formulate a r-th order SMC. A framework to design generic r-th order SMCs for nonlinear input-affine SISO systems is proposed by Levant (2003). The controller has the form

$$u = -\alpha \times \operatorname{sgn}(\varphi_r(\sigma, \dot{\sigma}, \ldots, \delta^{r-1}\sigma / \delta t^{r-1}), \qquad \alpha > 0, \tag{2.128}$$

where φ_r is a function dependent on the order r of the SMC and the time derivatives of σ. Another framework for the design of generic r-th order SMCs has been derived by Dinuzzo and Ferrara (2009). The approach of Dinuzzo and Ferrara (2009) solves an optimization problem that guarantees minimization of the sliding variable in the reaching phase under the influence of worst case disturbances.

Following Levant (2003) higher order sliding mode control (HOSMC) can also be applied to attenuate chattering. For instance, assume σ should be driven to zero in finite-time based on (2.126). Consider (2.126) to be derivated $l \geq 1$ times with respect to time. Consequently, an $r + l$ order description

$$\frac{\delta^{r+l}\sigma}{\delta t^{r+l}} = \bar{\Psi}(x, u, w) + \Gamma(x)v, \qquad v = \frac{\delta^l u}{\delta t^l}, \tag{2.129}$$

with virtual control input v can be obtained, where $\bar{\Psi}(x, u, w)$ may depend on the time derivatives of u up to the order of $l - 1$. Assuming the uncertainty bounds

$$|\bar{\Psi}(x, u, w)| \leq \Psi_M, \qquad 0 < \Gamma_m \leq \Gamma(x) \leq \Gamma_M, \tag{2.130}$$

to be finite a SMC of order $r + l$ can be formulated according to

$$\frac{\delta^l u}{\delta t^l} = v = -\alpha \times \operatorname{sgn}(\varphi_{r+l}(\sigma, \dot{\sigma}, \ldots, \delta^{r+l-1}\sigma/\delta t^{r+l-1}), \qquad \alpha > 0. \tag{2.131}$$

Based on the virtual control input v the SMC (2.131) drives σ and its corresponding time derivatives to zero in finite-time. The right hand side of (2.131) is discontinuous and the differential equation has to be interpreted in the sense of Filippov. However, as the time-derivative $\delta^l u/\delta t^l$ is defined the input signal u obtained from (2.131) is time-continuous for $l = 1$ and even smooth for $l > 1$. This is in contrast to the discontinuous signal given by (2.128). Consequently, the chattering is attenuated.

A drawback of the family of HOSMCs proposed by Levant (2003) is that for a r-th order SMC all time derivatives of σ up to the order of $r - 1$ are required to be known. In theory these time derivatives can be exactly determined by an $(r - 1)$-th order sliding mode differentiator but only under the assumption that the measured signal is noise-free. Typically the noise is amplified with every increasing order of the time derivative which can have a negative effect on the performance of the applied controller. A framework for the design of generic r-th order sliding mode differentiators has also been proposed by Levant (2003).

A popular HOSMC is the so-called supertwisting approach proposed by Levant (1993). The supertwisting approach is a second order SMC developed based on a first order description

$$\dot{\sigma} = \Psi(x, w) + \Gamma(x)u, \qquad |\Psi(x, w)| \leq \Psi_M, \quad 0 < \Gamma_m \leq \Gamma(x) \leq \Gamma_M. \tag{2.132}$$

It generates a time-continuous control input

$$u = -\lambda|\sigma|^{1/2} \times \operatorname{sgn}(\sigma) + u_1, \qquad \lambda > 0, \tag{2.133}$$

$$\dot{u}_1 = -\alpha \times \operatorname{sgn}(\sigma), \qquad \alpha > 0, \tag{2.134}$$

with attenuated chattering. The design parameters λ and α have to be chosen sufficient large to achieve finite-time convergence of σ and $\dot{\sigma}$ (Shtessel *et al.*, 2014; Levant, 1993).

Although the supertwisting approach is a second order SMC it does not require any time-derivative of σ to be known. Like for the first order relay and unit vector SMC approaches the sliding variable σ of the supertwisting approach can be defined based on the polynomial

$$\sigma = (\frac{d}{dt} + \lambda)^{r-1} e, \qquad \lambda > 0, \tag{2.135}$$

which allows reference tracking of systems with any order of relative degree r. The advantage of applying the supertwisting method instead of the first order unit vector or relay approaches is that the chattering is reduced without any loss of the control accuracy.

2.1.6 Nonlinear Sliding Manifolds

Besides higher order SMCs conventional first order relay or unit vector SMC approaches can provide finite-time convergence of the tracking error as well if they are combined with a class of nonlinear sliding manifolds named terminal sliding modes (TSM). Instead of asymptotic convergence known from linear sliding modes the nonlinear TSMs provide finite-time convergence improving e. g. the tracking performance of the closed loop system. Terminal sliding modes were introduced by Venkataraman and Gulati (1992). In addition, the approach described by Zhihong *et al.* (1994) is also often cited as an initial contribution to the field of TSM control. In Yu and Zhihong (2002) a sliding manifold with a linear and a nonlinear term has been proposed. The new method is denoted as fast terminal sliding mode (FTSM) control approach. In comparison to the TSM the convergence rate of the FTSM is increased for large tracking errors. A brief introduction to FTSM control is given as follows using the reformulation of the sliding manifolds from Yu *et al.* (2005). A nonlinear input-affine SISO system

$$\dot{x} = f(x) + g(x)u, \tag{2.136}$$
$$y_r = h(x), \tag{2.137}$$

with states $x \in \mathbb{R}^n$, input $u \in \mathbb{R}$, and control variable $y_r \in \mathbb{R}$ is considered. The system is assumed to have a well-defined relative degree of two. According to Yu *et al.* (2005) a FTSM is defined as

$$\sigma = \dot{e} + \alpha e + \beta |e|^{\gamma} \mathrm{sgn}(e) = 0, \qquad \alpha > 0, \quad \beta > 0, \quad 0 < \gamma < 1, \tag{2.138}$$
$$e = y_r - w, \tag{2.139}$$

where e denotes the tracking error with respect to reference $w(t)$ and quantities α, β, γ are tuning parameters that affect the error convergence. As the system has relative degree two it follows that the input u appears in the first time derivative of σ given by

$$\dot{\sigma} = L_f^2 h(x) + L_g L_f h(x) u - \ddot{w} + \alpha \dot{e} + \gamma \beta \dot{e} |e|^{\gamma - 1} = \Psi(x, w) + \Gamma(x) u. \tag{2.140}$$

The uncertainty bounds

$$|\Psi(x, w)| \leq \Psi_M, \qquad 0 < \Gamma_m \leq \Gamma(x) \leq \Gamma_M, \tag{2.141}$$

are assumed to be finite. Based on (2.140) a first-order SMC can be design to drive σ to zero in finite-time. After the sliding manifold has been reached the dynamics induced by the FTSM lead to finite-time convergence of the tracking error. More specifically (2.138)

can be solved for e which does not require any interpretation in the sense of Fillipov as all terms are continuous. Let t_0 be the time instant at which the sliding manifold is reached i. e. $\sigma(t_0) = 0$ then the tracking error decreases as

$$-\frac{1}{\alpha(1-\gamma)}\left(\ln\left(\frac{\alpha|e(t)|^{1-\gamma}+\beta}{\beta}\right)-\ln\left(\frac{\alpha|e(t_0)|^{1-\gamma}+\beta}{\beta}\right)\right)=t-t_0=\tau, \tag{2.142}$$

over the time interval τ (Yu and Zhihong, 2002).

Originally, TSMs have been proposed for relative degree two systems. However, using a chain of interconnected TSMs as proposed by Yu and Zhihong (2002) it becomes possible to achieve finite-time convergence of the tracking error for any systems with relative degree r greater two. Following Yu and Zhihong (2002) the chain has to be selected as

$$\begin{aligned}
\sigma_0 &= \dot{e} + \alpha_0 e + \beta_0 |e|^{\gamma_0}, \\
\sigma_1 &= \dot{\sigma}_0 + \alpha_1 \sigma_0 + \beta_1 |\sigma_0|^{\gamma_1}, \\
\sigma_2 &= \dot{\sigma}_1 + \alpha_2 \sigma_1 + \beta_2 |\sigma_1|^{\gamma_2}, \\
&\vdots \\
\sigma_i &= \dot{\sigma}_{i-1} + \alpha_i \sigma_{i-1} + \beta_i |\sigma_{i-1}|^{\gamma_i},
\end{aligned} \tag{2.143}$$

with $i = r - 2$ and relative degree $r \geq 2$. The tuning parameters that affect the error convergence may be chosen as

$$0 < \alpha_j, \quad 0 < \beta_j, \quad \frac{r-j-1}{r-j} < \gamma_j < 1, \quad 0 \leq j \leq i. \tag{2.144}$$

The control law is designed based on a conventional first order SMC that drives σ_i to zero in finite-time. When the sliding mode $\sigma_i = 0$ is reached the remaining sliding variables σ_j with $0 \leq j \leq i-1$ decrease to zero successively. Finally, when $\sigma_0 = 0$ is achieved the tracking error is forced to decrease to zero in finite-time.

The TSM as well as the FTSM approach may lead to singularities. In particular, if in (2.140) the expressions $e = 0$ and $\dot{e} \neq 0$ are assumed to hold then $\dot{\sigma}$ is undefined and no control input can be determined. A terminal sliding mode control approach that avoids this singularities is the nonsingular terminal sliding mode control method of Feng *et al.* (2002).

2.1.7 Adaptive Sliding Mode Control

Typically, in the field of sliding mode control the uncertainty bounds of the system are assumed unknown but finite. In this case convergence of the sliding variable can be achieved by choosing the gain of the SMC sufficient large. The SMC gain is usually chosen conservatively meaning that the uncertainty bounds are overestimated. Consequently, the selected gain is too large in the sense that convergence could also be achieved by a smaller gain. In practice that makes a difference because the chattering effect associated with the larger gain is also larger. This motivates the idea of an adaptive controller gain being sufficient large to achieve convergence of the sliding variable but not too large. Following Utkin and Poznyak (2013*a*) the existing gain adaptation strategies can be divided into two main categories: sigma based adaptive sliding mode control approaches and equivalent control based adaptive sliding mode control approaches.

The first sigma based adaptive SMC approach was proposed by Huang *et al.* (2008). It is a first order relay control approach for input-affine nonlinear SISO systems that guarantees finite-time convergence of the sliding variable by adaptively increasing the controller gain. Consider the first order description

$$\dot{\sigma} = \Psi + \Gamma u, \tag{2.145}$$

with finite but unknown uncertainty bounds

$$|\Psi| \leq \Psi_M, \qquad 0 < \Gamma_m \leq |\Gamma| \leq \Gamma_M. \tag{2.146}$$

From first order SMC design it is known that finite-time convergence of σ can be achieved by a relay controller

$$u = -k \times \operatorname{sgn}(\sigma) \tag{2.147}$$

with a sufficient large gain i. e. $k > \Psi_M/\Gamma_m$. However, the uncertainty bounds are unknown and defining the gain based on trial and error may lead to too large controller gains. Instead Huang *et al.* (2008) proposes to adapt the gain according to

$$\dot{k} = -k_a|\sigma|, \qquad k_a > 0, \tag{2.148}$$

where k_a is user-defined. It can be proven that adapting the gain based on (2.148) guarantees finite-time convergence of σ. However, applying (2.148) can easily lead to too large controller gains because in the moment when $|\sigma|$ already decreases and the gain is sufficient large it is still increased. Another drawback is that the gain can never be decreased.

Two first order SMCs based on the sigma adaptation scheme have been proposed by Plestan *et al.* (2010). These controllers have the ability to reduce the controller gain. However, in the simulation results depicted in Plestan *et al.* (2010) a noticeable amount of chattering is still present. In Obeid *et al.* (2018) the sigma adaption scheme is applied to guarantee that the sliding variable converges to a domain specified by the user. Once the domain has been reached the SMC gain is adapted based on control barrier functions (CBF). The adaptation based on CBFs guarantees the sliding variable to remain bounded with respect to a specified tunable domain. The approach achieves enhanced chattering mitigation in comparison to the method of Plestan *et al.* (2010).

An adaptive SMC approach based on the equivalent control method has been proposed by Edwards and Shtessel (2016). It can be applied to nonlinear input-affine MIMO systems that have a first order description of the form

$$\dot{\sigma} = \Psi + \Gamma u, \tag{2.149}$$

with $\sigma \in \mathbb{R}^m$. It is required that $\Gamma = I_m$ holds which typically can only be achieved based on model knowledge of the considered system. The bounds

$$\|\Psi\| \leq \Psi_M, \qquad \|\dot{\Psi}\| \leq \dot{\Psi}_M, \tag{2.150}$$

are required to be finite but may be unknown. The main idea of the adaptive equivalent control based approaches is to first estimate the equivalent control input. The equivalent control input is the input that keeps the system in sliding mode. In sliding mode it is

$\sigma = 0$ and to keep the system in sliding mode $\dot{\sigma} = 0$ is required to hold. Consequently, the equivalent control input is

$$u_{eq} = -\Psi, \tag{2.151}$$

according to (2.149). However, Ψ is not known. But it is known that the unit vector approach

$$u = -(k(t) + \eta)\frac{\sigma}{\|\sigma\|}, \qquad k(t) > 0, \quad \eta > 0, \tag{2.152}$$

with sufficient large gain $(k(t) + \eta)$ keeps the system in sliding mode. Assume the system to be in sliding mode and the gain of the unit vector control law to be sufficient large to keep the system in there. Under this conditions an estimation $\hat{u}_{eq} \in \mathbb{R}^m$ of the equivalent control input can be obtained from a bank of low pass filters of the form

$$\tau_i \dot{\hat{u}}_{i,eq} + \hat{u}_{i,eq} = -(k(t) + \eta)\frac{\sigma_i}{\|\sigma\|}, \qquad 1 \leq i \leq m. \tag{2.153}$$

It is proven in Utkin (1992, Lemma of Chap. 2.4) that under the assumption that the system is in sliding mode the estimation error $|\hat{u}_{i,eq} - u_{i,eq}|$ can be made arbitrary small by choosing the time constant $\tau_i > 0$ sufficient small. Following Edwards and Shtessel (2016) safety margins are introduced to guarantee

$$\frac{1}{\alpha}\|\hat{u}_{eq}\| + \epsilon > \frac{1}{\alpha}\|\hat{u}_{eq}\| - \frac{\epsilon}{2} > \|u_{eq}\|, \tag{2.154}$$

to hold. The parameters $\alpha \in]0, 1[$ and $\epsilon > 0$ are user-defined. Based on (2.154) and the adaptive gain $k(t)$ the quantity

$$\delta(t) = k(t) - \frac{1}{\alpha}\|\hat{u}_{eq}(t)\| - \epsilon, \tag{2.155}$$

is introduced that indicates if the gain should be reduced or increased. Consequently, the gain is adapted according to

$$\dot{k}(t) = -\rho(t) \times \operatorname{sgn}(\delta(t)). \tag{2.156}$$

In (2.156) the gain $\rho(t) > 0$ is also adaptive and further specified in Edwards and Shtessel (2016). The approach proposed by Edwards and Shtessel (2016) guarantees that the adaptive gain is finite-time stable with respect to the domain

$$|k(t) - \frac{1}{\alpha}\|\hat{u}_{eq}(t)\|| \leq \frac{\epsilon}{2}. \tag{2.157}$$

It follows from (2.154) that

$$k(t) > \|u_{eq}\| = \|\Psi\|, \tag{2.158}$$

holds true. Consequently, the gain is larger than the uncertainty term and it is guaranteed that the sliding mode remains established by applying the unit vector control input (2.152). The adaptation law of Edwards and Shtessel (2016) can also be applied to tune the gain of the supertwisting approach as well as the gain of a family of higher order SMCs. However,

in these cases not all controller parameters can be tuned by adaptation. At least one gain parameter is still required to be selected by the user which can be chosen too large. Another first order adaptive SMC based on the equivalent control method is proposed by Utkin and Poznyak (2013*b*). The approach is applicable to nonlinear input-affine SISO systems. Prior to the application of the controller a minimal gain value has to be selected by the user. During the runtime of the controller the approach has the ability to reduce the controller gain to the predefined minimal value but only if for that gain value the sliding mode is still guaranteed to remain established. The approach requires knowledge about the uncertainty bounds. The proposed method is also applied to adapt the parameters of the supertwisting approach. Again the problem appears that only one controller parameter is adapted and another parameter is required to be selected sufficient large by the user.

Gain adaptation of the twisting and the supertwisting approach has been subject to several contributions in the past. For instance in Shtessel *et al.* (2012) a law for the adaptation of both controller gains of the supertwisting approach is proposed. It can be guaranteed that the sliding variable and its time derivative converge towards a domain after a finite-time. However, the bounds of this domain remain imprecise and are not known. In addition the gains are known to remain bounded but it is not clear if minimal values are achieved for them.

2.2 Sliding Mode Observation

Sliding mode controllers have been shown to provide strong robustness features making them attractive for the control of linear and nonlinear uncertain systems. However, some of the considered approaches directly depend on the system states and others may benefit from the knowledge of those states. For example, in the field of linear systems the sliding surface is typically designed within the state space. As a consequence, the sliding variable directly depends on the system states and the state stability may only be achieved based on the knowledge of those states. For the control of nonlinear systems knowledge of the systems states may also be advantageous. Partial or nominal knowledge about the input-output dynamics can help to reduce the uncertainty bounds. As a result, the required controller gains can be decreased so that the occurring chattering is less severe. However, to state some nominal input-output dynamics knowledge about the system states is required.

In the following sliding mode observer design concepts are presented. The review of the approaches can be divided into two main sections: methods applicable to linear systems and methods applicable to nonlinear systems.

2.2.1 Linear Systems

A linear time-invariant system

$$\dot{x} = Ax + Bu + M\xi, \tag{2.159}$$

$$y = Cx, \tag{2.160}$$

with unknown states $x \in \mathbb{R}^n$, unknown uncertainties $\xi \in \mathbb{R}^q$, known inputs $u \in \mathbb{R}^m$, and known measurements $y \in \mathbb{R}^p$ is considered. In the following, $\hat{x}$ denotes the estimation of state x and $\hat{y}$ denotes the estimation of the system outputs y. Further, the state estimation error is denoted by $\tilde{x} = \hat{x} - x$ and the output estimation error is denoted by $\tilde{y} = \hat{y} - y$.

Assume the matrix pair (A, C) to be observable and the uncertainty to be zero i. e. $\xi = 0$. According to Shtessel *et al.* (2014, Chap. 3.2) an observer

$$\dot{\hat{x}} = A\hat{x} + Bu + G\nu, \tag{2.161}$$

is considered, where $\nu \in \mathbb{R}^p$ defines a discontinuous feedback of the output estimation error according to

$$\nu_i = \rho \times \operatorname{sgn}(\tilde{y}_i), \qquad \tilde{y}_i = \hat{y}_i - y_i. \tag{2.162}$$

The switching gain $0 < \rho \in \mathbb{R}$ and the matrix G are design parameters. The observer stated in (2.161) is denoted as Utkin observer. Its structure is identical to that of the classical Luenberger observer except for the discontinuous feedback. Under the premise of observability and sufficient boundedness of the initial estimation error $\tilde{x}(t_0)$ as well as proper design of ρ and G it can be shown that the Utkin observer guarantees finite-time convergence of the output estimation error $\tilde{y}(t)$ and asymptotic convergence of the state estimation error $\tilde{x}(t)$. For the design procedure see e. g. Shtessel *et al.* (2014, Chap. 3.2).

According to Edwards and Spurgeon (1998, Chap. 6.2.4) the Walcott-Zak observer is introduced as follows. The Walcott-Zak observer is an estimation approach that can handle model uncertainty. Let the input shaping matrix M of system (2.159) be equal to B so that the uncertainty is matched. Furthermore, let $p \geq m$ hold for the number of measurements and inputs. Assume the matrix pair (A, C) to be observable and the matrices B and C to have full rank. In addition, let the uncertainty be bounded as

$$\|\xi\| \leq \xi_M. \tag{2.163}$$

The observer

$$\dot{\hat{x}} = A\hat{x} + Bu - G\tilde{y} + P^{-1}C^T F^T \nu, \tag{2.164}$$

with discontinuous feedback

$$\nu = \begin{cases} -\rho \frac{F\tilde{y}}{\|F\tilde{y}\|}, & \text{if } \|F\tilde{y}\| \neq 0, \\ 0, & \text{else}, \end{cases} \tag{2.165}$$

of the output estimation error $\tilde{y}$ is denoted as Walcott-Zak observer. The scalar $0 < \rho \in \mathbb{R}$ and matrices G, P, and F are design parameters. As the system is observable G can be designed so that $A_0 = A - GC$ has eigenvalues with real parts smaller zero. It follows that some symmetric $P \succ 0$ can be found from the Lyapunov equation

$$A_0 P + P A_0^T = -Q, \tag{2.166}$$

with $Q \succ 0$ being a symmetric design matrix. Related to P and F the constraint

$$C^T F^T = PB, \tag{2.167}$$

has to be achieved. The switching gain has to be chosen sufficient large i. e.

$$\rho \geq \xi_M + \eta, \tag{2.168}$$

with $0 < \eta \in \mathbb{R}$ being user-defined. Under the made assumptions it can be shown that the output estimation error $\tilde{y}$ converges to zero in finite-time and that the state estimation error $\tilde{x}$ is quadratically stable (Edwards and Spurgeon, 1998, Chap. 6.2.4). The Walcott-Zak observer is a robust estimation approach with strong finite-time convergence. However, it requires the constraint (2.167) to be satisfied which is nontrivial and restrictive.

A more generic and well-established observer for linear uncertain system has been developed by Edwards and Spurgeon (1994). In the following explanation is given according to Edwards and Spurgeon (1994), Edwards and Spurgeon (1998), and Edwards *et al.* (2000). For the dynamic system (2.159)–(2.160) assume M and C to have full rank and assume

$$q \leq p < n, \tag{2.169}$$

to hold. Let the uncertainty be unmatched but bounded according to

$$\|\xi\| \leq \xi_M. \tag{2.170}$$

Consider an observer of the form

$$\dot{\hat{x}} = A\hat{x} + Bu - G_l\tilde{y} + G_n\nu, \tag{2.171}$$

with

$$\nu = \begin{cases} -\rho\|M\|\frac{P_2\tilde{y}}{\|P_2\tilde{y}\|}, & \text{if } \|P_2\tilde{y}\| \neq 0, \\ 0, & \text{else,} \end{cases} \tag{2.172}$$

like the Walcott-Zak observer. It is proven in Edwards *et al.* (2000, Proposition 1) that an observer of the form (2.171)–(2.172) with converging state estimation error in presence of bounded disturbances ξ exists if and only if

$$\operatorname{rank}\{CM\} = q, \tag{2.173}$$

holds and the invariant zeros

$$\mathcal{Z}_0 = \Big\{ z_0 \in \mathbb{C} \mid \operatorname{rank}\{P(z_0)\} < \min\{n + \operatorname{rank}\{M\}, n + \operatorname{rank}\{C\}\} \Big\}, \tag{2.174}$$

defined by

$$P(z) = \begin{bmatrix} zI_n - A & -M \\ -C & 0 \end{bmatrix}, \tag{2.175}$$

are all on the negative conjugate complex plane i. e. $\mathcal{Z}_0 \subseteq \mathbb{C}_-$. In the following it is assumed that (2.173) and $\mathcal{Z}_0 \subseteq \mathbb{C}_-$ hold true. Under the made assumptions it can be guaranteed that a state transformation $x \to Tx$ exists which brings the observer (2.171)–(2.172) into a special canonical form. For the exact definition of T and how to achieve it numerically see e. g. Edwards and Spurgeon (1998, Chap. 6.3.1). Let

$$\bar{A} = TAT^{-1} = \begin{bmatrix} \bar{A}_{11} & \bar{A}_{12} \\ \bar{A}_{21} & \bar{A}_{22} \end{bmatrix}, \tag{2.176}$$

with $\bar{A}_{11} \in \mathbb{R}^{(n-p)\times(n-p)}$, $\bar{A}_{12} \in \mathbb{R}^{(n-p)\times p}$, $\bar{A}_{21} \in \mathbb{R}^{p\times(n-p)}$, $\bar{A}_{22} \in \mathbb{R}^{p\times p}$ be the transformed system matrix. Assume G_l and G_n to be defined by

$$G_l = T^{-1}\begin{bmatrix}\bar{A}_{12}\\ \bar{A}_{22}-\bar{A}_{s,22}\end{bmatrix}, \qquad G_n = T^{-1}\begin{bmatrix}0\\ I_p\end{bmatrix}, \tag{2.177}$$

where $\bar{A}_{s,22} \in \mathbb{R}^{p\times p}$ is any matrix whose eigenvalues have real parts smaller zero. Further, let P_2 be the solution of the Lyapunov equation

$$\bar{A}_{s,22}P_2 + P_2\bar{A}_{s,22}^T = -Q, \tag{2.178}$$

with symmetric $Q \succ 0$ being user-defined and let the switching gain be chosen sufficient large according to

$$\rho \geq \xi_M + \eta, \tag{2.179}$$

where $0 < \eta \in \mathbb{R}$ is user-defined. Then for the observer (2.171)-(2.172) it can be proven that the output estimation error $\tilde{y}$ is finite-time stable and the state estimation error $\tilde{x}$ converges quadratically (Edwards and Spurgeon, 1998, Proposition 6.1 and Corollary 6.1). The observer developed by Edwards and Spurgeon (1994) can also be applied to estimate the unknown uncertainties themselves. An estimation $\hat{\xi}$ of the uncertainties can be achieved by a smoothed version

$$\hat{\xi} = -\rho\|M\|(M^TM)^{-1}M^T\frac{P_2\tilde{y}}{\|P_2\tilde{y}\|+\delta}, \tag{2.180}$$

of the output error feedback ν, where $0 < \delta \in \mathbb{R}$ denotes a tuning parameter. It can be shown that $\hat{\xi} \to \xi$ holds by choosing δ arbitrary small i. e. $\delta \to 0$.

2.2.2 Nonlinear Systems

Sliding mode observers for different classes of nonlinear systems are discussed as follows.

Consider a nonlinear system

$$\frac{\delta^n x_1}{\delta t^n} = f(x,u), \tag{2.181}$$

in companion form which is characterized by the definition

$$x = \begin{bmatrix}x_1 & \delta x_1/\delta t & \delta^2 x_1/\delta t^2 & \dots & \delta^{n-1}x_1/\delta t^{n-1}\end{bmatrix}, \tag{2.182}$$

of the state vector $x \in \mathbb{R}^n$. The inputs $u \in \mathbb{R}^m$ as well as the states are assumed unknown except for the first state which is assumed to be measured according to

$$y = x_1. \tag{2.183}$$

Due to the definition of the vector (2.182) the state estimation problem is in fact a differentiation problem. Consequently, a higher order sliding mode differentiator (HOSMD) can be applied to solve the problem. The differentiation approach proposed by Levant (2003) will be considered as follows. A suitable parameter tuning of the differentiator is

further described in Levant (2009). For system (2.181) it is assumed that $f\colon \mathbb{R}^n \times \mathbb{R}^m \to \mathbb{R}$ is unknown but has a known Lipschitz constant $L > 0$ i. e.

$$\forall t_1, t_2\colon |f(t_2) - f(t_1)| \leq L|t_2 - t_1|. \tag{2.184}$$

Then differentiation can be achieved according to

$$\dot{z}_0 = -\lambda_n L^{1/(n+1)} |z_0 - y|^{n/(n+1)} \operatorname{sgn}(z_0 - y) + z_1, \tag{2.185}$$
$$\dot{z}_1 = -\lambda_{n-1} L^{1/n} |z_1 - \dot{z}_0|^{(n-1)/n} \operatorname{sgn}(z_1 - \dot{z}_0) + z_2, \tag{2.186}$$
$$\vdots$$
$$\dot{z}_{n-1} = -\lambda_1 L^{1/2} |z_{n-1} - \dot{z}_{n-2}|^{1/2} \operatorname{sgn}(z_{n-1} - \dot{z}_{n-2}) + z_n, \tag{2.187}$$
$$\dot{z}_n = -\lambda_0 L \operatorname{sgn}(z_n - \dot{z}_{n-1}), \tag{2.188}$$

where z_i converges to $\delta^i x_1 / \delta t^i$ in finite-time if the parameters $0 < \lambda_i \in \mathbb{R}$ are suitably chosen. The parameters can be selected iteratively. Starting with $n = 1$ the parameters λ_0 and λ_1 are tuned then for $n = 2$ the parameters λ_0, λ_1 remain unchanged while λ_2 has to be selected sufficient large. In the next step λ_0, λ_1, λ_2 remain unchanged and λ_3 is selected sufficient large. The procedure is repeated up to the desired value of n. A suitable choice of parameters guaranteeing convergence always exists.

Sliding mode differentiators can also be applied to a wider class of nonlinear systems. Consider a nonlinear input-affine system

$$\dot{x} = f(x) + g(x)u, \tag{2.189}$$
$$y_r = h(x), \tag{2.190}$$

with states $x \in \mathbb{R}^n$, input $u \in \mathbb{R}$, and control variable $y_r \in \mathbb{R}$. Assume the system to have relative degree $r = n$. Then $\Phi\colon x \to \zeta$ with

$$\zeta = \begin{bmatrix} \zeta_1 \\ \zeta_2 \\ \vdots \\ \zeta_n \end{bmatrix} = \begin{bmatrix} h(x) \\ L_f h(x) \\ \vdots \\ L_f^{n-1} h(x) \end{bmatrix}, \tag{2.191}$$

defines a diffeomorphism (Isidori *et al.*, 1995, Proposition 4.1.3). In the new coordinates the system is in companion form with dynamics

$$\frac{\delta^n \zeta_1}{\delta t^n} = a(\zeta) + b(\zeta)u, \tag{2.192}$$

where

$$y = \zeta_1, \tag{2.193}$$

is assumed to be measured. The companion form is achieved as $r = n$ holds from which follows that no internal dynamics exist. Consequently, all transformed states ζ can be estimated by a sliding mode differentiator.

In the following a sliding mode observer for nonlinear systems in so-called triangular

input form is considered. The observer has originally been proposed by Barbot *et al.* (1996). The given explanation refers to Barbot *et al.* (2002, Chap. 4). Consider a nonlinear system

$$\dot{x} = f(x) + g(x,u), \tag{2.194}$$
$$y_r = h(x), \tag{2.195}$$

with states $x \in \mathbb{R}^n$, input $u \in \mathbb{R}$, and control variable $y_r \in \mathbb{R}$. The system is required to be input-to-state stable in finite-time, which is described as that the state cannot grow unbounded in finite-time if u is bounded. It is assumed that $g(x,0) = 0$ holds for all $x \in \mathbb{R}^n$. Let $\Phi\colon x \to \zeta$ with

$$\zeta = \begin{bmatrix} \zeta_1 \\ \zeta_2 \\ \vdots \\ \zeta_n \end{bmatrix} = \begin{bmatrix} h(x) \\ L_f h(x) \\ \vdots \\ L_f^{n-1} h(x) \end{bmatrix}, \tag{2.196}$$

define a state transformation. The Jacobian

$$\begin{bmatrix} \frac{\partial \zeta_1}{\partial x_1} & \frac{\partial \zeta_1}{\partial x_2} & \cdots & \frac{\partial \zeta_1}{\partial x_n} \\ \frac{\partial \zeta_2}{\partial x_1} & \frac{\partial \zeta_2}{\partial x_2} & \cdots & \frac{\partial \zeta_2}{\partial x_n} \\ \vdots & \vdots & \ddots & \vdots \\ \frac{\partial \zeta_n}{\partial x_1} & \frac{\partial \zeta_n}{\partial x_2} & \cdots & \frac{\partial \zeta_n}{\partial x_n} \end{bmatrix}, \tag{2.197}$$

is assumed nonsingular so that Φ is a diffeomorphism. The resulting dynamics are

$$\begin{bmatrix} \dot{\zeta}_1 \\ \dot{\zeta}_2 \\ \vdots \\ \dot{\zeta}_{n-1} \\ \dot{\zeta}_n \end{bmatrix} = \begin{bmatrix} \zeta_2 + b_1(\zeta,u) \\ \zeta_3 + b_2(\zeta,u) \\ \vdots \\ \zeta_n + b_{n-1}(\zeta,u) \\ a(\zeta) + b_n(\zeta,u) \end{bmatrix}, \tag{2.198}$$

with

$$a(\zeta,u) = L_f^n h(x), \qquad b_i(\zeta,u) = \frac{\partial L_f^{i-1} h(x)}{\partial x} g(x,u). \tag{2.199}$$

Further, it is required to assume that b_i only depends on u and $\zeta_1, \zeta_2, \ldots \zeta_i$ so that (2.198) can be written in so-called triangular input form

$$\begin{bmatrix} \dot{\zeta}_1 \\ \dot{\zeta}_2 \\ \vdots \\ \dot{\zeta}_{n-1} \\ \dot{\zeta}_n \end{bmatrix} = \begin{bmatrix} \zeta_2 + b_1(\zeta_1,u) \\ \zeta_3 + b_2(\zeta_1,\zeta_2,u) \\ \vdots \\ \zeta_n + b_{n-1}(\zeta_1,\zeta_2,\ldots,\zeta_{n-1},u) \\ a(\zeta) + b_n(\zeta,u) \end{bmatrix}, \tag{2.200}$$

where

$$y = \zeta_1, \tag{2.201}$$

is assumed to be measured to achieve estimation of state ζ. The sliding mode observer

$$\begin{bmatrix} \dot{\hat{\zeta}}_1 \\ \dot{\hat{\zeta}}_2 \\ \vdots \\ \dot{\hat{\zeta}}_{n-1} \\ \dot{\hat{\zeta}}_n \end{bmatrix} = \begin{bmatrix} \hat{\zeta}_2 + b_1(y,u) + \lambda_1 \mathrm{sgn}(y - \hat{\zeta}_1) \\ \hat{\zeta}_3 + b_2(y, \tilde{\zeta}_2, u) + \lambda_2 \mathrm{sgn}(\tilde{\zeta}_2 - \hat{\zeta}_2) \\ \vdots \\ \hat{\zeta}_n + b_{n-1}(y, \tilde{\zeta}_2, \ldots, \tilde{\zeta}_{n-1}, u) + \lambda_{n-1} \mathrm{sgn}(\tilde{\zeta}_{n-1} - \hat{\zeta}_{n-1}) \\ a(y, \tilde{\zeta}_2, \ldots, \tilde{\zeta}_n) + b_n(y, \tilde{\zeta}_2, \ldots, \tilde{\zeta}_n, u) + \lambda_n \mathrm{sgn}(\tilde{\zeta}_n - \hat{\zeta}_n) \end{bmatrix}, \tag{2.202}$$

with

$$\tilde{\zeta}_2 = \hat{\zeta}_2 + \lambda_1 \mathrm{sgn}(y - \hat{\zeta}_1), \tag{2.203}$$

$$\tilde{\zeta}_3 = \hat{\zeta}_3 + \lambda_2 \mathrm{sgn}(\tilde{\zeta}_2 - \hat{\zeta}_2), \tag{2.204}$$

$$\vdots$$

$$\tilde{\zeta}_n = \hat{\zeta}_n + \lambda_n \mathrm{sgn}(\tilde{\zeta}_{n-1} - \hat{\zeta}_{n-1}), \tag{2.205}$$

is proposed by Barbot *et al.* (1996). Under the made assumptions it can be guaranteed that a set of tuning parameters $0 < \lambda_i \in \mathbb{R}$ exists for which $\hat{\zeta}_i$ converges to ζ_i in finite-time (Barbot *et al.*, 2002, Theorem 50). Although the observer cannot handle model uncertainty it has the advantage that it only requires the first state to be measured which is also derivative-free.

2.3 Summary

In this chapter the basics of sliding mode control and sliding mode observation are introduced. With regards to sliding mode control definitions and explanations about the reaching and sliding phase are given. The design of sliding surfaces as well as control laws is considered. At the moment when the states reach the sliding surface the system is said to be in sliding mode. The dynamics in sliding mode are named the sliding dynamics. The sliding dynamics are of reduced order and are defined based on the design of the sliding surface. For linear MIMO systems well-known methods such as pole placement can be applied to design the sliding surface. This allows to achieve asymptotic convergence of the states if the underlying system is controllable. To achieve reference tracking an augmented system description with an integral state can be considered. For nonlinear MIMO systems a state transformation based on the vector of relative degree can be applied. The transformation serves as a basis to design the sliding surface to achieve either state stabilization or reference tracking. For linear as well as nonlinear systems the sliding dynamics are shown to be unaffected by matched uncertainties. This invariance is a strong property of sliding mode control and leads to its great robustness. The unit-vector and relay control approaches are introduced which guarantee that the sliding surface is reached in finite-time. The concept of integral sliding mode control allows to eliminate the reaching phase so that the states are on the sliding surface from the beginning. Furthermore, integral SMC provides a framework to combine sliding mode controllers with other control methods such as state feedback, MPC, etc. Chattering is introduced as an undesired effect resulting from the discontinuous switching of conventional first order sliding mode controllers. A boundary layer based approximation technique is presented which provides a trade-off between control accuracy and chattering mitigation. The concept of higher order sliding mode control

is introduced to design control laws that are continuous in time so that the chattering is highly attenuated. Higher order SMCs also give the possibility to achieve finite-time stabilization of systems with relative degree greater one. Similarly, finite-time convergence of the tracking error can be guaranteed. Nonlinear sliding manifolds have been presented with their ability to improve the closed loop behavior so that faster error convergence and stabilization can be achieved. The interconnection of nonlinear sliding manifolds allows finite-time convergence of systems with relative degree greater one even if conventional first order SMCs are applied. Adaptive SMC approaches are introduced with their ability to reduce the chattering. Sliding mode-based observation of linear and nonlinear systems is considered. The observers are typically designed based on a discontinuous feedback of the output estimation error. For linear systems general methods exist to estimate the state in presence of uncertainties. However, requirements related to e. g. invariant zeros have to be satisfied. Besides the states also the uncertainties themselves can be estimated which is denoted as unknown input estimation. States of nonlinear systems in companion form can be observed using sliding mode differentiators. These estimators only require Lipschitz continuity but not any model knowledge.

3 Combined Smooth Variable Structure and Kalman Filter Estimation Approach

State estimation plays an important role in the field of control. System states are required to be known for the calculation of commonly used controllers such as state feedback, exact input-output linearization approaches, equivalent control methods, or backstepping control approaches. Noise reduction of measured signals is desirable to improve the performance of controllers under real conditions. Unknown input estimation is beneficial for the rejection of disturbances that may affect the system behavior. In addition, model-based filtering approaches are useful for system monitoring in order to detect and localize faults.

As discussed in Section 2.2 sliding mode observers can be applied to achieve both state as well as unknown input estimation. However, SMO approaches are typically formulated with respect to deterministic systems. Measurement and process noise are not considered in the design process. High switching gains generally have a negative impact on the noise sensitivity of sliding mode differentiators (Levant and Yu, 2018; Levant, 2003). However, higher gains are required to achieve error convergence of the differentiator if noise with high amplitudes is present or if the Lipschitz constant of the underlying signal is large. Related to stochastic systems a relatively large variety of estimation approaches exists. Unknown input estimation approaches for linear systems may be divided into two main categories: the minimum variance unbiased and the augmented state Kalman filtering approaches. Minimum variance unbiased filtering approaches (Kitanidis, 1987; Gillijns and De Moor, 2007) are characterized by the fact that the dynamics of the unknown input is not modeled. Instead the unknown input is directly estimated from the innovation process of the filter. In the field of augmented state filtering (Anderson and Moore, 1979; Hmida *et al.*, 2012) the dynamics of the unknown input is assumed as piece-wise constant and integrated into the system description. Standard Kalman filtering is applied to estimate the augmented state including the unknown input. In Ding *et al.* (2020) it has been recently proven that minimum variance unbiased filtering is actually a special case of augmented state Kalman filtering. Apart from unknown input estimation approaches several other robust filtering methods exist. In case of known uncertainty bounds a so-called robust Kalman filter (Dong and You, 2006) can be applied to estimate the states of a linear uncertain system. In the field of H_∞ filtering robustness is achieved by minimizing the effect of the worst possible disturbance on the estimation error (Hassibi *et al.*, 1999). Multiple-model approaches (Blom and Bar-Shalom, 1988) are a powerful tool for state estimation of uncertain systems as well. In combination with particle filters the multiple model approach can also be applied to nonlinear systems (Martino *et al.*, 2017).

The smooth variable structure filter (SVSF) introduced in Habibi (2007) is claimed to be a robust estimation approach for the state estimation of uncertain nonlinear systems. It is formulated in discrete-time domain and explicitly considers measurement noise. The

SVSF follows the predictor-corrector scheme of the Kalman filter but also shows elements that are typical for sliding mode observers and sliding mode control. For instance, the SVSF discontinuously feds back the output estimation error which is common for sliding mode observers. In addition, the smoothing boundary layer concept is applied to the SVSF but not to mitigate the chattering rather to mitigate the negative impact of the measurement noise on the estimation performance of the filter.

In the following the working principle of the SVSF approach is explained in accordance to Habibi (2007). Based on the discontinuous feedback of the output error the estimated state trajectory is driven into a region around the true state trajectory called existence subspace. Due to measurement noise which is typically assumed to be white the estimated state trajectory shows a zigzag like motion characterized by high frequent switches when it reaches the existence subspace. This behavior of high frequent switches induced by noise is denoted as chattering although it differs from chattering known in the field of SMC. The chattering may be attenuated by introducing a smoothing boundary layer in which the hard switching of the filter gain is approximated by a saturation function. This may lead to improved estimation performance of the filter but depends on the selected width of the introduced boundary layer.

A serious limitation of the SVSF approach is that all system states have to be measured and the measurement model is required to be linear. However, at least in the field of object tracking it is possible to bypass the limitation. Although nonlinear measurement models are common in tracking a linear measurement model can be achieved by applying a measurement conversion (see e. g. Longbin *et al.*, 1998) and measurements of the object velocities can also be derived from the measured positions. An advantage of the SVSF approach is that neither measurement noise nor process noise covariances are required to be known. But as already mentioned the performance of the SVSF approach depends on the width of the introduced smoothing boundary layer. This width is a tuning parameter and has to be selected by the user. In Gadsden and Habibi (2010); Gadsden *et al.* (2011*b*) an optimization of the smoothing boundary layer width is considered. First, an estimation error model for the SVSF has been proposed in Gadsden and Habibi (2010) and later in Gadsden *et al.* (2011*b*) this error model is applied to minimized the estimation error with respect to the boundary layer width. As a consequence, optimal values for the tuning parameters are achieved in theory. However, the derived estimation error model is equivalent to the one of the Kalman filter. It is therefore only applicable to linear systems and requires exact model knowledge including a precise descriptions of the system dynamics and the noise covariances. This clearly contradicts the claim of the SVSF to be a robust estimation approach for nonlinear uncertain systems. Nevertheless, at least a maximum a posteriori estimation of the noise covariances can be obtained and is discussed in Tian *et al.* (2019). The requirement of the system dynamics to be precisely known and linear remains.

Combinations of the SVSF with the extended Kalman filter, the unscented Kalman filter, the cubature Kalman filter, and the particle filter have been studied in Al-Shabi *et al.* (2013); Gadsden *et al.* (2011*a*, 2014*a*). To combine the SVSF with the aforementioned filters the uncertainty of the system is estimated online based on a calculation of an optimal smoothing boundary layer width. In case of a large width (large uncertainty) the SVSF is applied to achieve robustness whereas in case of a small width (small uncertainty) the Kalman filtering approaches are applied to minimize the mean squared estimation error (MSE). However, the formulated combination of the SVSF approach and the Kalman

filter cannot be considered to be consistent. If the Kalman filter gain is applied at the moment when the model uncertainty is sufficient small then the calculated gain may still be erroneous. The reason for the erroneousness is that the Kalman filter gain requires knowledge of the error covariance which has to be updated at each time step. Assume the model to be imprecise. Then the error covariance will be updated incorrectly. If later the model becomes more precise and the Kalman filter gain is applied the gain may still be far away from being optimal as the error covariance has been update incorrectly in the previous time steps.

Further optimizations of the SVSF are studied in the literature. A SVSF that in addition to the states also estimates modeling errors is proposed in Cao *et al.* (2017). In Spiller *et al.* (2018) the SVSF gain is replaced by an adaptive gain with the goal to minimize the MSE and to guarantee boundedness of the estimation error.

Several applications of the SVSF approach can be found in the literature. The filter has been applied to estimate the states and parameters of an uncertain linear hydraulic system in Habibi (2007). A multiple-model approach has been formulated for fault detection e. g. to detect leakage of a hydraulic system (Gadsden *et al.*, 2013). The state of charge and state of health of batteries is estimated in Kim *et al.* (2015) and Afshari *et al.* (2018). A multiple-model approach has been applied for target tracking in Gadsden *et al.* (2010) and a SVSF based probabilistic data association (PDA) approach has been proposed for tracking in cluttered environment (Attari *et al.*, 2013). For multiple object tracking a SVSF based joint-PDA approach has been developed by Attari *et al.* (2015). Online multiple vehicle tracking on real road scenarios has been investigated in Luo *et al.* (2019). Several SVSF based simultaneous localization and mapping algorithms have been proposed e. g. Demim *et al.* (2016), Allam *et al.* (2017), Liu and Wang (2018). Training of neural networks based on the SVSF approach has been studied in Ahmed *et al.* (2011) with the goal to classify engine faults. Dual estimation of states and model parameters has been considered in Al-Shabi and Habibi (2011) based on a combination of the bi-section method and the SVSF. The attitudes of satellites are synchronized based on the SVSF approach in Cao *et al.* (2017).

In this chapter a combination of the SVSF and the Kalman filter is proposed to improve the estimation performance with respect to the original SVSF algorithm. First, a reformulation of the SVSF is derived from which unique features of the filter are identified. A new gain for the SVSF is proposed to achieve minimization of the MSE as well as robustness with respect to modeling errors. It is shown that if the new gain is applied to the SVSF then the obtained algorithm equals the one of the extended Kalman filter. A combined estimation approach is formulated that makes use of the original SVSF gain as well as the Kalman filter gain. A training scheme is developed to optimize the tuning parameters of the proposed filter. The optimized parameters provide insights on what contributes to the robustness of the proposed new filter: the SVSF gain, the Kalman filter gain, or the combination of both.

Some of the results presented in this chapter are preliminary discussed in Spiller and Söffker (2020*a*). This includes the proposed scheme for the optimization of the filter parameters and the theoretical analysis that establishes the link between the SVSF and the Kalman filter algorithm.

The chapter is structured as follows. In Section 3.1 the SVSF algorithm and its properties are studied. A reformulation of the SVSF is stated which facilitates the analysis of the filter. In Section 3.2 the SVSF gain is replaced by a new deterministic gain with the

goal to minimize the MSE. Based on the derived gain a direct link to the Kalman filter is drawn. The combination of the SVSF and the Kalman filter is proposed in Section 3.3. The scheme that is used for the tuning of the filter parameters is described in Section 3.4. The estimation performance of the SVSF in comparison to the novel combined filtering approach is studied in Section 3.5. The chapter is summarized in Section 3.6.

3.1 Smooth Variable Structure Filter

Let the dynamics of a nonlinear system be described by the discrete-time model

$$x_{k+1} = f_k(x_k, u_k), \tag{3.1}$$

$$y_k = x_k + r_k, \tag{3.2}$$

with states $x_k \in \mathbb{R}^n$, inputs $u_k \in \mathbb{R}^m$, and measurements $y_k \in \mathbb{R}^n$. Quantity r_k denotes the measurement noise which is assumed to be white. The measurement model (3.2) is introduced for notational convenience. It can always be obtained from the more general model

$$\bar{y}_k = Hx_k + \bar{r}_k, \tag{3.3}$$

with $\bar{y}_k, \bar{r}_k \in \mathbb{R}^n$ and $H \in \mathbb{R}^{n\times n}$ as the SVSF approach requires H to be invertible. The SVSF is derived in Habibi (2007). Although the requirement of H to be invertible is not explicitly stated in Habibi (2007) it is in fact necessary because otherwise the filters corrective switching term (Habibi, 2007, eq. (27)) may not satisfy the stability theorem that guarantees boundedness of the estimation error (Habibi, 2007, Theorem 1). From the full rank condition of H it follows that full state measurements are required which is the major limitation of the SVSF approach.

Consider $\breve{f}_k(\cdot)$ to be a nominal possibly imprecise description of the true system dynamics $f_k(\cdot)$. According to Habibi (2007) an estimation $\hat{x}_k$ of the system states x_k can be obtained based on the following filter algorithm

$$\tilde{y}_k = y_k - \hat{x}_k, \tag{3.4}$$

$$\hat{x}_{k+1|k} = \breve{f}_k(\hat{x}_k, u_k), \tag{3.5}$$

$$\tilde{y}_{k+1|k} = y_{k+1} - \hat{x}_{k+1|k}, \tag{3.6}$$

$$\Lambda_{k+1} = (|\tilde{y}_{k+1|k}| + \Phi|\tilde{y}_k|) \circ \operatorname{sgn}(\tilde{y}_{k+1|k}), \tag{3.7}$$

$$\hat{x}_{k+1} = \hat{x}_{k+1|k} + \Lambda_{k+1}, \tag{3.8}$$

where Λ_{k+1} is a corrective switching term. The diagonal matrix

$$\Phi = \operatorname{diag}\left\{\begin{bmatrix}\phi_1 & \phi_2 & \dots & \phi_n\end{bmatrix}^T\right\} \in \mathbb{R}^{n\times n}, \tag{3.9}$$

is defined by the filter parameters $0 \leq \phi_i < 1$ and is denoted as convergence rate. In Habibi (2007, Theorem 1) and more specifically in Habibi (2007, eq. (30)) it is shown that algorithm (3.4)–(3.8) guarantees asymptotic stability of the output estimation error $\tilde{y}_{k+1}$. The output error dynamics are given by

$$|\tilde{y}_{i,k+1}| = \phi_i|\tilde{y}_{i,k}|, \tag{3.10}$$

where $\tilde{y}_{i,k+1}$ denotes the i-th element of vector $\tilde{y}_{k+1}$ and $0 \leq \phi_i < 1$ is the eigenvalue making the dynamics asymptotically stable. As the output error converges to zero the statement

$$\lim_{k\to\infty} \hat{x}_k \to \lim_{k\to\infty} y_k, \tag{3.11}$$

holds true for the state estimations. If the measurement noise is bounded then (3.11) guarantees the estimation error to be bounded too. This error boundedness can even be achieved in presence of model uncertainties. However, from (3.11) it follows that it is unnecessary to apply the filter at all because the state estimations converge to the measurements and the measurements are all given. Consequently, the filter is useless.

The algorithm (3.4)–(3.8) generates a switching effect which is induced by noise and model uncertainty. When the a posteriori output error $\tilde{y}_{k+1}$ becomes close to zero the switching term Λ_{k+1} of (3.7) not necessarily converges to zero. The a priori output error $\tilde{y}_{k+1|k}$ that affects the switching gain may still significantly deviate from zero due to the measurement noise and the model uncertainty of $\breve{f}_k(\cdot)$. Because of the high frequent switching of the white noise a high frequent switching of the gain Λ_{k+1} may be induced to push the sliding variable $\tilde{y}_{k+1}$ in direction of the sliding surface $\tilde{y}_{k+1} = 0$. This effect is denoted as chattering in Habibi (2007) and it is suggested to apply the smoothing boundary layer concept known from SMC for its mitigation. Therefore, Habibi (2007) proposes to modify algorithm (3.4)–(3.8) as follows

$$\tilde{y}_k = y_k - \hat{x}_k, \tag{3.12}$$

$$\hat{x}_{k+1|k} = \breve{f}_k(\hat{x}_k, u_k), \tag{3.13}$$

$$\tilde{y}_{k+1|k} = y_{k+1} - \hat{x}_{k+1|k}, \tag{3.14}$$

$$\bar{\Lambda}_{k+1} = (|\tilde{y}_{k+1|k}| + \Phi|\tilde{y}_k|) \circ \mathrm{sat}(\Psi^{-1}\tilde{y}_{k+1|k}), \tag{3.15}$$

$$\hat{x}_{k+1} = \hat{x}_{k+1|k} + \bar{\Lambda}_{k+1}, \tag{3.16}$$

where $\mathrm{sat}(\cdot)$ is a smooth approximation of the switching function $\mathrm{sgn}(\cdot)$. The diagonal matrix Ψ is define as

$$\Psi = \mathrm{diag}\left\{\begin{bmatrix}\psi_1 & \psi_2 & \dots & \psi_n\end{bmatrix}^T\right\} \in \mathbb{R}^{n\times n}, \tag{3.17}$$

based on the smoothing boundary layer width $\psi_i > 0 \in \mathbb{R}$. Let $\tilde{y}_{i,k+1|k}$ denote the i-th element of vector $\tilde{y}_{k+1|k}$. The saturation function $\mathrm{sat}(\cdot)$ is defined according to

$$\mathrm{sat}(\Psi^{-1}\tilde{y}_{k+1|k}) = \begin{bmatrix} \varphi\left(\frac{\tilde{y}_{1,k+1|k}}{\psi_1}\right) \\ \varphi\left(\frac{\tilde{y}_{2,k+1|k}}{\psi_2}\right) \\ \vdots \\ \varphi\left(\frac{\tilde{y}_{n,k+1|k}}{\psi_n}\right) \end{bmatrix}, \qquad \varphi\left(\frac{a}{b}\right) = \begin{cases} 1 & \text{for } \frac{a}{b} > 1, \\ -1 & \text{for } \frac{a}{b} < -1, \\ \frac{a}{b} & \text{for } |\frac{a}{b}| \leq 1, \end{cases} \tag{3.18}$$

as it is known from the smoothing boundary layer concept of SMC. The introduced algorithm (3.12)–(3.16) is called the smooth variable structure filter. As the SVSF approximates the switching function by a saturation function asymptotic convergence of $|\tilde{y}_k|$

cannot be guaranteed anymore. This is to some extend desired as a zero output estimation error leads to estimations of the form $\hat{x}_k = y_k = x_k + r_k$ which deviate from the true states by the value of the measurement noise. However, it remains unclear how to select the boundary layer width to achieve mitigation of the noise so that the estimation performance is improved. In Habibi (2007) it is argued that the width ψ_i should be bounded from below. The width should exceed a threshold value which is defined by the assumed uncertainty of the model and the maximum amplitude of the noise (Habibi, 2007, eq. (33)). An upper bound of ψ_i is not considered in Habibi (2007). Nevertheless, assume $\psi_i \to \infty$ to hold for all $i \in \{1, \dots, n\}$. In this case $\bar{\Lambda}_k \to 0$ holds which can be seen from (3.15) and (3.18). For $\Lambda_k \to 0$ the filter ignores the measurements i. e. $\hat{x}_{k+1} \to \hat{x}_{k+1|k}$ (cf. (3.13), (3.16)). This may easily lead to unstable error dynamics due to the model uncertainty. In several papers e. g. Luo *et al.* (2019); Afshari *et al.* (2018); Ahmed *et al.* (2016) the SVSF parameters are tuned by trial and error using the root mean squared error (RMSE) of the true states. This tuning strategy appears to be unrealistic as the true states are not available in practice. To optimize the filter parameters the error covariance of the SVSF has been derived in (Gadsden and Habibi, 2010; Gadsden *et al.*, 2011*b*). The idea is to model the MSE of the SVSF and to propagate the error covariance similarly to the Kalman filter. The optimal tuning parameters of the SVSF are those ones that minimize the MSE. This optimized parameters are part of a couple of contributions (e. g. Gadsden *et al.*, 2011*a*, 2013, 2014*a*,*b*). But, as already mentioned in the introductory part of this chapter there are problems related to the error covariance derivation of the SVSF. Propagating the error covariance requires linearity of the system and exact model knowledge which contradicts the claim of the SVSF to be a robust estimation approach for nonlinear systems.

In the following the effect of the boundary layer width on the behavior of the SVSF is studied. Therefore a reformulation of the SVSF is stated in Theorem 1. The reformulation is originally derived in Spiller *et al.* (2018).

Theorem 1 (Reformulation of SVSF algorithm)**.**
Assume the convergence rate of the SVSF to be zero i. e. $\Phi = 0_{n\times n}$ *and the initial estimation to be* $\hat{x}_0 \in \mathbb{R}^n$*. Consider the following algorithm*

$$\hat{x}_{RF,k+1|k} = \breve{f}_k(\hat{x}_{RF,k}, u_k), \tag{3.19}$$

$$\tilde{y}_{RF,k+1|k} = y_{k+1} - \hat{x}_{RF,k+1|k}, \tag{3.20}$$

$$\hat{x}_{RF,k+1} = y_{k+1} - \tilde{\Lambda}_{k+1}\tilde{y}_{RF,k+1|k}, \tag{3.21}$$

$$\tilde{\Lambda}_{k+1} = \operatorname{diag}\left\{\mathbf{1}_n - \left|\operatorname{sat}(\Psi^{-1}\tilde{y}_{RF,k+1|k})\right|\right\}, \tag{3.22}$$

with initial estimation $\hat{x}_{RF,0} = \hat{x}_0$*. For identical inputs* $\mathcal{U}_k = \{u_0, u_1, \dots, u_k\}$ *and measurements* $\mathcal{Y}_k = \{y_0, y_1, \dots, y_k\}$ *the estimations of the SVSF and its reformulation (3.19)–(3.22) are identical i. e.* $\hat{x}_{k|k-1} = \hat{x}_{RF,k|k-1}$ *and* $\hat{x}_k = \hat{x}_{RF,k}$*.*

Proof. For $\Phi = 0$ the switching term (3.15) can be written as

$$\bar{\Lambda}_{k+1} = \operatorname{sat}(\Psi^{-1}\tilde{y}_{k+1|k}) \circ |\tilde{y}_{k+1|k}|. \tag{3.23}$$

It follows

$$\hat{x}_{k+1} = y_{k+1} - \tilde{y}_{k+1|k} + \operatorname{sat}(\Psi^{-1}\tilde{y}_{k+1|k}) \circ |\tilde{y}_{k+1|k}|, \tag{3.24}$$

for the a posteriori estimation (3.16). Let $\tilde{y}_{i,k+1|k}$ be the i-th element of $\tilde{y}_{k+1|k}$. From the definition of saturation function (3.18) and the boundary layer widths $\psi_i > 0 \in \mathbb{R}$ it follows

$$\begin{aligned}\varphi\left(\frac{\tilde{y}_{i,k+1|k}}{\psi_i}\right)|\tilde{y}_{i,k+1|k}| &= \operatorname{sgn}(\tilde{y}_{i,k+1|k})|\tilde{y}_{i,k+1|k}| = \tilde{y}_{i,k+1|k},\\ &= |\operatorname{sgn}(\tilde{y}_{i,k+1|k})|\tilde{y}_{i,k+1|k} = \left|\varphi\left(\frac{\tilde{y}_{i,k+1|k}}{\psi_i}\right)\right|\tilde{y}_{i,k+1|k},\end{aligned} \tag{3.25}$$

for $\left|\frac{\tilde{y}_{i,k+1|k}}{\psi_i}\right| > 1$ and

$$\begin{aligned}\varphi\left(\frac{\tilde{y}_{i,k+1|k}}{\psi_i}\right)|\tilde{y}_{i,k+1|k}| &= \frac{\tilde{y}_{i,k+1|k}}{\psi_i}|\tilde{y}_{i,k+1|k}|,\\ &= \frac{|\tilde{y}_{i,k+1|k}|}{\psi_i}\tilde{y}_{i,k+1|k} = \left|\varphi\left(\frac{\tilde{y}_{i,k+1|k}}{\psi_i}\right)\right|\tilde{y}_{i,k+1|k},\end{aligned} \tag{3.26}$$

for $\left|\frac{\tilde{y}_{i,k+1|k}}{\psi_i}\right| \leq 1$. Consequently,

$$\operatorname{sat}(\Psi^{-1}\tilde{y}_{k+1|k}) \circ |\tilde{y}_{k+1|k}| = |\operatorname{sat}(\Psi^{-1}\tilde{y}_{k+1|k})| \circ \tilde{y}_{k+1|k}, \tag{3.27}$$

holds which applied to (3.24) yields

$$\hat{x}_{k+1} = y_{k+1} - \tilde{\Lambda}_{k+1}\tilde{y}_{k+1|k}, \qquad \tilde{\Lambda}_{k+1} = \operatorname{diag}\left\{\mathbf{1}_n - \left|\operatorname{sat}(\Psi^{-1}\tilde{y}_{k+1|k})\right|\right\}. \tag{3.28}$$

□

From the stochastic gain (3.22) and the definition of saturation function (3.18) it can be stated that the filter relies more on the predictions $\hat{x}_{k+1|k}$ if the boundary layer widths ψ_i are increased. For decreasing widths ψ_i the filter tends to disregard the a priori estimations and relies more on the measurements. If the output error lies outside of the boundary layer, i. e. $|\tilde{y}_{i,k+1|k}|$ exceeds the boundary layer width ψ_i, then the filter has the ability to completely ignore the a priori estimations. This makes sense as the predictions may rely on an imprecise model description $\breve{f}(\cdot)$. However, the SVSF was not designed to minimize an estimation error criterion similar to the MSE. This motivates the idea to combine the SVSF with the Kalman filter gain so that robustness and to some extent minimization of the MSE can be achieved. Combinations of the SVSF with the EKF, the UKF, the cubature Kalman filter, and the particle filter can be found in Gadsden *et al.* (2014*a*,*b*, 2011*a*). All proposed combinations are based on the strategy to switch between the SVSF and the Kalman filter gain. If the uncertainty of the model is considered to be small the KF gain is applied otherwise the SVSF gain is used. To evaluate the uncertainty of the model a time-varying boundary layer width Ψ_{var} is calculated. If Ψ_{var} exceeds a user-defined threshold the model is considered as uncertain and the Kalman filter gain is replaced by the SVSF gain. However, the proposed method can not be considered to be consistent. The calculation of the Kalman filter gain is based on the error covariance which is required to be updated at each time step. Once modeling discrepancies exist the error

covariance matrix will be updated incorrectly. As a consequence the determined Kalman filter gain may be for away from being optimal even if the model fits well at a considered current time step. In addition, the calculation of the variable boundary layer width Ψ_{var} also directly depends on the erroneous error covariance. Further, it is not mentioned how the threshold value for the switching between the filter gains is determined. The threshold appears to be tuned by trial and error based on the RMSE which is not realistic.

3.2 Relation between Smooth Variable Structure and Kalman Filter

As discussed previously the robustness of the SVSF is achieved by the introduction of the smoothing boundary layer. The width of layer controls in the influence of the a priori estimation on the a posteriori estimation. If the output error exceeds the boundary layer width the a priori estimation is completely ignored. This leads to robustness as due the model uncertainty the a priori estimation is likely to be erroneous. However, the SVSF approach has not been derived to minimize an estimation error criterion such as the MSE. This motivates the idea to combine the SVSF with another filtering approach that minimizes the MSE. Therefore, the error covariance of the reformulated SVSF (3.19)–(3.22) is studied. The stochastic gain $\tilde{\Lambda}_k$ of (3.22) is replaced by a yet undefined deterministic gain K_k with the goal to minimize the MSE. This will give a direct link between the SVSF approach and the Kalman filter. The equations of the error covariances are derived as follows.

First, it is required to further specify the noise of the measurement model

$$y_k = x_k + r_k. \tag{3.29}$$

The noise $r_k \in \mathbb{R}^n$ is assumed as white with mutual stochastically independent samples described by the mean $E\{r_k\} = 0$ and the covariance matrix

$$E\{r_i r_j^T\} = R\delta_{ij}. \tag{3.30}$$

In (3.30) the symbol δ_{ij} denotes the Kronecker delta. The measurement noise covariance matrix is assumed to be positive definite i. e. $R \succ 0$.

From (3.1), (3.2), and (3.19)–(3.22) it follows that the state estimation error and the output estimation error can be determined as

$$\tilde{x}_{k+1} = x_{k+1} - \hat{x}_{k+1} = K_{k+1}\tilde{y}_{k+1|k} - r_{k+1}, \tag{3.31}$$

$$\tilde{x}_{k+1|k} = x_{k+1} - \hat{x}_{k+1|k}, \tag{3.32}$$

and

$$\tilde{y}_{k+1|k} = y_{k+1} - \hat{x}_{k+1|k} = \tilde{x}_{k+1|k} + r_{k+1}, \tag{3.33}$$

where the yet undefined deterministic gain K_{k+1} in (3.31) replaces the stochastic gain $\tilde{\Lambda}_{k+1}$ of the reformulation of the SVSF. Let the output error covariance be defined as $S_{k+1} = E\{\tilde{y}_{k+1|k}\tilde{y}_{k+1|k}^T\}$. From (3.33) it follows

$$S_{k+1} = E\left\{(\tilde{x}_{k+1|k} + r_{k+1})(\tilde{x}_{k+1|k} + r_{k+1})^T\right\}. \tag{3.34}$$

Assume the a priori error covariance to be defined as

$$P_{k+1|k} = E\{\tilde{x}_{k+1|k}\tilde{x}_{k+1|k}^T\}. \tag{3.35}$$

Expanding (3.34) and considering (3.35) as well as $R = E\{r_{k+1}r_{k+1}^T\}$ yields

$$S_{k+1} = P_{k+1|k} + R + E\{r_{k+1}\tilde{x}_{k+1|k}^T\} + E\{\tilde{x}_{k+1|k}r_{k+1}^T\}. \tag{3.36}$$

The value of the remaining expectations in (3.36) is studied as follows. The a priori estimation error $\tilde{x}_{k+1|k}$ is known to directly depend on the noise realizations r_j with $j \in \{0, 1, \ldots, k\}$ but not on the realization r_{k+1}. The realizations r_j with $j \in \{0, 1, \ldots, k\}$ and r_{k+1} are independent of each other due to the independent white noise assumption. Realization r_{k+1} can not have any effect on $\tilde{x}_{k+1|k}$. Both random variables are stochastically independent. It follows $E\{r_{k+1}\tilde{x}_{k+1|k}^T\} = E\{r_{k+1}\}E\{\tilde{x}_{k+1|k}^T\}$ and $E\{\tilde{x}_{k+1|k}r_{k+1}^T\} = E\{\tilde{x}_{k+1|k}\}E\{r_{k+1}^T\}$. The zero-mean noise assumption i. e. $E\{r_k\} = 0$ leads to

$$S_{k+1} = P_{k+1|k} + R. \tag{3.37}$$

Let the a posteriori error covariance be defined as

$$P_{k+1} = E\left\{\tilde{x}_{k+1}\tilde{x}_{k+1}^T\right\}. \tag{3.38}$$

Substituting (3.31) in (3.38) yields

$$P_{k+1} = E\left\{(K_{k+1}\tilde{y}_{k+1|k} - r_{k+1})(\tilde{y}_{k+1|k}^T K_{k+1}^T - r_{k+1}^T)\right\}. \tag{3.39}$$

Expanding (3.39) and considering the definition of the output error covariance S_{k+1} yields

$$P_{k+1} = K_{k+1}S_{k+1}K_{k+1}^T + R - E\{r_{k+1}\tilde{y}_{k+1|k}^T K_{k+1}^T\} - E\{K_{k+1}\tilde{y}_{k+1|k}r_{k+1}^T\}. \tag{3.40}$$

Based on (3.33) the two remaining expectations in (3.40) can be written as

$$E\left\{r_{k+1}(\tilde{x}_{k+1|k}^T + r_{k+1}^T)K_{k+1}^T\right\} = RK_{k+1}^T, \tag{3.41}$$

$$E\left\{K_{k+1}(\tilde{x}_{k+1|k} + r_{k+1})r_{k+1}^T\right\} = K_{k+1}R, \tag{3.42}$$

where $E\{r_{k+1}\tilde{x}_{k+1|k}^T\}$ and $E\{\tilde{x}_{k+1|k}r_{k+1}^T\}$ again vanish due to the stochastic independency of r_{k+1} and $\tilde{x}_{k+1|k}$. Finally, the a posteriori error covariance is achieved as

$$P_{k+1} = K_{k+1}S_{k+1}K_{k+1}^T + R - RK_{k+1}^T - K_{k+1}R. \tag{3.43}$$

The error covariance (3.43) can also be written as

$$\begin{aligned} P_{k+1} = {} & K_{k+1}S_{k+1}K_{k+1}^T + R \\ & - RS_{k+1}^{-1}S_{k+1}K_{k+1}^T - K_{k+1}S_{k+1}S_{k+1}^{-1}R + RS_{k+1}^{-1}R - RS_{k+1}^{-1}R, \end{aligned} \tag{3.44}$$

which is equivalent to

$$P_{k+1} = R - RS_{k+1}^{-1}R + (K_{k+1} - RS_{k+1}^{-1})S_{k+1}(K_{k+1} - RS_{k+1}^{-1})^T. \tag{3.45}$$

Based on the derived error covariance (3.45) the filter performance is optimized as follows. A new filter gain that minimizes the MSE is obtained from Theorem 2. In Theorem 3 the new gain is applied to the SVSF which gives a link to the Kalman filter. The presented connection between the SVSF and the Kalman filter is originally described in Spiller and Söffker (2020*b*).

Theorem 2 (Optimal deterministic gain of reformulated SVSF)**.**
The gain

$$K_{k+1} = K_{opt,k+1} = RS_{k+1}^{-1} = R(P_{k+1|k} + R)^{-1}, \tag{3.46}$$

minimizes the a posteriori MSE i. e. the trace of P_{k+1} according to (3.45).

Proof. From (3.45) it is known that K_{k+1} only affects the term

$$\Pi_{k+1} = (K_{k+1} - RS_{k+1}^{-1})S_{k+1}(K_{k+1} - RS_{k+1}^{-1})^T. \tag{3.47}$$

Matrix S_{k+1} is a covariance matrix. Consequently, it is positive semi-definite. Matrix Π_{k+1} is also positive semi-definite as

$$0 \leq b(a)S_{k+1}b^T(a), \qquad b(a) \triangleq a(K_{k+1} - RS_{k+1}^{-1}), \tag{3.48}$$

holds for any $a \in \mathbb{R}^n$. The minimal trace of a positive semi-definite matrix is zero. As that zero value is achieved for $K_{opt,k+1}$ from (3.46) it is the optimal gain. □

Theorem 3 (Relation between SVSF and KF)**.**
The state prediction (3.19) and the correction (3.21) of the SVSF approach equal the one of the extended Kalman filter if the switching gain $\tilde{\Lambda}_{k+1}$ of (3.22) is replaced by the optimal gain $K_{opt,k+1}$ from (3.46).

Proof. [1] The state prediction (3.19) obviously equals the one of the extended Kalman filter. Regarding the correction step (3.21) it follows that

$$\begin{aligned} \hat{x}_{k+1} &= y_{k+1} - K_{opt,k+1}\tilde{y}_{k+1|k} = \hat{x}_{k+1|k} + \tilde{y}_{k+1|k} - K_{opt,k+1}\tilde{y}_{k+1|k}, \\ &= \hat{x}_{k+1|k} + (I_n - K_{opt,k+1})\tilde{y}_{k+1|k} = \hat{x}_{k+1|k} + K_{kal,k+1}\tilde{y}_{k+1|k}, \end{aligned} \tag{3.49}$$

with

$$K_{kal,k+1} = I_n - K_{opt,k+1}, \tag{3.50}$$

holds if $\tilde{\Lambda}_{k+1}$ of (3.22) is replaced by $K_{opt,k+1}$ known from (3.46). As the introduced $K_{kal,k+1}$ of (3.50) equals the Kalman filter gain

$$\begin{aligned} K_{kal,k+1} &= I_n - K_{opt,k+1} = I_n - R(P_{k+1|k} + R)^{-1}, \\ &= (P_{k+1|k} + R)(P_{k+1|k} + R)^{-1} - R(P_{k+1|k} + R)^{-1}, \\ &= P_{k+1|k}(P_{k+1|k} + R)^{-1}, \end{aligned} \tag{3.51}$$

step (3.49) and thus (3.21) is identical to the correction step of the Kalman filter. □

[1] The authors thank the anonymous reviewers of the European Control Conference 2020 for the insightful comments and suggestions related to the proof of the theorem.

3.3 Combined Estimation Approach

In this section a combination of the SVSF and the extended Kalman filter is proposed. As mentioned before a combination of both filters has already been described in Gadsden *et al.* (2014*b*). The approach developed by Gadsden *et al.* (2014*b*) simply switches between the Kalman filter and the SVSF gain. To apply the Kalman filter gain the estimation error covariance is needed to be known. For the update of the error covariance a precise linear system description is required which makes the approach of Gadsden *et al.* (2014*b*) insufficient for the state estimation of nonlinear uncertain systems. The combined estimation approach that is described in this section is based on a weighted sum of the SVSF and the Kalman filter gain. The error covariance that is required to calculate the Kalman filter gain is also estimated. As a consequence the proposed approach is applicable to nonlinear uncertain systems. The filter introduces additional tuning parameters. This tuning parameters are determined in a subsequently described parameter optimization process.

To apply the Kalman filter gain $K_{opt,k+1}$ of (3.46) the a priori error covariance $P_{k+1|k}$ has to be determined. The error covariance cannot be updated based on the Kalman filter equations as that would require linearity of the system and full model knowledge. Consequently, the error matrix $P_{k+1|k}$ itself is estimated. This avoids a wrong update of the error covariance based on an imprecise system description. The estimation of the error covariance is described as follows.

According to (3.37) the state error covariance $P_{k+1|k}$ is related to the output error covariance S_{k+1} which motivates to estimate $P_{k+1|k}$ as

$$\hat{P}_{k+1|k} = \hat{S}_{k+1} - R, \tag{3.52}$$

with

$$\begin{aligned}\hat{S}_{k+1} &= \frac{1}{N}\sum_{j=k-N+2}^{k+1} \tilde{y}_{j|j-1}\tilde{y}_{j|j-1}^T, \\ &= \frac{1}{N}\sum_{j=k-N+2}^{k+1} \left(\tilde{x}_{j|j-1}\tilde{x}_{j|j-1}^T + r_j\tilde{x}_{j|j-1}^T + \tilde{x}_{j|j-1}r_j^T + r_j r_j^T\right),\end{aligned} \tag{3.53}$$

and $1 \leq N$. Estimating $\hat{S}_{k+1}$ based on the output error $\tilde{y}_{k+1|k}$ is common in the field of adaptive Kalman filtering (e. g. Yang and Gao, 2006; Hide *et al.*, 2003). Assume the estimation error $\tilde{x}_{k+1|k}$ to be constant. Let r_{k+1} be ergodic in the sense of

$$\frac{1}{N}\sum_{j=k-N+2}^{k+1} r_j = 0, \qquad \frac{1}{N}\sum_{j=k-N+2}^{k+1} r_j r_j^T = R, \tag{3.54}$$

then the true error covariance

$$P_{k+1|k} = \hat{S}_{k+1} - R, \tag{3.55}$$

can be obtained from (3.53).

Additional information about $P_{k+1|k}$ is obtained by considering the suboptimal gain $K_{sub,k+1} = 0_{n\times n}$. Let $P_{opt,k+1}$ denote the error covariance if the optimal gain $K_{opt,k+1}$ is applied and let $P_{sub,k+1}$ denote the error covariance if the suboptimal gain $K_{sub,k+1}$ is

applied. Substituting K_{k+1} of (3.45) by $K_{sub,k+1}$ gives $P_{sub,k+1} = R$. As the filter with the optimal gain minimizes the MSE the inequality

$$\mathrm{tr}\{P_{opt,k+1}\} \leq \mathrm{tr}\{R\} = \mathrm{tr}\{P_{sub,k+1}\}, \tag{3.56}$$

can be stated. If $P_{k+1} \approx P_{k+1|k}$ is assumed which holds for a sufficient small sampling time then

$$\hat{P}_{k+1|k} = \zeta R, \qquad \zeta \in [0,1], \tag{3.57}$$

may be considered as an estimation of $P_{k+1|k}$.

As the SVSF is a recursive estimation approach the relation of $P_{k+1|k}$ to its previous value $P_{k|k-1}$ should be considered. For a small sampling time this can be roughly described by

$$\hat{P}_{k+1|k} = \hat{P}_{k|k-1}. \tag{3.58}$$

To find an estimation $\hat{P}^{\star}_{k+1|k}$ of $P_{k+1|k}$ that fits best to the established equations (3.52), (3.57), and (3.58) a weighted least squares (WLS) estimation problem is formulated. The importance of the individual equations is expressed by weighting factors $0 < \alpha, \beta, \gamma \in \mathbb{R}$ which are determined subsequently in a parameter optimization process. Based on the vector operator "vec" the WLS problem

$$p^{\star}_{k+1|k} = \underset{p_{k+1|k}}{\arg\min} \|b_{k+1} - A p_{k+1|k}\|^2_W, \qquad \hat{P}^{\star}_{k+1|k} = \mathrm{vec}^{-1}\left\{p^{\star}_{k+1|k}\right\}, \tag{3.59}$$

with

$$A = I_n \otimes \begin{bmatrix} I_n \\ I_n \\ I_n \end{bmatrix}, \qquad b_{k+1} = \mathrm{vec}\left\{\begin{bmatrix} \hat{S}_{k+1} - R \\ \zeta R \\ \hat{P}^{\star}_{k|k-1} \end{bmatrix}\right\}, \qquad \zeta \in [0,1],$$

$$W = I_n \otimes \begin{bmatrix} \alpha I_n & 0 & 0 \\ 0 & \beta I_n & 0 \\ 0 & 0 & \gamma I_n \end{bmatrix},$$

and $0 < \alpha, \beta, \gamma$ is considered. The solution of this WLS estimation problem is

$$\hat{P}^{\star}_{k+1|k} = \frac{1}{\alpha + \beta + \gamma}\left(\alpha(\hat{S}_{k+1} - R) + \beta\zeta R + \gamma \hat{P}^{\star}_{k|k-1}\right), \tag{3.60}$$

which is a weighted sum of the solutions of the individual equations (3.52), (3.57), and (3.58). Based on the substitution

$$\bar{\alpha} = \frac{\alpha}{\alpha + \beta + \gamma}, \qquad \bar{\beta} = \frac{\beta}{\alpha + \beta + \gamma}, \qquad \bar{\gamma} = \frac{\gamma}{\alpha + \beta + \gamma}, \tag{3.61}$$

with

$$\bar{\alpha} + \bar{\beta} + \bar{\gamma} = 1, \tag{3.62}$$

the number of weighting factors is reduced by one yielding

$$\hat{P}^{\star}_{k+1|k} = \bar{\alpha}(\hat{S}_{k+1} - R) + \bar{\beta}\zeta R + (1 - \bar{\alpha} - \bar{\beta})\hat{P}^{\star}_{k|k-1}, \tag{3.63}$$

subject to

$$0 < \bar{\alpha}, \bar{\beta}, \qquad \bar{\alpha} + \bar{\beta} < 1. \tag{3.64}$$

The estimated error covariance $\hat{P}^{\star}_{k+1|k}$ of (3.63) is not guaranteed to be positive semi-definite. However, from the definition of a covariance matrix it can be shown that every covariance matrix must be positive semi-definite. To solve the problem all negative eigenvalues of $\hat{P}^{\star}_{k+1|k}$ are replaced by non-negative ones. The resulting positive semi-definite matrix is denoted as $\hat{P}^{\dagger}_{k+1|k}$. The post-processing step that guarantees positive semi-definiteness is described as follows. Matrix $\hat{P}^{\star}_{k+1|k}$ is symmetric according to (3.63) if a symmetric initial matrix $\hat{P}_0$ is chosen which is assumed to hold. As $\hat{P}^{\star}_{k+1|k}$ is symmetric it can always be diagonalized according to

$$D^{\star}_{k+1} = L^{T}_{k+1}\hat{P}^{\star}_{k+1|k}L_{k+1}, \tag{3.65}$$

where $D^{\star}_{k+1} \in \mathbb{R}^{n\times n}$ is a diagonal matrix with diagonal elements $d^{*}_{ii,k+1}$ corresponding to the eigenvalues of matrix $\hat{P}^{\star}_{k+1|k}$. Let $D_{k+1} \in \mathbb{R}^{n\times n}$ define a diagonal matrix with diagonal elements $d_{ii,k+1}$. Based on $d^{*}_{ii,k+1}$ the diagonal elements $d_{ii,k+1}$ are determined according to

$$d_{ii,k+1} = \begin{cases} d^{\star}_{ii,k+1} & \text{if } d^{\star}_{ii,k+1} \text{ is } > 0, \\ \eta \times \tilde{r}_{ii,k+1} & \text{if } d^{\star}_{ii,k+1} \text{ is } \leq 0, \end{cases} \qquad \eta \in (0, 1]. \tag{3.66}$$

In (3.66) the scalar $\tilde{r}_{ii,k+1} \geq 0$ denotes the i-th diagonal element of the transformed noise covariance $\tilde{R}_{k+1} = L^{T}_{k+1}RL_{k+1}$ and the parameter η is a scaling factor. The scaling factor is optimized subsequently. The modified error covariance $\hat{P}^{\dagger}_{k+1|k}$ is calculated as

$$\hat{P}^{\dagger}_{k+1|k} = L_{k+1}D_{k+1}L^{T}_{k+1}. \tag{3.67}$$

Finally, an estimation $\hat{P}^{\dagger}_{k+1|k}$ of the state error covariance is achieved. Substituting $P_{k+1|k}$ of (3.46) by $\hat{P}^{\dagger}_{k+1|k}$ gives an estimation of the Kalman filter gain according to

$$\hat{K}_{opt,k+1} = R(\hat{P}^{\dagger}_{k+1|k} + R)^{-1}. \tag{3.68}$$

The combination of the SVSF and the Kalman filter is described as follows. Let Ξ_{k+1} denote the gain of the combined approach. To some extent it should be equal to the estimated Kalman filter gain

$$\Xi_{k+1} = \hat{K}_{opt,k+1} = R(\hat{P}^{\dagger}_{k+1|k} + R)^{-1}, \tag{3.69}$$

and to some extend it should also be equal to the gain of the SVSF approach

$$\Xi_{k+1} = \operatorname{diag}\left\{\mathbf{1}_n - |\Psi^{-1}\tilde{y}_{k+1|k}|\right\}. \tag{3.70}$$

The SVSF gain of (3.70) is the gain $\tilde{\Lambda}_{k+1}$ of the reformulation of the SVSF according to (3.22) for the case that all output errors lie inside the boundary layer i. e. $\forall i\colon |\tilde{y}_{i,k+1|k}| \leq \psi_i$. Based on (3.69) and (3.70) the WLS estimation problem

$$\xi^{\star}_{k+1} = \underset{\xi_{k+1}}{\arg\min} \|b_{k+1} - A\xi_{k+1}\|^2_W, \qquad \Xi^{\star}_{k+1} = \mathrm{vec}^{-1}\left\{\xi^{\star}_{k+1}\right\}, \tag{3.71}$$

with

$$A = I_n \otimes \begin{bmatrix} I_n \\ I_n \end{bmatrix}, \qquad b_{k+1} = \mathrm{vec}\left\{\begin{bmatrix} R(\hat{P}^{\dagger}_{k+1|k} + R)^{-1} \\ \mathrm{diag}\left\{\mathbf{1}_n - \left|\Psi^{-1}\tilde{y}_{k+1|k}\right|\right\} \end{bmatrix}\right\},$$
$$W = I_n \otimes \begin{bmatrix} \iota I_n & 0 \\ 0 & \upsilon I_n \end{bmatrix},$$

and $0 < \iota, \upsilon$ is formulated which has the solution

$$\Xi^{\star}_{k+1} = \frac{1}{\iota + \upsilon}\left(\iota\left(R(\hat{P}^{\dagger}_{k+1|k} + R)^{-1}\right) + \upsilon \times \mathrm{diag}\left\{\mathbf{1}_n - \left|\Psi^{-1}\tilde{y}_{k+1|k}\right|\right\}\right). \tag{3.72}$$

The number of weighting factors is reduced by one using the substitution

$$\bar{\iota} = \frac{\iota}{\iota + \upsilon}, \qquad \bar{\upsilon} = \frac{\upsilon}{\iota + \upsilon}, \qquad \bar{\iota} + \bar{\upsilon} = 1. \tag{3.73}$$

As a consequence

$$\Xi^{\star}_{k+1} = \bar{\iota}\left(R(\hat{P}^{\dagger}_{k+1|k} + R)^{-1}\right) + (1 - \bar{\iota}) \times \mathrm{diag}\left\{\mathbf{1}_n - \left|\Psi^{-1}\tilde{y}_{k+1|k}\right|\right\}, \tag{3.74}$$

is obtained which is subject to

$$0 \leq \bar{\iota} \leq 1. \tag{3.75}$$

The matrix $\Xi^{\star}_{k+1}$ of (3.74) is the gain of the combined approach. Substituting $\tilde{\Lambda}_{k+1}$ of (3.21) by $\Xi^{\star}_{k+1}$ gives the a posteriori estimation

$$\hat{x}_{k+1} = y_{k+1} - \Xi^{\star}_{k+1}\tilde{y}_{k+1|k}, \tag{3.76}$$

of the combined filter. As previously discussed the SVSF has the ability to completely ignore the a priori estimations if the the output error exceeds the boundary layer width. To implement this feature on the combined filter the a posteriori estimation of (3.76) is slightly modified. The modification is described as follows. The function $\Theta\colon \Psi, \tilde{y}_{k+1|k} \rightarrow \Theta(\Psi, \tilde{y}_{k+1|k}) \in \mathbb{R}^{n\times n}$ is introduced according to

$$\Theta(\Psi, \tilde{y}_{k+1|k}) = \mathrm{diag}\left\{\left[\vartheta_1 \ldots \vartheta_n\right]^T\right\}, \qquad \vartheta_i = \begin{cases} 0 & \text{for } |\tilde{y}_{i,k+1|k}| > \psi_i, \\ 1 & \text{for } |\tilde{y}_{i,k+1|k}| \leq \psi_i. \end{cases} \tag{3.77}$$

Modifying the a posteriori estimation as

$$\hat{x}_{k+1} = y_{k+1} - \Theta(\Psi, \tilde{y}_{k+1|k}) \times \Xi^{\star}_{k+1}\tilde{y}_{k+1|k}, \tag{3.78}$$

implements the desired feature on the combined filter.

Finally, the combined estimating approach of the SVSF and the Kalman filter is summarized as

$$\hat{x}_{k+1|k} = \breve{f}_k(\hat{x}_k, u_k), \tag{3.79}$$

$$\tilde{y}_{k+1|k} = y_{k+1} - \hat{x}_{k+1|k}, \tag{3.80}$$

$$\hat{x}_{k+1} = y_{k+1} - \Theta(\Psi, \tilde{y}_{k+1|k}) \times \Xi^{\star}_{k+1} \tilde{y}_{k+1|k}, \tag{3.81}$$

$$\Theta(\Psi, \tilde{y}_{k+1|k}) = \operatorname{diag}\left\{ \begin{bmatrix} \vartheta_1 \dots \vartheta_n \end{bmatrix}^T \right\}, \tag{3.82}$$

$$\vartheta_i = \begin{cases} 0 & \text{for } |\tilde{y}_{i,k+1|k}| > \psi_i, \\ 1 & \text{for } |\tilde{y}_{i,k+1|k}| \leq \psi_i, \end{cases} \tag{3.83}$$

$$\Xi^{\star}_{k+1} = \bar{\iota} \left(R(\hat{P}^{\dagger}_{k+1|k} + R)^{-1} \right) + (1 - \bar{\iota}) \times \operatorname{diag}\left\{ \mathbf{1}_n - \left| \Psi^{-1} \tilde{y}_{k+1|k} \right| \right\}, \tag{3.84}$$

with

$$\Psi = \operatorname{diag}\left\{ \begin{bmatrix} \psi_1 & \psi_2 & \dots & \psi_n \end{bmatrix}^T \right\}, \qquad 0 < \psi_i, \qquad 0 \leq \bar{\iota} \leq 1,$$

and

$$\hat{P}^{\dagger}_{k+1|k} = L_{k+1} D_{k+1} L^T_{k+1},$$

so that L_{k+1} diagonalizes $\hat{P}^{\star}_{k+1|k}$ according to

$$D^{\star}_{k+1} = L^T_{k+1} \hat{P}^{\star}_{k+1|k} L_{k+1},$$

with

$$\hat{P}^{\star}_{k+1|k} = \bar{\alpha}(\hat{S}_{k+1} - R) + \bar{\beta}\zeta R + (1 - \bar{\alpha} - \bar{\beta}) \hat{P}^{\dagger}_{k|k-1}, \tag{3.85}$$

subject to

$$\hat{S}_{k+1} = \frac{1}{N} \sum_{j=k-N+2}^{k+1} \tilde{y}_{j|j-1} \tilde{y}^T_{j|j-1}, \qquad 0 < \bar{\alpha}, \bar{\beta}, \quad \bar{\alpha} + \bar{\beta} < 1, \quad 1 \leq N, \quad \zeta \in [0, 1],$$

and diagonal matrix D_{k+1} being obtained from

$$d_{ii,k+1} = \begin{cases} d^{\star}_{ii,k+1} & \text{if } d^{\star}_{ii,k+1} \text{ is } > 0, \\ \eta \times \tilde{r}_{ii,k+1} & \text{if } d^{\star}_{ii,k+1} \text{ is } \leq 0, \end{cases} \qquad \eta \in (0, 1],$$

where $d_{ii,k+1}$ denotes the i-th diagonal element of diagonal matrix D_{k+1}, $d^{\star}_{ii,k+1}$ denotes the i-th diagonal element of diagonal matrix $D^{\star}_{k+1}$, and $\tilde{r}_{ii,k+1}$ denotes the i-th diagonal element of the transformed noise covariance $\tilde{R}_{k+1} = L^T_{k+1} R L_{k+1}$.

As the proposed filter requires full state measurements a direct link between the known output estimation error and the unknown state estimation error can be stated by the following theorem.

Theorem 4 (Estimation error of combined filtering approach)**.**
The estimation error of the a posteriori estimation

$$\begin{aligned} \hat{x}_{k+1} &= y_{k+1} - \Xi^{\dagger}_{k+1}\tilde{y}_{k+1|k}, \\ \Xi^{\dagger}_{k+1} &\triangleq \Theta(\Psi, \tilde{y}_{k+1|k}) \times \Xi^{\star}_{k+1}, \end{aligned} \tag{3.86}$$

of the combined filtering approach (3.79)–(3.84) is bounded by

$$\|\tilde{x}_{k+1}\| \leq \|\Xi^{\dagger}_{k+1}\tilde{y}_{k+1|k}\| + a, \tag{3.87}$$

if the measurement noise is bounded by $\|r_k\| < a$*. In addition, if* $|\tilde{y}_{i,k+1|k}| > \psi_i$ *is satisfied and the measurement noise is bounded by* $|r_{i,k+1}| < b_i$ *then also*

$$|\tilde{x}_{i,k+1}| \leq b_i, \tag{3.88}$$

holds.

Proof. Substituting (3.86) in the definition of the a posteriori error gives

$$\tilde{x}_{k+1} = x_{k+1} - y_{k+1} + \Xi^{\dagger}_{k+1}\tilde{y}_{k+1|k} = \Xi^{\dagger}_{k+1}\tilde{y}_{k+1|k} - r_{k+1}. \tag{3.89}$$

The general statement (3.87) follows by applying the triangle inequality on (3.89). The specific statement (3.88) results from the definition of switching function (3.77) which yields the a posteriori estimation $\hat{x}_{i,k+1} = y_{i,k+1}$ in case of $|\tilde{y}_{i,k+1|k}| > \psi_i$ (cf. (3.81)). Then it is

$$\tilde{x}_{i,k+1} = x_{i,k+1} - \hat{x}_{i,k+1} = x_{i,k+1} - y_{i,k+1} = -r_{i,k+1}, \tag{3.90}$$

which leads to (3.88). □

3.4 Parameter Optimization

The previously described combined filtering approach introduces tuning parameters that are required to be optimized to achieve improved estimation performance. In this section a scheme for the parameter optimization is described which is originally proposed in Spiller and Söffker (2020*b*). The considered optimization scheme can be applied to optimize any state estimator that has to deal with an imprecise model description. For the optimization neither the true systems states are required to be know nor any experiments on the real system have to be undertaken. A nominal system description is assumed to be available which is not required to accurately describe the true dynamics of the system. Some a priori knowledge is assumed to be given that describes the maximum range that the true system parameters may vary from the known nominal values. Based on that knowledge training models are generated. The training models consist of system parameters that vary from the nominal values by the specified parameter ranges. The optimization can be divided into two steps: training and test procedure. The main idea of the training process is to simulate the true system behavior based on training models but to let the filter run based on the nominal model. The true states of the training models are known so that the estimation performance can be optimized with respect to those states. As a consequence, during training the parameters of the filter are optimized to achieve improved performance

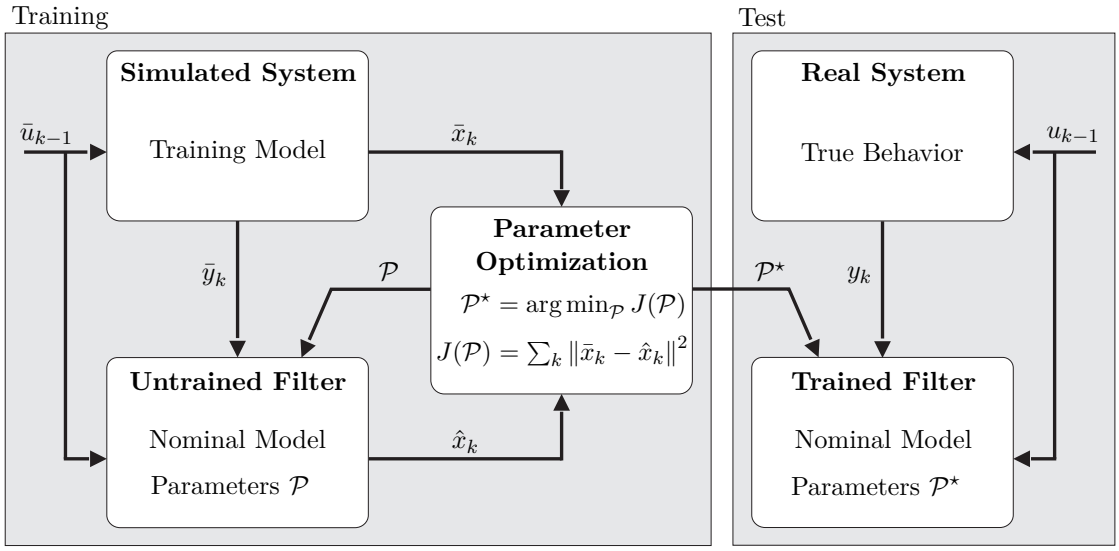

Figure 3.1: Filter parameter optimization. Training: the training is based on a specific system description called training model which simulates model uncertainty. The training model equals the known nominal system description but with varied system parameters to account for the model uncertainty. The filter receives measurements from the training model but uses the nominal model for the state estimation. The filter parameters are optimized by comparing the filter estimates with the true states of the training model. Test: the filter is applied to the real system, it runs with the optimized tuning parameters, and uses the known nominal system description for the state estimation.

in presence of model discrepancy. In the test phase the filter is applied to the true system using the optimized parameters from the training procedure. A formal description of the optimization concept is given as follows.

A nonlinear discrete-time system of the form

$$x_{k+1} = f_k(x_k, u_k) + q_r, \tag{3.91}$$

$$y_k = h_k(x_k) + r_k, \tag{3.92}$$

is considered, where q_k and r_k are assumed to be noise processes with known probability density functions p_q and p_r. It is assumed that a possible imprecise description of the dynamics of (3.91) is given by $\breve{f}_k(\cdot)$. In addition, it is assumed that the discrepancy between $f_k(\cdot)$ and $\breve{f}_k(\cdot)$ is not structural meaning that the discrepancy only results from different values of the system parameters. The model $\breve{f}_k(\cdot)$ is denoted as the nominal system description which has system parameters with so-called nominal values. The measurement model $h_k(\cdot)$ is assumed to be precisely known. For the training procedure the training models have to be generated. Let N_p be the number of system parameters and let $p_{nom,i}$ denote the nominal value of parameter i. Some a priori knowledge about the amount of model uncertainty is assumed to be available. More precisely, parameter $p_{nom,i}$ is known to be varied by ϱ_i percent to account for the severity of model uncertainty that is related to the parameter i. Let the uniform distribution

$$Z \sim \mathcal{U}(a, b), \tag{3.93}$$

of a random variable Z be defined by the probability density function

$$f_Z(z|a,b) = \begin{cases} \frac{1}{b-a} & \text{if } b \geq z \geq a, \\ 0 & \text{else.} \end{cases} \tag{3.94}$$

It is suggested to obtain the i-th parameter $p_i^{(j)}$ of the j-th training model by drawing a sample from

$$p_i^{(j)} \sim \mathcal{U}\left((1-\varrho_i/100)p_{nom,i}, (1+\varrho_i/100)p_{nom,i}\right). \tag{3.95}$$

Repeating the procedure for all N_p system parameters forms one set of training parameters which defines one training model j. The training procedure is described as follows.

Assume $\mathcal{P}$ to be the sequence of filter parameters that are required to be optimized. Let $\bar{u}_k^{(j)}$ be the inputs that are applied to training model j. Based on $\bar{u}_k^{(j)}$ and the probability density function p_q of the process noise the states $\bar{x}_k^{(j)}$ of the j-th training model are generated. Using the known measurement model $h_k(\cdot)$ and the probability density function p_r of the measurement noise the measurements $\bar{y}_k^{(j)}$ of the j-th training model are generated. Suppose $\hat{x}_k|\Omega_k^{(j)}$ to be the estimations of a filter that runs based on the nominal model but receives data $\Omega_k^{(j)} = \{\bar{U}_k^{(j)}, \bar{Y}_k^{(j)}\}$ from the training model j, i. e. inputs $\bar{U}_k^{(j)} = (\bar{u}_0^{(j)}, \bar{u}_1^{(j)}, \ldots, \bar{u}_k^{(j)})$ and measurements $\bar{Y}_k^{(j)} = (\bar{y}_0^{(j)}, \bar{y}_1^{(j)}, \ldots, \bar{y}_k^{(j)})$. The optimized parameters $\mathcal{P}_j^\star$ for that filter are given by

$$\mathcal{P}_j^\star = \arg\min_{\mathcal{P}} J_j(\mathcal{P}) = \arg\min_{\mathcal{P}} \sum_k \|\bar{x}_k^{(j)} - \hat{x}_k|\Omega_k^{(j)}(\mathcal{P})\|^2, \tag{3.96}$$

where J_j denotes the cost function. The optimization problem (3.96) can be solved by e. g. genetic approaches.

During training several training models can be generated so that several sets of optimized filter parameters $\mathcal{P}_1^\star, \mathcal{P}_2^\star, \mathcal{P}_3^\star \ldots$ are obtained. For the test procedure a selection has to be made with respect to these sets. For instance, the mean or the median of the optimized parameters can be taken into consideration to define the parameters of the filter that is applied to the real system. Finally, an overview of the discussed filter optimization strategy is given in Fig. 3.1.

In the following the parameter optimization of the combined estimation approach (3.79)–(3.84) of Section 3.3 is considered. The set of tuning parameters of the combined approach is given by

$$\mathcal{S}_{CA} = (\bar{\alpha}, \bar{\beta}, \bar{\iota}, \eta, \zeta, \Psi, N). \tag{3.97}$$

Assume the optimization scheme to be applied to the SVSF and the combined estimation approach. As both filters are related to each other a statement about the estimation performance during the training phase can be made by the following theorem.

Theorem 5 (Training performance of combined filtering approach)**.**
Let the parameters of the reformulated SVSF and the combined filtering approach be tuned as illustrated in Fig. 3.1. Assume the filters to be run with the same initial state estimation and same data $\Omega_k^{(j)}$ generated by a training model j. Suppose that the obtained solutions of

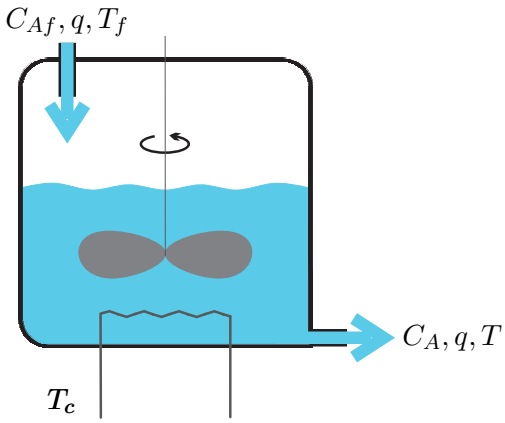

Figure 3.2: Continuous stirred tank reactor (Spiller et al. IFAC2020)

the optimization process (3.96) are global minima, i. e. the optimization procedure e. g. a genetic approach finds the best possible solution for (3.96). Let $J_{RF,j}$ be the global minimum found for the reformulated SVSF approach and let $J_{CA,j}$ be the global minimum found for the combined approach. Then the statement $J_{RF,j} \geq J_{CA,j}$ holds true.

Proof. The space of the tuning parameters of the reformulated SVSF is

$$\mathcal{S}_{RF} = \Psi \tag{3.98}$$

and the tuning parameters of the combined approach are defined by the parameter space

$$\mathcal{S}_{CA} = (\bar{\alpha}, \bar{\beta}, \bar{\iota}, \eta, \zeta, \Psi, N). \tag{3.99}$$

From (3.79)–(3.84) it can be seen that for

$$\mathcal{S}^{\star}_{CA} = (\bar{\alpha}, \bar{\beta}, 0, \eta, \zeta, \Psi, N) \tag{3.100}$$

the combined approach reduces to the reformulated SVSF and the parameter space $\mathcal{S}_{\mathrm{RF}}$ lies within $\mathcal{S}^{\star}_{\mathrm{CA}}$. □

3.5 Application to Nonlinear Uncertain System

In this section state estimation of a chemical plant is considered to evaluate the performance of the original SVSF and the combined estimation approach (CA). In addition, the extended Kalman filter (EKF) with tuned parameters is applied. According to Seborg *et al.* (2010) and Magni *et al.* (2001) a chemical reaction in a continuous stirred tank reactor (CSTR) is considered. The reactor with its inputs and outputs is visualized in Fig. 3.2. In the reactor a species A reacts to a species B. The inlet stream is only composed of species A whereas the effluent flow is composed of a mixture of A and B. The effluent flow concentration of species A is denoted as C_A and the reactor temperature is denoted as T. The dynamics of C_A and T are described by the nonlinear time-continuous model

$$\underbrace{\begin{bmatrix}\dot{x}_1\\ \dot{x}_2\end{bmatrix}}_{\dot{x}} = \underbrace{\begin{bmatrix}\frac{q}{V}(C_{Af} - x_1) - k_0 x_1 \exp\left(-\frac{E}{Rx_2}\right)\\ a(x) + \frac{UA}{V\rho C_p}(u + T_{eq,c} - x_2)\end{bmatrix}}_{f(x,u)}, \tag{3.101}$$

Table 3.1: Parameters of continuous stirred tank reactor (Magni *et al.* (2001))

Description	Parameter	Unit	Nominal	Real	Training
Tank volume	V	l	100	92	[80, 120]
Feed flow rate	q	l/min	100	94	[80, 120]
Feed concentration	C_{Af}	mol/l	1	0.98	[0.8, 1.2]
Feed temperature	T_f	K	350	354	[280, 420]
Density	ρ	g/l	1000	953	[800, 1200]
Enthalpy	$-\Delta H$	J/mol	$5e^4$	$4.91e^4$	[$4e^4$, $6e^4$]
Exponential factor	$\frac{E}{R}$	K	8750	8893	[7000, 10500]
Frequency factor	k_0	min^{-1}	$7.2e^{10}$	$7.68e^{10}$	[$5.76e^{10}$, $8.64e^{10}$]
Heat transfer	UA	J/minK	$5e^4$	$4.68e^4$	[$4e^4$, $6e^4$]
Specific heat	C_p	J/gK	0.239	0.299	[0.191, 0.287]
Cooling temperature	$T_{eq,c}$	K	300	300	300

Interval [a,b]: parameter for training equals a sample z drawn from uniform distribution $Z \sim U(a, b)$.

$$a(x) = \frac{q}{V}(T_f - x_2) + \frac{(-\Delta H)k_0 x_1}{\rho C_p}\exp\left(-\frac{E}{Rx_2}\right),$$

where state x_1 denotes C_A and state x_2 denotes T. The input $u = \Delta T_c$ is the change of the coolant stream temperature related to a nominal value $T_{eq,c}$. The system parameters are given in Table 3.1. As all considered filters are formulated in the discrete-time domain a discretization of the considered system is performed. Based on the Euler method the nonlinear discrete-time system

$$x_{k+1} = f(x_k, u_k) \times T_s + x_k, \tag{3.102}$$

is obtained, where T_s denotes the sampling time. The system has slow dynamics and the sampling time is chosen as $T_s = 0.1\,\text{s}$. The measurement model is

$$y_k = x_k + r_k, \tag{3.103}$$

where r_k is assumed to be zero-mean, white Gaussian noise described by the covariance matrix

$$R = E\{r_k r_k^T\} = \begin{bmatrix} \sigma_{C_A}^2 & 0 \\ 0 & \sigma_T^2 \end{bmatrix}, \qquad \sigma_{C_A} = 0.8 \times 10^{-3} \left[\frac{\text{mol}}{\text{l}}\right], \quad \sigma_T = 0.5\,[\text{K}]. \tag{3.104}$$

The initial state of the system is assumed to be

$$x_0 = \begin{bmatrix} 0.875\,[\text{mol/l}] \\ 325\,[\text{K}] \end{bmatrix}. \tag{3.105}$$

The considered filters are all initialized based on the measurement

$$\hat{x}_0 = y_0 = x_0 + r_0, \tag{3.106}$$

Table 3.2: Training process: computational effort and achieved accuracy with respect to the five training models (Training I, Training II, Training III, Training IV, Training V)

		Iterations	Convergence	$J(\mathcal{P}^\star)$	FLOPS	Time [min]
Training I	EKF	4189	yes	0.3755	181e7	3.59
	SVSF	4800	yes	0.4951	86e7	2.38
	CA	7074	yes	0.3697	11071e7	215.18
Training II	EKF	2873	yes	0.5908	124e7	2.59
	SVSF	5223	yes	0.5139	94e7	2.67
	CA	11045	yes	0.3659	20625e7	410.51
Training III	EKF	3907	yes	0.8531	169e7	3.28
	SVSF	3672	yes	0.8538	66e7	1.74
	CA	9093	yes	0.5751	1664e7	34.70
Training IV	EKF	3296	yes	0.4280	142e7	2.87
	SVSF	4753	yes	0.3167	86e7	2.40
	CA	11542	yes	0.2018	21387e7	414.53
Training V	EKF	4001	yes	0.8534	173e7	3.45
	SVSF	3578	yes	0.8538	64e7	1.78
	CA	9093	yes	0.5751	1664e7	34.36

Based on the Genetic Algorithm of MATLAB with default parameters, Iterations: calls of cost function, Convergence: change of cost function falls below tolerance, $J(\mathcal{P}^\star)$: minimum value of cost function, FLOPS: floating point operations, Time: computational time, Hardware: 4xCPU@3.7GHz with 8 GB memory

with the initial error covariance

$$\hat{P}_0^\dagger = P_0 = R. \tag{3.107}$$

The Jacobian of the system which is required to be known to apply the extended Kalman filter is stated in Appendix A.1.

3.5.1 Training Results

In the following the optimization of the tuning parameters of the SVSF, the combined estimation approach, and the extended Kalman filter is discussed. As previously explained, training models are required to be generated first. These training models are obtained by varying the values of the system parameters as follows. To account for the model uncertainty of the plant a variation of 20 percent from the nominal value is considered. This variation of 20 percent is a guess of the true model uncertainty and is assumed as a priorly known. Following the optimization scheme the i-th parameter of the training model j is obtained from the uniform distribution $p_i^{(j)} \sim U((1-0.2)p_{\text{nom},i}, (1+0.2)p_{\text{nom},i})$. Repeating the step for all parameters $i \in \{1, 2, \ldots, 10\}$ forms one training model. To account for the different combinations and variations of the system parameters five training models are

Table 3.3: Combined approach: optimized parameters and total exceedings of the boundary layer width related to the five training models (Training I, Training II, Training III, Training IV, Training V)

	Training I	Training II	Training III	Training IV	Training V
$\bar{\alpha}$	0.194050	0.267800	0.008947	0.279587	0.008947
$\bar{\beta}$	0.000121	0.000063	0.000046	0.026638	0.000046
$1-\bar{\alpha}-\bar{\beta}$	0.805829	0.732138	0.991007	0.693775	0.991007
$\bar{\iota}$	0.999999	0.999996	0.999996	0.970876	0.999996
$1-\bar{\iota}$	0.000001	0.000004	0.000004	0.029124	0.000004
η	0.406164	0.070489	0.147509	0.047929	0.147509
ζ	0.782612	0.998330	0.915384	0.603115	0.915384
ψ_1	782730	344703	361599	528841	361599
ψ_2	338831	564855	86378	370922	86378
N	293	356	5	353	5
$\lvert\Theta\rvert^*$	0/12000	0/12000	0/12000	0/12000	0/12000

* Counts the times the boundary layer width is exceeded according to (3.77) and divides it by the maximum number of possible exceedings.

build which are denoted as Training I, Training II, and so on. For each training model the filter parameters are optimized so that five sets of optimized parameters are obtained for each filter. In Table 3.1 an overview of the true system parameters, the nominal system parameters, and the parameter ranges used to build the training models is given.

The following filter parameters are optimized. For the SVSF the original filter algorithm (3.12)–(3.16) is considered with the tuning parameters

$$\mathcal{S}_{SVSF} = (\phi_1, \phi_2, \psi_1, \psi_2), \tag{3.108}$$

where ϕ_1, ϕ_2 denote the convergence rates and ψ_1, ψ_2 the boundary layer widths of the two system states. The parameters of the combined approach are

$$\mathcal{S}_{CA} = (\bar{\alpha}, \bar{\beta}, \bar{\iota}, \eta, \zeta, \psi_1, \psi_2, N). \tag{3.109}$$

To account for the model uncertainty the extended Kalman filter is applied based on a parametrization of the process noise covariance. Therefore, the process model (3.102) is considered to be affected by an additive noise term according to

$$x_{k+1} = f(x_k, u_k) \times T_s + x_k + q_k. \tag{3.110}$$

The noise q_k is assumed to be zero-mean, white noise with covariance $Q = E\{q_k q_k^T\}$. The covariance Q is unknown and according to

$$\mathcal{S}_{EKF} = (q_{11}, q_{12}, q_{22}), \qquad Q = \begin{bmatrix} q_{11} & q_{12} \\ q_{12} & q_{22} \end{bmatrix}, \tag{3.111}$$

the elements of Q are considered to be the tuning parameters of the EKF approach. The measurement noise covariance R is known as stated in (3.104).

The optimization problem (3.96) is solved based on the "genetic algorithm" of MATLAB with default settings. One iteration of the optimizer simulates the system response of the input

$$u_k = 2\sin\left(\frac{2\pi}{8\times 60}T_s k\right) + 1, \tag{3.112}$$

for a time span of 60 [min]. After the end of the iteration the filter parameters change according to the optimizer and the next iteration starts. During the optimization only one realization of measurement noise is considered so that the cost function does not vary due to noise. The computational time required for the optimization and the achieved estimation accuracy are shown in Table 3.2. For all training models the combined approach achieves the best estimation performance. Compared to the EKF the SVSF approach does not show improved estimation accuracy in general. The EKF as well as the SVSF are computationally more efficient than the combined approach. The optimized parameters of the combined approach are given by Table 3.3. Considering the gain

$$\Xi^{\star}_{k+1} = \bar{\iota}\left(R(\hat{P}^{\dagger}_{k+1|k} + R)^{-1}\right) + (1-\bar{\iota}) \times \operatorname{diag}\left\{I_n - \left|\Psi^{-1}\tilde{y}_{k+1|k}\right|\right\}, \tag{3.113}$$

of the combined approach it can be stated that the second term with the prefactor $1-\bar{\iota}$ is of minor importance as the optimized values of $1-\bar{\iota}$ are very small. As the second term denotes the SVSF gain it can be concluded that the SVSF gain does not contribute well to the achieved performance of the combined approach. In addition, from the last row of Table 3.3 it can be seen that the optimized boundary layer widths are so large that the output error never exceeds the boundary layer widths. As a consequence, the switching function Θ described by (3.82)–(3.83) does not have any effect on the combined approach. The feature of the SVSF to neglect the a priori estimation if the output error exceeds the boundary layer width does not contribute at all to the performance of the combined approach. The gain (3.113) of the combined approach is dominated by the first term which is the estimated Kalman filter gain. The estimated Kalman filter gain is affected by the estimation

$$\hat{P}^{\star}_{k+1|k} = \bar{\alpha}(\hat{S}_{k+1} - R) + \bar{\beta}\zeta R + (1-\bar{\alpha}-\bar{\beta})\hat{P}^{\dagger}_{k|k-1}, \tag{3.114}$$

of the error covariance according to (3.85). Regarding the optimized parameters of Table (3.3) it can be stated that the last term of (3.114) contributes most. The first term may have a noticeable effect whereas the second one is of minor importance. Consequently, a Kalman filter with a gain that is mostly steady-state but may have small adaption according to (3.52) shows best results in the training process. As the gain is mostly steady state the initial value is of great importance. The initial gain value depends on the initial error covariance P_0. The true initial error covariance is always known if the states are initialized based on the measurements as stated in (3.106). In that case the initial estimation error is R and the true initial error covariance is given by (3.107). For the sake of completeness the optimized parameters of the EKF and the SVSF are given in Appendix A.2.

Table 3.4: Test performance: mean μ and variance σ^2 of the estimation error criterion c_{error} over 100 realizations of the system response

System input	Parameter set		EKF	SVSF	CA	Meas.*
Step $u_k = +5\,\mathrm{K}$	Training I	μ	0.2867	0.2738	0.1995	0.8887
		σ^2	7.94e-05	1.42e-04	8.90e-05	3.76e-04
	Training II	μ	0.5086	0.2715	0.1978	0.8887
		σ^2	1.14e-04	1.39e-04	8.99e-05	3.76e-04
	Training III	μ	0.8475	0.8090	0.1963	0.8887
		σ^2	3.35e-04	3.77e-04	7.80e-05	3.76e-04
	Training IV	μ	0.3997	0.2361	0.1844	0.8887
		σ^2	7.78e-05	7.63e-05	7.54e-05	3.76e-04
	Training V	μ	0.8480	0.8090	0.1963	0.8887
		σ^2	3.36e-04	3.77e-04	7.80e-05	3.76e-04
Step $u_k = -5\,\mathrm{K}$	Training I	μ	0.2834	0.2566	0.1187	0.8925
		σ^2	6.34e-05	1.32e-04	5.03e-05	2.83e-04
	Training II	μ	0.5079	0.2540	0.1210	0.8925
		σ^2	1.07e-04	1.29e-04	6.60e-05	2.83e-04
	Training III	μ	0.8512	0.8121	0.1094	0.8925
		σ^2	2.57e-04	3.01e-04	3.98e-05	2.83e-04
	Training IV	μ	0.3788	0.1980	0.1054	0.8925
		σ^2	6.88e-05	5.86e-05	4.74e-05	2.83e-04
	Training V	μ	0.8516	0.8120	0.1094	0.8925
		σ^2	2.57e-04	3.01e-04	3.98e-05	2.83e-04

* Meas.: Considering the measurements as state estimations i. e. $\hat{x}_k = y_k$

3.5.2 Test Results

In this section the SVSF, the combined estimation approach, and the EKF are applied to the CSTR system with their previously optimized filter parameters. The considered real system parameters that are used to simulate the true behavior of the CSTR system are shown in Table 3.1. The step responses of the states C_A and T are generated for each step input that is applied to the system. In total two step inputs are considered: $u = 5\,[\mathrm{K}]$ and $u = -5\,[\mathrm{K}]$. The time span of the step responses is 6 [min]. All considered filters are run in parallel with the same inputs i. e. the same system inputs and the same measurements which have same noise realizations. The filtering performance is evaluated based on the mean squared estimation error according to

$$c_{error} = \frac{1}{N_s} \sum_{k=0}^{N_s} \tilde{x}_k^T \tilde{x}_k, \tag{3.115}$$

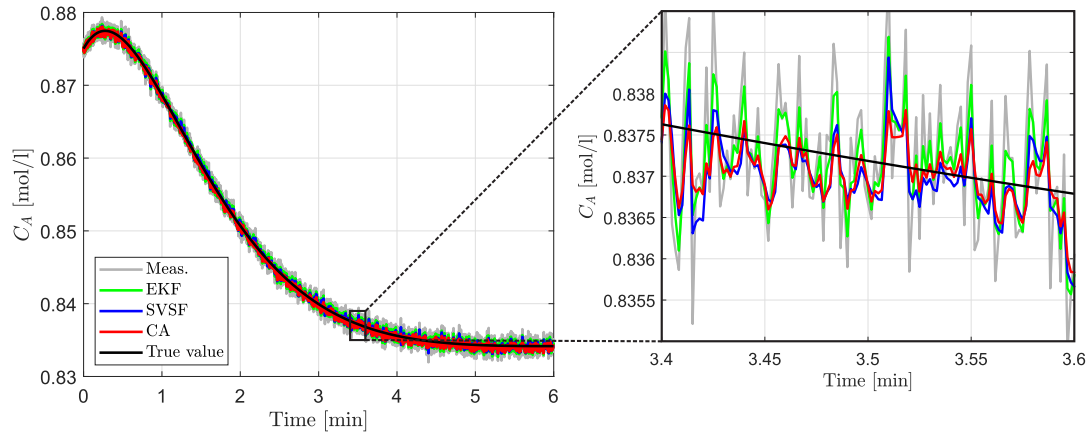

(a)

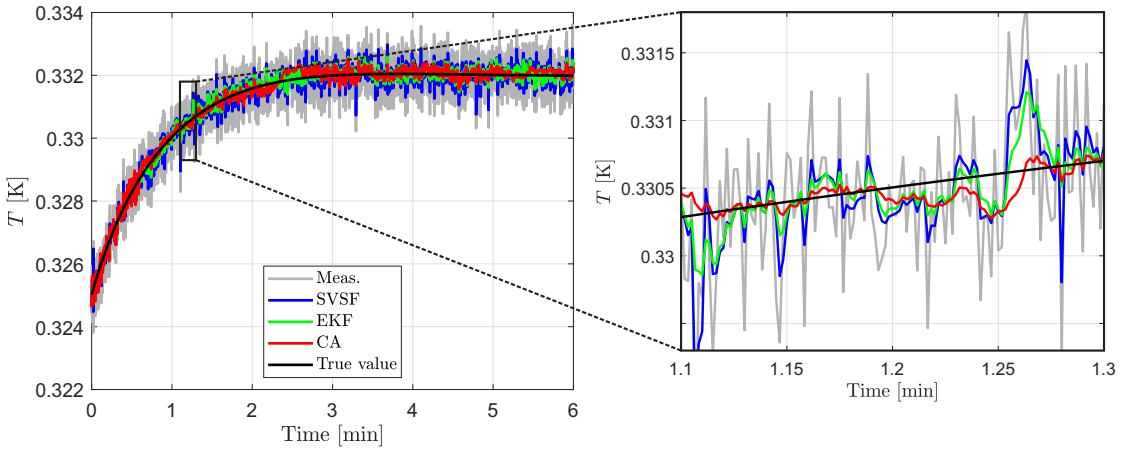

(b)

Figure 3.3: Comparison of the estimated states for step response $u_k = +5\,[\mathrm{K}]$. The filters are run with the parameter set that achieved the best test performance according to Table 3.4: EKF (Training I), SVSF (Training IV), CA (Training IV). Achieved estimation performance of the shown time series: EKF ($c_{error} = 0.2986$), SVSF ($c_{error} = 0.2482$), CA ($c_{error} = 0.1883$), Meas. ($c_{error} = 0.9067$). (a) State estimations of C_A (b) State estimations of T

where N_s denotes the number of samples that are generated within the simulated time span of 6 [min]. To account for variations of the estimation performance due to noise the step responses of the CSTR system are simulated 100 times. The filters are applied to that 100 realizations and the mean μ and variance σ^2 of the estimation error criterion c_{error} are determined. The obtained results are visualized in Table 3.4.

Considering the results for the step inputs $u = 5\,[\mathrm{K}]$ and $u = -5\,[\mathrm{K}]$ separately it can be stated that the worst estimation result of the combined approach is still better than the best estimation result of the other filters. For both step inputs $u = 5\,[\mathrm{K}]$ and $u = -5\,[\mathrm{K}]$ one realization of the step responses is plotted in Fig. 3.3 and 3.4. In addition, the estimated states of the filters are visualized. Each filter is applied with the set of

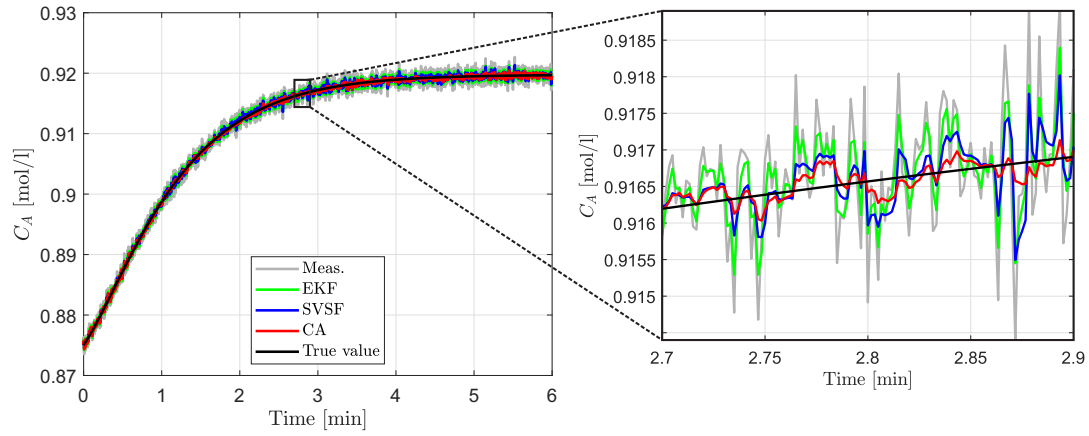

(a)

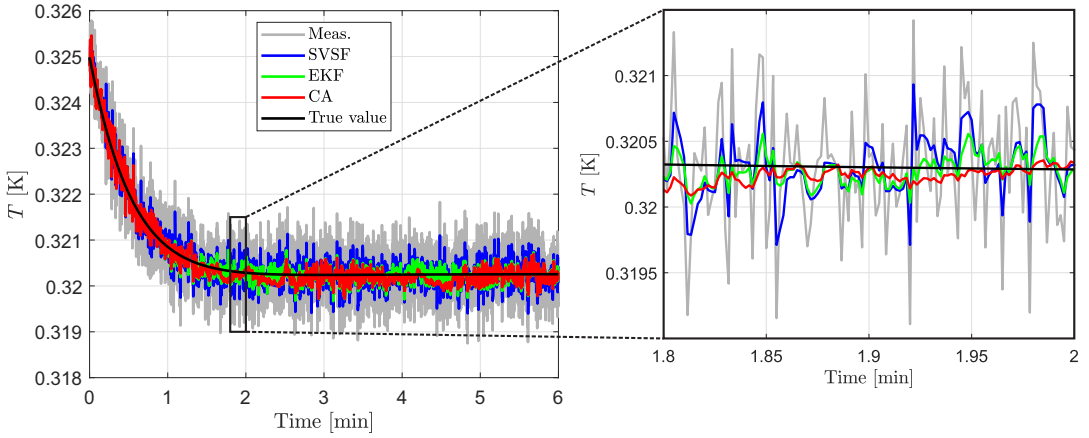

(b)

Figure 3.4: Comparison of the estimated states for step response $u_k = -5\,[\mathrm{K}]$. The filters are run with the parameter set that achieved the best test performance according to Table 3.4: EKF (Training I), SVSF (Training IV), CA (Training IV). Achieved estimation performance of the shown time series: EKF ($c_{error} = 0.2888$), SVSF ($c_{error} = 0.2063$), CA ($c_{error} = 0.1034$), Meas. ($c_{error} = 0.9162$). (a) State estimations of C_A (b) State estimations of T

optimized parameters that achieved the best estimation performance according to Table 3.4. From visual inspection of the graphs it can be seen that the deviation between the true and the estimated states is less severe in case of the combined estimation approach than it is for the other filters.

3.6 Summary

This chapter is about state estimation of nonlinear uncertain systems. The smooth variable structure filter and its theory are introduced. The SVSF is an estimation approach that can be applied to nonlinear uncertain systems. It is a nonlinear discrete-time filtering

approach that follows the predictor-corrector scheme of the Kalman filter. The boundary layer concept is applied to the SVSF to handle erroneousness of the a priori estimation that may arise from the imprecise system description. It is shown in this chapter that the a priori estimation is neglected if the output error exceeds the boundary layer width. This feature is identified as a feature that may make the SVSF more robust in comparison to other estimation approaches. However, the performance of the SVSF highly depends on user-defined parameters. In addition, the SVSF does not minimize any estimation performance criterion such as the mean squared error. Therefore, a combination of the SVSF and the Kalman filter is proposed. First, a reformulation of the SVSF is stated. The reformulation facilitates the design of the combined estimation approach as it gives a direct link between the Kalman filter and the SVSF. The combined approach should unify the robustness of the SVSF and the optimality of the Kalman filter. Therefore, the gain of the combined approach is formulated as a weighted sum of the SVSF and the Kalman filter gain. To apply the Kalman filter gain the error covariance is required to be known. The error covariance can not be recursively updated at each time step as that would require a linear precisely known system description. For that reason the error covariance itself is also estimated. The proposed combined estimation approach introduces several new tuning parameters like the weighting factors of the combined gain. A parameter optimization scheme is developed that can be applied to optimize any state estimation approach that is required to handle parametric model uncertainty. Parametric model uncertainty means that the discrepancy of the models only arises from the system parameters and is not structural. The proposed optimization scheme neither requires the true states of the real system to be known nor does it require any experimental data from the real system. The main idea of the proposed scheme is to design so-called training models from the known uncertain model description. This uncertain system description is denoted as the nominal model. The parameters of the nominal model are varied to determine the training models. The training models are used to simulate model discrepancy. This discrepancy arises as the filters make use of the nominal model but the incoming measurements are generated by the training models. As a consequence, the filter parameters can be optimized to handle the artificially generated model discrepancy. The developed combined estimation approach, the SVSF, as well as the extended Kalman filter are applied to a chemical plant to evaluate their estimation performance. All considered filters are optimized based on the proposed scheme. The combined estimation approach achieves the best performance during the optimization. It is also most accurate when it is applied to the real system. From the optimized weighting factors of the combined approach it can be stated that neither the boundary layer concept nor the SVSF gain contribute well to the achieved robustness. The combined approach with optimal weights behaves similar to a Kalman filter with a gain that is nearly steady-state. Only small gain adaptions may appear initiated by changes of the output estimation error. Finally, the originally claimed superiority of the SVSF against the Kalman filter cannot be confirmed in general. For future comparisons of the SVSF and the Kalman filter it is recommended to also tune the parameters of the Kalman filter in a suitable manner to achieve a fair comparison.

4 Chattering Mitigated Control of Uncertain Nonlinear Systems with Slow Dynamics

Chattering is known to be an undesired effect of conventional first order sliding mode control. It describes the high frequent switching of the control input that results from the discontinuity of the control law. Chattering mitigation has been subject to many research contributions in the past. A simple concept is the boundary layer approach introduced in Slotine (1984). It approximates the control law of the SMC in the near of the sliding surface. As a consequence, the chattering is mitigated but also the control accuracy is reduced. The approach requires to find a compromise between control accuracy and chattering attenuation. Higher order SMCs which drive the sliding variable and its time derivatives of corresponding order to zero can be applied to achieve chattering mitigation without any loss of the control accuracy (Levant, 2003). However, higher order SMCs require knowledge of higher order time derivatives. The time derivatives can be estimated by means of sliding mode differentiators. But the differentiators are sensitive to measurement noise which may have negative effects on the controlled system. Additionally, the higher order SMCs of Levant (2003) are restricted to the SISO case and require tuning of the controller gains. Another possibility to reduce chattering is the usage of exponential power reaching laws. These reaching laws reduce the switching gain in the near of the sliding surface so that mitigation of the chattering is achieved. The idea of the power reaching law is introduced in Gao and Hung (1993) and improved regarding the reaching time in Fallaha *et al.* (2010). Another problem appearing in practice is that the unknown uncertainty bounds of the system are overestimated. As the switching gain depends on these bounds the chattering effect can increase if the bounds are chosen too large. Therefore, SMC approaches with adaptive gains are proposed (Huang *et al.*, 2008; Plestan *et al.*, 2010; Obeid *et al.*, 2018; Edwards and Shtessel, 2016). The goal is to adaptively control the SMC gain so that the value of the gain is as small as possible but still large enough to keep the sliding mode established.

To mitigate the chattering combinations of SMC with other control methods may be considered. Due to its robustness sliding mode control is typically applied when the system description is not precisely known. As a consequence, the additional controller has to deal with model uncertainty too. Model-free control obviously does not require a precise model description. The combination of SMC and model-free control may provide some advantages. The SMC may dominate the control law during the reaching phase so that boundedness of the tracking error can be guaranteed whereas the model-free controller may dominate the control law in the near of the sliding surface so that chattering mitigation is achieved. Combinations of sliding mode and model-free control have already been considered in the literature. In Weng and Gao (2017) the dynamics of the sliding variable is estimated using input-output data. For the identified dynamics an equivalent control

law can be stated which reduces the required gain of the switching function and mitigates chattering. Also in Fei and Ding (2012) factors of the equivalent control law are adapted online using a radial basis function neural network. Intelligent PID control is combined with SMC in Wang *et al.* (2016). The PID controller is formulated with respect to a local system description to achieve reference tracking. As a result the SMC gain can be reduced but must be sufficient to account for the modeling errors of the local model. In Esmaeili *et al.* (2019); Ren *et al.* (2019) a dynamic linearization of the system behavior is obtained from input-output data to state an equivalent control law that reduces the required SMC gain.

To avoid high control inputs of the SMC, to mitigate chattering, and to make tracking more efficient combinations of SMC and MPC have also been proposed. However, the design of the MPC typically requires at least some local description of the input-output dynamics of the system. In Garcia-Gabin *et al.* (2009); Mitić *et al.* (2013) the quadratic value of the sliding variable is minimized over a considered time horizon. The obtained solution defines a predictive controller which keeps the states on the sliding surface. To guarantee that the sliding surface will be reached a conventional SMC with saturation function is added. The approach of Xu and Li (2011) is based on a MPC that is designed to reach the sliding surface. A switching gain is not required and the MPC guarantees to reach the sliding surface even in the presence of disturbances. However, only linear systems are considered. In Rubagotti *et al.* (2010) MPC is combined with integral SMC. The integral SMC is used to eliminate matched uncertainties which simplifies the design of a robust MPC approach.

In this chapter chattering mitigated control of nonlinear uncertain systems with sufficient slow dynamics is considered. A data-driven approach is developed. Based on input-output data of the system a linear local model is identified. The parameters of the local model are estimated by means of a Kalman filter. This allows to identify the system dynamics recursively and to update the local model online. The local model is used to predict the future system behavior. An optimization problem is formulated to minimize the squared tracking error and the input energy. The solution of the optimization problem defines a so-called receding horizon controller. As the identified dynamics are not guaranteed to describe the true system behavior exactly the receding horizon controller is combined with an adaptive SMC. The combined control law is designed in such a way that boundedess of the control tracking error can be guaranteed. In addition, the model-free controller dominates the control law in the vicinity of the sliding surface so that chattering mitigation is achieved. The focus of the proposed data-driven approach is to achieve chattering mitigated control without concrete system knowledge. The proposed approach makes adaptive SMC more efficient. The drawback of existing adaptive SMC strategies is that the controller gain cannot be reduced to small values. Sufficient large controller gains are always required to keep the system in sliding mode. However, the proposed method allows to scale down the SMC gain to zero as the model-free controller can take over. As a consequence, the chattering is highly reduced. The developed controller is tested on an uncertain nonlinear systems with slow dynamics. The proposed control method achieves accurate tracking without noticeable chattering in the stationary phase. For the considered specific system it is also shown that the control goals are achieve without knowing any concrete value of the system parameters.

The chapter is organized as follows. In Section 4.1 the model-free receding horizon controller is designed and as a proof of concept it is applied to a nonlinear system. The

proposed data-driven approach that combines the receding horizon controller with an adaptive SMC is described in Section 4.2. The section also considers a performance evaluation of the proposed control method.

4.1 Model-Free Control

In traditional model-based control a system model is derived based on the physical understanding of the underlying process. The obtained model may be imprecise due to parameter uncertainties, unmodeled dynamics, or changes of the operating conditions (Villagra *et al.*, 2012; Hou and Wang, 2013). Additionally, the modeling process may be complex, time consuming, and expensive (Piga *et al.*, 2017; Tanaskovic *et al.*, 2017).

Due to increased computational capabilities data-driven controllers (DDC) are getting more and more popular. According to Hou and Zhu (2013) DDC approaches can be splitted up into two main categories.

The first category considers approaches in which a priori knowledge about the controller structure is assumed to be known. Typically, the parameters of the controllers are determined or tuned by experiment. The classical PID controller belongs to this kind of DDC approaches as it is usually tuned by experiments based on e. g. the method of Ziegler-Nichols. Another approach of the category is the intelligent PID (iPID) controller proposed by Fliess and Join (2008). The iPID controller has a fixed structure that is formulated based on a local system description. The parameters of the controller are required to be tuned by experiment. In comparison to the original PID the proposed iPID shows better tracking performance and increased robustness (Agee *et al.*, 2015). Virtual reference control introduced in Campi *et al.* (2002) is another DDC approach. It can be applied to linear SISO systems and requires a desired closed loop transfer function to be stated. Based on input-output data the transfer function of the controller is calculated in such a way that the desired closed loop dynamics is achieved as accurately as possible. Iterative feedback tuning is a DDC approach proposed by Hjalmarsson *et al.* (1994). The goal is to find optimal controller parameters that minimize the squared tracking error. Therefore, the gradient of the system output with respect to the controller parameters is estimated based on experiments. Iterative learning control is a DDC approach for repetitive control tasks (Longman, 2000). The control task is repeated iteratively to update a sequence of control inputs so that after repeating the task several times the control accuracy improves. A learning rule is applied that feds back the control error to update the sequence of control inputs. The feedback gain of the learning rule is required to be tuned by experiment.

The second class of DDC approaches is based on the strategy to first identify an approximate system description and then calculate a generic control input based on that. Classical subspace identification approaches which determine a linear prediction equation based on orthogonal projections belong to this group (Favoreel *et al.*, 1999). The usage of neural networks (Doherty *et al.*, 1997) or support vector machines (Iplikci, 2006; Shin *et al.*, 2010) for the identification process is also common practice. Another strategy for the identification is the so-called dynamic linearization method proposed by Hou and Jin (2011). The approach continuously updates a linear prediction model based on input and output data.

In the following sections a receding horizon controller is determined based on a data-driven approach. In Section 4.1.1 the local dynamics of a nonlinear system are identified. A prediction equation is formulated that describes the input and output dynamics of the

system. In Section 4.1.2 an optimization problem is stated and a receding horizon controller is determined that minimizes the squared tracking error and the input energy. In Section 4.1.3 the receding horizon controller is tested on a nonlinear MIMO system. For the performance evaluation a set-point tracking problem with constraints is considered. In addition, the prediction capabilities of the identified local model are evaluated.

4.1.1 Recursive System Identification

In the following a local model is identified that describes the input and output dynamics of a nonlinear system. The local model is assumed to be linear which simplifies the identification process and the subsequently considered determination of the control input. To achieve adequate approximation capabilities of the local model the nonlinear system is required to have sufficient slow dynamics. As the local model is linear its parameters can be identified recursively through a Kalman filter. This allows to update the local model at every time step based on the incoming data of the system. Finally, the local model is rewritten to form a linear prediction equation of the system dynamics. This prediction equation is subsequently used to formulate an optimization problem from which a receding horizon controller is obtained.

The recursive system identification that is described as follows is originally proposed in Spiller *et al.* (2020).

A nonlinear discrete-time MIMO system is considered with an input-output behavior that is described by the nonlinear autoregressive exogenous (NARX) model

$$y_{k+1} = f_k(y_k, \dots, y_{k-n_y+1}, u_k, \dots, u_{k-n_u+1}), \qquad 1 \leq n_y \in \mathbb{N}, \quad 2 \leq n_u \in \mathbb{N}. \tag{4.1}$$

In (4.1) the number of delayed outputs is denoted by n_y and the number of delayed inputs is denoted by n_u. Let the outputs $y_k \in \mathbb{R}^r$ and inputs $u_k \in \mathbb{R}^m$ define the argument

$$s_k = \begin{bmatrix} y_k^T & \dots & y_{k-n_y+1}^T & u_k^T & \dots & u_{k-n_u+1}^T \end{bmatrix}^T \in \mathbb{R}^{rn_y+mn_u}, \tag{4.2}$$

of function $f_k(s_k)$. Based on the Taylor series the i-th component of y_{k+1} can be expressed as

$$\begin{aligned} y_{i,k+1} = y_{i,k} &+ (s_k - s_{k-1})^T Df_{i,k}(s_{k-1}) \\ &+ \frac{1}{2}(s_k - s_{k-1})^T D^2 f_{i,k}(s_{k-1})(s_k - s_{k-1}) + \dots, \qquad 1 \leq i \leq r, \end{aligned} \tag{4.3}$$

where $Df_{i,k}$ and $D^2 f_{i,k}$ denote the gradient and Hessian of the i-th component of f_k. Let the considered system have sufficient slow dynamics meaning that $\Delta s_k = |s_k - s_{k-1}|$ is sufficient small so that the influence of the higher order terms in (4.3) can be neglected. It follows that the dynamics are approximately described by the linearized input-output behavior

$$\begin{aligned} y_{k+1} \approx A_{1,k}y_k + A_{2,k}y_{k-1} + \dots + A_{n_y+1,k}y_{k-n_y} \\ + N_k u_k + B_{1,k}u_{k-1} + B_{2,k}u_{k-2} + \dots + B_{n_u,k}u_{k-n_u}, \end{aligned} \tag{4.4}$$

with $A_{i,k} \in \mathbb{R}^{r\times r}$, $B_{j,k} \in \mathbb{R}^{r\times m}$, and $N_k \in \mathbb{R}^{r\times m}$. The quantities $A_{i,k}, B_{j,k}, N_k$ in (4.4) define the transfer function matrix of a linear MIMO system. As a consequence, equation (4.4) completely describes the input-output behavior of a linear system (Isermann and

Münchhof, 2010, Chap. 17). The matrix polynomial (4.4) can be rewritten as a linear neural network

$$y_{k+1} \approx A_k \bar{y}_k + N_k u_k + B_k \bar{u}_{k-1} + b_k = \underbrace{\begin{bmatrix} A_k & N_k & B_k & b_k \end{bmatrix}}_{Z_k} \underbrace{\begin{bmatrix} \bar{y}_k^T & u_k^T & \bar{u}_{k-1}^T & 1 \end{bmatrix}^T}_{p_k}, \quad (4.5)$$

with weighting matrices

$$A_k = \begin{bmatrix} A_{1,k} & A_{2,k} & \dots & A_{n_y+1,k} \end{bmatrix}, \qquad B_k = \begin{bmatrix} B_{1,k} & B_{2,k} & \dots & B_{n_u,k} \end{bmatrix}, \qquad N_k, \quad (4.6)$$

inputs

$$\bar{y}_k = \begin{bmatrix} y_k^T & \dots & y_{k-n_y}^T \end{bmatrix}^T, \qquad \bar{u}_{k-1} = \begin{bmatrix} u_{k-1}^T & \dots & u_{k-n_u}^T \end{bmatrix}^T, \qquad u_k, \quad (4.7)$$

and bias vector $b_k \in \mathbb{R}^r$. The matrix of the network weights has the dimension $Z_k \in \mathbb{R}^{r \times n}$ with $n = r(n_y + 1) + m(n_u + 1) + 1$ and the input vector is of dimension $p_k \in \mathbb{R}^n$.

A vector

$$\zeta_k = \mathrm{vec}(Z_k) \quad (4.8)$$

of the unknown network parameters is obtained by applying the vector operator on the weighting matrix Z_k. The dimension of $\zeta_k \in \mathbb{R}^{nr}$ grows quadratically with r. Based on the vectorization the unknown network parameters can be estimated and recursively adapted by means of a Kalman filter. This allows online adaptation of the matrix polynomial (4.4) so that an updated system description is available at each time step k. According to Haykin (2001) a well-known Kalman filter-based estimation of the network parameters

$$\hat{\zeta}_k = \mathrm{vec}(\hat{Z}_k), \quad (4.9)$$

is given as

$$\hat{\zeta}_{k+1|k} = \hat{\zeta}_k, \quad (4.10)$$

$$P_{k+1|k} = P_k + Q, \quad (4.11)$$

$$\hat{\zeta}_{k+1} = \hat{\zeta}_{k+1|k} + K_{k+1}(y_{k+1} - H_{k+1}\hat{\zeta}_{k+1|k}), \quad (4.12)$$

$$K_{k+1} = P_{k+1|k} H_{k+1}^T (H_{k+1} P_{k+1|k} H_{k+1}^T + R)^{-1}, \quad (4.13)$$

$$P_{k+1} = K_{k+1} R K_{k+1}^T + (I_{nr} - K_{k+1} H_{k+1}) P_{k+1|k} (I_{nr} - K_{k+1} H_{k+1})^T, \quad (4.14)$$

where the output matrix

$$H_{k+1} = p_k^T \otimes I_r, \quad (4.15)$$

is obtained by applying the vector operator on (4.5). The output matrix is time-variant and has to be updated at each time step based on the vector p_k. The received data of the real system

$$\{y_{k+1}, p_k\} = \{y_{k+1}, \bar{y}_k, u_k, \bar{u}_{k-1}\}, \quad (4.16)$$

that is required to run the Kalman filter algorithm is assumed to be noise-free. Otherwise the measurement noise would affect the output matrix in (4.15). The Kalman filter is

known to be the solution of a recursive WLS estimation problem (see e. g. Sorenson, 1970). Consequently, algorithm (4.10)–(4.14) minimizes

$$\Lambda = \underset{(\zeta_i^\star)_{i=0}^k}{\arg\min} \|\zeta_0 - \zeta_0^\star\|^2_{P_0^{-1}} + \sum_{i=0}^{k} \|y_k - H_k\zeta_k^\star\|^2_{R^{-1}} + \sum_{i=0}^{k-1} \|\zeta_{k+1}^\star - \zeta_k^\star\|^2_{Q^{-1}}, \tag{4.17}$$

where $\Lambda = (\hat{\zeta}_i)_{i=0}^k$ are the Kalman filter estimations. The weighting matrices $Q = \alpha I_{nr}$ and $R = \beta I_r$ with scaling factors $0 \leq \alpha \in \mathbb{R}$, $0 < \beta \in \mathbb{R}$ are considered to be design variables to control the training process of the neural network. From the WLS problem (4.17) it can be seen that matrix R determines how exact the network parameters are estimated so that the predicted output fits to the received output of the true system. The matrix Q influences the learning rate of the network i.e. the rate of change of the estimated parameters. The estimated parameters of the network have to adapt during offline training but also online. The online adaptation is important as the behavior of the true system may change due to e. g. different operating conditions. The mean reason to apply the Kalman filter for the estimation process is the possibility to recursively update the local linear model online. It would also be possible to apply subspace identification methods. However, orthogonal projections actually solve least squares estimation problems (see e. g. Favoreel *et al.*, 1999). Consequently, also from subspace identification a least squares estimation of the matrix polynomial (4.5) would be obtained.

Based on the estimated matrix polynomial (4.5) the linear one step ahead prediction equation

$$y_{k+1} \approx \hat{A}_k \bar{y}_k + \hat{N}_k u_k + \hat{B}_k \bar{u}_{k-1} + \hat{b}_k, \tag{4.18}$$

is formulated. By defining a state vector

$$\bar{x}_k = \begin{bmatrix} \bar{y}_k^T & \bar{u}_{k-1}^T & \hat{b}_k^T \end{bmatrix}^T, \tag{4.19}$$

the linear state space description

$$\underbrace{\begin{bmatrix} \bar{y}_{k+1} \\ \bar{u}_k \\ \hat{b}_{k+1} \end{bmatrix}}_{\bar{x}_{k+1}} \approx \underbrace{\begin{bmatrix} \bar{A}_{11} & \bar{A}_{12} & \bar{A}_{13} \\ 0 & \bar{A}_{22} & 0 \\ 0 & 0 & I_r \end{bmatrix}}_{\bar{A}} \underbrace{\begin{bmatrix} \bar{y}_k \\ \bar{u}_{k-1} \\ \hat{b}_k \end{bmatrix}}_{\bar{x}_k} + \underbrace{\begin{bmatrix} \bar{N}_1 \\ \bar{N}_2 \\ 0 \end{bmatrix}}_{\bar{B}} u_k, \tag{4.20}$$

$$y_k = \underbrace{\begin{bmatrix} I_r & 0 & \dots & 0 \end{bmatrix}}_{\bar{C}} \bar{x}_k, \tag{4.21}$$

with

$$\bar{A}_{11} = \begin{bmatrix} \hat{A}_k \\ T \end{bmatrix}, \quad \bar{A}_{12} = \begin{bmatrix} \hat{B}_k \\ 0 \end{bmatrix}, \quad \bar{A}_{13} = \begin{bmatrix} I_r \\ 0 \end{bmatrix},$$
$$\bar{N}_1 = \begin{bmatrix} \hat{N}_k \\ 0 \end{bmatrix}, \quad \bar{A}_{22} = \begin{bmatrix} 0 \\ S \end{bmatrix}, \quad \bar{N}_2 = \begin{bmatrix} I_m \\ 0 \end{bmatrix},$$

and

$$T = \begin{bmatrix} I_r & 0 & \dots & 0 & 0 \\ 0 & I_r & \dots & 0 & 0 \\ \vdots & \vdots & \ddots & \vdots & \vdots \\ 0 & 0 & \dots & I_r & 0 \end{bmatrix}, \qquad S = \begin{bmatrix} I_m & 0 & \dots & 0 & 0 \\ 0 & I_m & \dots & 0 & 0 \\ \vdots & \vdots & \ddots & \vdots & \vdots \\ 0 & 0 & \dots & I_m & 0 \end{bmatrix},$$

is obtained. The dimension of the state vector $\bar{x}_k$ is $\bar{n} \times 1$ with $\bar{n} = r(n_y + 2) + mn_u$. The matrix $\bar{C}$ is of dimension $r \times \bar{n}$, the matrix T is of dimension $rn_y \times r(n_y + 1)$, and the matrix S is of dimension $m(n_u - 1) \times mn_u$.

4.1.2 Predictive Control

In this section two model-free control strategies are considered. First, a LS solution with minimal Euclidean norm is determined from the one step ahead prediction (4.18). Second, a receding horizon controller is realized based on the identified linear state space description (4.20)–(4.21).

Suppose y_k to be the measured system outputs and

$$z_k = Ly_k, \tag{4.22}$$

to be the control variables with $z_k \in \mathbb{R}^l$ and $L \in \mathbb{R}^{l \times r}$. A set-point tracking problem is considered where the reference values are denoted by $z_{ref,k}$. Multiplying the prediction equation (4.18) by L yields

$$z_{ref,k+1} = L\hat{A}_k\bar{y}_k + L\hat{N}_k u_k + L\hat{B}_k\bar{u}_{k-1} + L\hat{b}_k, \tag{4.23}$$

with u_k being the desired control input to achieve $z_{ref,k+1} \approx y_{k+1}$. A solution u_k of the equation

$$c_k = z_{ref,k+1} - L\hat{A}_k\bar{y}_k - L\hat{B}_k\bar{u}_{k-1} - L\hat{b}_k = L\hat{N}_k u_k, \tag{4.24}$$

can always be found if matrix $L\hat{N}_k \in \mathbb{R}^{l \times m}$ has full row rank. However, the rank of $L\hat{N}_k$ is unknown as the matrix depends on the network weights which are estimated online. What can be guaranteed is that at least one LS solution of (4.24) exists as the so-called normal equation

$$(L\hat{N}_k)^T c_k = (L\hat{N}_k)^T L\hat{N}_k u_k, \tag{4.25}$$

always has at least one solution u_k (see Kailath *et al.*, 2000, Lemma 2.A.2). If $L\hat{N}_k$ does not have full column rank then an infinity amount of LS solutions exists (Kailath *et al.*, 2000, Lemma 2.2.3). As in control minimization of the input energy is desirable it is suggested to choose the LS solution with minimal norm $\|u_k\|$. This solution with minimal norm can be obtained from a singular value decomposition (SVD). Let p be the rank of $L\hat{N}_k$. It follows that the SVD of $L\hat{N}_k$ is given by

$$L\hat{N}_k = \begin{bmatrix} U_1 & U_2 \end{bmatrix} \begin{bmatrix} \Sigma_1 & 0 \\ 0 & 0 \end{bmatrix} \begin{bmatrix} V_1 & V_2 \end{bmatrix}^T, \tag{4.26}$$

where $\Sigma_1 \in \mathbb{R}^{p \times p}$ is a diagonal matrix of the form

$$\Sigma_1 = \operatorname{diag}\left\{ \begin{bmatrix} \sigma_1 & \dots & \sigma_p \end{bmatrix}^T \right\}, \tag{4.27}$$

with $0 \leq \sigma_i \in \mathbb{R}$ denoting the singular values of $L\hat{N}_k$. Matrices U_1 and V_1 have p columns. According to Demmel (1997, Proposition 3.3) the LS solution with minimal Euclidean norm $\|\cdot\|$ can be determined as

$$u_k^\dagger = V_1\Sigma_1^{-1}U_1^T c_k. \tag{4.28}$$

In the sequel $u_k^\dagger$ will be denoted as min-LS solution i. e. minimal Euclidean norm LS solution. If the matrix $L\hat{N}_k$ has full column rank then the LS solution is unique and coincides with the min-LS solution (4.28). This follows from the fact that the SVD equals the Moore–Penrose inverse (Demmel, 1997, Definition 3.2).

The min-LS solution is based on a one step ahead prediction of the system outputs. However, from MPC it is known that consideration of a prediction horizon is more effective regarding minimization of input energy and squared tracking error. Consequently, the receding horizon control problem

$$\begin{aligned} \vec{u}^* &= \arg\min_{\vec{u}} \frac{1}{2} \left(\sum_{i=k}^{k+n_p-1} e_i^T Q_{cont} e_i + \sum_{i=k}^{k+n_c-1} u_i^T R_{cont} u_i \right), \\ \vec{u} &= \begin{bmatrix} u_k^T & u_{k+1}^T & \dots & u_{k+n_c-1}^T \end{bmatrix}^T, \end{aligned} \tag{4.29}$$

subject to

$$y_{k+1} = \hat{A}_k \bar{y}_k + \hat{N}_k u_k + \hat{B}_k \bar{u}_{k-1} + \hat{b}_k, \tag{4.30}$$

$$\bar{y}_k = \begin{bmatrix} y_k^T & y_{k+1}^T & \dots & y_{k-n_y}^T \end{bmatrix}^T, \tag{4.31}$$

$$\bar{u}_{k-1} = \begin{bmatrix} u_{k-1}^T & y_k^T & \dots & u_{k-n_u}^T \end{bmatrix}^T, \tag{4.32}$$

$$z_k = L y_k, \tag{4.33}$$

$$e_k = z_k - z_{ref,k} \tag{4.34}$$

$$A_c \vec{u} \leq b_c, \tag{4.35}$$

is considered. The quantities $Q_{cont} \succeq 0$ and $R_{cont} \succeq 0$ denote weighting matrices. The length of the control horizon is quantified by $1 \leq n_c \in \mathbb{N}$ and the length of the prediction horizon n_p is chosen as $n_c < n_p$. Within the control horizon the input u_k can be varied. After the end of the control horizon the input is kept fixed until the end of the prediction horizon is reached. This distinction between control and prediction horizon is made to reduce the computational load as less control inputs are required to be determined (Wang, 2009). Equations (4.30)–(4.33) describe the assumed system dynamics according to the identified model (4.18). The tracking error e_k is defined by equation (4.34). Output constraints $y_k \in \mathcal{Y}_k \subseteq \mathbb{R}^r$ as well as input constraints $u_k \in \mathcal{U}_k \subseteq \mathbb{R}^m$ are defined by the convex polytope (4.35). Let $0 \leq n_{const} \in \mathbb{N}$ denote the number of constraints then $A_c \in \mathbb{R}^{n_{const} \times n_c m}$ and $b_c \in \mathbb{R}^{n_{const}}$. The optimization problem (4.29) can be solved by rewriting it as a quadratic program see e. g. Wang (2009). This is a standard problem in linear MPC and a brief solution according to Wang (2009) is given as follows. The state space model (4.20)–(4.21) is augmented by the reference variable according to

$$\underbrace{\begin{bmatrix} \bar{x}_{k+1} \\ z_{ref,k+1} \end{bmatrix}}_{\tilde{x}_{k+1}} = \underbrace{\begin{bmatrix} \bar{A} & 0 \\ 0 & I_l \end{bmatrix}}_{\tilde{A}} \underbrace{\begin{bmatrix} \bar{x}_k \\ z_{ref,k} \end{bmatrix}}_{\tilde{x}_k} + \underbrace{\begin{bmatrix} \bar{B} \\ 0 \end{bmatrix}}_{\tilde{B}} u_k. \tag{4.36}$$

The tracking error

$$e_k = \underbrace{\begin{bmatrix} L\bar{C} & -I_l \end{bmatrix}}_{\tilde{C}} \tilde{x}_k, \tag{4.37}$$

is considered to be the output of the augmented model. From (4.36)–(4.37) the prediction equation of the tracking error

$$\underbrace{\begin{bmatrix} e_k \\ e_{k+1} \\ e_{k+2} \\ e_{k+3} \\ \vdots \\ e_{k+n_p-1} \end{bmatrix}}_{\vec{e}} = \underbrace{\begin{bmatrix} \tilde{C} \\ \tilde{C}\tilde{A} \\ \tilde{C}\tilde{A}^2 \\ \tilde{C}\tilde{A}^3 \\ \vdots \\ \tilde{C}f_{\tilde{A}}(n_p-1) \end{bmatrix}}_{\mathcal{Q}} \tilde{x}_k + \underbrace{\begin{bmatrix} 0 & 0 & 0 & \dots \\ \tilde{C}\tilde{B} & 0 & 0 & \dots \\ \tilde{C}\tilde{A}\tilde{B} & \tilde{C}\tilde{B} & 0 & \dots \\ \tilde{C}\tilde{A}^2\tilde{B} & \tilde{C}\tilde{A}\tilde{B} & \tilde{C}\tilde{B} & \dots \\ \vdots & \vdots & \vdots & \ddots \\ \tilde{C}f_{\tilde{A}}(n_p-2)\tilde{B} & \tilde{C}f_{\tilde{A}}(n_p-3)\tilde{B} & \tilde{C}f_{\tilde{A}}(n_p-4)\tilde{B} & \dots \end{bmatrix}}_{\mathcal{T}} \underbrace{\begin{bmatrix} u_k \\ \vdots \\ u_{k+n_p-2} \end{bmatrix}}_{\vec{u}}, \tag{4.38}$$

with

$$f_{\tilde{A}}(x) = \begin{cases} \tilde{A}^x & \text{if } x \geq 0, \\ 0_{(\bar{n}+l)\times(\bar{n}+l)} & \text{else,} \end{cases} \tag{4.39}$$

is obtained. Substituting (4.38) in (4.29) yields the quadratic program

$$\vec{u}^* = \arg\min_{\vec{u}} \frac{1}{2}\vec{u}^T G\vec{u} + d^T\vec{u}, \tag{4.40}$$

subject to

$$A_c\vec{u} \leq b_c, \tag{4.41}$$

with

$$G = M^T\mathcal{T}^T\tilde{Q}_{cont}\mathcal{T}M + \tilde{R}_{cont}, \qquad \tilde{Q}_{cont} = I_{n_p} \otimes Q_{cont},$$
$$d^T = \tilde{x}_k^T\mathcal{Q}^T\tilde{Q}_{cont}\mathcal{T}M, \qquad \tilde{R}_{cont} = I_{n_c} \otimes R_{cont}.$$

The matrix M is the move blocking matrix which is defined according to

$$\underbrace{\begin{bmatrix} \tilde{u}_k \\ \tilde{u}_{k+1} \\ \vdots \\ \tilde{u}_{k+n_c-2} \\ \tilde{u}_{k+n_c-1} \\ \tilde{u}_{k+n_c} \\ \vdots \\ \tilde{u}_{k+n_p-2} \end{bmatrix}}_{\vec{\tilde{u}}} = \underbrace{\begin{bmatrix} I_m & 0 & \dots & 0 & 0 \\ 0 & I_m & \dots & 0 & 0 \\ \vdots & \vdots & \ddots & \vdots & \vdots \\ 0 & 0 & \dots & I_m & 0 \\ 0 & 0 & \dots & 0 & I_m \\ 0 & 0 & \dots & 0 & I_m \\ \vdots & \vdots & & \vdots & \vdots \\ 0 & 0 & \dots & 0 & I_m \end{bmatrix}}_{M} \underbrace{\begin{bmatrix} u_k \\ u_{k+1} \\ \vdots \\ u_{k+n_c-1} \end{bmatrix}}_{\vec{u}}. \tag{4.42}$$

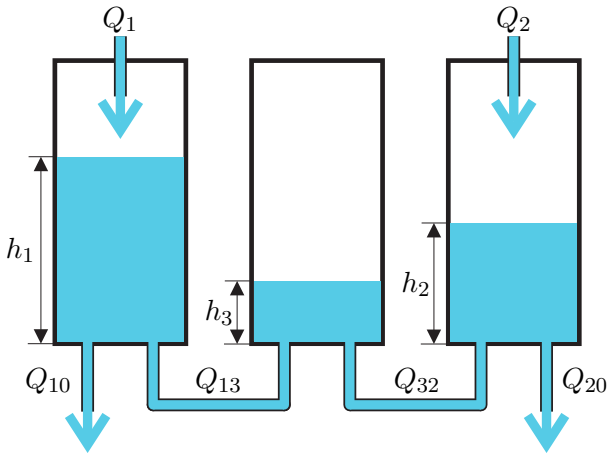

Figure 4.1: Three tank water system

To reduce the computational load the move blocking matrix keeps the system inputs fixed if the end of the control horizon has been reached. As stated in Hiriart-Urruty and Lemaréchal (2013, p. 291) an optimization problem is convex if its objective function is convex and the feasibility set is a convex set. The objective function of (4.40) is convex as G is positive semi-definite. The feasibility set is convex as (4.41) is a convex polytope. The hard constraints of (4.41) may lead to infeasibility problems as discussed in e. g. Kerrigan and Maciejowski (2000). If the output variables leave the admissible region caused by some disturbance (like inaccuracy of the trained system model) then the optimization problem is unfeasible. Even if the output variables are inside the admissible region a conflict of constraints may appear. It could happen that the control input has to exceed its limits to keep the output variables in the admissible region. To avoid infeasibility problems the hard constraints are reformulated as soft constraints. Soft constraints do not guarantee the hard constraints to be satisfied in general. However, using so-called slack variables the hard constraints will be almost satisfied in practice. A description of the considered optimization problem with reformulated soft constraints based on slack variables can be found in Appendix B. From the optimized chain of control inputs

$$\vec{u}^* = \begin{bmatrix} u_k^{*T} & u_{k+1}^{*T} & \dots & u_{k+n_c-1}^{*T} \end{bmatrix}^T,$$

the first input u_k^* is applied to the system. In the sequel u_k^* is denoted as predictive control (PC) solution.

4.1.3 Application Example

In this section the previously discussed model-free controllers namely the PC approach and the min-LS approach are applied to a nonlinear uncertain system with slow dynamics. A three tank water system as shown in Fig. 4.1 is considered. According to Hou and Jin (2011) the dynamics of the water levels in the tanks are described by

$$S_A \dot{h}_1 = Q_1 - Q_{13} - Q_{10}, \tag{4.43}$$
$$S_A \dot{h}_3 = Q_{13} - Q_{32}, \tag{4.44}$$
$$S_A \dot{h}_2 = Q_2 + Q_{32} - Q_{20}, \tag{4.45}$$

Table 4.1: Parameters of three tank water system (Hou and Jin (2011))

Parameter	Symbol	Value
Section of cylinders	S_A	$0.0154\,[\mathrm{m}^2]$
Section of connections	S_n	5e-5 $[\mathrm{m}^2]$
Maximum liquid levels	h_{max}	$0.6\,[\mathrm{m}]$
Maximum supply flow rates	$Q_{\max}$	$0.0001\,[\mathrm{m}^3/\mathrm{s}]$
Outflow coefficient	γ_1	0.22
Outflow coefficient	γ_2	0.28
Outflow coefficient	γ_3	0.27

with

$$Q_{13} = \gamma_1 S_n \mathrm{sgn}(h_1 - h_3)\sqrt{2g|h_1 - h_3|}, \tag{4.46}$$

$$Q_{32} = \gamma_3 S_n \mathrm{sgn}(h_3 - h_2)\sqrt{2g|h_3 - h_2|}, \tag{4.47}$$

$$Q_{20} = \gamma_2 S_n \mathrm{sgn}(h_2)\sqrt{2g|h_2|}, \tag{4.48}$$

$$Q_{10} = \gamma_2 S_n \mathrm{sgn}(h_1)\sqrt{2g|h_1|}, \tag{4.49}$$

where h_1, h_2, h_3 are the water levels of the three tanks, Q_1, Q_2 are the incoming water flows from pump 1 and 2, Q_{10}, Q_{20} are the flows in the outflow valves of tank 1 and 2, and Q_{13}, Q_{32} are flows in the connecting pipes of tank 1, 2, and 3. The system parameters are assumed as unknown and are summarized in Table 4.1. The control goal is to achieve set-point tracking of the water levels h_1 and h_2 based on the inlet streams Q_1 and Q_2. The input signals are restricted to

$$0 \leq Q_1 \leq Q_{max}, \qquad 0 \leq Q_2 \leq Q_{max}. \tag{4.50}$$

All levels h_1, h_2, h_3 are measured. The system is discretized based on the Euler method with a sampling time of 1 [s], and a simulation duration of 1500 [s]. The initial water levels are zero i. e. $h_1(t_0) = h_2(t_0) = h_3(t_0) = 0\,[\mathrm{m}]$. The network parameters are tuned by trial and error based on the tracking performance of the resulting controllers. The number of delayed network inputs is set to $n_y = n_u = 2$ and the network weights are initialized with $\hat{x}_0 = \mathbf{1}_{33}$, $P_0 = I_{33} \times 10^{10}$. A learning rate of $\alpha = 0.001$ is considered and β is chosen as $\beta = 0.01$. The network is initially trained from $t^* = 0...5000\,[\mathrm{s}]$ based on the system outputs generated by the inputs

$$Q_1 = Q_2 = \begin{cases} 0.00002\,\cos\left(\frac{2\pi}{1000}t^*\right) + 0.00008 & \text{if } t^* \bmod 333 \text{ is even,} \\ 0 & \text{otherwise.} \end{cases} \tag{4.51}$$

Related to the cost function of the PC approach the weighting matrices $Q_{cont} = I_2$ and $R_{cont} = I_2$ are considered.

Table 4.2: Performance evaluation w/o constraints

	Time horizon	$\sum_{i=1}^{N} u_i^2/N$	$\sum_{i=1}^{N} e_i^2/N$
min-LS	one step	2.7332569e-9	0.0032333
PC	$n_p = 10, n_c = 9$	2.7643026e-9	0.0032186
PC	$n_p = 20, n_c = 19$	2.7650868e-9	0.0032099
PC	$n_p = 30, n_c = 29$	2.7655725e-9	0.0032064
PC	$n_p = 40, n_c = 39$	2.7665269e-9	0.0032047
PC	$n_p = 50, n_c = 49$	2.7666369e-9	0.0032041
PC	$n_p = 60, n_c = 59$	2.7669043e-9	0.0032039
PC	$n_p = 70, n_c = 69$	2.7672953e-9	0.0032039
PC	$n_p = 80, n_c = 79$	2.7743995e-9	0.0032062
PC	$n_p = 90, n_c = 89$	2.7746371e-9	0.0032063

Unconstrained Control Problem

For the set-point tracking problem the reference values of h_1 and h_2 are chosen as

$$h_{ref,1}(t) = \begin{cases} 0.15\,[\mathrm{m}] & \text{if } t \leq 400\,[\mathrm{s}], \\ 0.3\,[\mathrm{m}] & \text{if } 400\,[\mathrm{s}] < t \leq 700\,[\mathrm{s}], \\ 0.15\,[\mathrm{m}] & \text{if } 700\,[\mathrm{s}] < t \leq 1500\,[\mathrm{s}], \end{cases} \tag{4.52}$$

$$h_{ref,2}(t) = \begin{cases} 0.2\,[\mathrm{m}] & \text{if } t \leq 400\,[\mathrm{s}], \\ 0.4\,[\mathrm{m}] & \text{if } 400\,[\mathrm{s}] < t \leq 700\,[\mathrm{s}], \\ 0.2\,[\mathrm{m}] & \text{if } 700\,[\mathrm{s}] < t \leq 1000\,[\mathrm{s}], \\ 0.05\,[\mathrm{m}] & \text{if } 1000\,[\mathrm{s}] < t \leq 1500\,[\mathrm{s}], \end{cases} \tag{4.53}$$

where $t = 0 \ldots 1500\,[\mathrm{s}]$ denotes the simulation time.

The tracking performance of both controllers is evaluated in Table 4.2. Different lengths of the prediction horizon are considered for the PC approach. The min-LS approach has no tuning parameters and always achieve the given result. The best tracking performance of the PC approach is achieved if 60 or 70 time steps (60 or 70 seconds) are chosen for the length of the prediction horizon. Due to the limited prediction capabilities of the neural network further enhancement of the prediction horizon leads to a loss of control accuracy. The closed loop behavior is visualized by the time series of Fig. 4.2. The main difference between the two controllers occurs after 16.67 seconds when the set-point switches from $h_{ref,2} = 0.2\,[\mathrm{m}]$ to $h_{ref,2} = 0.05\,[\mathrm{m}]$. This switching instantly leads to a relatively high tracking error of control variable h_2. The predictive control approach anticipates that a reduction of the water level h_1 will improve the overall control accuracy. Although the reduction initially induces a control error related to h_1 it reduces the water level h_3 of the middle tank. As the amount of water in the middle tank is reduced the water level h_2 can decrease more quickly so that the overall control performance is improved. This effect is only present if the length of the prediction horizon is sufficient large. In Fig.

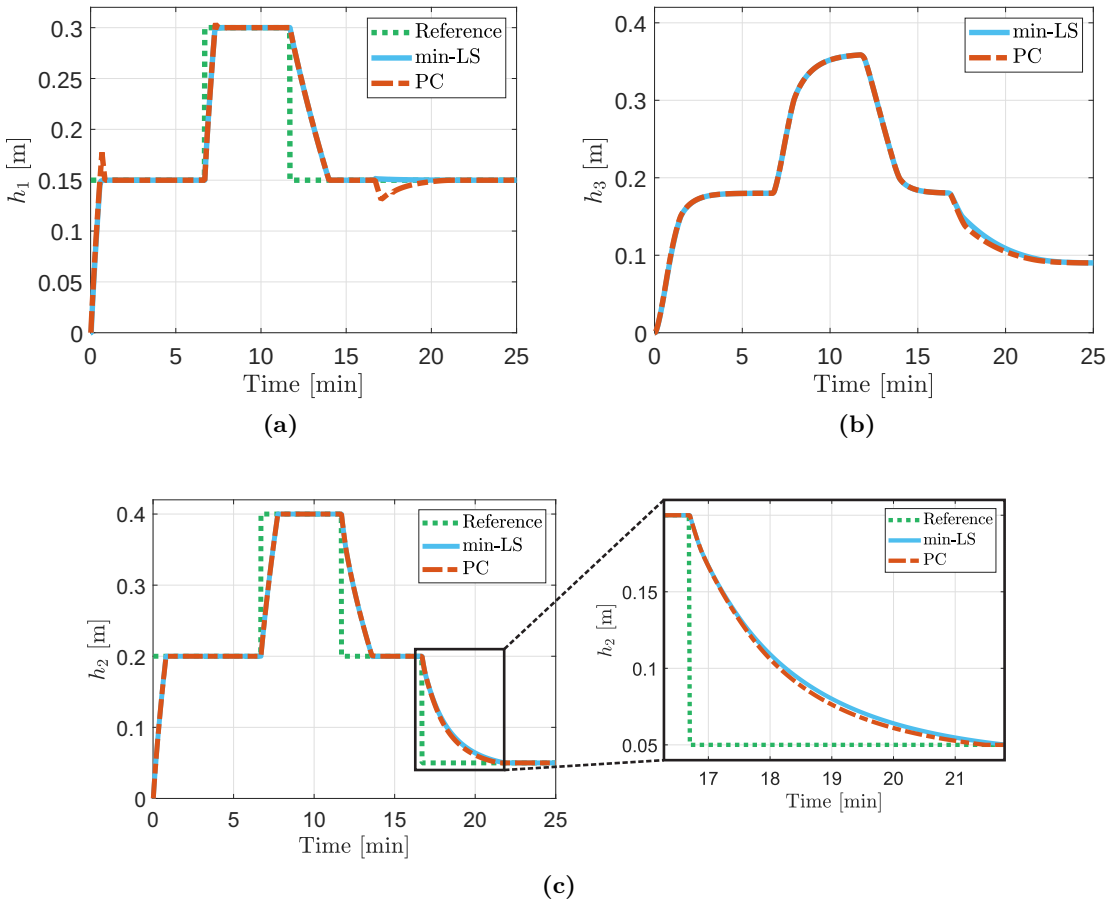

Figure 4.2: Tracking performance of model-free controllers. Parameters of PC approach: $n_p = 60$ and $n_c = 59$ (prediction horizon of 60 [s]). (a) Water level h_1 of left tank. (b) Water level h_3 of middle tank. (c) Water level h_2 of right tank.

4.3 the control inputs of both approaches are visualized. At around 16.67 seconds when the switching from $h_{ref,2} = 0.2$ [m] to $h_{ref,2} = 0.05$ [m] occurs control input Q_1 of the PC approach temporarily goes to zero leading to the improved overall performance.

The prediction capabilities of the network are evaluated in Fig. 4.4a. Starting from time instant 10 [min] the network is fed with its own outputs for a considered prediction horizon of 15 [min]. Naturally, the prediction accuracy decreases over time. To measure the adaption of the network the change of the network weights according to

$$\Delta Z_k = Z_k - Z_{k-1}, \tag{4.54}$$

is considered. Matrix Z_k as defined in (4.5) contains all network parameters. It is suggested to apply the Frobenius norm to (4.54) to obtain a scalar value reflecting the absolute change of the network parameters. The resulting time series $\|\Delta Z_k\|$ is visualized in Fig. 4.4b. It can be observed that the amount of adaption decreases over time. Adaption is present especially when set-points and control inputs change.

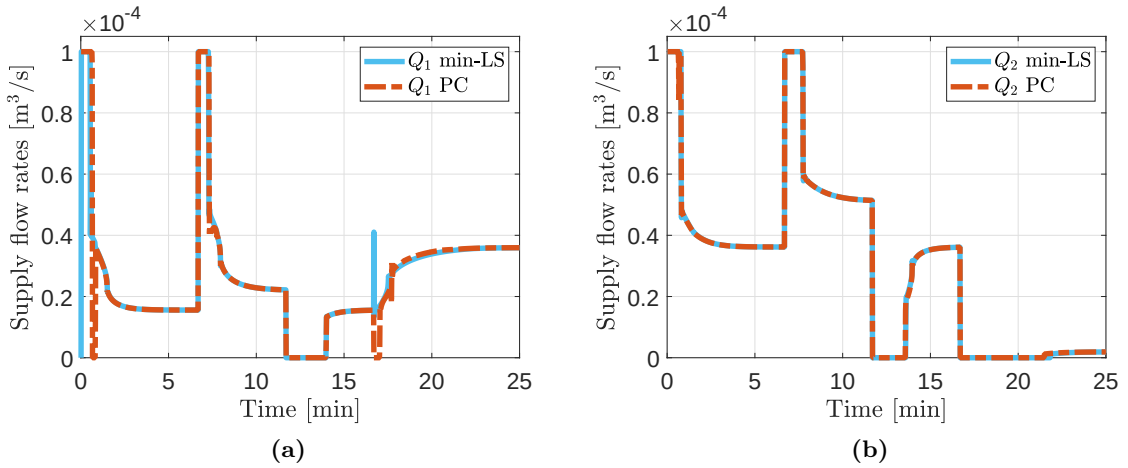

Figure 4.3: Control inputs of model-free controllers. (a) Input flow Q_1 of left tank. (b) Input flow Q_2 of right tank.

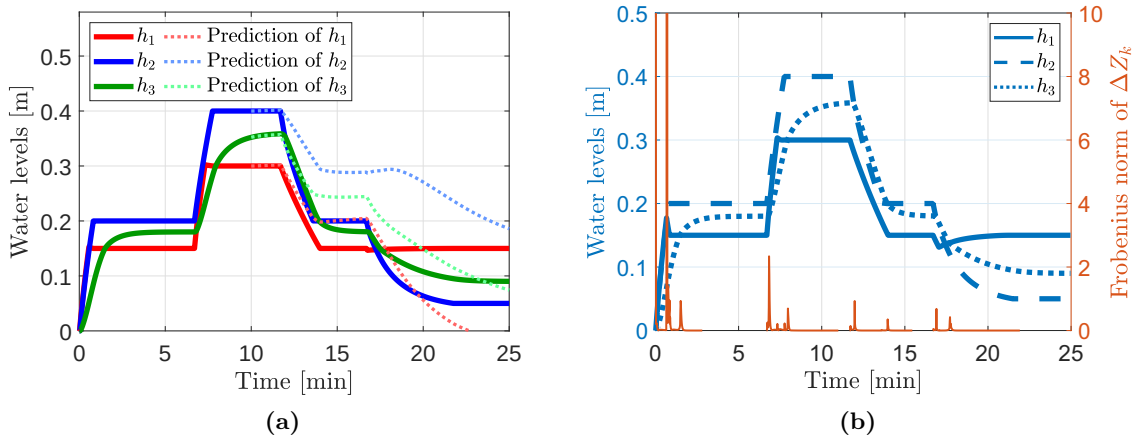

Figure 4.4: Performance evaluation of neural network. (a) Network predictions compared with true system outputs. Prediction starts at 10 [min] and ends at 25 [min] so that a prediction horizon of 15 [min] is considered. (b) Adaption of network weights exemplarily given for the closed loop system controlled by the min-LS approach.

Constrained Control Problem

For the constrained control problem the references defined by (4.52) and (4.53) remain the same. In addition, the water level of tank three is restricted according to

$$h_3 \leq 0.3\,[\mathrm{m}]. \tag{4.55}$$

By modifying the output matrix $\tilde{C}$ in (4.38) the constraint can be formulated as a polytope $A_c\vec{u} \leq b_c$. The constraint is implemented as a soft-constraint using a vector of slack variables ν. Details about the implementation of the constraint can be found in Appendix B. Minimizing the term $\nu^T\nu$ enforces the slack variables to be close to zero which guarantees the constraints to be almost satisfied. The performance of the PC approach for the

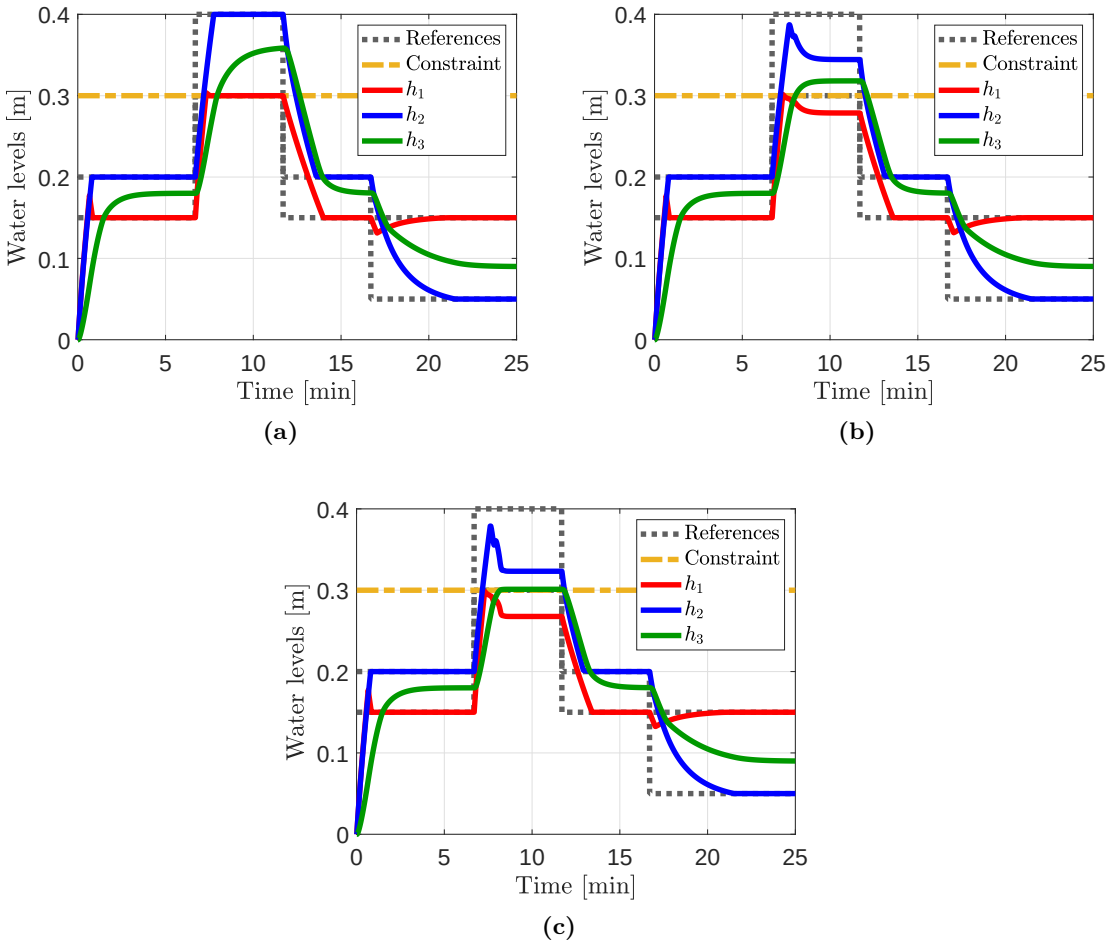

Figure 4.5: Constrained model-free control. Application of PC approach with $n_p = 60$, $n_c = 59$, and weights $W = I_{60} \times w$, where $w \geq 0$ is related to the minimization of the slack variables ν according to Appendix B equations (B.5)–(B.7). Minimization of $\nu^T\nu$: (a) Not enforced ($w = 0$). (b) Slightly enforced ($w = 5$). (c) Highly enforced ($w = 100$).

constrained control problem is visualized in Fig. 4.5. The figure shows that the constraint is enforced by minimizing the term $\nu^T\nu$. From the figure also the predictive nature of the controller can be detected. The water levels of tanks h_1 and h_2 decrease before h_3 reaches the bound of the constraint.

4.1.4 Summary

In this section model-free control of nonlinear systems with sufficient slow dynamics is considered. A data-driven approach is proposed which identifies a local model that describes the input-output dynamics. The system identification is achieved through a Kalman filter. That allows to update the local model at each time step based on the incoming measurements of the true system. The local model is applied to predict the future behavior of the nonlinear system. Two controllers for set-point tracking problems are proposed. The min-LS approach considers a one step ahead prediction of the system behavior. The goal

is to determine a control input that generates the desired system outputs after one time step. As such a control input is not guaranteed to exist the LS solution is considered instead. The LS solution is guaranteed to exist and it provides the solution with the least squared tracking error. The LS solution is not guaranteed to be unique. Therefore, the LS solution with minimal Euclidean norm is selected to achieve minimization of the input energy. The second proposed method is the model-free predictive controller. An optimization problem is stated in which the system behavior is predicted over a horizon of multiple time steps. For the considered horizon the squared tracking error and the input energy are minimized. In addition, input and output constraints may be considered. The solution of the optimization problem defines the predictive controller. Both proposed controllers are applied to a nonlinear MIMO system with slow dynamics. The dynamics of the system are completely unknown. Two set-point tracking problems are considered. One with and one without constraints. The min-LS approach solves the set-point tracking problem without constraints whereas the predictive controller can solve both the unconstrained and the constrained set-point tracking problem. In comparison to the min-LS approach the predictive controller achieves better control accuracy. In addition, the prediction capabilities of the local model are confirmed. The local model is also shown to adapt online especially if changes of the control set-point appear.

4.2 Combined Adaptive Sliding Mode and Receding Horizon Control

In this section the previously developed model-free predictive controller is combined with an adaptive SMC. The primary goal of the controller design is to achieve chattering mitigated sliding mode control. In addition, the proposed combination of the controllers should guarantee the control tracking error to be bounded. To achieve the desired goals a boundary layer is introduced. Outside of the boundary layer the control input of the model-free controller is suppressed and the gain of the SMC is increased. As a result, the states are guaranteed to be pushed towards the sliding surface. When the sliding surface is approached and the states are within the boundary layer the model-free predictive controller becomes active and the gain of the SMC is scaled down. Consequently, in the vicinity of the sliding surface the control input is dominated by the model-free controller which greatly mitigates the chattering effect.

The subsequently described concept is originally developed in Spiller and Söffker (2020*a*).
The section is organized as follows. In Section 4.2.1 additional assumptions are made that are required to combine the proposed model-free predictive controller with an adaptive SMC. In Section 4.2.2 the new chattering mitigated controller is proposed. In Section 4.2.3 the developed control method is applied to a nonlinear uncertain system and its performance with regards to chattering mitigation is studied.

4.2.1 Additional Assumptions

In addition to the requirements that are stated in Section 4.1.1 the following assumptions are made. The nonlinear system is assumed to be input-affine according to

$$\begin{aligned} \dot{x} &= a(x) + b(x)u, \\ y &= h(x). \end{aligned} \tag{4.56}$$

Further, it is assumed that the number of inputs $u \in \mathbb{R}^m$ equals the number of control variables $z \in \mathbb{R}^m$. The control variable $z(t)$ and the tracking error $e(t)$ are defined identical to its discrete-time pendants i. e.

$$z(t) = Ly(t), \qquad e(t) = z_{ref}(t) - z(t). \tag{4.57}$$

For each control variable a sliding manifold is defined. Let $\sigma \in \mathbb{R}^m$ be a vector of sliding variables then the sliding manifolds are defined by

$$\sigma_i = a_{n_i,i}\frac{\partial^{n_i}}{(\partial t)^{n_i}}e_i + a_{n_i-1,i}\frac{\partial^{n_i-1}}{(\partial t)^{n_i-1}}e_i + \cdots + a_{0,i}e_i = 0, \qquad 1 \leq i \leq m, \tag{4.58}$$

with $1 \leq n_i \in \mathbb{N}$. The coefficients $a_{j,i}$ with $j = 1, \ldots, n_i$ are chosen so that the dynamics of e_i are asymptotically stable. The nonlinear system (4.56) is restricted to the class of systems for which the following holds true. It is assumed that n_i of (4.58) can be chosen so that the input u_i appears in the first time derivative of σ_i but not the inputs u_j with $j \neq i$. As a consequence, the dynamics of the sliding variables are of the form

$$\dot{\sigma} = v\left(x, z_{ref}, t\right) + M\left(x,t\right)u, \tag{4.59}$$

where $M\left(x,t\right)$ is a diagonal matrix

$$M\left(x,t\right) = \begin{bmatrix} m_1\left(x,t\right) & 0 & \ldots & 0 \\ 0 & m_2\left(x,t\right) & \ldots & 0 \\ \vdots & \vdots & \ddots & \vdots \\ 0 & 0 & \ldots & m_m\left(x,t\right) \end{bmatrix}. \tag{4.60}$$

The quantity $\operatorname{sgn}(m_i)$ is assumed as known and the uncertainty bounds

$$|v_i| \leq v_{M,i}, \qquad 0 < m_{m,i} \leq |m_i|, \tag{4.61}$$

are assumed to be finite but with unknown concrete values.

4.2.2 Chattering Mitigated Control Approach

In the following the model-free predictive controller is combined with an adaptive SMC to guarantee boundedness of the tracking error and to achieve chattering mitigated control. The SMC is designed in the continuous-time domain. Therefore, the predictive control input $u_k^\star$ is transformed into the time-continuous signal

$$u^\star(t) = u_k^\star, \tag{4.62}$$

where t and k are selected from

$$kT_s \leq t < (k+1)T_s, \tag{4.63}$$

with T_s denoting the sampling time. The proposed combined control input is

$$u_i = \eta_i(\sigma_i)u_i^\star - \frac{\mu_i(\sigma_i)}{\operatorname{sgn}\left(m_i\left(x,t\right)\right)}\operatorname{sgn}\left(\sigma_i\right), \qquad 1 \leq i \leq m, \tag{4.64}$$

Algorithm 1 Chattering mitigated sliding mode controller

Inputs σ_i, $u_i^\star$, $\psi_i \geq 0$, $\kappa_i > 0$, $\tilde{\eta}_i$ from (4.67), $\tilde{\mu}_i$ from (4.68), $k_i(t_0) > 0$

```
if |σ_i| ≤ ψ_i then                    ▷ If σ_i is inside the boundary layer then ...
    k_i ← μ̃_i(ψ_i)                                          ▷ Reset SMC gain
    η_i(σ_i) ← η̃_i(σ_i)
    μ_i(σ_i) ← μ̃_i(σ_i)
else if |σ_i| > ψ_i then               ▷ If σ_i is outside the boundary layer then ...
    k̇_i ← κ_i|σ_i|                                          ▷ Increase SMC gain
    η_i(σ_i) ← 0                                        ▷ Suppress predictive controller
    μ_i(σ_i) ← k_i(t)                                     ▷ Apply adaptive SMC gain
end if
u_i ← η_i(σ_i) u_i^⋆ − μ_i(σ_i)/sgn(m_i(x,t)) sgn(σ_i)
```

Output $u_i(t)$

with weighting functions $\eta_i(\sigma_i) \in \mathbb{R}$ and $\mu_i(\sigma_i) \in \mathbb{R}$ selected as

$$\eta_i(\sigma_i) \in [0,1], \qquad 0 \leq \mu_i(\sigma_i). \tag{4.65}$$

The weighting functions adapt online based on a boundary layer that is introduced. The boundary layer is assumed to have a user-defined width $0 < \psi_i \in \mathbb{R}$. The adaptation of the weighting functions is given by Algorithm 1 and is described in detail as follows. Outside the boundary layer ($|\sigma_i| > \psi_i$) the predictive control input is suppressed as $\eta_i = 0$ holds and the SMC gain k_i is continuously increased based on the dynamics

$$\dot{k}_i = \kappa_i |\sigma_i|, \tag{4.66}$$

where $0 < \kappa_i \in \mathbb{R}$ is user-defined.

The SMC gain adaptation (4.66) is originally published by Huang *et al.* (2008) with the goal to avoid an overestimation of the controller gain by the user. As a result, the amount of chattering may be reduced. However, the approach of Huang *et al.* (2008) does not allow the SMC gain to decrease, it can only be increased as stated by (4.66). As a consequence, the controller gain may easily become too large as in the moment when $|\sigma_i|$ starts to decrease and to converge to zero the gain k_i is still increased.

In contrast to the adaptive SMC proposed by Huang *et al.* (2008) the newly developed chattering mitigated SMC allows a resetting of the controller gain to a smaller value. As stated by Algorithm 1 the SMC gain is increased according to (4.66) as long as the sliding variable is outside the boundary layer i. e. $|\sigma_i| > \psi_i$. As outside the boundary layer the SMC gain is continuously increased it can be guaranteed that $|\sigma_i|$ converges towards the domain ψ_i in finite-time. As a consequence, the boundary layer is reached in finite-time. Within the boundary layer the SMC gain k_i is set back to a user-defined value $\tilde{\mu}_i(\psi_i)$ and the weighting functions η_i and μ_i are defined based on some utility functions $\tilde{\eta}_i(\sigma_i) \in \mathbb{R}$ and $\tilde{\mu}_i(\sigma_i) \in \mathbb{R}$. Withing the boundary layer it is desired to scale down the gain of the SMC so that chattering mitigation is achieved when the sliding surface is approached. On the other hand the model-free predictive controller has to be become active to take over

control. Therefore, it is suggested that the utility functions should satisfy the conditions

$$\lim_{|\sigma_i|\to 0}\tilde{\eta}_i(\sigma_i)=1, \qquad \frac{\partial\tilde{\eta}_i(\sigma_i)}{\partial|\sigma_i|}<0, \qquad \lim_{|\sigma_i|\to\psi_i}\tilde{\eta}_i(\sigma_i)=0, \tag{4.67}$$

$$\lim_{|\sigma_i|\to 0}\tilde{\mu}_i(\sigma_i)=0, \qquad \frac{\partial\tilde{\mu}_i(\sigma_i)}{\partial|\sigma_i|}>0, \tag{4.68}$$

for $|\sigma_i|\in[0,\psi_i[$. A family of functions satisfying (4.67) and (4.68) is e. g.

$$\tilde{\eta}_i(\sigma_i)=\frac{(|\psi_i|-|\sigma_i|)^p}{|\psi_i|^p}, \qquad \frac{\partial\tilde{\eta}_i(\sigma_i)}{\partial|\sigma_i|}=-p\frac{(|\psi_i|-|\sigma_i|)^{p-1}}{|\psi_i|^p}, \tag{4.69}$$

$$\tilde{\mu}_i(\sigma_i)=\xi|\sigma_i|, \qquad \frac{\partial\tilde{\mu}_i(\sigma_i)}{\partial|\sigma_i|}=\xi, \tag{4.70}$$

with $0<p\in\mathbb{R}$ and $0<\xi\in\mathbb{R}$ being tuning parameters.

For the sake of completeness the following theorem is stated which shows that the tracking error of the proposed control method is bounded.

Theorem 6 (Boundedness of tracking error of Algorithm 1)**.**
Suppose $|\sigma_i(t_1)|>\psi_i$ to hold at time instant t_1. Then a finite-time $t_2\geq t_1$ exists so that $|\sigma_i(t_2)|\leq\psi_i$ holds true. As the sliding variable is a continuous function it follows that $|\sigma_i(t)|$ is bounded from above. If (4.58) is selected Hurwitz then boundedness of the sliding variable implies boundedness of the tracking error.

Proof. The control law outside the boundary layer is given by

$$u_i=-\frac{\mu_i(\sigma_i)}{\operatorname{sgn}\left(m_i(x,t)\right)}\operatorname{sgn}\left(\sigma_i\right), \tag{4.71}$$

which is obtained from (4.64) with $\eta_i(\sigma_i)=0$. Substituting (4.71) in (4.59) yields

$$\dot{\sigma}_i=v_i(x,t)-\mu_i(\sigma_i)|m_i(x,t)|\operatorname{sgn}(\sigma_i). \tag{4.72}$$

Consider

$$\mu_i(\sigma_i)\geq\frac{\gamma+v_{M,i}}{m_{m,i}}, \tag{4.73}$$

with any $0<\gamma\in\mathbb{R}$ to be satisfied by the controller gain. The right hand side of (4.73) is known to be bounded as quantities $v_{M,i}$ and $m_{m,i}$ are finite according to (4.61). Substituting (4.73) in (4.72) yields

$$\dot{\sigma}_i\leq-\gamma, \tag{4.74}$$

in case of $\sigma_i>0$ and

$$\dot{\sigma}_i\geq\gamma, \tag{4.75}$$

in case of $\sigma_i<0$. Suppose $|\sigma(t_1)|>\psi_i$ to hold at time instant t_1. From Algorithm 1 it is known that as long as $|\sigma_i|>\psi_i$ holds the control input coincides with (4.71) and the gain k_i is continuously increased. Consequently, a finite-time instant $\tilde{t}_1\geq t_1$ exists at which (4.73) is satisfied. It follows that equations (4.74) and (4.75) hold true and a finite-time instant $t_2\geq\tilde{t}_1\geq t_1$ can be found at which $|\sigma(t_2)|\leq\psi_i$ holds. □

4.2.3 Application Example

In this section the performance of the previously introduced chattering mitigated sliding mode controller (CM-SMC) is evaluated. The CM-SMC from (4.64) is compared with the developed predictive controller (PC) from (4.40), and a conventional adaptive SMC from the literature. The continuous stirred tank reactor (CSTR) from Section 3.5 is considered for the performance evaluation. The dynamics of the system is given by

$$\underbrace{\begin{bmatrix}\dot{x}_1\\ \dot{x}_2\end{bmatrix}}_{\dot{x}} = \underbrace{\begin{bmatrix}\frac{q}{V}(C_{Af}-x_1)-k_0x_1\exp\left(-\frac{E}{Rx_2}\right)\\ a(x)+\frac{UA}{V\rho C_p}(T_{eq,c}-x_2)\end{bmatrix}}_{\tilde{f}(x,u)} + \underbrace{\begin{bmatrix}0\\ \frac{UA}{V\rho C_p}\end{bmatrix}}_{g} u, \tag{4.76}$$

$$a(x) = \frac{q}{V}(T_f - x_2) + \frac{(-\Delta H)k_0x_1}{\rho C_p}\exp\left(-\frac{E}{Rx_2}\right),$$

where state $x_1 \in \mathbb{R}$ denotes the effluent flow concentration C_A and state $x_2 \in \mathbb{R}$ denotes the reactor temperature T. The input $u \in \mathbb{R}$ denotes the change of the coolant stream temperature ΔT_c which is limited by $|\Delta T_c| \leq 50\,[\mathrm{K}]$. All states are measured according to

$$y = x = \begin{bmatrix}x_1\\ x_2\end{bmatrix}, \tag{4.77}$$

and the control goal is to achieve reference tracking of the effluent flow concentration

$$z = y_1 = x_1. \tag{4.78}$$

To apply the developed controllers it first has to be checked if the CSTR system satisfies the assumptions related to the CM-SMC and the PC approach. In the following only the requirements of the CM-SMC approach are checked as this also guarantees the requirements of the PC approach to be satisfied. As required, the system (4.76) is input-affine and also the number of inputs and control variables is identical. The input-output behavior of the CSTR system is required to be described by the NARX model (4.1). Substituting x of (4.76) by y and applying the Euler discretization shows that the discrete-time input-output behavior of system (4.76)–(4.77) is of the form (4.1). It is also known that the CSTR system has slow dynamics which can be seen from the step responses in Section 3.5. Consequently, the input-output behavior is approximately described by the linearized model (4.4) as required. In the following it is shown that the dynamics of the sliding variable can have the form (4.59) as it is required. The relative degree of system (4.76)–(4.77) is two which yields the dynamics

$$\ddot{z} = L_{\tilde{f}}^2 h\,(x) + L_g L_{\tilde{f}} h\,(x)\,u, \tag{4.79}$$

where the Lie derivatives are

$$L_{\tilde{f}}^2 h\,(x) = \frac{q^2}{V^2}(C_{Af}-x_1) + x_1k_0\exp\left(-\frac{E}{Rx_2}\right) \times \left[\exp\left(-\frac{E}{Rx_2}\right)\left(k_0 - x_1\frac{-\Delta HEk_0}{\rho C_pRx_2^2}\right) + \phi(x)\right], \tag{4.80}$$

and

$$L_g L_{\tilde{f}} h\left(x\right) = -k_0 x_1 \frac{UAE}{V\rho C_p R x_2^2} \exp\left(-\frac{E}{R x_2}\right), \tag{4.81}$$

with

$$\phi(x) = \frac{q}{V} - \frac{q}{V x_1}\left(C_{Af} - x_1\right) - \frac{Eq}{R x_2^2 V}(T_f - x_2) - \frac{UAE}{V\rho C_p R x_2^2}(T_{eq,c} - x_2).$$

Let the sliding variable be defined as

$$\sigma = \dot{e} + \lambda e = \dot{z}_{ref} - \dot{z} + \lambda(z_{ref} - z), \qquad \lambda > 0, \tag{4.82}$$

leading to

$$\dot{\sigma} = \ddot{z}_{ref} - \ddot{z} + \lambda \dot{z}_{ref} - \lambda \dot{z}, \tag{4.83}$$

with the reference signal z_{ref} assumed smooth and bounded. Substituting $\ddot{z}$ of (4.79) in (4.83) and $\dot{z} = \dot{x}_1$ of (4.76) in (4.83) gives

$$\dot{\sigma} = v\left(x,t\right) + m\left(x,t\right) u, \tag{4.84}$$

with

$$v\left(x,t\right) = \ddot{z}_{ref} - L_{\tilde{f}}^2 h\left(x\right) + \lambda \dot{z}_{ref} - \lambda \frac{q}{V}(C_{Af} - x_1) + \lambda k_0 x_1 \exp\left(-\frac{E}{R x_2}\right), \tag{4.85}$$

$$m\left(x,t\right) = -L_g L_{\tilde{f}} h\left(x\right). \tag{4.86}$$

Consequently, the dynamics (4.84) of the sliding variable is in the desired form (4.59). The uncertainty bounds of $v(x,t)$ and $m(x,t)$ are assumed to be finite as it is required. According to (4.64) the sign of $m(x,t)$ is also required to be known to state the control law of the CM-SMC approach. From (4.81) and (4.86) it follows that

$$\operatorname{sgn}\left(m\left(x,t\right)\right) = \operatorname{sgn}\left(k_0 x_1 \frac{UAE}{V\rho C_p R x_2^2} \exp\left(-\frac{E}{R x_2}\right)\right), \tag{4.87}$$

has to be evaluated. Comparing (4.87) with the system parameters shown in Table 3.1 the following can be stated. The flow concentration x_1, the tank volume V, the density ρ, the reactor temperature x_2, the specific heat capacity C_p are all positive. According to Seborg *et al.* (2010) quantity UA is the product of heat area A and heat transfer coefficient U which are both positive. Following Seborg *et al.* (2010) quantity k_0 is a positive prefactor of the Arrhenius equation and E/R is the fraction of activation energy E and gas constant R which are both positive. Consequently, without knowing any concrete system parameter the sign of $m(x,t)$ is known to be positive. Finally, all requirements of the CM-SMC approach are achieved.

As the sign of $m(x,t)$ is known it follows from (4.64) that the control law of the CM-SMC approach can be stated as

$$u = \eta(\sigma) u^\star - \mu(\sigma) \operatorname{sgn}\left(\sigma\right). \tag{4.88}$$

The utility functions $\tilde{\eta}(\sigma)$ and $\tilde{\mu}(\sigma)$ that in combination with Algorithm 1 define the weightings $\eta(\sigma)$ and $\mu(\sigma)$ are chosen in accordance to (4.67)–(4.68). Following (4.69)–(4.70) the utility functions are given as

$$\tilde{\eta}(\sigma) = \frac{(|\psi| - |\sigma|)^p}{|\psi|^p}, \qquad \tilde{\mu}(\sigma) = \xi|\sigma|, \qquad \psi = 0.5, \qquad p = 1, \qquad \xi = 10, \tag{4.89}$$

with ψ, p, and ξ being determined by trial and error based on the tracking performance of the resulting controller. In the same way the controller parameters κ and $k(t_0)$ are determined as $\kappa = 10$ and $k(t_0) = 20$. The parameter λ of (4.82) is chosen as $\lambda = 0.05$ so that the sliding dynamics are asymptotically stable.

From Theorem 6 it is known that the CM-SMC approach provides boundedness of the tracking error. However, it is also required to show that the states x_1 and x_2 of the CSTR system (4.76) remain stable. Let

$$\Phi : \begin{bmatrix} x_1 \\ x_2 \end{bmatrix} \rightarrow \begin{bmatrix} z \\ \dot{z} \end{bmatrix}, \tag{4.90}$$

define a state transformation. According to the dynamics $\dot{z} = \dot{x}_1$ of system (4.76) and the definition of the control variable $z = x_1$ it is

$$\begin{bmatrix} z \\ \dot{z} \end{bmatrix} = \begin{bmatrix} x_1 \\ \frac{q}{V}(C_{Af} - x_1) - k_0 x_1 \exp\left(-\frac{E}{Rx_2}\right) \end{bmatrix}. \tag{4.91}$$

In the following it will be checked if Φ defines a diffeomorphism so that stability of the transformed states z and $\dot{z}$ implies stability of the states x_1 and x_2. The stability of z and $\dot{z}$ is guaranteed. This follows directly from (4.82) as boundedness of σ is provided by the controller as stated in Theorem 6. Consequently, it is only required to show that Φ defines a diffeomorphism which according to Slotine and Li (1991, Lemma 6.2) is the case if the Jacobian $d\Phi/dx$ has full rank. The Jacobian is

$$\frac{d\Phi}{dx} = \begin{bmatrix} 1 & 0 \\ -\frac{q}{V}x_1 - k_0 \exp\left(-\frac{E}{Rx_2}\right) & -k_0 x_1 \frac{E}{Rx_2^2} \exp\left(-\frac{E}{Rx_2}\right) \end{bmatrix}, \tag{4.92}$$

and it has full rank if

$$-k_0 x_1 \frac{E}{Rx_2^2} \exp\left(-\frac{E}{Rx_2}\right) \neq 0, \tag{4.93}$$

holds. It follows that the effluent flow concentration $x_1 \geq 0$ has to be nonzero to achieve (4.93) and the reactor temperature $x_2 \geq 0$ has also to be nonzero as (4.93) is not defined for $x_2 = 0$. A reactor temperature of $x_2 = 0\,[\mathrm{K}]$ cannot be achieved due to physical limits. The effluent flow concentration of species A is very unlikely to become zero as this would mean that in the reactor the complete input flow C_{Af} of species A has to react to species B. However, $x_1 > 0$ can be guaranteed by choosing $z_{ref} \gg 0$ as the tracking error is bounded.

For the simulation of the considered system the following initializations and reference

values are considered. The initial flow concentration is $C_A(t_0) = 0.875\,[\text{mol/l}]$ and the initial reactor temperature is $T(t_0) = 325\,[\text{K}]$. The set-points

$$z_{ref}(t) = \begin{cases} 0.80\,[\text{mol/l}] & \text{if } t \leq 4\,[\text{min}], \\ 0.75\,[\text{mol/l}] & \text{if } 4\,[\text{min}] < t \leq 8\,[\text{min}], \\ 0.70\,[\text{mol/l}] & \text{if } 8\,[\text{min}] < t \leq 12\,[\text{min}], \\ 0.85\,[\text{mol/l}] & \text{if } 12\,[\text{min}] < t \leq 15\,[\text{min}], \end{cases} \tag{4.94}$$

define the reference values for tracking, where the simulation duration is $15\,[\text{min}]$. The sampling time is chosen as $T_s = 1\,[\text{s}]$.

The CM-SMC approach is compared with the adaptive SMC approach (A-SMC) of Plestan *et al.* (2010). The A-SMC approach is further described in Appendix C including the selection of the related controller parameters. The selection of the parameters of the local linear model (neural network) that is recursively identified through the Kalman filter is discussed as follows. The number of delayed inputs is selected as $n_y = 3$ and the number of delayed outputs is selected as $n_u = 2$ based on trial and error. The network weights are initialized based on the estimated initial state $\hat{\xi}_0 = \mathbf{1}_{18}$ with an initial error covariance selected as $P_0 = I_{18} \times 10^{10}$. The learning rate α is chosen as $\alpha = 0.01$ and the weighting factor β is selected as $\beta = 0.001$. The network is initially trained based on the system outputs generated by the input

$$u(t^\star) = A_t(t^\star) \times \cos\left(\omega_t(t^\star)t^\star\right), \qquad t^\star = 0...20\,[\text{min}], \tag{4.95}$$

where $\omega_t(t^\star)$ and $A_t(t^\star)$ vary according to $\omega_t(t^\star) \in [2\pi/3000, 2\pi/50]$ and $A_t(t^\star) \in [0.5, 2.5]$. The weighting matrices that define the receding horizon control problem (4.29) are selected as $Q_{cont} = 1$ and $R_{cont} = 0.001$. According to (4.78) the matrix L of (4.22) is $L = \begin{bmatrix} 1 & 0 \end{bmatrix}$. The prediction and control horizon are chosen as $n_p = 20$ (20 seconds) and $n_c = 19$ (19 seconds).

The performance of the controllers is evaluated based on Fig. 4.6 and Table 4.3. From a principal point of view set-point tracking is achieved by all considered approaches. However, the PC approach shows overshooting when the set-point switches. The CM-SMC approach avoids the overshooting and requires least time to become stationary accurate. Regarding the control inputs all approaches show chattering when the set-point changes. But the PC and the CM-SMC approach are stationary accurate without noticeable chattering whereas the A-SMC approach shows chattering all the time. In Fig. 4.6d the weighting functions of the CM-SMC approach are shown for a specific time interval. It can be seen that the switching of the set-point leads to higher activity of the SMC. The

Table 4.3: Tracking performance with respect to the reference values defined by (4.94).

	CM-SMC	A-SMC	PC
$\int (e(t)^2/T_{sim})dt$	584.61	623.59	605.90
$\int (u(t)^2/T_{sim})dt$	327.18	742.45	564.23
Switchings	28	257	62

Switchings: Number of switchings from $\text{sgn}(u) = 1$ to $\text{sgn}(u) = -1$ and vice versa, $T_{sim} = 15\,[\text{min}]$.

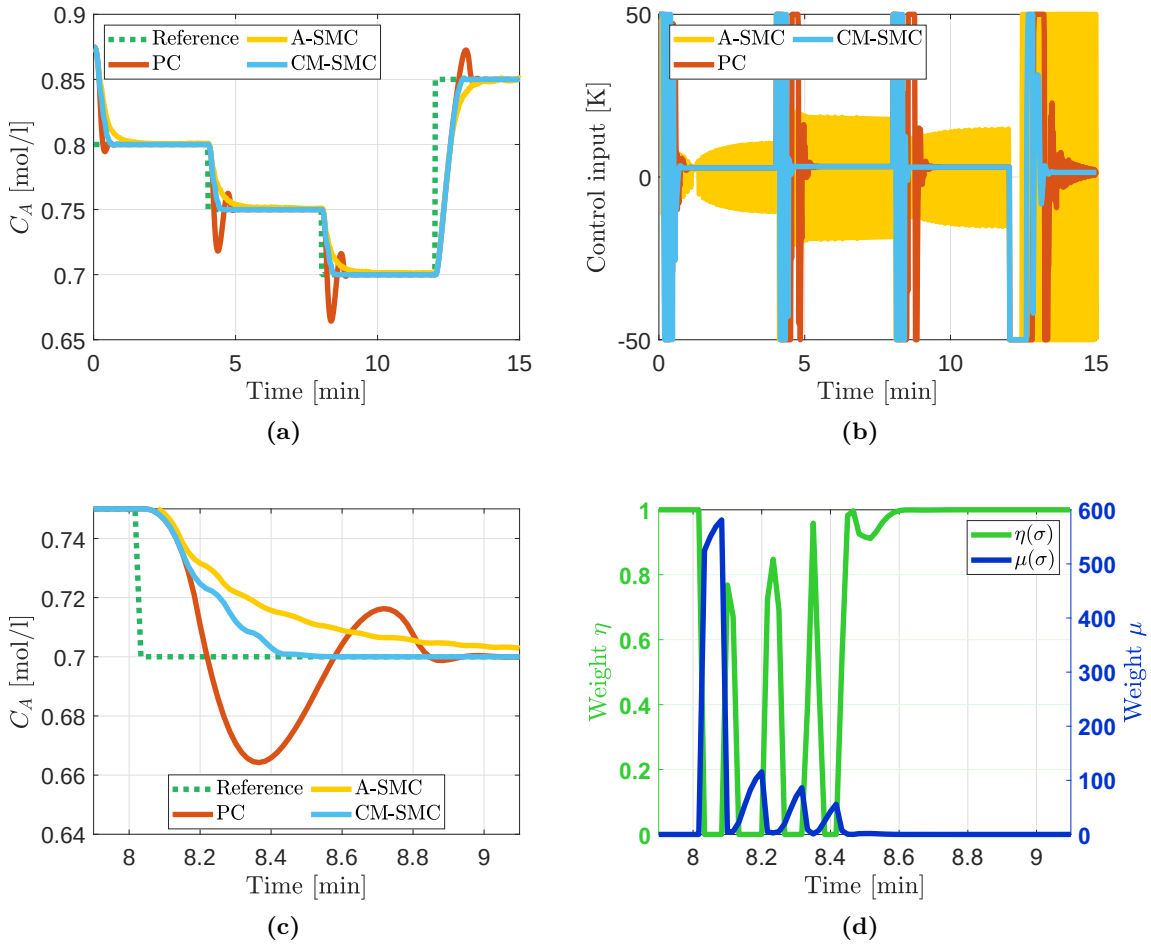

Figure 4.6: Performance evaluation of chattering mitigated SMC (CM-SMC), adaptive SMC (A-SMC), and predictive controller (PC). (a) Tracking performance. (b) Control inputs. (c) Tracking performance on specific time interval. (d) Weighting functions on specific time interval.

adaptive gain of the SMC shows several peaks. As a result, the states are pushed towards the sliding surface which reduces the tracking error in the transient phase and avoids the overshooting. At the end of the transient phase the SMC gain decreases whereas the receding horizon controller is scaled up. As a consequence, in the subsequently following stationary phase no visible chattering occurs.

Although the proposed CM-SMC method is only compared with the A-SMC approach of Plestan *et al.* (2010) similar results can be expected for comparisons with other adaptive SMC approaches. In adaptive sliding mode control it is common to estimate the equivalent control input in order to reduce the SMC gain. However, in general the equivalent control input is not zero because some control effort is required to keep the system in sliding mode. Consequently, the SMC gain can not be scaled down to zero by any adaptive SMC approach. But from the conducted simulation it can be seen that the adaptive gain of the proposed CM-SMC method can be scaled down to a value close to zero. This is possible

because the predictive controller takes over the control action when the SMC becomes inactive. As the SMC gain is scaled down closely to zero no noticeable chattering is present in the stationary phase.

4.2.4 Summary

In the previous sections chattering mitigated control of uncertain nonlinear systems with sufficient slow dynamics is considered. A model-free predictive controller is combined with an adaptive SMC to mitigated the chattering and guarantee boundedness of the tracking error. The activity of the predictive controller and the adaptive SMC is controlled by weighting functions. The weighting functions adapt online based on the concept of a boundary layer. Within the boundary layer when the sliding surfaced is approached the model-free predictive controller dominates the control law so that chattering mitigation is achieved. Outside the boundary layer the gain of the SMC is continuously increased so that the states are pushed towards the sliding surface and the tracking error is guaranteed to be bounded. A nonlinear system with slow dynamics is considered to study the performance of the proposed chattering mitigated control approach. For the considered system the proposed approach can be applied without knowing any concrete values of the system parameters. In comparison to a conventional adaptive SMC from the literature the proposed approach shows less chattering. In particular, the proposed controller is stationary accurate without any noticeable chattering. The mitigation of the chattering is achieved as the predictive controller takes over the control action in the vicinity of the sliding surface. This allows to scale down the adaptive SMC gain of the proposed approach to very small values. As a result, the chattering problem is in fact avoided. The ability to scale down the SMC gain to very small values makes the proposed method advantageous in comparison to the existing adaptive SMCs from the literature. The existing adaptive SMC approaches cannot scale down the gain to values close to zero as a minimal amount of control action is required to keep the system in sliding mode.

5 Constrained Control of Uncertain Relative Degree Two Nonlinear Systems

Constrained control problems arise in many applications such as in autonomous vehicles, process industry, traffic control, or robotics.

Model predictive control is widely applied in industry due to its ability to control MIMO systems that are subject to constraints. In addition, MPC approaches forecasts the future system behavior in order to minimize a defined performance index so that a high control accuracy can be achieved (Rawlings and Mayne, 2009). However, MPC is model-based which means that parametric or external uncertainties may have a negative influence on the control performance. To overcome the problem so-called robust MPC approaches have been developed. The strategy behind the min-max approaches is to minimize the performance index for the worst possible sequence of the disturbance (Raimondo *et al.*, 2009). The method is known to be computationally demanding and due to its conservative selection strategy it may lead to suboptimal performance results (Bemporad *et al.*, 2003). Scenario optimization is another robust MPC approach (Calafiore and Fagiano, 2012; Schildbach *et al.*, 2014). A finite number of disturbance realizations is drawn from a known probability measure of the disturbance. The obtained finite number of realizations forms one scenario for which the performance index is minimized. Dependent on the number of disturbance realizations it can be determined how likely it is that the solution of the optimization problem indeed satisfies the constraints and reaches the terminal region. Tube based MPC is another robust control strategy. It guarantees the system states to remain in a tube around the nominal trajectory although some disturbances may be present (Langson *et al.*, 2004). The method was first proposed for linear systems (Langson *et al.*, 2004) and later extended to nonlinear systems (e. g. Cannon *et al.*, 2011).

Besides MPC several other constrained control approaches exist. An important approach is the invariance control method proposed by Wolff and Buss (2004). It can be applied to nonlinear systems that are subject to constraints. The approach is based on an exact input-output linearization. The time derivatives of the output variable form a set of transformed states. Constraints imposed on the original states can be expressed in the transformed state domain based on a so-called invariance function. The control strategy is based on two control laws. The nominal controller and the invariance controller. The nominal controller can be any control law guaranteeing stability of the system or convergence of the tracking error. The invariance controller guarantees satisfaction of the constraints. The invariance function serves as a switching condition to decide if it is required to apply the invariance controller or the nominal controller. In Kimmel and Hirche (2014) the switching between the invariance controller and the nominal controller is formulated with respect to an optimization problem. This ensures that the invariance controller equals the nominal controller as close as possible. Another constrained control method is the refer-

ence governor approach. As described in Garone *et al.* (2017) an asymptotically stable closed loop system is considered as a basis for the reference governor design. It is assumed that state or input constraints are required to be satisfied. The main idea of the reference governor method is to modify the reference signal so that satisfaction of the constraints can be guaranteed for all future time steps. The approach was first established for linear systems (Gilbert and Tan, 1991) and later extended to nonlinear systems (Bemporad, 1998). Control barrier functions (CBF) in combination with control Lyapunov functions (CLF) can also be applied to enforce constraints. In Ames *et al.* (2014) a quadratic program is formulated with the goal to minimize a desired performance index. In addition, the quadratic program is subject to a CBF and a CLF. The solution of the optimization problem gives a control input that guarantees the constraints to be satisfied. The approach has been extended in Rauscher *et al.* (2016) to handle multiple constraints. In addition, the work of Rauscher *et al.* (2016) provides a framework to adapt a given nominal control input in such a way that the adapted solution guarantees the constraints to be satisfied. Therefore, a quadratic program subject to a set of CBFs is formulated. The solution of the optimization problem not only guarantees the constraints to be satisfied it also provides the control input that is most similar to the nominal controller. In Hsu *et al.* (2015) a method for the construction of CBFs is developed. Based on the obtained CBFs it is exemplarily shown that a constrained robot locomotion control problem can be solved.

Constrained SMC approaches can also be found in the literature. The authors in Incremona *et al.* (2016) make use of a state transformation to express the constraints in terms of the sliding variables. A combination of first order and higher order SMCs is applied to drive the sliding variables to zero without violating the constraints. The approach provides a maximum domain of attraction for relative degree one and two systems. A constrained sliding mode control approach that can be applied to nonlinear relative degree two systems and also guarantees a maximum domain of attraction is described in Ding *et al.* (2018). The proposed controller requires the constraints to be stated in terms of the sliding variables. In contrast to the approach of Incremona *et al.* (2016) the constrained control method of Ding *et al.* (2018) is not based on a combination of sub-controllers and therefore avoids switching effects. In Bartoszewicz and Nowacka-Leverton (2010) parameters of a linear time-varying sliding surface are optimized to achieve either input saturation or satisfaction of velocity or acceleration constraints. The considered system has relative degree three. Another approach optimizing the parameters of a nonlinear sliding surface is proposed in Pietrala and Jaskuła (2019). The controller can be applied to relative degree two systems to achieve position control under velocity constraints. Sliding mode reference conditioning (SMRC) proposed by Garelli *et al.* (2011) is a control strategy that is similar to the reference governor approaches. The SMRC method is an outer loop control approach that manipulates the reference signal of an already controlled system. By manipulating the reference signal the closed loop system is kept in a sliding mode in which the constraints are satisfied. The constraints can be formulated with respect to the closed loop states. Only bounds of the time derivatives of the closed loop states are required to be known for the design of the SMRC approach. The method can also be applied to nonlinear systems. In Richter *et al.* (2007) the class of linear time-invariant systems with bounded disturbances is considered. A sliding mode controller is applied and robust positive invariant (RPI) sets of the closed loop dynamics are determined. The intersection of a state constraint set and the RPI of the closed loop dynamics is studied further. Conditions are derived to check if this intersection itself is a RPI. In Richter (2011) output constrained

control of linear single input systems is considered. Multiple sliding mode controllers are combined with each other using a min-max selection strategy. The min-max selection scheme is a multi-controller approach known from e. g. aerospace industry where it is used for constrained turbo engine control (Litt *et al.*, 2009). Instead of linear controllers the approach of Richter (2011) applies SMCs within the framework. The approach proposed in Song *et al.* (2016) considers robust constrained control of nonlinear systems that satisfy the so-called conic sector constraint (ElBsat and Yaz, 2013). State feedback and SMC are combined in order to guarantee that the quadratic norm of the output variables does not exceed a defined threshold neither in the reaching phase nor within the sliding mode. In Pietrala *et al.* (2018) a time-varying nonlinear sliding mode is designed. The parameters of the sliding manifold are optimized to achieve velocity-constrained control of relative degree two systems. For the consideration of input and state constraints a control scheme that combines first order SMCs is proposed in Jaskuła and Leśniewski (2020). The approach can be applied to linear time-invariant systems with bounded disturbances. In Liu and Yang (2017) prescribed performance functions are formulated to guarantee that the tracking error remains within prescribed performance bounds. This also allows to satisfy constraints that are formulated with respect to the tracking error. The contribution of Innocenti and Falorni (1998) considers sliding mode control of linear systems. Conditions are derived under which satisfaction of polygonal state constraints can be achieved.

In this chapter a robust constrained sliding mode control approach for nonlinear relative degree two systems is developed. The first time derivative of the control variable is assumed to be constrained with bounds that may explicitly depend on time. The system description may be imprecise. Only the control variable and its first time derivative are assumed to be known. The uncertainty bounds of the system are assumed to be finite. The developed controller is a combination of SMC sub-controllers. Discontinuities that may result from the switching of the sub-controllers are avoided by a proper controller design. In addition, mitigation of the chattering effect is considered. For the proposed controller it is analytically shown that the constrained control problem can be solved. The convergence of the tracking error is studied and error bounds dependent on the controller parameters are stated. Chattering mitigation is achieved by introducing a boundary layer. Although the boundary layer is applied the constraints can still be guaranteed to be satisfied if the controller parameters are suitably chosen. In contrast to the already existing constrained SMC approaches the proposed method has the following advantages. The considered constraints may have time-varying bounds, whereas most of the existing approaches deal with box constraints. As a consequence, the application field of the proposed approach is less limited. Most of the existing constrained SMCs are based on discontinuous control laws. Due to the discontinuities chattering occurs and the controllers can not be applied in practice. To mitigate the chattering the boundary layer concept may be used. However, the boundary layer approach modifies the control law so that constraint violation may occur. In contrast to that the proposed constrained SMC guarantees the constraints to be satisfied also if the chattering is mitigated through the boundary layer concept. The existing approaches that are based on combination of sub-controllers may introduce additional discontinuities that result from the switching between the control laws. Although the proposed control strategy is also based on a combination of sub-controllers the transition between the introduced sub-controllers is guaranteed to be smooth.

A preliminary version of the proposed constrained SMC is studied in Spiller and Söffker (2021). However, this preliminary version of the controller does not consider the nonlinear

sliding manifold that is presented in this chapter to improve the error convergence of the controller. In addition, the preliminary version described in Spiller and Söffker (2021) does not consider the analysis of the relevant practical controller implementation that is given within this chapter.

The chapter can be divided into two main sections. In Section 5.1 the new robust constrained sliding mode control approach is introduced. This includes the introduction of mathematical assumptions and definitions, the derivation of the control laws and the definition of the input selection strategy as well as the mathematical analysis of the controller properties, and finally the consideration of an application example. In Section 5.2 human-robot collaboration is considered as a specific application example of robust constrained control. Based on the introduced new constrained sliding mode control approach a safety concept applicable in the field of human-robot collaboration is proposed. The concept is mathematically analyzed and finally tested on a simulated robotic system.

5.1 Controller Design

In this section the new constrained sliding mode control approach is presented. First, a detailed review of the constrained control approach of Incremona *et al.* (2016) is given in Section 5.1.1. In Section 5.1.2 the constrained control problem is formulated and mathematical preliminaries are introduced. The new constrained SMC is described in Section 5.1.3 and the controller properties are studied in Section 5.1.4. Constrained control of a robotic system based on the developed approach is considered in Section 5.1.5.

5.1.1 Review of Constrained Control Approach

Among the aforementioned constrained SMC approaches the contribution of Incremona *et al.* (2016) arises special interest as it provides a maximum domain of attraction for nonlinear relative degree one and two SISO systems. In addition it is to some extent a general approach as it can handle any constraints that may be expressed in terms of the sliding variables. Following Incremona *et al.* (2016) an input-affine nonlinear system

$$\begin{aligned} \dot{x} &= f(x) + g(x)u, \\ y_r &= h(x), \end{aligned} \tag{5.1}$$

with states $x \in \mathbb{R}^n$, input $u \in \mathbb{R}$, and control variable $y_r \in \mathbb{R}$ is considered. The relative degree r is assumed to be one or two. Let the sliding variable $\sigma \in \mathbb{R}^r$ be defined as

$$\sigma = \begin{cases} \sigma_1 & \text{if } r = 1, \\ \begin{bmatrix} \sigma_1 & \sigma_2 \end{bmatrix}^T = \begin{bmatrix} \sigma_1 & \dot{\sigma}_1 \end{bmatrix}^T & \text{if } r = 2, \end{cases} \tag{5.2}$$

with $\sigma_1 \in \mathbb{R}$. An admissible region of σ is introduced according to

$$\mathcal{S}_b = \begin{cases} \{\sigma \in \mathbb{R} \colon \sigma_1 \in [\underline{\sigma}_1, \bar{\sigma}_1]\}, & \text{if } r = 1, \\ \{\sigma \in \mathbb{R}^2 \colon \sigma_1 \in [\underline{\sigma}_1, \bar{\sigma}_1] \wedge \sigma_2 \in [\underline{\sigma}_2, \bar{\sigma}_2]\}, & \text{if } r = 2, \end{cases} \tag{5.3}$$

with constants $\underline{\sigma}_1, \underline{\sigma}_2 < 0$ and $\bar{\sigma}_1, \bar{\sigma}_2 > 0$. The admissible region (5.3) describes box constraints that are formulated with respect to the sliding variables. Following Incremona

et al. (2016) a domain of attraction $\mathcal{S}_I \subseteq \mathbb{R}^r$ is defined. The subspace $\mathcal{S}_I$ defines all initial values for which the sliding variables decrease to zero in finite-time without violating the constraints. Formally $\mathcal{S}_I$ is given by

$$\mathcal{S}_I = \{\sigma_0 = \sigma(t_0) \in \mathbb{R}^r \colon \sigma(t, \sigma_0) \in [\underline{\sigma}, \bar{\sigma}] \wedge \sigma(t^\star, \sigma_0) = 0\}, \qquad t^\star \geq t_f, \tag{5.4}$$

where $\sigma(t, \sigma_0)$ is the trajectory of $\sigma(t)$ with initial value σ_0, quantities $\underline{\sigma}, \bar{\sigma} \in \mathbb{R}^r$ are the bounds of the box constraints, and t_f is a finite-time instant (Incremona *et al.*, 2016).

For the relative degree one case the dynamics of the sliding variable $\sigma_1 = y_r - w$ is given by

$$\dot{\sigma}_1 = L_f h(x) + L_g h(x) u - \dot{w} = \Psi(x, w) + \Gamma(x) u, \tag{5.5}$$

where w denotes the reference value. The uncertainty bounds

$$\Psi(x, w) \leq \Psi_M, \qquad 0 < \Gamma_m \leq \Gamma(x) \leq \Gamma_M, \tag{5.6}$$

are assumed to be finite. The controller design is trivial and leads to a conventional first-order SMC

$$u = -\alpha \times \operatorname{sgn}(\sigma_1), \tag{5.7}$$

which drives σ_1 to zero in finite-time for sufficient large gains $\alpha > \frac{\Psi_M}{\Gamma_m}$. If $\sigma_1(t_0) \in [\underline{\sigma}_1, \bar{\sigma}_1]$ holds initially then the controller naturally avoids constraint violation because satisfying the reachability condition implies that $\dot{\sigma}_1 < 0$ holds in case of $\sigma_1 > 0$ and that $\dot{\sigma}_1 > 0$ holds in case of $\sigma_1 < 0$. Consequently, the achieved domain of attraction is maximal.

The controller for the relative degree two case is studied as follows. The controller is described based on Incremona *et al.* (2016) although a very similar controller has already been proposed before in Rubagotti *et al.* (2010). The dynamics of the sliding variable $\sigma_1 = y_r - w$ is given by

$$\ddot{\sigma}_1 = \dot{\sigma}_2 = L_f^2 h(x) + L_g L_f h(x) u - \ddot{w} = \Psi(x, w) + \Gamma(x) u, \tag{5.8}$$

where the uncertainty bounds

$$\Psi(x, w) \leq \Psi_M, \qquad 0 < \Gamma_m \leq \Gamma(x) \leq \Gamma_M, \tag{5.9}$$

are assumed finite. The control law is stated as

$$u = \begin{cases} -\alpha \times \operatorname{sgn}\Big(\sigma_1 + \dfrac{\sigma_2 |\sigma_2|}{2\alpha_l}\Big) & \text{if } (\sigma_1, \sigma_2) \in \mathcal{S}_b, \quad (5.10) \\ -\alpha \times \operatorname{sgn}(\sigma_2) & \text{if } (\sigma_1, \sigma_2) \notin \mathcal{S}_b, \quad (5.11) \end{cases}$$

with $\alpha > \frac{\Psi_M}{\Gamma_m}$ being sufficient large and α_l being defined as $\alpha_l = \Gamma_m \alpha - \Psi_M$ (Incremona *et al.*, 2016). As proven in Dinuzzo and Ferrara (2009) control law (5.10) is a second order SMC meaning that if the sliding variables remain in the admissible region $\mathcal{S}_b$ and (5.10) is active all the time then σ_1 and σ_2 reach the sliding surface

$$\sigma_1 + \frac{\sigma_2 |\sigma_2|}{2\alpha_l} = 0, \tag{5.12}$$

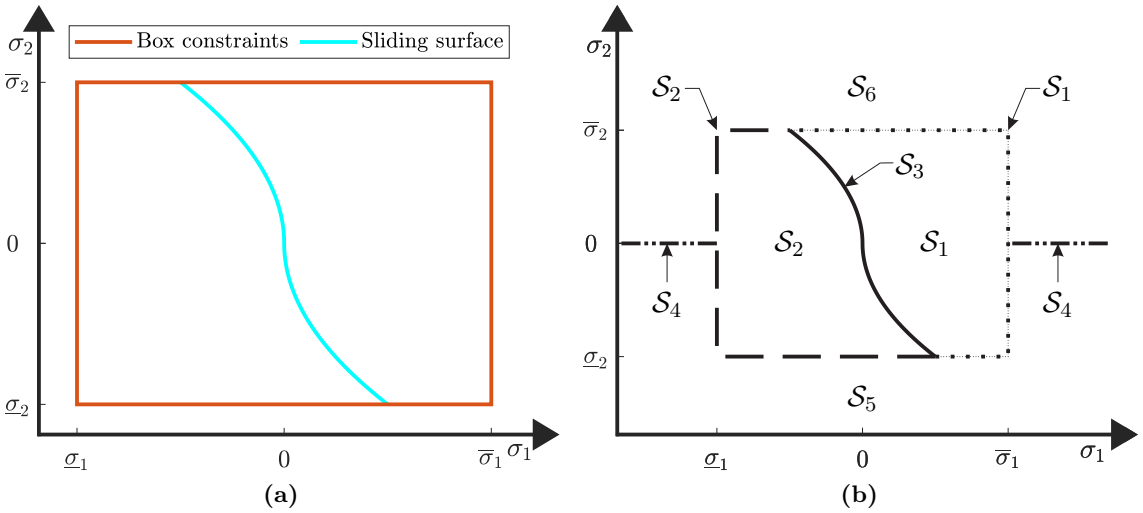

Figure 5.1: Visualization of space $\sigma \in \mathcal{S} \subseteq \mathbb{R}^2$. (a) Box constraints of admissible region $\mathcal{S}_b$ and sliding surface $\sigma_1 + \frac{\sigma_2|\sigma_2|}{2\alpha_1} = 0$ according to (5.12). (b) Regions of $\mathcal{S}$ defining $\dot{\sigma}_2$ as stated by (5.21).

in finite-time. Further, after the sliding surface has been reached the variables σ_1 and σ_2 slide on the sliding surface towards the origin and become zero in finite-time. The sliding manifold (5.12) is visualized in Fig. 5.1 (a). If the sliding variables do not remain within the admissible region $\mathcal{S}_b$ it follows that the control law (5.11) becomes active to push σ_2 back towards the bounds $\underline{\sigma}_2$ and $\bar{\sigma}_2$ of the admissible region. The closed loop dynamics of σ_1 and σ_2 are studied as follows. Defining $\alpha_h = \Gamma_M \alpha + \Psi_M$ and substituting (5.10)–(5.11) in (5.8) yields

$$|\dot{\sigma}_2| \in \{x \in \mathbb{R} \colon 0 \leq x \leq \Psi_M \vee \alpha_l \leq x \leq \alpha_h\}, \tag{5.13}$$

as $u = \alpha$, $u = -\alpha$, or $u = 0$ may be applied. According to (5.8) and (5.10)–(5.11) the following cases

$$\mathcal{S}_1 = \{(\sigma_1, \sigma_2) \in \mathbb{R}^2 \colon (\sigma_1, \sigma_2) \in \mathcal{S}_b \wedge \sigma_1 > -\frac{\sigma_2|\sigma_2|}{2\alpha_l}\}, \tag{5.14}$$

$$\mathcal{S}_2 = \{(\sigma_1, \sigma_2) \in \mathbb{R}^2 \colon (\sigma_1, \sigma_2) \in \mathcal{S}_b \wedge \sigma_1 < -\frac{\sigma_2|\sigma_2|}{2\alpha_l}\}, \tag{5.15}$$

$$\mathcal{S}_3 = \{(\sigma_1, \sigma_2) \in \mathbb{R}^2 \colon (\sigma_1, \sigma_2) \in \mathcal{S}_b \wedge \sigma_1 = -\frac{\sigma_2|\sigma_2|}{2\alpha_l}\}, \tag{5.16}$$

$$\mathcal{S}_4 = \{(\sigma_1, \sigma_2) \in \mathbb{R}^2 \colon (\sigma_1, \sigma_2) \notin \mathcal{S}_b \wedge \sigma_2 = 0\}, \tag{5.17}$$

$$\mathcal{S}_5 = \{(\sigma_1, \sigma_2) \in \mathbb{R}^2 \colon (\sigma_1, \sigma_2) \notin \mathcal{S}_b \wedge \sigma_2 < 0\}, \tag{5.18}$$

$$\mathcal{S}_6 = \{(\sigma_1, \sigma_2) \in \mathbb{R}^2 \colon (\sigma_1, \sigma_2) \notin \mathcal{S}_b \wedge 0 < \sigma_2\}, \tag{5.19}$$

can be defined as shown in Fig. 5.1 (b) to further evaluate the dynamics $\dot{\sigma}_2$ of (5.8). Considering the different cases the closed loop dynamics

$$\dot{\sigma}_1 = \sigma_2, \tag{5.20}$$

$$\dot{\sigma}_2 = \begin{cases} U^+ & \text{if } (\sigma_1, \sigma_2) \in \mathcal{S}_2 \cup \mathcal{S}_5, \\ U^- & \text{if } (\sigma_1, \sigma_2) \in \mathcal{S}_1 \cup \mathcal{S}_6, \\ U^0 & \text{if } (\sigma_1, \sigma_2) \in \mathcal{S}_3 \cup \mathcal{S}_4, \end{cases} \tag{5.21}$$
$$\alpha_l \leq U^+ \leq \alpha_h, \qquad -\alpha_h \leq U^- \leq -\alpha_l, \qquad -\Psi_M \leq U^0 \leq \Psi_M,$$

are achieved. Based on the system dynamics (5.20)–(5.21) the phase portrait of σ_1 and σ_2 can be analyzed. For instance, assume σ_1 and σ_2 to remain in $\mathcal{S}_1$ during a time interval $[t_1, t_2]$ then the right hand side of the differential equation (5.21) equals U^- which is continuous and allows integration. Studying the phase portrait requires the relation between σ_1 and σ_2 to be known. Consequently,

$$\delta\sigma_1 = \sigma_2 \delta t, \tag{5.22}$$
$$\delta\sigma_2 = U^- \delta t, \tag{5.23}$$

is considered which leads to

$$\delta\sigma_1 = \frac{\sigma_2}{U^-}\delta\sigma_2. \tag{5.24}$$

Integration of (5.24) yields

$$-\frac{1}{2\alpha_l}\Big(\sigma_2^2(t_1^\star) - \sigma_2^2(t_1)\Big) \leq \sigma_1(t_1^\star) - \sigma_1(t_1) \leq -\frac{1}{2\alpha_h}\Big(\sigma_2^2(t_1^\star) - \sigma_2^2(t_1)\Big), \tag{5.25}$$

for $\sigma_2(t) \geq 0$ with $t \in [t_1, t_1^\star]$ where $t_1 \leq t_1^\star \leq t_2$ and

$$-\frac{1}{2\alpha_h}\Big(\sigma_2^2(t_2) - \sigma_2^2(t_2^\star)\Big) \leq \sigma_1(t_2) - \sigma_1(t_2^\star) \leq -\frac{1}{2\alpha_l}\Big(\sigma_2^2(t_2) - \sigma_2^2(t_2^\star)\Big), \tag{5.26}$$

for $\sigma_2(t) \leq 0$ with $t \in [t_2^\star, t_2]$ where $t_1 \leq t_2^\star \leq t_2$. Let

$$\sigma_1(t_1) = \bar{\sigma}_1 - \bar{\sigma}_2{}^2/(2\alpha_l), \qquad \sigma_2(t_1) = \bar{\sigma}_2, \tag{5.27}$$

be the initial values of the sliding variables then the resulting trajectory $\sigma(t, \sigma(t_1))$ lies between the bounds shown in Fig. 5.2 (a).

It can be seen that the trajectory may reach the sliding surface or the bound $\underline{\sigma}_2$ of the constraints. If the sliding surface is reached directly then σ slides towards the origin and becomes zero. If the bound is reached and slightly exceeded afterwards then control law (5.11) is activated and σ moves alongside of the bound in direction of the sliding surface. So finally also in this case the sliding surface is reached and σ becomes zero. Similar results regarding convergence and achievement of constraints can be obtained for region $\mathcal{S}_2$. For instance, if the trajectories of $\mathcal{S}_1$ shown in Fig. 5.2 (a) are reflected on the σ_1 and σ_2 axis then possible trajectories of region $\mathcal{S}_2$ are obtained.

Regarding the shape of the trajectories shown in Fig. 5.2 (a) it can be seen that if the initial point (5.27) would be shifted to the right then the trajectory may violate the constraints. Consequently, the admissible region does not coincide with the domain of attraction. In fact it is shown in Incremona *et al.* (2016, Theorem 2) that the domain of attraction $\mathcal{S}_I$ has the shape shown in Fig. 5.2 (b) which is also the maximum obtainable domain of attraction. In Incremona *et al.* (2016, Theorem 2) it is as well formally proven that $\sigma(t)$ converges to zero in finite-time if $\sigma(t_0) \in \mathcal{S}_I$ holds for the initial value.

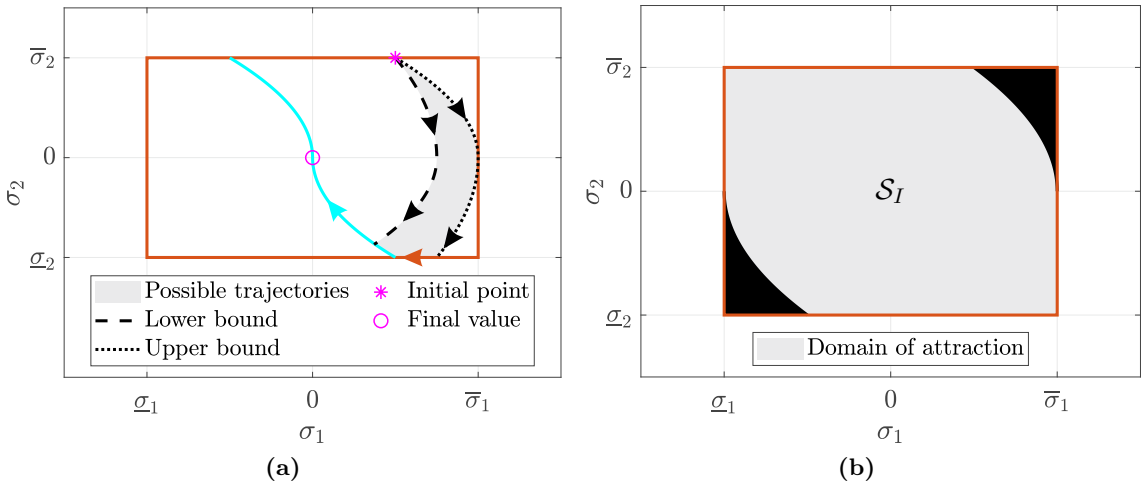

Figure 5.2: (a) Evolving trajectories of region $\mathcal{S}_1$ with specific initial value (5.27) on the bound $\bar{\sigma}_2$. (b) Visualization of domain of attraction $\mathcal{S}_I$ which is also a positive invariant set.

It is also shown that $\mathcal{S}_I$ is a positive invariant set meaning that if $\sigma(t_0) \in \mathcal{S}_I$ holds then $\sigma(t, \sigma(t_0)) \in \mathcal{S}_I$ holds for the trajectory and the constraints are never violated.

In summary the considered constrained control approach provides a maximum domain of attraction and finite-time convergence of the sliding variables. It can handle any constraints formulated in terms of the sliding variables. However, the approach also has disadvantages. For instance, consider the initial values $\sigma_1(t_0) < \underline{\sigma}_1$ and $\sigma_2(t_0) = 0$. Then control law (5.11) is applied as $\notin \mathcal{S}_b$ holds. Control law (5.11) forces $\sigma_2(t)$ to remain zero. As $\sigma_2 = \dot{\sigma}_1 = 0$ holds it follows that σ_1 remains smaller $\underline{\sigma}_1$ and never converges to zero. Another drawback of the consider approach is that the control laws (5.10) and (5.11) themselves are discontinuous and in addition switching between the control laws takes place when entering or leaving the admissible region. From a practical point of view such a controller is inapplicable as it induces chattering in the input signal. The chattering may be attenuated by introducing a smoothing boundary layer. However, in this case achievement of constrained control cannot be guaranteed anymore which is also explicitly stated in Incremona *et al.* (2016, Remark 3). Another disadvantage of the approach proposed by Incremona *et al.* (2016) is that the bounds of the constraints are required to be static. This widely limits the field of applications. For instance, consider a relative degree two mechanical system that should be controlled with respect to some position. Then constraints could be formulated with respect to position and velocity. However, the approach of Incremona *et al.* (2016) does not allow the velocity constraints to be updated online based on a distance to some obstacle for example.

5.1.2 Problem Formulation and Assumptions

In the following the class of nonlinear input-affine systems

$$\dot{x} = f(x) + g(x)u, \tag{5.28}$$

$$y_r = h(x), \tag{5.29}$$

with states $x \in \mathbb{R}^n$, control variable $y_r \in \mathbb{R}$, and control input $u \in \mathbb{R}$ is considered. The control goal is to achieve set-point tracking according to

$$\lim_{t\to\infty} y_r(t) = w, \tag{5.30}$$

in compliance with constraints that are defined by the upper bound

$$c_1\colon \quad y_{c_1}(t) = s_{c_1}\dot{y}_r(t) \leq l_{c_1}(t), \qquad s_{c_1} = +1, \qquad l_{c_1}(t) > 0, \tag{5.31}$$

and the lower bound

$$c_2\colon \quad y_{c_2}(t) = s_{c_2}\dot{y}_r(t) \leq l_{c_2}(t), \qquad s_{c_2} = -1, \qquad l_{c_2}(t) > 0, \tag{5.32}$$

of the constrained variable $\dot{y}_r(t)$. The reference variable $w \in \mathbb{R}$ is assumed constant and the bounds $0 < l_{c_i}(t) \in \mathbb{R}$ of the constraints may depend on time. The only accessible, measured quantity is the control variable y_r and its first order time derivative $\dot{y}_r$. The system (5.28)–(5.29) is assumed to have a relative degree of two. Consequently, the input appears in the second time derivative of the control variable according to

$$\ddot{y}_r = L_f^2 h(x) + L_g L_f h(x) u = \Psi(x) + \Gamma(x) u. \tag{5.33}$$

The uncertainty bounds

$$\big|\Psi(x)\big| \leq \Psi_M, \qquad 0 < \Gamma_m \leq \Gamma(x) \leq \Gamma_M, \tag{5.34}$$

are assumed to be finite.

In the following mathematical definitions are introduced which later on play an important role for the design of the controller. A sliding manifold related to the each of the constraints is defined as

$$\sigma_{c_i}(t) = -\eta_{c_i}(t) + y_{c_i}(t) = 0, \tag{5.35}$$

with $\eta_{c_i}(t) \in \mathbb{R}$ being a continuous function and $\eta_{m,c_i} \in \mathbb{R}$ being a constant chosen as

$$\forall t\colon 0 < \eta_{m,c_i} < \eta_{c_i}(t) < l_{c_i}(t). \tag{5.36}$$

Related to the lower bound η_{m,c_i} of the auxiliary function $\eta_{c_i}(t)$ the constant $\eta_m \in \mathbb{R}$ is introduced according to

$$0 < \eta_m < \min\{\eta_{m,c_1}, \eta_{m,c_2}\}. \tag{5.37}$$

The auxiliary function $\eta_{c_i}(t)$ is assumed to be continuously differentiable with $\dot{\eta}_{c_i}(t)$ satisfying the condition

$$0 \leq \max_t \left\{|\dot{\eta}_{c_1}(t)|, |\dot{\eta}_{c_2}(t)|\right\} < \dot{\eta}_M, \tag{5.38}$$

where $\dot{\eta}_M \in \mathbb{R}$ is assumed to be a finite constant. A nonlinear sliding manifold

$$\sigma_r = -\dot{e}_r - \alpha e_r - \beta |e_r|^\gamma \mathrm{sgn}(e_r) = 0, \qquad 0 < \gamma < 1, \tag{5.39}$$

with tuning parameters $0 < \alpha \in \mathbb{R}$, $0 < \beta \in \mathbb{R}$, and $\gamma \in \mathbb{R}$ is introduced. The sliding manifold (5.39) defines a so-called terminal sliding mode which provides finite-time convergence of the tracking error

$$e_r = w - y_r. \tag{5.40}$$

The sliding manifold (5.39) is originally developed by Yu and Zhihong (2002). More details about terminal sliding modes including the concept proposed by Yu and Zhihong (2002) can be found in the introductory Section 2.1.6. In order to solve the constrained control problem it is further assumed that factor α of (5.39) satisfies

$$\alpha = \frac{\dot{\eta}_M}{\eta_m} + \mu_\alpha > 0, \qquad \mu_\alpha > 0, \tag{5.41}$$

where $\mu_\alpha \in \mathbb{R}$ is a user-defined parameter. In the subsequently discussed analysis of the developed controller it will be shown that (5.41) is a sufficient condition ensuring the convergence of sliding variable σ_r. Finally, it is assumed that $y_r = h(x)$ and $\dot{y}_r = L_f h(x)$ are continuous functions so that σ_r and σ_{c_i} are continuous.

5.1.3 Controller Design and Implementation Issues

In the following the proposed constrained controller is derived in a bottom-up manner. That means that the controller is first stated as a combination of SMC sub-controllers and afterwards it is analytically shown that the proposed control method can solve the constrained control problem. The main idea that motivates the design of the proposed controller can be understood as follows. The controller consists of two SMC sub-controllers. The first SMC is designed to guarantee reaching of the sliding manifold $\sigma_r = 0$ that is defined based on (5.39). The terminal sliding mode that is induced by $\sigma_r = 0$ provides fast finite-time convergence of the tracking error. The second SMC guarantees reaching of the additional sliding manifold $\sigma_{c_i} = 0$ defined by (5.35). The sliding manifold $\sigma_{c_i} = 0$ is used to avoid constraint violation. Therefore, the manifold $\sigma_{c_i} = 0$ is placed in the admissible region below the bound $l_{c_i}(t)$ of the constraint. If the constrained variable lays inside the admissible region but is going to violate one of the bounds the second SMC becomes active to force the constrained variable towards the manifold $\sigma_{c_i} = 0$. As the manifold $\sigma_{c_i} = 0$ lays below the bound $l_{c_i}(t)$ it follows that the violation of the constraint is avoided.

The challenges that are related to the proposed controller design are: the derivation of control laws that guarantee reaching of the introduced sliding manifolds, the achievement of smooth transition between the SMC sub-controllers, the mitigation of chattering, the handling of the time-variant bounds, and the analysis of the controller performance.

In the following the two SMC sub-controllers are designed. In particular it is required to derive the control laws that guarantee reaching of the introduced sliding manifolds $\sigma_r = 0$ and $\sigma_{c_i} = 0$. The control law that guarantees reaching of the manifold $\sigma_r = 0$ is denoted as u_r and is studied first. A Lyapunov function candidate $V_r = 0.5\sigma_r^2$ is considered to reach $\sigma_r = 0$ in finite-time. Consequently, it has to be shown that $\dot{V}_r = \dot{\sigma}_r \sigma_r \leq -\frac{\mu_r}{\sqrt{2}}|\sigma_r|$ with $\mu_r > 0$ holds true for $\sigma_r \neq 0$. Derivating (5.39) with respect to time yields

$$\dot{\sigma}_r = \ddot{y}_r + \alpha \dot{y}_r + \beta\gamma \dot{y}_r |e_r|^{\gamma-1}, \tag{5.42}$$

and substituting (5.33) in (5.42) gives

$$\dot{\sigma}_r = \Psi + \Gamma u_r + \alpha \dot{y}_r + \beta\gamma \dot{y}_r |e_r|^{\gamma-1}. \tag{5.43}$$

Substituting (5.42) in $\dot{V}_r$ leads to the reachability condition

$$\dot{\sigma}_r\sigma_r = \Psi\sigma_r + \Gamma u_r\sigma_r + \alpha\dot{y}_r\sigma_r + \beta\gamma\dot{y}_r|e_r|^{\gamma-1}\sigma_r \leq -\frac{\mu_r}{\sqrt{2}}|\sigma_r|, \qquad \mu_r > 0, \tag{5.44}$$

of the sliding surface $\sigma_r = 0$. Dividing (5.44) by $0 > -|\sigma_r|$ and $\Gamma > 0$ yields

$$-\text{sgn}(\sigma_r)u_r \geq \frac{\mu_r + \Psi_M\sqrt{2}}{\Gamma_m\sqrt{2}} + \frac{\alpha + \beta\gamma|e_r|^{\gamma-1}}{\Gamma}\dot{y}_r\text{sgn}(\sigma_r), \tag{5.45}$$

which is solved by

$$u_r = \begin{cases} -\text{sgn}(\sigma_r)\left(\frac{\mu_r+\Psi_M\sqrt{2}}{\Gamma_m\sqrt{2}} + \frac{\alpha+\beta\gamma|e_r|^{\gamma-1}}{\Gamma_m}|\dot{y}_r|\right), & \text{if } \dot{y}_r\text{sgn}(\sigma_r) \geq 0, \\ -\text{sgn}(\sigma_r)\left(\frac{\mu_r+\Psi_M\sqrt{2}}{\Gamma_m\sqrt{2}} - \frac{\alpha+\beta\gamma|e_r|^{\gamma-1}}{\Gamma_M}|\dot{y}_r|\right), & \text{if } \dot{y}_r\text{sgn}(\sigma_r) < 0. \end{cases} \tag{5.46}$$

In the following the control law u_{c_i} is derived which guarantees reaching of the manifold $\sigma_{c_i} = 0$. A Lyapunov function candidate $V_{c_i} = 0.5\sigma_{c_i}^2$ is considered and the structure of the control law is assumed to be

$$u_{c_i} = u_r - s_{c_i}k_{c_i}\text{sgn}(\sigma_{c_i}). \tag{5.47}$$

Derivating (5.35) with respect to time and substituting (5.31)–(5.33) into the time derivative leads to

$$\dot{\sigma}_{c_i} = -\dot{\eta}_{c_i} + s_{c_i}\Psi + s_{c_i}\Gamma u_{c_i}. \tag{5.48}$$

Multiplying (5.48) by σ_{c_i} yields the reachability condition

$$\sigma_{c_i}\dot{\sigma}_{c_i} = \sigma_{c_i}s_{c_i}\Psi + \sigma_{c_i}s_{c_i}\Gamma u_{c_i} - \sigma_{c_i}\dot{\eta}_{c_i} \leq -\frac{\mu_{c_i}}{\sqrt{2}}|\sigma_{c_i}|, \qquad \mu_{c_i} > 0. \tag{5.49}$$

Dividing (5.49) by $|\sigma_{c_i}|$ and $-\Gamma < 0$ and considering the uncertainty bounds gives

$$-\text{sgn}(\sigma_{c_i})s_{c_i}u_{c_i} \geq \frac{\mu_{c_i} + \Psi_M\sqrt{2}}{\Gamma_m\sqrt{2}} - \frac{\dot{\eta}_{c_i}}{\Gamma}\text{sgn}(\sigma_{c_i}). \tag{5.50}$$

Substituting the controller structure (5.47) in (5.50) leads to the condition

$$k_{c_i} \geq \frac{\mu_{c_i} + \Psi_M\sqrt{2}}{\Gamma_m\sqrt{2}} - \frac{\dot{\eta}_{c_i}}{\Gamma}\text{sgn}(\sigma_{c_i}) + s_{c_i}\text{sgn}(\sigma_{c_i})u_r, \tag{5.51}$$

which is required to be satisfied by the controller gain. From (5.51) the control law

$$u_{c_i} = u_r - s_{c_i}k_{c_i}\text{sgn}(\sigma_{c_i}), \tag{5.52}$$

with gain

$$k_{c_i} = \frac{\mu_{c_i} + \Psi_M\sqrt{2}}{\Gamma_m\sqrt{2}} + \frac{|\dot{\eta}_{c_i}|}{\Gamma_m} + s_{c_i}\text{sgn}(\sigma_{c_i})u_r + \frac{\alpha + \beta\gamma|e_r|^{\gamma-1}}{\Gamma_m}|\dot{y}_r|, \tag{5.53}$$

Algorithm 2 Ideal constrained sliding mode controller

Inputs $\sigma_{c_i}(t)$ from (5.35), $\sigma_r(t)$ from (5.39), $\dot{y}_r(t)$ from (5.29), $\dot{\eta}_{c_i}(t)$ from (5.36), μ_r from (5.44), μ_{c_i} from (5.49), α from (5.41), β, γ both from (5.39), Γ_m, Γ_M, Ψ_M all from (5.34)

if $\forall c_i \colon s_{c_i}\dot{y}_r \leq \eta_{c_i}$ **then** ▷ Inside admissible region and distant from bounds

if $\dot{y}_r \mathrm{sgn}(\sigma_r) \geq 0$ **then**

$u \leftarrow -\mathrm{sgn}(\sigma_r) \times \left(\frac{\mu_r + \Psi_M\sqrt{2}}{\Gamma_m\sqrt{2}} + \frac{\alpha+\beta\gamma|e_r|^{\gamma-1}}{\Gamma_m}|\dot{y}_r| \right)$

else

$u \leftarrow -\mathrm{sgn}(\sigma_r) \times \left(\frac{\mu_r + \Psi_M\sqrt{2}}{\Gamma_m\sqrt{2}} - \frac{\alpha+\beta\gamma|e_r|^{\gamma-1}}{\Gamma_M}|\dot{y}_r| \right)$

end if

else if $\exists c_i \colon s_{c_i}\dot{y}_r > \eta_{c_i}$ **then** ▷ Outside admissible region or approaching a bound

$u \leftarrow -s_{c_i}\mathrm{sgn}(\sigma_{c_i}) \times \left(\frac{\mu_{c_i} + \Psi_M\sqrt{2}}{\Gamma_m\sqrt{2}} + \frac{|\dot{\eta}_{c_i}|}{\Gamma_m} + \frac{\alpha+\beta\gamma|e_r|^{\gamma-1}}{\Gamma_m}|\dot{y}_r| \right)$

end if

Output $u(t)$

is obtained. The additional term $+\frac{\alpha+\beta\gamma|e_r|^{\gamma-1}}{\Gamma_m}|\dot{y}_r|$ becomes relevant for the subsequently discussed controller analysis. By substituting (5.53) in (5.52) it can be shown that control law (5.52) is equivalent to

$$u_{c_i} = -s_{c_i}\mathrm{sgn}(\sigma_{c_i}) \times \left(\frac{\mu_{c_i} + \Psi_M\sqrt{2}}{\Gamma_m\sqrt{2}} + \frac{|\dot{\eta}_{c_i}|}{\Gamma_m} + \frac{\alpha+\beta\gamma|e_r|^{\gamma-1}}{\Gamma_m}|\dot{y}_r| \right). \tag{5.54}$$

However, to achieve smooth transitions between the control laws u_r and u_{c_i} it is desirable to have control law u_{c_i} in the form of (5.52) which will be further discussed.

An ideal version of the proposed controller that does not consider any smoothness of the input signal is described by Algorithm 2. It is a simple switching between the control laws (5.46) and (5.54) of the SMC sub-controllers. If the constrained variables are inside the admissible region and in sufficient distance to the bounds then the control law (5.46) is applied to achieve reference tracking. If the constrained variable violates a bound or lays inside the admissible region but is approaching a bound too closely then control law (5.54) is applied to enforce the constraints. However, Algorithm 2 can not be applied in practice. Due to the discontinuous control laws and the discontinuous switching between the sub-controllers chattering is generated which makes the whole approach infeasible.

To avoid the problem of discontinuities smoothing boundary layers are introduced as follows. Therefore, the smooth approximation

$$\mathrm{sat}(a) = \begin{cases} \mathrm{sgn}(a) & \text{for } |a| \geq 1, \\ a & \text{for } |a| < 1, \end{cases} \tag{5.55}$$

of the signum function is defined. The smooth approximation (5.55) is applied to the reaching laws (5.46) and (5.52) to replace the signum function. Consequently, an approx-

Algorithm 3 Practical implementation of constrained sliding mode controller

Inputs $\sigma_{c_i}(t)$ from (5.35), $\sigma_r(t)$ from (5.39), $\dot{y}_r(t)$ from (5.29), $\dot{\eta}_{c_i}(t)$ from (5.36), μ_r from (5.44), μ_{c_i} from (5.49), α from (5.41), β, γ both from (5.39), Γ_m, Γ_M, Ψ_M all from (5.34), $\epsilon_{c_i} > 0$, $\epsilon_r > 0$

if $\dot{y}_r \mathrm{sgn}(\sigma_r) \geq 0$ **then**

$u_r^* \leftarrow -\mathrm{sat}(\frac{\sigma_r}{\epsilon_r}) \times \left(\frac{\mu_r + \Psi_M\sqrt{2}}{\Gamma_m\sqrt{2}} + \frac{\alpha+\beta\gamma|e_r|^{\gamma-1}}{\Gamma_m}|\dot{y}_r| \right)$

else

$u_r^* \leftarrow -\mathrm{sat}(\frac{\sigma_r}{\epsilon_r}) \times \left(\frac{\mu_r + \Psi_M\sqrt{2}}{\Gamma_m\sqrt{2}} - \frac{\alpha+\beta\gamma|e_r|^{\gamma-1}}{\Gamma_M}|\dot{y}_r| \right)$

end if

if $\forall c_i \colon s_{c_i}\dot{y}_r \leq \eta_{c_i}$ **then** ▷ Inside admissible region and distant from bounds

$u \leftarrow u_r^*$

else if $\exists c_i \colon s_{c_i}\dot{y}_r > \eta_{c_i}$ **then** ▷ Outside admissible region or approaching a bound

$u \leftarrow u_r^* - s_{c_i}\mathrm{sat}\left(\frac{\sigma_{c_i}}{\epsilon_{c_i}}\right) \times \left(\frac{\mu_{c_i} + \Psi_M\sqrt{2}}{\Gamma_m\sqrt{2}} + \frac{|\dot{\eta}_{c_i}|}{\Gamma_m} + s_{c_i}\mathrm{sat}\left(\frac{\sigma_{c_i}}{\epsilon_{c_i}}\right) u_r^* + \frac{\alpha+\beta\gamma|e_r|^{\gamma-1}}{\Gamma_m}|\dot{y}_r| \right)$

end if

Output $u(t)$

imation

$$u_r^* = \begin{cases} -\mathrm{sat}(\frac{\sigma_r}{\epsilon_r}) \times \left(\frac{\mu_r + \Psi_M\sqrt{2}}{\Gamma_m\sqrt{2}} + \frac{\alpha+\beta\gamma|e_r|^{\gamma-1}}{\Gamma_m}|\dot{y}_r| \right), & \text{if } \dot{y}_r\mathrm{sgn}(\sigma_r) \geq 0, \\ -\mathrm{sat}(\frac{\sigma_r}{\epsilon_r}) \times \left(\frac{\mu_r + \Psi_M\sqrt{2}}{\Gamma_m\sqrt{2}} - \frac{\alpha+\beta\gamma|e_r|^{\gamma-1}}{\Gamma_M}|\dot{y}_r| \right), & \text{if } \dot{y}_r\mathrm{sgn}(\sigma_r) < 0, \end{cases} \tag{5.56}$$

of the reaching law u_r is obtained by substituting $\mathrm{sgn}(\sigma_r)$ of (5.46) with $\mathrm{sat}(\frac{\sigma_r}{\epsilon_r})$ and an approximation

$$\begin{aligned} u_{c_i}^* = u_r^* &- s_{c_i}\mathrm{sat}\left(\frac{\sigma_{c_i}}{\epsilon_{c_i}}\right) \\ &\times \left(\frac{\mu_{c_i} + \Psi_M\sqrt{2}}{\Gamma_m\sqrt{2}} + \frac{|\dot{\eta}_{c_i}|}{\Gamma_m} + s_{c_i}\mathrm{sat}\left(\frac{\sigma_{c_i}}{\epsilon_{c_i}}\right) u_r^* + \frac{\alpha+\beta\gamma|e_r|^{\gamma-1}}{\Gamma_m}|\dot{y}_r| \right), \end{aligned} \tag{5.57}$$

of the reaching law u_{c_i} is obtained by substituting $\mathrm{sgn}(\sigma_{c_i})$ of (5.52) with $\mathrm{sat}(\frac{\sigma_{c_i}}{\epsilon_{c_i}})$. In (5.56) the parameter $0 < \epsilon_r \in \mathbb{R}$ defines the width of the smoothing boundary layer that is introduced with respect to the sliding surface $\sigma_r = 0$ and in (5.57) the parameter $0 < \epsilon_{c_i} \in \mathbb{R}$ defines the width of the smoothing boundary layer that is introduced with respect to the sliding surface $\sigma_{c_i} = 0$. Based on the approximated reaching laws u_r^* and $u_{c_i}^*$ a practical controller implementation is formulated that avoids the problem of the discontinuities. The practical controller implementation is described by Algorithm 3. In the following it is shown that the practical controller implementation provides a smooth transition between the SMC sub-controllers. First, the conditions $\forall c_i \colon s_{c_i}\dot{y}_r \leq \eta_{c_i}$ and $\exists c_i \colon s_{c_i}\dot{y}_r > \eta_{c_i}$ are studied that according to Algorithm 3 induce the switching of the sub-controllers. From (5.31), (5.32), and (5.35) it follows that statement $\forall c_i \colon s_{c_i}\dot{y}_r \leq \eta_{c_i}$

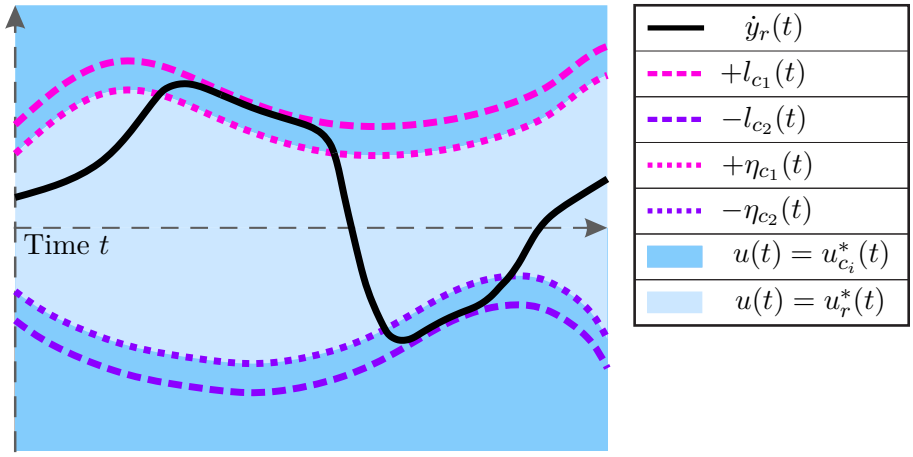

Figure 5.3: Control input selection dependent on constrained variable $\dot{y}_r(t)$.

is equivalent to $\forall c_i \colon \sigma_{c_i} \leq 0$ and statement $\exists c_i \colon s_{c_i}\dot{y}_r > \eta_{c_i}$ is equivalent to $\exists c_i \colon \sigma_{c_i} > 0$. According to Algorithm 3 the switch between the sub-controllers (5.56) and (5.57) occurs if σ_{c_i} changes from zero to a positive value or vice versa. Let $\sigma_{c_i} \to 0_+$ denote that σ_{c_i} approaches 0 from the right hand side. In case of $\sigma_{c_i} \to 0_+$ it follows from (5.57) that $u^*_{c_i} \to u^*_r$ holds. Consequently, the transition between the control laws is smooth. In addition, the chattering effect occurring around the sliding surfaces $\sigma_r = 0$ and $\sigma_{c_i} = 0$ can be mitigated by choosing the boundary layer widths ϵ_r and ϵ_{c_i} properly.

Finally, a graphical illustration of the practical controller implementation is given by Fig. 5.3. It can be seen that the control input equals $u^*_r(t)$ if the constrained variable is in the region between the auxiliary functions $\eta_{c_1}(t)$ and $\eta_{c_2}(t)$. In this region the constraints are satisfied so that $u^*_r(t)$ is applied to achieve reference tracking. If the constrained variable leaves the region between $\eta_{c_1}(t)$ and $\eta_{c_2}(t)$ then the control input switches to $u^*_{c_i}(t)$. The switch of the control input guarantees the constraints to remain satisfied if the auxiliary function $\eta_{c_i}(t)$ is properly chosen. That can be understood as follows. First, the sliding surfaces $\sigma_{c_1}(t) = \dot{y}_r(t) - \eta_{c_1}(t) = 0$ and $\sigma_{c_2}(t) = -\dot{y}_r(t) - \eta_{c_2}(t) = 0$ are considered. Both surfaces are illustrated in Fig. 5.3 by the graphs $\eta_{c_1}(t)$ and $-\eta_{c_2}(t)$. From the controller design it is known that the control input $u_{c_i}(t)$ guarantees reaching of the sliding manifold $\sigma_{c_i}(t) = 0$. Consequently, if $u_{c_1}(t)$ would be applied it can be guaranteed that $\dot{y}_r(t)$ is pushed towards the graph $\eta_{c_1}(t)$ and if $u_{c_2}(t)$ would be applied it can be guaranteed that $\dot{y}_r(t)$ is pushed towards the graph $-\eta_{c_2}(t)$. Both graphs $\eta_{c_1}(t)$ and $-\eta_{c_2}(t)$ are located inside the admissible region defined by the bounds of $l_{c_1}(t)$ and $l_{c_2}(t)$. As a result, constraint violation can be avoided by applying input $u_{c_i}(t)$. The remaining problem is that the practical controller implementation generates the control input $u^*_{c_i}(t)$ instead of the desired input $u_{c_i}(t)$. Nevertheless, satisfaction of the constraints can still be guaranteed if the auxiliary function is properly chosen. Assume the auxiliary function $\eta_{c_i}(t) > 0$ to be chosen in sufficient distance to the bound $l_{c_i}(t) > 0$ so that $\sigma_{c_i}(t) = s_{c_i}\dot{y}_r(t) - \eta_{c_i}(t) > \epsilon_{c_i}$ holds in case of $s_{c_i}\dot{y}_r(t) = l_{c_i}(t)$. As $\sigma_{c_i}(t) > \epsilon_{c_i}$ holds for the considered case it follows from the smooth approximation (5.55) that $\mathrm{sat}(\sigma_{c_i}/\epsilon_{c_i})$ and $\mathrm{sgn}(\sigma_{c_i}/\epsilon_{c_i})$ are identical. The boundary layer width ϵ_{c_i} is always positive leading to $\mathrm{sgn}(\sigma_{c_i}/\epsilon_{c_i}) = \mathrm{sgn}(\sigma_{c_i})$. Finally, as $\mathrm{sat}(\sigma_{c_i}/\epsilon_{c_i}) = \mathrm{sgn}(\sigma_{c_i})$ holds the control inputs $u^*_{c_i}(t)$ and $u_{c_i}(t)$ equal each other in case of $s_{c_i}\dot{y}_r(t) = l_{c_i}(t)$ and the constraint violation

is avoided.

5.1.4 Controller Analysis

In the following it is shown that the proposed control method can solve the constrained control problem. The mathematical properties of the proposed approach are discussed. That includes the analysis of the tracking error convergence as well as the study on how the tuning parameters affect the controller performance. The ideal controller (Algorithm 2) is a special case of the practical controller implementation (Algorithm 3) which can be seen by choosing the boundary layer widths $\epsilon_r > 0$ and $\epsilon_{c_i} > 0$ arbitrary small. As a consequence, Algorithm 3 is discussed subsequently as it is the more general approach and the method that is relevant in practice.

The main results of this section are summarized as follows. In Theorem 8 it is proven that the constraints can be guaranteed to be satisfied if the auxiliary function η_{c_i} is suitably chosen. The condition that the auxiliary function has to met is given by the inequality (5.61). In Theorem 12 the convergence of the sliding variable σ_r is studied. It can be guaranteed that $|\sigma_r|$ converges to a domain that depends on the boundary layer widths ϵ_r and ϵ_{c_i}. The domain is specified by the inequality (5.95). The convergence of $|\sigma_r|$ with respect to the specified domain can be achieved in finite time. A maximum time interval that is required for the convergence is given by (5.97). In Theorem 14 the convergence of the tracking error e_r is proven. The tracking error is shown to be bounded after a finite time. The error bounds can be determined by solving the nonlinear equation (5.119). The bounds depend on several controller parameters such as the tuning parameters of the sliding manifold $\sigma_r = 0$ and the smoothing boundary layer widths ϵ_r and ϵ_{c_i}. A maximum time interval after which the tracking error is guaranteed to be within the specified bounds is given by (5.121). In Corollary 15 the domain of attraction is discussed. The considered domain of attraction is specified by (5.141). It is shown that the proposed control method provides the maximum possible domain of attraction.

In the following the theorems and the corollary as well as required lemmata are stated.

Lemma 7.
Consider control of system (5.28)–(5.29) based on Algorithm 3. There exists some finite-time t_f so that σ_{c_i} is upper bounded by the smoothing boundary layer width ϵ_{c_i} i. e.

$$\sigma_{c_i}(t) \leq \epsilon_{c_i}, \tag{5.58}$$

holds for $t \geq t_f$.

Proof. From Algorithm 3 it is known that if

$$\sigma_{c_i} = -\eta_{c_i} + s_i \dot{y}_r \geq \epsilon_{c_i} > 0, \tag{5.59}$$

holds then the control input equals (5.57) which in fact equals (5.52) as $\mathrm{sat}(\sigma_{c_i}/\epsilon_{c_i}) = \mathrm{sgn}(\sigma_{c_i})$ holds due to (5.59) and (5.55). As control input (5.52) satisfies the reachability condition (5.49) it follows that

$$\sigma_{c_i}(t) \leq \epsilon_{c_i}, \tag{5.60}$$

holds for $t \geq t_f$ with t_f being some finite-time instant. □

Theorem 8 (Achievement of constraints related to Algorithm 3)**.**
Consider control of system (5.28)–(5.29) based on Algorithm 3. Let the auxiliary function $\eta_{c_i}(t)$ *be chosen as*

$$\epsilon_{c_i} \leq l_{c_i}(t) - \eta_{c_i}(t), \tag{5.61}$$

with bound $l_{c_i}(t) > 0$ *and smoothing boundary layer width* $\epsilon_{c_i} > 0$*. There exists some finite-time* t_f *so that the constraints are satisfied for* $t \geq t_f$ *i. e.*

$$-l_{c_2}(t) \leq \dot{y}_r(t) \leq l_{c_1}(t), \tag{5.62}$$

holds for $t \geq t_f$*. If* $\forall c_i \colon \sigma_{c_i}(t_0) \leq \epsilon_{c_i}$ *holds true for the initial time instant* t_0 *then* $t_f = t_0$*.*

Proof. From Lemma 7 it is known that

$$\sigma_{c_i} = -\eta_{c_i}(t) + s_{c_i}\dot{y}_r(t) \leq \epsilon_{c_i}, \tag{5.63}$$

holds for $t \geq t_f$ with t_f being finite. Substituting (5.61) in (5.63) leads to $s_{c_i}\dot{y}_r(t) \leq l_{c_i}(t)$ from which (5.62) follows. □

Lemma 9.
Consider control of system (5.28)–(5.29) based on Algorithm 3 with μ_{c_1} *chosen as* $\mu_{c_1} \geq \mu_r$*. Let* $\sigma_r(t) \geq \epsilon_r > 0$ *hold for* $t \in [t_1, t_2]$ *where* $\epsilon_r > 0$ *is the user-defined smoothing boundary layer width. It follows that* $\sigma_r(t)$ *decreases to* ϵ_r *in finite-time according to*

$$\begin{aligned} &\sigma_r(t) \leq \kappa - \varrho(t - t_1), \\ &\quad \kappa = \max\Big\{\sigma_r(t_1), \sigma_r(t_1) + \sigma_{c_2}(t_1)\Big\}, \qquad \sigma_{c_2}(t_1) = -\dot{y}_r(t_1) - \eta_{c_2}(t_1), \\ &\quad \varrho = \min\left\{\frac{\mu_r}{\sqrt{2}}, \mu_a \eta_m\right\}, \end{aligned} \tag{5.64}$$

with $t \in [t_1, t_2]$*.*

Proof. It will be shown that for the possible control inputs $u = u_r^*$, $u = u_{c_1}^*$, and $u = u_{c_2}^*$ the sliding variable $\sigma_r \geq \epsilon_r > 0$ decreases to ϵ_r in finite-time.

Step 1: Consideration of control input $u = u_r^*$ according to (5.56). From the reachability condition (5.44) and the definition of the smooth approximation (5.55) it follows that

$$\dot{\sigma}_r \leq -\frac{\mu_r}{\sqrt{2}}, \tag{5.65}$$

holds in case of $\sigma_r \geq \epsilon_r$.

Step 2: Consideration of control input

$$u = u_{c_1}^* = u_r^* - \operatorname{sat}\left(\frac{\sigma_{c_1}}{\epsilon_{c_1}}\right) \times k_{c_1}^*, \tag{5.66}$$

with

$$k_{c_1}^* = \left(\frac{\mu_{c_1} + \Psi_M\sqrt{2}}{\Gamma_m\sqrt{2}} + \frac{|\dot{\eta}_{c_1}|}{\Gamma_m} + \operatorname{sat}\left(\frac{\sigma_{c_1}}{\epsilon_{c_1}}\right) u_r^* + \frac{\alpha + \beta\gamma|e_r|^{\gamma-1}}{\Gamma_m}|\dot{y}_r|\right), \tag{5.67}$$

according to (5.57). The saturation function $\text{sat}(\sigma_{c_1}/\epsilon_{c_1})$ is bounded as

$$0 \leq \text{sat}\left(\frac{\sigma_{c_1}}{\epsilon_{c_1}}\right) \leq 1, \tag{5.68}$$

because $\sigma_{c_1} > 0$ holds if $u = u_{c_1}^*$ is applied. Input u_r^* is part of (5.66) and (5.67). As $u = u_{c_1}^*$ is only applied if $\sigma_{c_1} = -\eta_{c_1} + \dot{y}_r > 0$ holds it follows that $\dot{y}_r > 0$ holds and according to (5.56) quantity u_r^* is

$$u_r^* = -\frac{\mu_r + \Psi_M\sqrt{2}}{\Gamma_m\sqrt{2}} - \frac{\alpha + \beta\gamma|e_r|^{\gamma-1}}{\Gamma_m}|\dot{y}_r| < 0, \tag{5.69}$$

in case of $\sigma_r \geq \epsilon_r > 0$ and $\dot{y}_r > 0$. Substituting (5.69) in (5.67) and considering (5.68) yields

$$0 \leq \frac{\mu_{c_1} - \mu_r}{\Gamma_m\sqrt{2}} + \frac{|\dot{\eta}_{c_1}|}{\Gamma_m} \leq k_{c_1}^*, \tag{5.70}$$

in case of $\mu_{c_1} \geq \mu_r > 0$. As $k_{c_1}^*$ is non-negative and due to (5.68) it follows $u_{c_1}^* \leq u_r^*$ from (5.66). For $\sigma_r > 0$ the reachability condition

$$\dot{\sigma}_r = \Psi + \Gamma u + \alpha\dot{y}_r + \beta\gamma\dot{y}_r|e_r|^{\gamma-1} \leq -\frac{\mu_r}{\sqrt{2}}, \qquad \mu_r > 0, \tag{5.71}$$

known from (5.44) is satisfied if inequality

$$u \leq -\frac{\mu_r + \Psi_M\sqrt{2}}{\Gamma_m\sqrt{2}} - \frac{\alpha + \beta\gamma|e_r|^{\gamma-1}}{\Gamma}\dot{y}_r, \tag{5.72}$$

holds. As stated in Step 1 the reachability condition is satisfied for $u = u_r^*$ if $\sigma_r \geq \epsilon_r$ holds. As $u_{c_1}^* \leq u_r^*$ holds it is

$$u_{c_1}^* \leq u_r^* \leq -\frac{\mu_r + \Psi_M\sqrt{2}}{\Gamma_m\sqrt{2}} - \frac{\alpha + \beta\gamma|e_r|^{\gamma-1}}{\Gamma}\dot{y}_r, \tag{5.73}$$

and the reachability condition is also satisfied for $u = u_{c_1}^*$. Consequently,

$$\dot{\sigma}_r \leq -\frac{\mu_r}{\sqrt{2}}, \tag{5.74}$$

holds.

Step 3: Consideration of control input $u = u_{c_2}^*$ according to (5.57).

Case I:

It is first studied the behavior of σ_r if input $u(t) = u_{c_2}^*(t)$ is applied on some time interval $t \in [t_1, t_2)$ but not at time instant t_2. As $u = u_{c_2}^*$ is applied if and only if $\sigma_{c_2} > 0$ holds it is $\sigma_{c_2}(t) > 0$ and $\sigma_{c_2}(t_2) = 0$. Consequently, $\sigma_{c_2}(t^\star) \geq 0$ with $t^\star \in [t_1, t_2]$ holds. According to (5.39) and (5.40) it is

$$\sigma_r(t^\star) = \dot{y}_r(t^\star) - \alpha e_r(t^\star) - \beta|e_r(t^\star)|^\gamma \text{sgn}(e_r(t^\star)), \tag{5.75}$$

for $t^\star \in [t_1, t_2]$. As $\sigma_{c_2}(t^\star) = -\eta_{c_2}(t^\star) - \dot{y}_r(t^\star) \geq 0$ holds it follows from (5.36) and (5.37) that

$$\dot{y}_r(t^\star) \leq -\eta_{c_2}(t^\star) < -\eta_m < 0, \qquad \eta_m > 0, \tag{5.76}$$

holds. As $\sigma_r(t^\star) > 0$ and $\dot{y}_r(t^\star) < 0$ hold it can be seen from (5.75) that $e_r(t^\star) < 0$ holds. Consequently, equation (5.75) is

$$\sigma_r(t^\star) = \dot{y}_r(t^\star) - \alpha e_r(t^\star) + \beta |e_r(t^\star)|^\gamma, \tag{5.77}$$

for $t^\star \in [t_1, t_2]$. From (5.77), (5.76), and $e_r = w - y_r$ it follows that

$$\begin{aligned}\sigma_r(t^\star) \leq -\eta_{c_2}(t^\star) - \alpha w + \alpha y_r(t_1) + \beta |e_r(t_1)|^\gamma \\ + \int_{t_1}^{t^\star} \alpha \dot{y}_r(\tau) d\tau + \int_{t_1}^{t^\star} \gamma \beta \dot{y}_r(\tau) |e_r(\tau)|^{\gamma-1} d\tau,\end{aligned} \tag{5.78}$$

holds for any time $t^\star \in [t_1, t_2]$, where $\gamma\beta\dot{y}_r|e_r|^{\gamma-1}$ is the time derivative of $\beta|e_r|^\gamma$ in case of $e_r < 0$. Consider α to be a positive constant

$$\alpha = \frac{\dot{\eta}_M}{\eta_m} + \mu_\alpha, \tag{5.79}$$

as stated in (5.41). From (5.76) and (5.38) it follows that inequality

$$\alpha = \frac{\dot{\eta}_M}{\eta_m} + \mu_\alpha \geq \frac{\dot{\eta}_{c_2}(t)}{\dot{y}_r(t)} + \mu_\alpha, \qquad \mu_\alpha > 0, \tag{5.80}$$

holds. Substituting $\alpha > 0$ from (5.80) in (5.78), considering $\dot{y}_r(t^\star) \leq -\eta_m < 0$ from (5.76), and considering that β, γ are positive leads to

$$\sigma_r(t^\star) \leq -\alpha w + \alpha y_r(t_1) + \beta |e_r(t_1)|^\gamma - \eta_{c_2}(t_1) - \mu_\alpha \eta_m (t^\star - t_1). \tag{5.81}$$

Adding $\dot{y}_r(t_1) - \dot{y}_r(t_1)$ to (5.81) and considering the definition of σ_r according to (5.77) yields

$$\begin{aligned}\sigma_r(t^\star) &\leq \dot{y}_r(t_1) - \alpha e_r(t_1) + \beta |e_r(t_1)|^\gamma - \dot{y}_r(t_1) - \eta_{c_2}(t_1) - \mu_\alpha \eta_m (t^\star - t_1), \\ &= \sigma_r(t_1) - \dot{y}_r(t_1) - \eta_{c_2}(t_1) - \mu_a \eta_m (t^\star - t_1), \qquad \mu_a \eta_m > 0,\end{aligned} \tag{5.82}$$

for $t^\star \in [t_1, t_2]$.

Case II:

It is now studied the behavior of σ_r if input $u(t) = u^*_{c_2}(t)$ is applied on some time interval $t \in (t_1, t_2)$ but not at time instants t_1 and t_2. It follows that $\sigma_{c_2}(t) > 0$, $\sigma_{c_2}(t_1) = 0$, $\sigma_{c_2}(t_2) = 0$, and $\sigma_{c_2}(t^\star) \geq 0$ with $t^\star \in [t_1, t_2]$ hold. According to (5.39) it is

$$\sigma_r(t^\star) = \dot{y}_r(t^\star) - \alpha e_r(t^\star) - \beta |e_r(t^\star)|^\gamma \mathrm{sgn}(e_r(t^\star)), \tag{5.83}$$

for $t^\star \in [t_1, t_2]$. As $\sigma_{c_2}(t^\star) = -\eta_{c_2}(t^\star) - \dot{y}_r(t^\star) \geq 0$ holds it follows from (5.35), (5.36), and (5.37) that

$$\dot{y}_r(t^\star) \leq -\eta_{c_2}(t^\star) < -\eta_m < 0, \qquad \eta_m > 0, \tag{5.84}$$

holds. Considering $\dot{y}_r(t^\star) < 0$ and $\sigma(t^\star) > 0$ it can be seen from (5.83) that $e_r(t^\star) < 0$ holds which leads to

$$\sigma_r(t^\star) = \dot{y}_r(t^\star) - \alpha e_r(t^\star) + \beta |e_r(t^\star)|^\gamma. \tag{5.85}$$

From (5.84), (5.85), and $e_r = w - y_r$ it follows that

$$\sigma_r(t^\star) \leq -\eta_{c_2}(t^\star) - \alpha w + \alpha y_r(t_1) + \beta |e_r(t_1)|^\gamma + \int_{t_1}^{t^\star} \alpha \dot{y}_r(\tau) d\tau + \int_{t_1}^{t^\star} \gamma\beta \dot{y}_r(\tau) |e_r(\tau)|^{\gamma-1} d\tau, \tag{5.86}$$

holds for any time $t^\star \in [t_1, t_2]$. Substituting

$$\alpha = \frac{\dot{\eta}_M}{\eta_m} + \mu_\alpha \geq \frac{\dot{\eta}_{c_2}(t)}{\dot{y}_r(t)} + \mu_\alpha, \qquad \mu_\alpha > 0, \tag{5.87}$$

in (5.86) and considering $\dot{y}_r(t^\star) \leq -\eta_m < 0$ as well as $\beta > 0$, $\gamma > 0$ leads to

$$\sigma_r(t^\star) \leq -\alpha w + \alpha y_r(t_1) + \beta |e_r(t_1)|^\gamma - \eta_{c_2}(t_1) - \mu_\alpha \eta_m (t^\star - t_1). \tag{5.88}$$

As $\sigma_{c_2}(t_1) = -\eta_{c_2}(t_1) - \dot{y}_r(t_1) = 0$ holds it follows $-\eta_{c_2}(t_1) = \dot{y}_r(t_1)$. Replacing $-\eta_{c_2}(t_1)$ by $\dot{y}_r(t_1)$ in (5.88) and considering the definition of σ_r from (5.85) yields

$$\sigma_r(t^\star) \leq \sigma_r(t_1) - \mu_a \eta_m (t^\star - t_1), \qquad \mu_a \eta_m > 0, \tag{5.89}$$

for $t^\star \in [t_1, t_2]$.

Step 4: Occurrence of Case I and Case II of Step 3. It will be shown that Case I of Step 3 can only occur if $u = u^*_{c_2}$ is applied first, meaning that once input $u = u^*_r$ or $u = u^*_{c_1}$ has been applied Case I of Step 3 can not occur anymore.

According to Algorithm 3 input $u = u^*_r$ or $u = u^*_{c_1}$ are only applied if $\sigma_{c_2} = -\eta_{c_2} - \dot{y}_r \leq 0$ holds. Consider $u = u^*_r$ or $u = u^*_{c_1}$ to be applied before the input switches to $u = u^*_{c_2}$. That means that there exists a time instant t_1 with $\sigma_{c_2}(t_1) = -\eta_{c_2}(t_1) - \dot{y}_r(t_1) = 0$ just before σ_{c_2} switches to a positive number inducing the switch of the input to $u = u^*_{c_2}$. As $\sigma_{c_2}(t_1) = 0$ holds it is Case II that has to be considered and not Case I which would require $\sigma_{c_2}(t_1) > 0$.

Step 5: Rate of decrease. Let $\mu_{c_1} \geq \mu_r$ and $\sigma_r(t) \geq \epsilon_r > 0$ hold for some interval $t \in [t_1, t_2]$. From (5.65), (5.74), (5.82), (5.89), and Step 4 it follows that $\sigma_r(t)$ decreases to ϵ_r in finite-time according to

$$\begin{aligned} \sigma_r(t) &\leq \kappa - \varrho(t - t_1), \\ \kappa &= \max\Big\{\sigma_r(t_1), \sigma_r(t_1) - \dot{y}_r(t_1) - \eta_{c_2}(t_1)\Big\}, \\ \varrho &= \min\left\{\frac{\mu_r}{\sqrt{2}}, \mu_a \eta_m\right\}, \end{aligned} \tag{5.90}$$

with $t \in [t_1, t_2]$. □

Lemma 10.
Consider control of system (5.28)–(5.29) based on Algorithm 3 with μ_{c_2} chosen as $\mu_{c_2} \geq \mu_r$. Let $\sigma_r(t) \leq -\epsilon_r < 0$ hold for $t \in [t_1, t_2]$ where $\epsilon_r > 0$ is the user-defined smoothing boundary layer width. It follows that $\sigma_r(t)$ increases to $-\epsilon_r$ in finite-time according to

$$\begin{aligned} \sigma_r(t) &\geq \kappa + \varrho(t - t_1), \\ \kappa &= \min\Big\{\sigma_r(t_1), \sigma_r(t_1) - \sigma_{c_1}(t_1)\Big\}, \qquad \sigma_{c_1}(t_1) = \dot{y}_r(t_1) - \eta_{c_1}(t_1), \end{aligned} \tag{5.91}$$

$$\varrho = \min\left\{\frac{\mu_r}{\sqrt{2}}, \mu_a\eta_m\right\},$$

with $t \in [t_1, t_2]$.

Proof. The proof can be found in Appendix D. It is similar to the proof of Lemma 9. □

Lemma 11.
Consider control of system (5.28)–(5.29) based on Algorithm 3. Let

$$\forall t\colon \max\Big\{\sigma_{c_1}(t), \sigma_{c_2}(t)\Big\} \leq \zeta, \tag{5.92}$$

$$\sigma_{c_1}(t) = \dot{y}_r(t) - \eta_{c_1}(t), \qquad \sigma_{c_2}(t) = -\dot{y}_r(t) - \eta_{c_2}(t), \tag{5.93}$$

hold for $t \geq t_f$ *and let* $\mu_{c_i} \geq \mu_r$ *hold. Then* $|\sigma_r(t)|$ *is finite-time stable with respect to the domain* $\epsilon_r + \zeta$ *with* $\epsilon_r > 0$ *being the user-defined smoothing boundary layer width. More specifically* $|\sigma_r(t^\star)|$ *decreases as*

$$|\sigma_r(t^\star)| \leq |\sigma_r(t_1)| - \varrho(t^\star - t_1), \qquad \varrho = \min\left\{\frac{\mu_r}{\sqrt{2}}, \mu_a\eta_m\right\}, \tag{5.94}$$

if $|\sigma_r(t^\star)| \geq \epsilon_r + \zeta$ *with* $t^\star \in [t_1, t_2]$ *and* $t_1 \geq t_f$.

Proof. Let condition (5.92) hold for $t \geq t_f$. It follows from Lemma 9 and 10 that a finite-time instant $t_{f2} \geq t_f$ exists for which $|\sigma_r(t_{f2})| = \epsilon_r$ holds. Then according to Lemma 9 and 10 and condition (5.92) it follows that $|\sigma_r(t)|$ is captured within the domain $\epsilon_r + \zeta$ for $t \geq t_{f2}$. Sliding variable $|\sigma_r(t)|$ is finite-time stable with respect to the domain $\epsilon_r + \zeta$ for $t \geq t_f$. □

Theorem 12 (Boundedness of sliding variable related to Algorithm 3)**.**
Consider control of system (5.28)–(5.29) based on Algorithm 3. Let the controller parameters be chosen as $\mu_{c_i} \geq \mu_r$. *There exists a finite-time instant* t_f *so that*

$$|\sigma_r(t)| \leq \epsilon_r + \epsilon_{c,M}, \qquad \epsilon_{c,M} = \max\{\epsilon_{c_1}, \epsilon_{c_2}\}, \tag{5.95}$$

holds for $t \geq t_f$ *with* $\epsilon_r, \epsilon_{c_1}, \epsilon_{c_2} > 0$ *being the user-defined smoothing boundary layers. Assume*

$$|\sigma_r(t^\star)| > \epsilon_r + \epsilon_{c,M}, \tag{5.96}$$

to hold at some time instant $t^\star$. *Further assume* $|\sigma_r(t^\star)| \leq \sigma_{r,M}$ *and* $\sigma_{c_i}(t^\star) \leq \epsilon_{c_i}$ *to hold at* $t^\star$. *It can be stated that (5.95) is achieved for* $t_f = t^\star + \tau$ *at the latest with*

$$\tau = \frac{\sigma_{r,M} - (\epsilon_r + \epsilon_{c,M})}{\varrho}, \qquad \varrho = \min\left\{\frac{\mu_r}{\sqrt{2}}, \mu_a\eta_m\right\}. \tag{5.97}$$

If $\forall c_i\colon \sigma_{c_i}(t_0) \leq \epsilon_{c_i}$ *holds initially then* $t^\star = t_0$.

Proof. From Lemma 7 it is known that

$$\sigma_{c_i}(t) \leq \epsilon_{c_i}, \tag{5.98}$$

holds for $t \geq t^\star$ with $t^\star$ being some finite-time instant. Following Lemma 11 the upper bound of σ_{c_i} as stated in (5.92) can be defined based on (5.98) which leads to

$$\zeta = \epsilon_{c,M} = \max\{\epsilon_{c_1}, \epsilon_{c_2}\}. \tag{5.99}$$

It follows from Lemma 11 that $|\sigma_r|$ remains in the domain $\epsilon_r + \epsilon_{c,M}$ after a finite-time. The statement (5.97) about τ is achieved by rearranging (5.94). □

Lemma 13.
Assume the constraints to be satisfied according to Theorem 8 i. e.

$$-l_{c_2}(t) \leq \dot{y}_r(t) \leq l_{c_1}(t), \tag{5.100}$$

holds for $t \geq t_f$. Let the sliding variable σ_r be bounded as $|\sigma_r(t)| \leq \sigma_{r,M}$ for $t \geq t_f$. For $t \geq t_f$ the tracking error $|e_r(t)|$ is finite-time stable with respect to a domain $e_{r,M} > 0$. The domain is obtained as the solution of

$$\alpha e_{r,M} + \beta e_{r,M}^{\gamma} = \sigma_{r,M} + \frac{\mu_e}{\sqrt{2}}, \tag{5.101}$$

with α, β, and γ known from the sliding manifold (5.39) where α is chosen as stated in (5.41). Quantity μ_e may be selected as

$$0 < \mu_e \leq \eta_m \sqrt{2}. \tag{5.102}$$

More specifically $|e_r(t)|$ decreases as

$$\frac{d|e_r(t)|}{dt} \leq -\frac{\mu_e}{\sqrt{2}}, \tag{5.103}$$

for $t \geq t_f$ if $|e_r(t)| > e_{r,M}$ holds.

Proof. Let some function $V(t)$ be defined as $V(t) = |e_r(t)|$. To make $|e_r(t)|$ finite-time stable it is desired to achieve

$$\dot{V} = \operatorname{sgn}(e_r)\, \dot{e}_r \leq -\frac{\mu_e}{\sqrt{2}}, \qquad \mu_e > 0, \tag{5.104}$$

for $e_r \neq 0$. Based on the definition of the sliding variable σ_r from (5.39) it can be stated that

$$-\dot{y}_r = \dot{e}_r = -\sigma_r - \alpha e_r - \beta |e_r|^{\gamma} \operatorname{sgn}(e_r), \tag{5.105}$$

holds. Substituting (5.105) in (5.104) gives

$$\alpha|e_r| + \beta|e_r|^{\gamma} = \alpha e_r + \beta|e_r|^{\gamma} \geq \frac{\mu_e}{\sqrt{2}} - \sigma_r, \tag{5.106}$$

for $e_r > 0$ and

$$\alpha|e_r| + \beta|e_r|^{\gamma} = -\alpha e_r + \beta|e_r|^{\gamma} \geq \frac{\mu_e}{\sqrt{2}} + \sigma_r. \tag{5.107}$$

for $e_r < 0$. As

$$\frac{\mu_e}{\sqrt{2}} + \sigma_{r,M} \geq \frac{\mu_e}{\sqrt{2}} - \sigma_r, \qquad \frac{\mu_e}{\sqrt{2}} + \sigma_{r,M} \geq \frac{\mu_e}{\sqrt{2}} + \sigma_r, \tag{5.108}$$

hold true, the equations (5.106) and (5.107) can be achieved for all $|e_r| \geq e_{r,M}$ with $e_{r,M}$ being the solution of

$$\alpha|e_{r,M}| + \beta|e_{r,M}|^\gamma = \frac{\mu_e}{\sqrt{2}} + \sigma_{r,M}. \tag{5.109}$$

As a result $|e_r|$ is finite-time stable with respect to the domain $e_{r,M}$.

The rate of decrease according to (5.104) is restricted as it depends on the constrained variable $\dot{e}_r = -\dot{y}_r$. The bounds of the constrained variable are given by (5.100).

The largest and smallest values of $\dot{y}_r$ that are obtainable in presence of the constraints can be seen if σ_{c_i} is rearranged according to

$$\sigma_{c_i} + \eta_{c_i} = s_i \dot{y}_r \leq l_{c_i}. \tag{5.110}$$

As stated in the proof of Theorem 8 satisfaction of the constraints (5.100) is achieved by enforcing

$$\sigma_{c_i}(t) \leq \epsilon_{c_i}, \tag{5.111}$$

to hold for $t \geq t_f$. Consequently, in presence of the constraints the maximum value σ_{c_i} can have is $\epsilon_{c_i} > 0$. Quantity η_{c_i} is known to be lower bounded by η_m as stated in (5.36) and (5.37), so that the values of $\dot{y}_r$ that surely can be achieved may be in the range of

$$s_i \dot{y}_r = \sigma_{c_i} + \eta_{c_i} \leq \epsilon_{c_i} + \eta_m. \tag{5.112}$$

However, from Algorithm 3 it is known that $\dot{y}_r$ is only not constrained by the controller if it is in the range of $-\eta_{c_2}(t) \leq \dot{y}_r(t) \leq \eta_{c_1}(t)$. Consequently,

$$\dot{y}_r \in [-a, +a], \qquad a \triangleq \eta_m, \quad \eta_m < \min_t\{\eta_{c_1}(t), \eta_{c_2}(t)\}, \tag{5.113}$$

describes a range of values of $\dot{y}_r = -\dot{e}_r$ that can be achieved by (5.104) for sure as for that specific range the values of $\dot{y}_r$ are guaranteed to be not constrained by the controller. Rewriting (5.104) as

$$-\operatorname{sgn}(e_r)\dot{y}_r \leq -\frac{\mu_e}{\sqrt{2}}, \tag{5.114}$$

it follows that μ_e can be selected as stated in (5.102). Consequently, the rate of decrease is suitably described by (5.103). □

Theorem 14 (Convergence of tracking error related to Algorithm 3)**.**
Consider control of system (5.28)–(5.29) based on Algorithm 3. Let

$$\forall c_i \colon \sigma_{c_i}(t_0) \leq \epsilon_{c_i}, \tag{5.115}$$

and

$$|\sigma_r(t_0)| \leq \sigma_{r,M}, \tag{5.116}$$

hold initially and let η_{c_i} *be selected as*

$$\epsilon_{c_i} \leq l_{c_i}(t) - \eta_{c_i}(t). \tag{5.117}$$

Further assume μ_{c_i} *to be chosen as* $\mu_{c_i} \geq \mu_r$*. There exists a finite-time* t_f *for which the tracking error* $|e_r|$ *remains in the domain* $e_{r,M}$ *i. e.*

$$|e_r(t)| \leq e_{r,M}, \tag{5.118}$$

holds for $t \geq t_f$*. The domain* $e_{r,M}$ *is given by the solution of*

$$\alpha e_{r,M} + \beta e_{r,M}^{\gamma} = \epsilon_r + \epsilon_{c,M} + \frac{\mu_e}{\sqrt{2}}, \qquad 0 < \mu_e \leq \eta_m \sqrt{2}, \tag{5.119}$$

where $\epsilon_{c,M}$ *is related to the smoothing boundary layer widths according to*

$$\epsilon_{c,M} = \max\{\epsilon_{c_1}, \epsilon_{c_2}\}. \tag{5.120}$$

The time instant t_f *is achieved at*

$$t_f = t_0 + \tau_1 + \tau_2, \tag{5.121}$$

$$\tau_1 = \frac{\sigma_{r,M} - (\epsilon_r + \epsilon_{c,M})}{\varrho}, \qquad \varrho = \min\left\{\frac{\mu_r}{\sqrt{2}}, \mu_a \eta_m\right\}, \tag{5.122}$$

$$\tau_2 = (e_{r,M^\star} - e_{r,M})\frac{\sqrt{2}}{\mu_e}, \tag{5.123}$$

at the latest where $e_{r,M^\star}$ *solves*

$$\alpha e_{r,M^\star} + \beta e_{r,M^\star}^{\gamma} = \epsilon_r + \epsilon_{c,M} + l_c(t_0 + \tau_1), \tag{5.124}$$

with l_c *being defined by*

$$l_c(t) = \max\{l_1(t), l_2(t)\}. \tag{5.125}$$

If $l_c(t_0 + \tau_1)$ *is not known beforehand* $e_{r,M^\star}$ *can also be obtained as the solution of*

$$\alpha e_{r,M^\star} + \beta e_{r,M^\star}^{\gamma} = \epsilon_r + \epsilon_{c,M} + l_M, \qquad \forall t\colon l_c(t) \leq l_M. \tag{5.126}$$

In addition to the constraints defined by l_{c_i} *the inequality*

$$|\dot{y}_r(t)| \leq \epsilon_r + \epsilon_{c,M} + \alpha e_{r,M} + \beta e_{r,M}^{\gamma}, \tag{5.127}$$

holds for $t \geq t_f$*.*

Proof. As (5.115), (5.116), and $\mu_{c_i} \geq \mu_r$ hold Theorem 12 can be applied from which follows that

$$|\sigma_r(t)| \leq \epsilon_r + \epsilon_{c,M}, \tag{5.128}$$

is achieved for $t \geq t_0 + \tau_1$ at the latest with τ_1 as stated in (5.122). Due to (5.115) and (5.117) it follows from Theorem 8 that the constraints are satisfied from the beginning i. e.

$$-l_{c_2}(t) \leq \dot{y}_r(t) \leq l_{c_1}(t), \tag{5.129}$$

holds for $t \geq t_0$. It follows from Lemma 13 that for $t \geq t_0 + \tau_1$ the tracking error $|e_r(t)|$ is finite-time stable with respect to the domain $e_{r,M}$ given by the solution of (5.119).

In the following it is shown that $|e_r(t_0 + \tau_1)|$ is bounded as

$$|e_r(t_0 + \tau_1)| \leq e_{r,M^\star}, \tag{5.130}$$

where $e_{r,M^\star}$ may be taken as the solution of any of the two equations: (5.124) or (5.126). Consider σ_r to be rearranged as

$$-\alpha e_r(t_0 + \tau_1) - \beta |e_r(t_0 + \tau_1)|^\gamma \mathrm{sgn}(e_r(t_0 + \tau_1)) = \sigma_r(t_0 + \tau_1) - \dot{y}_r(t_0 + \tau_1), \tag{5.131}$$

according to its definition stated in (5.39). Multiplying (5.131) by minus one gives

$$\alpha e_r(t_0 + \tau_1) + \beta |e_r(t_0 + \tau_1)|^\gamma \mathrm{sgn}(e_r(t_0 + \tau_1)) = -\sigma_r(t_0 + \tau_1) + \dot{y}_r(t_0 + \tau_1). \tag{5.132}$$

From (5.131) statement

$$-\alpha e_r(t_0 + \tau_1) - \beta |e_r(t_0 + \tau_1)|^\gamma \mathrm{sgn}(e_r(t_0 + \tau_1)) \leq \epsilon_r + \epsilon_{c,M} + |\dot{y}_r(t_0 + \tau_1)|, \tag{5.133}$$

and from (5.132) statement

$$\alpha e_r(t_0 + \tau_1) + \beta |e_r(t_0 + \tau_1)|^\gamma \mathrm{sgn}(e_r(t_0 + \tau_1)) \leq \epsilon_r + \epsilon_{c,M} + |\dot{y}_r(t_0 + \tau_1)|, \tag{5.134}$$

may be concluded, where $|\sigma_r(t_0 + \tau_1)| \leq \epsilon_r + \epsilon_{c,M}$ is known to hold due to (5.128). Considering (5.133) for $e_r < 0$ and (5.134) for $e_r \geq 0$ both times yields

$$\alpha |e_r(t_0 + \tau_1)| + \beta |e_r(t_0 + \tau_1)|^\gamma \leq \epsilon_r + \epsilon_{c,M} + |\dot{y}_r(t_0 + \tau_1)|. \tag{5.135}$$

Consequently, $|e_r(t_0 + \tau_1)|$ is bounded as stated in (5.130).

It was already shown that $|e_r(t)|$ is finite-time stable with respect to the domain $e_{r,M}$ for $t \geq t_0 + \tau_1$. In the following a time span τ_2 is specified so that (5.118) holds for $t \geq t_0 + \tau_1 + \tau_2$ at the latest. With the result of (5.130) the missing time span τ_2 can be determined. From Lemma 13 it follows that τ_2 is obtained as

$$\tau_2 = \left(e_{r,M^\star} - e_{r,M}\right) \frac{\sqrt{2}}{\mu_e} \geq \left(|e_r(t_0 + \tau_1)| - e_{r,M}\right) \frac{\sqrt{2}}{\mu_e}, \tag{5.136}$$

by integrating (5.103).

The remaining statement (5.127) follows by rearranging σ_r according to

$$\dot{y}_r(t) = \sigma_r(t) + \alpha e_r(t) + \beta |e_r(t)|^\gamma \mathrm{sgn}(e_r(t)). \tag{5.137}$$

Applying the triangle inequality on (5.137) and considering that $e_r(t)$ is bounded by $e_{r,M}$ for $t \geq t_f$ yields

$$|\dot{y}_r(t)| = |\sigma_r(t) + \alpha e_r(t) + \beta |e_r(t)|^\gamma \mathrm{sgn}(e_r(t))| \leq \epsilon_r + \epsilon_{c,M} + \alpha e_{r,M} + \beta e_{r,M}^\gamma, \tag{5.138}$$

with $t \geq t_f$. □

Corollary 15 (Domain of attraction related to Algorithm 3)**.**
Let

$$\forall c_i \colon \sigma_{c_i}(t_0) \leq \epsilon_{c_i}, \tag{5.139}$$

hold initially and let η_{c_i} *be selected as*

$$\epsilon_{c_i} \leq l_{c_i}(t) - \eta_{c_i}(t). \tag{5.140}$$

Suppose μ_{c_i} *to be chosen as* $\mu_{c_i} \geq \mu_r$*. Consider a domain of attraction to be specified as*

$$\begin{aligned} &\mathcal{S}_I = \{\mathcal{Y}_0 \colon -l_2(t) \leq \dot{y}_r(t, \mathcal{Y}_0) \leq l_1(t) \wedge |w - y_r(t^\star, \mathcal{Y}_0)| \leq e_{r,M}\}, \\ &\mathcal{Y}_0 = \{y_{r,0}, \dot{y}_{r,0}\}, \end{aligned} \tag{5.141}$$

where $y_{r,0} = y_r(t_0)$*,* $\dot{y}_{r,0} = \dot{y}_r(t_0)$ *denote initial values and* $y_r(t, \mathcal{Y}_0)$*,* $\dot{y}_r(t, \mathcal{Y}_0)$ *denote trajectories initiated by those initial values. Further,* $t^\star$ *is specified as* $t^\star \geq t_f$ *with* t_f *being a finite-time instant and* $e_{r,M}$ *is defined by the solution of*

$$\begin{aligned} &\alpha e_{r,M} + \beta e_{r,M}^\gamma = \epsilon_r + \epsilon_{c,M} + \frac{\mu_e}{\sqrt{2}}, \qquad 0 < \mu_e \leq \eta_m \sqrt{2}, \\ &\epsilon_{c,M} = \max\{\epsilon_{c_1}, \epsilon_{c_2}\}. \end{aligned} \tag{5.142}$$

Consider system (5.28)–(5.29) to be controlled based on Algorithm 3. A maximum possible domain of attraction according to (5.141) is achieved.

Proof. The desired goal

$$-l_2(t) \leq \dot{y}_r(t, \mathcal{Y}_0) \leq l_1(t), \qquad |w - y_r(t^\star, \mathcal{Y}_0)| \leq e_{r,M}, \tag{5.143}$$

can be achieved by satisfying the constraints (Theorem 8) and reaching the domain $e_{r,M}$ of the tracking error in finite-time (Theorem 14). From Theorem 8 and 14 it is known that the only restrictions that are made with respect to $y_{r,0}$, $\dot{y}_{r,0}$ are (5.115)–(5.117) which can be reformulated as

$$\forall t, c_i \colon \sigma_{c_i}(t_0) = -\eta_{c_i}(t_0) + s_{c_i}\dot{y}_r(t_0) \leq \epsilon_{c_i} \leq l_{c_i}(t) - \eta_{c_i}(t), \tag{5.144}$$

based on (5.35) and

$$|\sigma_r(t_0)| = |\dot{y}_r(t_0) - \alpha(w - y_r(t_0)) - \beta|w - y_r(t_0)|^\gamma \mathrm{sgn}(w - y_r(t_0))| \leq \sigma_{r,M}, \tag{5.145}$$

based on (5.39). Related to (5.145) it is required that some finite $\sigma_{r,M} > 0$ exists that solves the inequality. Such a $\sigma_{r,M}$ can always be found as $|\sigma_r(t_0)|$ is just the initial value of $|\sigma_r|$ which is always finite. Consequently, $y_{r,0}$ and $\dot{y}_{r,0}$ are not restricted by (5.145). Considering (5.144) it follows

$$s_{c_i}\dot{y}_r(t_0) \leq l_{c_i}(t_0) \qquad \Leftrightarrow \qquad -l_{c_2}(t_0) \leq \dot{y}_r(t_0) \leq l_{c_1}(t_0). \tag{5.146}$$

Consequently, only $\dot{y}_r(t_0)$ is restricted. But it is restricted to the maximal possible domain. □

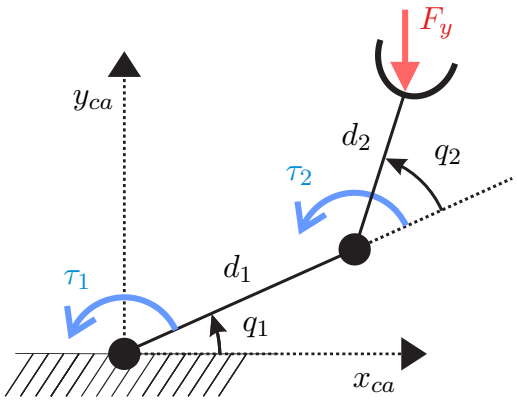

Figure 5.4: Two-link robot with rotary joints. The joint angles are denoted by q_1 and q_2, the link length are given by d_1 and d_2, the input torques are symbolized by τ_1 and τ_2, and the unknown payload is denoted as F_y. The input torques are highlighted in blue and the unknown payload is shown in red.

5.1.5 Application Example

In this section the proposed constrained controller is applied to a robotic system. The robot is a two-link robot with rotary joints as shown in Fig. 5.4. The goal is to achieve velocity-constrained point to point control of the robot. In particular, the end effector should be driven to different way points while the angular velocities of the joints are restricted. As shown in Siciliano *et al.* (2010) the dynamics of the considered two-link robot can be derived based on Lagrange equations of the second kind. Following Siciliano *et al.* (2010, Chap. 7) the dynamic equation

$$B(q)\ddot{q} + C(q,\dot{q})\dot{q} + f_v\dot{q} + f_s\mathrm{sgn}(\dot{q}) + g(q) = \tau + \xi(q, F_y), \tag{5.147}$$

is obtained where $B(q)$ describes the moments of inertia, $C(q,\dot{q})$ accounts for the centrifugal and Coriolis effects, f_v and f_s represent coefficients of static and viscous friction torques, $g(q)$ are the moments generated by earth gravity, τ are the actuator torques, and $\xi(q, F_y)$ are the moments generated by an external force F_y applied to the end effector. The related terms are given by

$$B(q) = \begin{bmatrix} b_1 + b_2\cos(q_2) & b_3 + b_4\cos(q_2) \\ b_3 + b_4\cos(q_2) & b_5 \end{bmatrix}, \quad C(q,\dot{q}) = -c_1\sin(q_2)\begin{bmatrix} \dot{q}_1 & \dot{q}_1 + \dot{q}_2 \\ -\dot{q}_1 & 0 \end{bmatrix},$$
$$g(q) = \begin{bmatrix} g_1\cos(q_1) + g_2\cos(q_1+q_2) \\ g_2\cos(q_1+q_2) \end{bmatrix}, \qquad f_f(\dot{q}) = f_v\dot{q} + f_s\mathrm{sgn}(\dot{q}),$$
$$\xi(q, F_y) = F_y\begin{bmatrix} d_1\cos(q_1) + d_2\cos(q_1+q_2) \\ d_2\cos(q_1+q_2) \end{bmatrix},$$

in detail. The model parameters are summarized in Table 5.1. The joint angles, angular velocities, and actuator torques are defined as

$$q = \begin{bmatrix} q_1 \\ q_2 \end{bmatrix}, \qquad \dot{q} = \begin{bmatrix} \dot{q}_1 \\ \dot{q}_2 \end{bmatrix}, \qquad \tau = \begin{bmatrix} \tau_1 \\ \tau_2 \end{bmatrix}, \tag{5.148}$$

Table 5.1: Parameters of two-link robot according to Siciliano *et al.* (2010)

b_1	131.5	$[\mathrm{kg\,m^2/rad}]$	b_2	6.0	$[\mathrm{kg\,m^2/rad}]$
b_3	13.0	$[\mathrm{kg\,m^2/rad}]$	b_4	3.0	$[\mathrm{kg\,m^2/rad}]$
b_5	112.0	$[\mathrm{kg\,m^2/rad}]$	c_1	3.0	$[\mathrm{kg\,m^2/rad^2}]$
g_1	309.0	$[\mathrm{kg\,m^2/s^2}]$	g_2	98.1	$[\mathrm{kg\,m^2/s^2}]$
f_v	0.2	$[\mathrm{kg\,m^2\,(s\,rad)^{-1}}]$	f_s	0.4	$[\mathrm{kg\,m^2/s^2}]$
d_1	0.6	[m]	d_2	0.4	[m]

and the position of the end effector in the Cartesian domain is given by

$$h_{ca}(q) = \begin{bmatrix} x_{ca} \\ y_{ca} \end{bmatrix} = \begin{bmatrix} d_1\cos(q_1) + d_2\cos(q_1+q_2) \\ d_1\sin(q_1) + d_2\sin(q_1+q_2) \end{bmatrix}. \tag{5.149}$$

The control goal is to move the end effector from an initial waypoint A (WP-A) to a waypoint C (WP-C) via an interim waypoint B (WP-B). During the movement the angular velocities of the joints are restricted. In addition a pick and place problem is considered. At WP-B a payload of 80 [kg] is picked up simulated by an external force $F_y = 80\,[\mathrm{kg}] \times 9.81\,[\mathrm{m/s^2}]$. The goal is to move the robot to WP-C while carrying the payload. The external force is unknown to the controller same as the friction coefficients f_v and f_s of the robot.

The Cartesian coordinates of the waypoints and their corresponding joint angles are shown in Table 5.2. The initial angular velocities of the links are zero i. e. $\dot{q}_1(t_0) = \dot{q}_2(t_0) = 0\,[\mathrm{rad/s}]$. The constraints of the angular velocities depend on time and are introduced as follows. Let $l_{c_i,j}$ define the i-th constraint of the angular velocity $\dot{q}_j$ i. e.

$$-l_{c_2,j} \leq \dot{q}_j \leq l_{c_1,j}. \tag{5.150}$$

The bound $l_{c_i,j}$ of the constraints is given by a quadratic function

$$l_{c_i,j}(q_j) = \begin{cases} \phi_{c_i,j}(q_j) & \text{if } \phi_{c_i,j}(q_j) \leq c_c, \\ c_c & \text{if } \phi_{c_i,j}(q_j) > c_c, \end{cases} \tag{5.151}$$
$$\phi_{c_i,j}(q_j) = a_c(w_j - q_j)^2 + b_c, \qquad 0 < b_c \leq c_c, \qquad i,j \in \{1,2\},$$

where w_j denotes the reference angle of joint angle q_j in radiant. Consequently, the bound $l_{c_i,j} > 0$ decreases quadratically dependent on the tracking error $w_j - q_j$. Based on c_c an upper limit and based on b_c a lower limit of $l_{c_i,j}$ is defined. For the considered example

Table 5.2: Reference values in Cartesian coordinates (x_{ca}, y_{ca}) and joint angles (w_1, w_2)

	$x_{ca}\,[\mathrm{m}]$	$y_{ca}\,[\mathrm{m}]$	$w_1\,[^\circ]$	$w_2\,[^\circ]$
WP-A	0.900	0.100	26.511	−51.318
WP-B	−0.700	0.500	168.873	−62.720
WP-C	0.100	0.400	117.562	−136.817

the constants a_c, b_c, c_c in (5.151) are given as $a_c = 0.6\,[1/(\mathrm{s\,rad})]$, $b_c = 10 \times 2\pi/360\,[\mathrm{rad/s}]$, and $c_c = 70 \times 2\pi/360\,[\mathrm{rad/s}]$.

To achieve the desired control goals the actuator torques τ have to be suitably selected. Therefore, the following MIMO controller

$$\tau = C(q, \dot{q})\dot{q} + g(q) + B(q)\nu, \tag{5.152}$$

with auxiliary control inputs

$$\nu = \begin{bmatrix} \nu_1 & \nu_2 \end{bmatrix}^T, \tag{5.153}$$

is introduced. Substituting (5.152) in (5.147) gives the input-output dynamics

$$\ddot{q}_1 = \Psi_1(q, \dot{q}, F_y) + \Gamma_1 \nu_1, \qquad \Gamma_1 = 1, \tag{5.154}$$

and

$$\ddot{q}_2 = \Psi_2(q, \dot{q}, F_y) + \Gamma_2 \nu_2, \qquad \Gamma_2 = 1, \tag{5.155}$$

where Ψ_1 and Ψ_2 denote uncertainties related to the unknown friction terms f_s, f_v, and the unknown external disturbance ξ. The input-output dynamics (5.154) and (5.155) have both a relative degree of two with respect to the control variable q_j and the introduced auxiliary control input ν_j. The uncertainty bound $\Psi_{M,j}$ defined by

$$|\Psi_j| \leq \Psi_{M,j}, \qquad j \in \{1, 2\}, \tag{5.156}$$

is assumed to be finite. According to (5.154)-(5.155) quantity Γ_j equals one. As a consequence, suitable values of the bounds $\Gamma_{m,j}$ and $\Gamma_{M,j}$ defined by

$$0 < \Gamma_{m,j} \leq \Gamma_j = 1 \leq \Gamma_{M,j}, \qquad j \in \{1, 2\}, \tag{5.157}$$

are known and can be selected based on (5.157). As the input-output dynamics have relative degree two and the uncertainty bounds are finite the proposed constrained controller can be applied. The proposed controller guarantees that set-point tracking of q_j can be achieved while constraints are imposed on the angular velocity $\dot{q}_j$. Consequently, the proposed constrained controller solves the constrained control problem by applying suitable control inputs ν_j. The auxiliary control inputs ν_j that the constrained controller provides are defined by Algorithm 3. To apply the algorithm the following auxiliary functions and sliding variables are introduced. According to (5.36) the auxiliary functions $\eta_{c_i,j}(t)$ are stated as

$$\forall t\colon 0 < \eta_{m,c_i,j} < \eta_{c_i,j}(t) < l_{c_i,j}(t), \tag{5.158}$$

and the quantities $\eta_{m,j}$ and $\dot{\eta}_{M,j}$ related to the auxiliary functions are defined by

$$0 < \eta_{m,j} < \min\{\eta_{m,c_1,j}, \eta_{m,c_2,j}\}, \tag{5.159}$$

and

$$0 \leq \max_t \left\{|\dot{\eta}_{c_1,j}(t)|, |\dot{\eta}_{c_2,j}(t)|\right\} < \dot{\eta}_{M,j}. \tag{5.160}$$

In accordance to (5.35) the sliding variable related to the sliding surface $\sigma_{c_i,j} = 0$ is defined as

$$\sigma_{c_i,j} = -\eta_{c_i,j} + s_{c_i}\dot{q}_j, \tag{5.161}$$

and based on (5.39) the sliding variable related to the sliding surface $\sigma_{r,j} = 0$ is introduced as

$$\sigma_{r,j} = \dot{q}_j - \alpha_j e_{r,j} - \beta_j |e_{r,j}|^{\gamma_j} \mathrm{sgn}(e_{r,j}). \tag{5.162}$$

In (5.162) the quantities α_j and $e_{r,j}$ are defined by

$$\alpha_j = \frac{\dot{\eta}_{M,j}}{\eta_{m,j}} + \mu_{\alpha,j}, \qquad e_{r,j} = w_j - q_j. \tag{5.163}$$

The quantities $\beta_j > 0$ and $0 < \gamma_j < 1$ are tuning parameters of the sliding surface $\sigma_{r,j} = 0$ and the parameter $\mu_{\alpha,j} > 0$ is user-defined. Following Algorithm 3 the auxiliary control inputs are given by

$$\nu_j(t) = \begin{cases} u^*_{r,j}(t) & \text{if } \forall i\colon \sigma_{c_i,j}(t) \leq 0, \\ u^*_{c_i,j}(t) & \text{if } \exists i\colon \sigma_{c_i,j}(t) > 0, \end{cases} \tag{5.164}$$

with $u^*_{r,j}$ and $u^*_{c_i,j}$ being defined as

$$u^*_{r,j} = \begin{cases} -\mathrm{sat}(\frac{\sigma_{r,j}}{\epsilon_{r,j}}) \times \left(\frac{\mu_{r,j} + \Psi_{M,j}\sqrt{2}}{\Gamma_{m,j}\sqrt{2}} + \frac{\alpha_j + \beta_j\gamma_j |e_{r,j}|^{\gamma_j - 1}}{\Gamma_{m,j}} |\dot{q}_j| \right), & \text{if } \dot{q}_j \mathrm{sgn}(\sigma_{r,j}) \geq 0, \\ -\mathrm{sat}(\frac{\sigma_{r,j}}{\epsilon_{r,j}}) \times \left(\frac{\mu_{r,j} + \Psi_{M,j}\sqrt{2}}{\Gamma_{m,j}\sqrt{2}} - \frac{\alpha_j + \beta_j\gamma_j |e_{r,j}|^{\gamma_j - 1}}{\Gamma_{M,j}} |\dot{q}_j| \right), & \text{if } \dot{q}_j \mathrm{sgn}(\sigma_{r,j}) < 0, \end{cases}$$

and

$$u^*_{c_i,j} = u^*_{r,j} - s_{c_i} \mathrm{sat}\left(\frac{\sigma_{c_i,j}}{\epsilon_{c_i,j}}\right) \times \left(\frac{\mu_{c_i,j} + \Psi_{M,j}\sqrt{2}}{\Gamma_{m,j}\sqrt{2}} + \frac{|\dot{\eta}_{c_i,j}|}{\Gamma_{m,j}} + s_{c_i} \mathrm{sat}\left(\frac{\sigma_{c_i,j}}{\epsilon_{c_i,j}}\right) u^*_{r,j} + \frac{\alpha_j + \beta_j\gamma_j |e_{r,j}|^{\gamma_j - 1}}{\Gamma_{m,j}} |\dot{q}_j| \right).$$

The smoothing boundary layer widths $\epsilon_{r,j}$ and $\epsilon_{c_i,j}$ may be chosen greater zero same as the tuning-parameters $\mu_{r,j}$ and $\mu_{c_i,j}$.

In the following a valid selection of the controller parameters is discussed. The auxiliary function $\eta_{c_i,j}(t)$ has to be greater zero and smaller than $l_{c_i,j}(t)$ and is chosen as

$$\eta_{c_i,j}(t) = l_{c_i,j}(t) - \epsilon_{c_i,j}, \tag{5.165}$$

where it is assumed that the smoothing boundary layer width $\epsilon_{c_i,j} > 0$ is sufficient small so that $l_{c_i,j}(t) \geq b_c = 0.1745 > \epsilon_{c_i,j}$ holds. The choice of the upper bound $\dot{\eta}_{M,j}$ defined by (5.160) is discussed next. Based on (5.151) the time derivative of $\eta_{c_i,j}$ is obtained as

$$|\dot{\eta}_{c_i,j}| = |\dot{l}_{c_i,j}| = \begin{cases} |\dot{\phi}_{c_i,j}|, & \text{if } \phi_{c_i,j} \leq c_c, \\ 0, & \text{else}, \end{cases} \tag{5.166}$$

Table 5.3: Controller parameters related to control input ν_j (parameterization of both controllers identical)

$\mu_{r,j}$	75	$\mu_{c_i,j}$	75	$\mu_{a,j}$	35	β_j	5	γ_j	0.8	$\epsilon_{r,j}$	0.007
$\epsilon_{c_i,j}$	0.007	$\dot{\eta}_{M,j}$	1.94	$\eta_{m,j}$	0.166	$\hat{\Psi}_{M,j}$	10	$\Gamma_{M,j}$	1	$\Gamma_{m,j}$	1

where $|\dot{\phi}_{c_i,j}|$ is given by

$$|\dot{\phi}_{c_i,j}| = |\frac{d\phi_{c_i,j}}{dq_j}\dot{q}_j| = | - 2a_c(w_j - q_j)\dot{q}_j| = 2a_c|w_j - q_j||\dot{q}_j|. \tag{5.167}$$

According to (5.151) the terms $|w_j - q_j|$ and $|\dot{q}_j|$ of (5.167) become maximal for

$$\max\{|w_j - q_j|\} = \sqrt{\frac{c_c - b_c}{a_c}}, \qquad \max\{|\dot{q}_j|\} = c_c. \tag{5.168}$$

By substituting (5.168) in (5.167) it follows that the upper bound $\dot{\eta}_{M,j}$ can be selected in accordance to

$$\forall i, t\colon |\dot{\eta}_{c_i,j}(t)| \leq 2a_c c_c\sqrt{\frac{c_c - b_c}{a_c}} = 1.9368 < \dot{\eta}_{M,j}. \tag{5.169}$$

The choice of the lower bound $\eta_{m,j}$ defined by (5.159) is discussed as follows. From (5.151) it is known that the auxiliary function $\eta_{c_i,j}$ is bounded as

$$\forall i\colon \eta_{m,j} < 0.1745 = b_c - \epsilon_{c_i,j} \leq l_{c_i,j} - \epsilon_{c_i,j} = \eta_{c_i,j}, \tag{5.170}$$

so that $\eta_{m,j}$ can be obtained from (5.170). The parameter α_j is chosen based on (5.163). As stated in (5.157) the uncertainty bounds $\Gamma_{m,j}$ and $\Gamma_{M,j}$ are known to be $\Gamma_{m,j} = \Gamma_{M,j} = 1$. The uncertainty bound $\Psi_{M,j}$ is assumed to be finite. In the field of sliding mode control it is typically to assume that the uncertainty bounds are finite (Shtessel *et al.*, 2014). Based on that assumption the bound $\Psi_{M,j}$ can be increased by trial and error until the controller provides the desired convergence. For the considered example $\hat{\Psi}_{M,j} = 10$ is assumed to be a suitable choice of $\Psi_{M,j}$. In a post-processing step it will be shown by simulation that $\hat{\Psi}_{M,j}$ is indeed a sufficient upper bound of $|\Psi_j(q, \dot{q}, F_y)|$. The remaining controller parameters $\mu_{r,j}$, $\mu_{c_i,j}$, μ_a, β_j, γ_j are chosen based on Theorem 14 to achieve desired convergence of the tracking error. Finally, the controller parameters are summarized in Table 5.3.

In the following it is shown that for the chosen controller parameters it can be guaranteed that the constrained point to point robot control problem is solved. Moreover, the bounds of the tracking error can be quantified and a maximum time interval that is required for the error convergence can be stated as well. This allows to determine a maximum time interval that the controller requires to solve the control problem without conducting any simulation at all. The following proposition considers the movement of the end effector from WP-A to WP-B. The remaining tracking error of the end effector with respect to WP-B is determined and the maximum time interval is stated that is required to guarantee that the tracking error will be in the given bounds.

Proposition 16.
Consider the robot to be initially located at WP-A with the configuration stated in Table 5.2

and with zero angular velocities. The control goal is to move the end effector from WP-A to WP-B without violation of the constraints. Let the bounds $l_{c_i,j}$ be given by (5.151) with $a_c = 0.6\,[1/(\mathrm{s\,rad})]$, $b_c = 10 \times 2\pi/360\,[\mathrm{rad/s}]$, $c_c = 70 \times 2\pi/360\,[\mathrm{rad/s}]$, let the auxiliary functions $\eta_{c_i,j}$ be defined as stated in (5.165), and let the controller parameters be chosen as shown in Table 5.3 assuming that $\hat{\Psi}_{M,j}$ is sufficient large to be an upper bound of $|\Psi_j|$. By applying the MIMO controller (5.152) the following can be stated:

- *The reference angle $w_1 = 168.873\,[°]$ of WP-B is reached after $34.2\,[\mathrm{s}]$ at the latest with a remaining tracking error in the range of $\pm 0.0122\,[°]$.*
- *The reference angle $w_2 = -62.720\,[°]$ of WP-B is reached after $14.3\,[\mathrm{s}]$ at the latest with a remaining tracking error in the range of $\pm 0.0122\,[°]$.*
- *The constraints defined by (5.151) are never violated and after $34.2\,[\mathrm{s}]$ the angular velocities are bounded as $|\dot{q}_j| \leq 1.71\,[°/\mathrm{s}]$.*

Proof.
Consideration of tracking performance: The initial values of the sliding variables are bounded as

$$|\sigma_{r,1}(t_0)| = |\dot{q}_1(t_0) - \alpha_1 e_{r,1}(t_0) - \beta_1 |e_{r,1}(t_0)|^{\gamma_1} \mathrm{sgn}(e_{r,1}(t_0))| \leq 127 \triangleq \sigma_{r,M,1}, \tag{5.171}$$

and

$$|\sigma_{r,2}(t_0)| = |\dot{q}_2(t_0) - \alpha_2 e_{r,2}(t_0) - \beta_2 |e_{r,2}(t_0)|^{\gamma_2} \mathrm{sgn}(e_{r,2}(t_0))| \leq 11 \triangleq \sigma_{r,M,2}. \tag{5.172}$$

Based on Theorem 14 stability of the tracking error with respect to the domain

$$|e_{r,j}(t)| \leq e_{r,M,j}, \tag{5.173}$$

can be achieved for $t \geq t_{f,j}$ and $t_{f,j} = t_0 + \tau_{1,j} + \tau_{2,j}$ being finite. Let $\mu_{e,j}$ be chosen as $\mu_{e,j} = \eta_{m,j}\sqrt{2}/100$ it follows from Theorem 14 that $e_{r,M,j}$ is given by the solution of

$$\begin{aligned} &\alpha_j e_{r,M,j} + \beta_j e_{r,M,j}^{\gamma_j} = \epsilon_{r,j} + \epsilon_{c,M,j} + \frac{\mu_{e,j}}{\sqrt{2}}, \qquad 0 < \mu_{e,j} \leq \eta_{m,j}\sqrt{2}, \\ &\epsilon_{c,M,j} = \max\{\epsilon_{c_1,j}, \epsilon_{c_2,j}\}, \end{aligned} \tag{5.174}$$

which yields $e_{r,M,j} = 0.0122\,[°]$ for $j = 1$ and $j = 2$. The time period $\tau_{1,j}$ can be calculated as

$$\tau_{1,j} = \frac{\sigma_{r,M,j} - (\epsilon_{r,j} + \epsilon_{c,M,j})}{\varrho_j}, \qquad \varrho_j = \min\left\{\frac{\mu_{r,j}}{\sqrt{2}}, \mu_{a,j}\eta_{m,j}\right\}, \tag{5.175}$$

leading to $\tau_{1,1} = 21.86\,[s]$ and $\tau_{1,2} = 1.90\,[s]$. Time period $\tau_{2,j}$ is given by

$$\tau_{2,j} = (e_{r,M^\star,j} - e_{r,M,j})\frac{\sqrt{2}}{\mu_{e,j}}, \tag{5.176}$$

where $e_{r,M^\star,j}$ is obtained from

$$\alpha_j e_{r,M^\star,j} + \beta_j e_{r,M^\star,j}^{\gamma_j} = \epsilon_{r,j} + \epsilon_{c,M,j} + l_M. \tag{5.177}$$

From (5.151) it is known that $l_M = 70 \times 2\pi/360\,[\mathrm{rad/s}]$ holds. Then $e_{r,M^\star,j}$ is obtained as $e_{r,M^\star,j} = 1.2321\,[^\circ]$ and $\tau_{2,j}$ is $\tau_{2,j} = 12.31\,[\mathrm{s}]$.
Achievement of constrained control: As the initial angular velocities are zero it is $\sigma_{c_i,j}(t_0) < 0$. According to (5.165) the auxiliary function is chosen as

$$\eta_{c_i,j} = l_{c_i,j} - \epsilon_{c_i,j}. \tag{5.178}$$

It follows from Theorem 8 that the constraints are always satisfied. The statement $|\dot{q}_j| \leq 1.71\,[^\circ/\mathrm{s}]$ is obtained from (5.127) of Theorem 14 which states

$$|\dot{q}_j(t)| \leq \epsilon_{r,j} + \epsilon_{c,M,j} + \alpha_j e_{r,M,j} + \beta_j e_{r,M,j}^{\gamma_j} = 1.7034\,[^\circ/\mathrm{s}], \tag{5.179}$$

for $t \geq t_{f,j}$. □

In Proposition 16 the movement of the end effector from WP-A to WP-B is considered. In the next proposition the movement from WP-B to WP-C is studied. The initial conditions of the robot at WP-B are defined by the results of Proposition 16. In particular, the error bound provided by Proposition 16 defines the initial location of the end effector around WP-B and the bounds of the constrained variable provided by Proposition 16 define the initial values of the angular velocities.

Proposition 17.
Consider the robot to be initially located in the near of WP-B according to

$$|168.873\,[^\circ] - q_1(t_0)| \leq 0.0122\,[^\circ], \qquad |-62.750\,[^\circ] - q_2(t_0)| \leq 0.0122\,[^\circ]. \tag{5.180}$$

Let the initial angular velocities be bounded as

$$|\dot{q}_j(t_0)| \leq 1.71\,[^\circ/\mathrm{s}]. \tag{5.181}$$

The control goal is to move the end effector from WP-B to WP-C without violation of the constraints. Let the bounds $l_{c_i,j}$ be given by (5.151) with $a_c = 0.6\,[1/(\mathrm{s\,rad})]$, $b_c = 10 \times 2\pi/360\,[\mathrm{rad/s}]$, $c_c = 70 \times 2\pi/360\,[\mathrm{rad/s}]$, let the auxiliary functions $\eta_{c_i,j}$ be defined as stated in (5.165), and let the controller parameters be chosen as shown in Table 5.3 assuming that $\hat{\Psi}_{M,j}$ is sufficient large to be an upper bound of $|\Psi_j|$. By applying the MIMO controller (5.152) the following can be stated:

- *The reference angle $w_1 = 117.562\,[^\circ]$ of WP-C is reached after $20.5\,[\mathrm{s}]$ at the latest with a remaining tracking error in the range of $\pm 0.0122\,[^\circ]$.*
- *The reference angle $w_2 = -136.817\,[^\circ]$ of WP-C is reached after $24.0\,[\mathrm{s}]$ at the latest with a remaining tracking error in the range of $\pm 0.0122\,[^\circ]$.*
- *The constraints defined by (5.151) are never violated and after $24.0\,[\mathrm{s}]$ the angular velocities are bounded as $|\dot{q}_j| \leq 1.71\,[^\circ/\mathrm{s}]$.*

Proof.
Consideration of tracking performance: According to Table 5.2 the initial tracking errors are bounded as

$$|e_{r,1}(t_0)| \leq |117.562\,[^\circ] - 168.873\,[^\circ]| + 0.0122\,[^\circ] = 0.8958\,[\mathrm{rad}], \tag{5.182}$$

$$|e_{r,2}(t_0)| \leq |-136.817\,[°] - 62.720\,[°]| + 0.0122\,[°] = 1.2934\,[\text{rad}], \tag{5.183}$$

leading to

$$|\sigma_{r,1}(t_0)| \leq |\dot{q}_1(t_0)| + \alpha_1|e_{r,1}(t_0)| + \beta_1|e_{r,1}(t_0)|^{\gamma_1} \leq 47 \triangleq \sigma_{r,M,1}, \tag{5.184}$$

$$|\sigma_{r,2}(t_0)| \leq |\dot{q}_2(t_0)| + \alpha_2|e_{r,2}(t_0)| + \beta_2|e_{r,2}(t_0)|^{\gamma_2} \leq 67 \triangleq \sigma_{r,M,2}. \tag{5.185}$$

Then according to Theorem 14

$$|e_{r,j}(t)| \leq e_{r,M,j}, \tag{5.186}$$

can be achieved for $t \geq t_0 + \tau_{1,j} + \tau_{2,j}$ with $\mu_{e,j} = \eta_{m,j}\sqrt{2}/100$, $e_{r,M,j} = 0.0122\,[°]$, $\tau_{1,1} = 8.1\,[\text{s}]$, $\tau_{1,2} = 11.6\,[\text{s}]$, and $\tau_{2,j} = 12.4\,[\text{s}]$.
Achievement of constrained control: From Theorem 8 it is known that

$$\sigma_{c_i,j}(t_0) = -\eta_{c_i,j}(t_0) + s_{c_i}\dot{q}_j(t_0) \leq \epsilon_{c_i,j}, \tag{5.187}$$

has to hold to guarantee the constraints to be always satisfied. From (5.151) and (5.165) it follows that

$$\begin{aligned}\eta_{c_i,1}(t_0) &\geq 37\frac{2\pi}{360}\,[\text{rad/s}] - \epsilon_{c_i,1},\\ &= a_c\Big((|117.562 - 168.873| - 0.0122)\frac{2\pi}{360}\,[\text{rad}]\Big)^2 + b_c - \epsilon_{c_i,1},\end{aligned} \tag{5.188}$$

$$\begin{aligned}\eta_{c_i,2}(t_0) &\geq 67\frac{2\pi}{360}\,[\text{rad/s}] - \epsilon_{c_i,2},\\ &= a_c\Big((|-136.817 - 62.720| - 0.0122)\frac{2\pi}{360}\,[\text{rad}]\Big)^2 + b_c - \epsilon_{c_i,2},\end{aligned} \tag{5.189}$$

holds. Multiplying (5.188) and (5.189) by minus one and adding $s_{c_i}\dot{q}_1(t_0)$ respectively $s_{c_i}\dot{q}_2(t_0)$ yields

$$\sigma_{c_i,1}(t_0) = -\eta_{c_i,1}(t_0) + s_{c_i}\dot{q}_1(t_0) \leq -37\frac{2\pi}{360}\,[\text{rad/s}] + \epsilon_{c_i,1} + s_{c_i}\dot{q}_1(t_0), \tag{5.190}$$

$$\sigma_{c_i,2}(t_0) = -\eta_{c_i,2}(t_0) + s_{c_i}\dot{q}_2(t_0) \leq -67\frac{2\pi}{360}\,[\text{rad/s}] + \epsilon_{c_i,2} + s_{c_i}\dot{q}_2(t_0). \tag{5.191}$$

According to (5.181) it is known that $|\dot{q}_j(t_0)| \leq 1.71\,[°/\text{s}]$ holds so that from (5.190) and (5.191) it can be concluded that (5.187) is achieved.

The remaining statement that $|\dot{q}_j|$ is bounded by $1.71\,[°/\text{s}]$ after $24\,[\text{s}]$ is obtained from (5.127) of Theorem 14 stating

$$|\dot{q}_j(t)| \leq \epsilon_{r,j} + \epsilon_{c,M,j} + \alpha_j e_{r,M,j} + \beta_j e_{r,M,j}^{\gamma_j} = 1.7034\,[°/\text{s}], \tag{5.192}$$

for $t \geq t_{f,j}$. □

By considering the results of Propositions 16 and 17 it can be guaranteed that the constrained robot control problem is solved in finite time. From Proposition 16 it follows that the movement of the end effector from WP-A to WP-B takes a maximum of $34.2\,[\text{s}]$. The remaining tracking error with respect to WP-B is in the range of $\pm 0.0122\,[°]$. Considering the end effector to be located around WP-B with an error of $\pm 0.0122\,[°]$ it follows from Proposition 17 that the end effector reaches WP-C within $24.0\,[\text{s}]$. After the

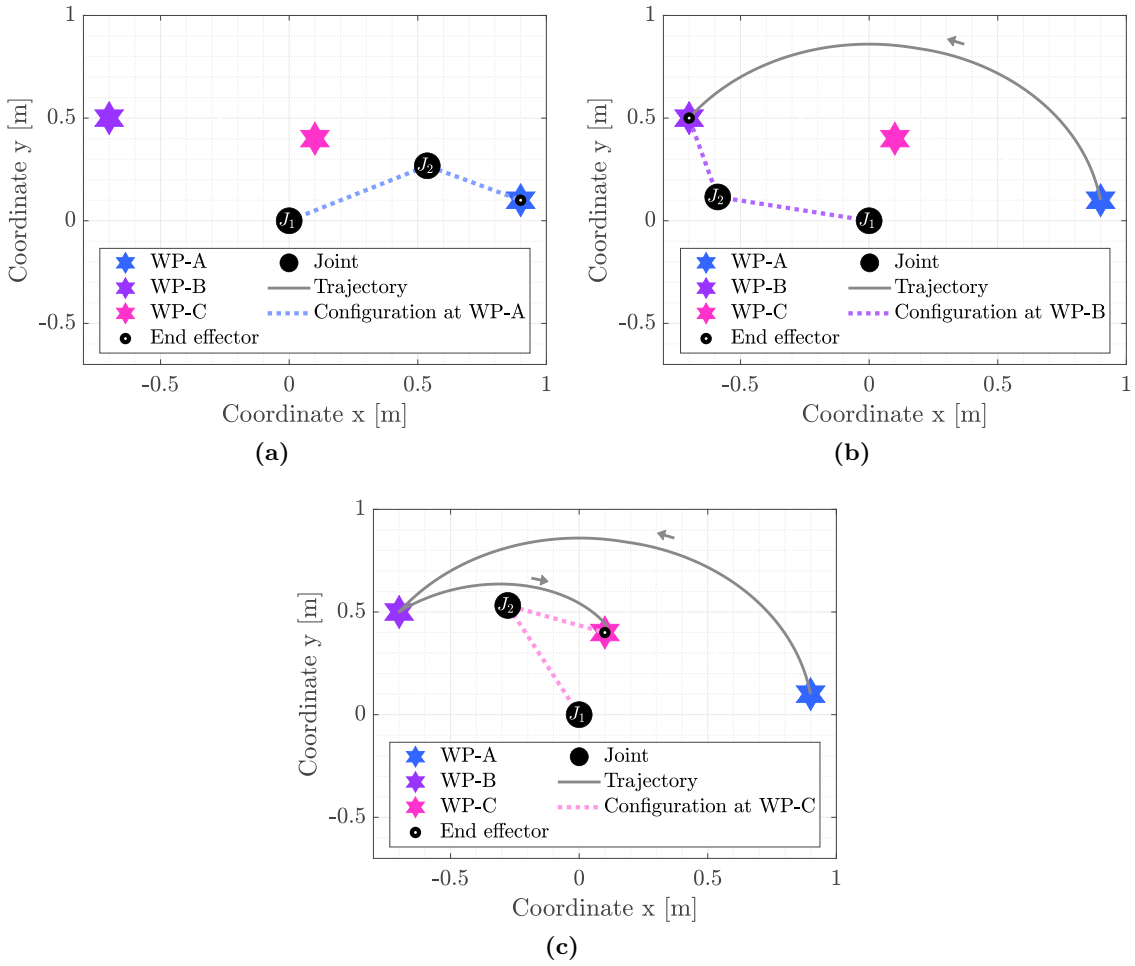

Figure 5.5: Trajectory of the end effector in the Cartesian domain and visualization of the robot configuration (joint angles) at the waypoints. (a) At WP-A. (b) At WP-B. (b) At WP-C.

24.0 [s] the tracking error with respect to WP-C is also guaranteed to be in the range of ± 0.0122 [°]. Finally, the constrained control problem is considered as a whole. Based on the stated results it follows that the movement of the end effector from the initial WP-A to WP-C takes at most 58.2 [s]. The final tracking error with respect to WP-C is in the range of ± 0.0122 [°]. The propositions 16 and 17 also guarantee that the constraints are never violated, neither during the movement from WP-A to WP-C, nor after WP-C has been reached with the stated accuracy.

The control problem has been shown to be solved. However, it is also required to guarantee that the system remains stable. Therefore, the following proposition is stated.

Proposition 18.
Consider the robotic system (5.147) to be controlled by the proposed MIMO controller (5.152). Assume the initial angular velocities of the system to be bounded as

$$\sigma_{c_i,j}(t_0) \leq \epsilon_{c_i,j}. \tag{5.193}$$

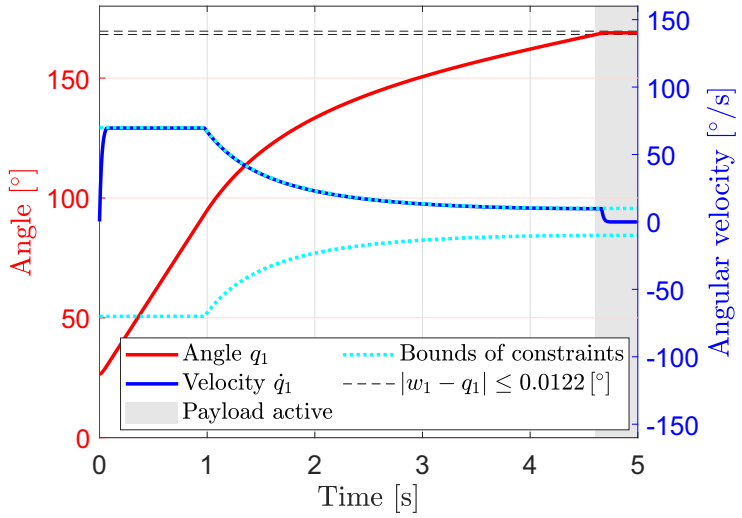

(a)

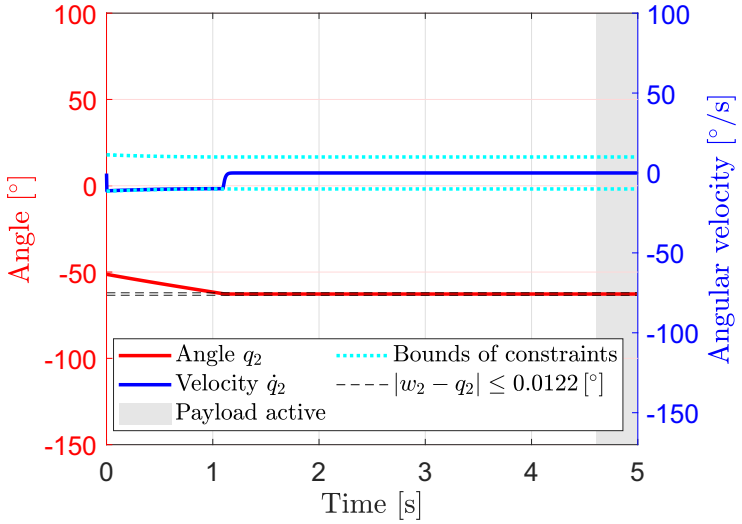

(b)

Figure 5.6: Controller performance during movement from WP-A to WP-B. Time series of joint angles and angular velocities. Visualization of tracking performance, constrained variables, and effect of the payload. (a) First joint. (b) Second joint.

Let the bounds $l_{c_i,j}$ be given by (5.151) with $a_c = 0.6\,[1/(\mathrm{s\,rad})]$, $b_c = 10 \times 2\pi/360\,[\mathrm{rad/s}]$, $c_c = 70 \times 2\pi/360\,[\mathrm{rad/s}]$, let the auxiliary functions $\eta_{c_i,j}$ be defined as stated in (5.165), and let the controller parameters be chosen as shown in Table 5.3 assuming that $\hat{\Psi}_{M,j}$ is sufficient large to be an upper bound of $|\Psi_j|$. Then the closed loop system is always state-stable.

Proof. The states of the system are: q_1, q_2, $\dot{q}_1$, $\dot{q}_2$. From Theorem 14 it follows that the tracking error is bounded which yields boundedness of states q_1 and q_2. From Theorem 8 it follows that the constraints are always satisfied meaning that the constrained variables

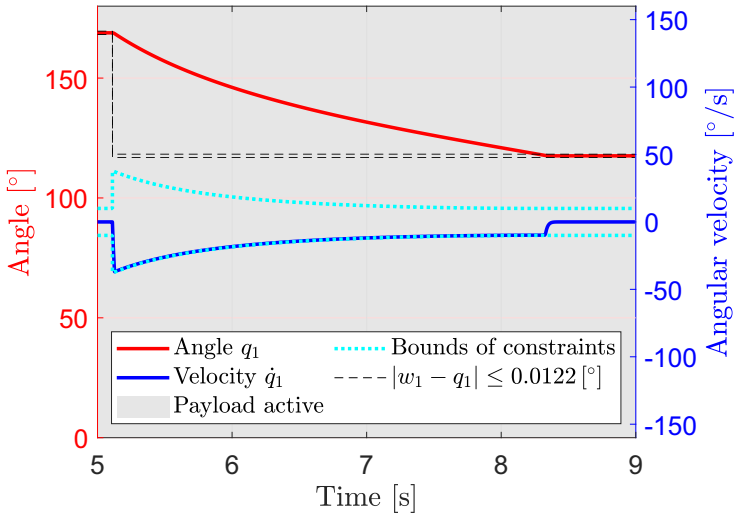

(a)

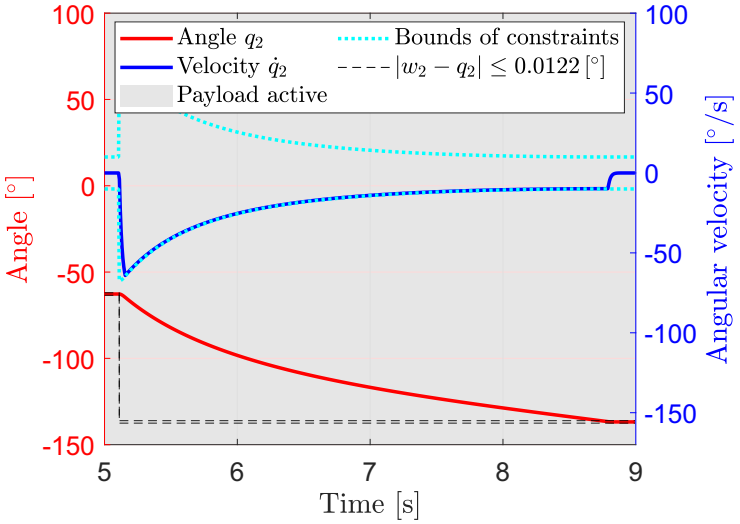

(b)

Figure 5.7: Controller performance during movement from WP-B to WP-C. Time series of joint angles and angular velocities. Visualization of tracking performance, constrained variables, and effect of the payload. (a) First joint. (b) Second joint.

$\dot{q}_1$ and $\dot{q}_2$ remain within finite bounds. □

In the following a simulation is conducted to confirm the results provided by the Propositions 16 and 17. Therefore, the closed loop robotic system is discretized based on the Euler method and simulated with a sampling time of 0.1 [ms]. The simulation is performed as follows. The reference angles only change from WP-B to WP-C if the tracking errors of both joint angles related to WP-B reach the domain of ± 0.0122 [°]. The simulation only terminates if the tracking errors of both joint angles related to WP-C reach the domain of ± 0.0122 [°].

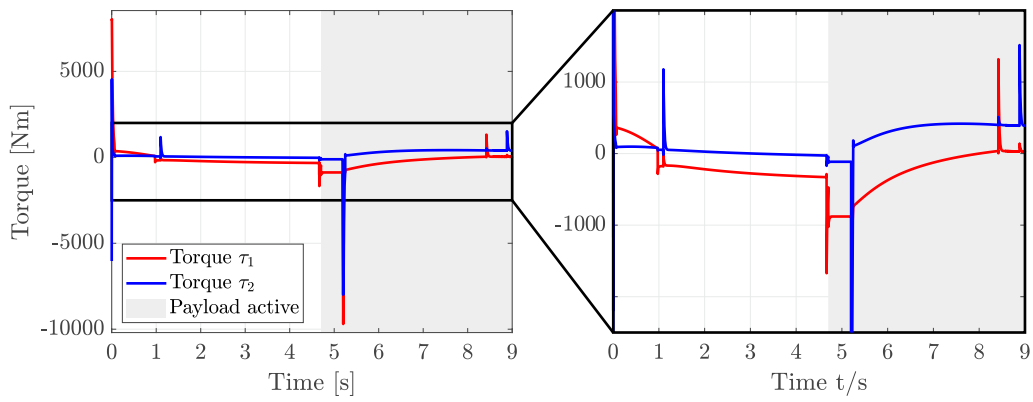

(a)

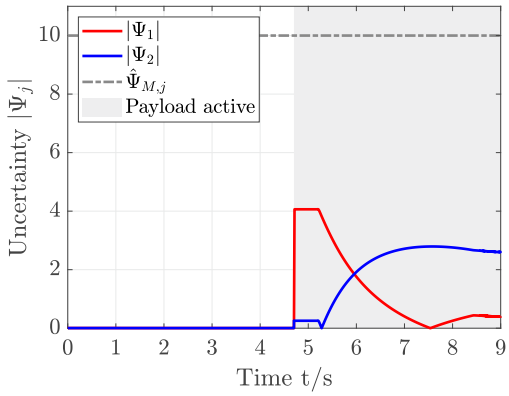

(b)

Figure 5.8: Further controller performance evaluation. (a) Visualization of input torques and rejection effect related to the payload. (b) Proof that $\hat{\Psi}_{M,j}$ is indeed an upper bound of $|\Psi_j|$.

The simulation results are visualized by the Fig. 5.5–5.8. In Fig. 5.5 the trajectory of the end effector is shown in the Cartesian domain. It can be seen that the point to point control problem is solved from a principal point of view. In addition, it can be observed that the robot configurations at the waypoints correspond to the desired joint angles of Table 5.2. In Fig. 5.6 the movement of the end effector from WP-A to WP-B is considered. The angles q_1 and q_2 of the first and second joint are shown as well as the corresponding angular velocities $\dot{q}_1$ and $\dot{q}_2$. In addition, the bounds of the constraints are visualized and the desired domain $|w_j - q_j| \leq 0.0122$ [°] of the tracking error is shown that can be achieve according to Proposition 16. From Fig. 5.6 it can be seen that the tracking error bounds are reached within 5 [s] for both joints. That confirms the results of Proposition 16 which states that the tracking error convergence is guaranteed to be achieved after a maximum of 34.2 [s]. It can also be seen from Fig. 5.6 that during the movement from WP-A to WP-B the constraints are never violated. In Fig. 5.7 the movement of the end effector from WP-B to WP-C is visualized. Again, the angles q_1 and q_2 of the first and second joint and their corresponding angular velocities $\dot{q}_1$ and $\dot{q}_2$ are illustrated. The bounds of the constraints are shown as well as the domain $|w_j - q_j| \leq 0.0122$ [°] of the tracking error that is desired to be achieved according to Proposition 17. It can be seen from Fig. 5.7

that WP-C is reached with the desired accuracy after 4 [s] at the latest. That confirms the results of Proposition 17 which guarantees that the convergence of the tracking error is achieved within 24 [s]. From Fig. 5.7 it can also be observed that the constraints are never violated while the end effector moves to WP-C and remains there. The input torques τ_1 and τ_2 that are generated by the proposed constrained controller are shown in Fig. 5.8a. The chattering is well attenuated but some peaks of the control input can be observed. From Fig. 5.8a also a rejection effect can be detected which occurs in the moment when the payload is applied to the robot for the first time. In Fig. 5.8b it is confirmed that the assumed upper bound $\hat{\Psi}_{M,j}$ of the uncertainty term $|\Psi_j|$ is indeed chosen sufficient large. As shown by Fig. 5.8b the unknown payload mainly contributes to the uncertainty term.

Finally, the simulation results confirm that the proposed constrained controller solves the desired control problem. For an uncertain nonlinear MIMO system constrained control is achieved with bounds that depend on time. The controller is shown to provide the desired tracking error convergence. The control goals are achieved also in presence of an unknown exogenous disturbance.

5.1.6 Summary

In the previous sections a robust control approach for constrained control of nonlinear relative degree two systems is proposed. The developed controller is a combination of two SMC sub-controllers. Based on these sub-controllers reaching of two sliding manifolds is achieved. One sliding manifold is formulated for the tracking error convergence. The other sliding manifold avoids the constraint violation. A control algorithm is stated that defines the conditions for the input selection of the SMC sub-controllers. The algorithm guarantees that the transition between the control inputs of the sub-controllers is smooth. In addition, the chattering effect can be mitigated by adapting some tuning parameters of the controller. The proposed controller assumes the first time derivative of the control variable to be constrained. The bounds of the constraints may be time-varying. The developed approach is robust as the model description of the nonlinear system is allowed to be imprecise. Only finite uncertainty bounds are assumed. For the proposed controller it is analytically proven that the constrained control problem can be solved. Moreover, tracking error bounds are stated that dependent on the controller parameters. Finite-time convergence of the tracking error with respect to those bounds is guaranteed. A maximum time interval can be determined after which the convergence is achieved. A condition dependent on the tuning parameters is formulated which guarantees that the constraints are always satisfied. The condition is only slightly restrictive. The controller is tested on a nonlinear MIMO robotic system. A constrained point to point control problem is considered in which the robot is disturbed by an unknown payload that is applied to the end effector. It is analytically shown that the proposed controller solves the constrained robot control problem. Moreover, the tracking error bounds can be quantified and a maximum time interval can be stated after which the control problem is guaranteed to be solved. The analytical results are confirmed by simulation.

5.2 Safe Robot Control in Human-Robot Collaboration Tasks

Human-robot interaction and collaboration appears in an increasing amount of applications. This includes the field of healthcare, service, and assistance (Yu *et al.*, 2015; Su *et*

al., 2018) as well as the domain of manufacturing (Zanchettin *et al.*, 2015; Robla-Gómez *et al.*, 2017). In industry robots typically take over repetitive or dangerous tasks. In the past the workspace of the robot was clearly separated from that of humans. However, an increasing demand of shared workspaces in which humans and robots collaborate with each other can be expected for the future (Robla-Gómez *et al.*, 2017). In assembly lines skillful operations undertaken by humans may be directly supported by the capabilities of robots to increase flexibility and efficiency (Robla-Gómez *et al.*, 2017; Ceriani *et al.*, 2015).

Human-robot collaboration requires shared workspaces or even physical contact between robots and humans. In order to avoid injuries the robot velocity is typically restricted dependent on the distance between the robot and the human (Zanchettin *et al.*, 2015). However, the robot should still be able to efficiently complete desired control tasks (Kimmel and Hirche, 2017). Trajectory planning is an approach that offers the ability to achieve desired goals subject to constraints. But in the field of human-robot collaboration this kind of path planning methods may be considered to be unsafe as they require a prediction of the human behavior (Mainprice and Berenson, 2013). Instead of planning a collision-free trajectory the approach of Zanchettin *et al.* (2015) calculates the maximal velocity along a predefined nominal path for which the robot is still able to stop without colliding with the human. To improve safety in shared workspaces Faroni *et al.* (2019) formulates an optimization problem in which the distance between the human and the robot is maximized. However, this kind of spatial separation may be undesired for the collaboration of humans and robots. So-called dynamic windowing approaches are proposed in e. g. Wilkie *et al.* (2009); Saranrittichai *et al.* (2013). They assume the velocities of the obstacles to be known and to remain constant. Based on that assumption suitable robot velocities are determined that do not lead to collisions in the future. Another class of robot control approaches are the reactive control methods that generate repulsive forces that are applied to the robot. Among this methods the potential field method may be most known which is originally described in Khatib (1986). The potential field method generates repulsive forces dependent on how the robot and the obstacles are located to each other. The forces are applied to the robot to avoid collisions. In addition to the original approach proposed by Khatib (1986) various extensions can be found (e. g. Ceriani *et al.*, 2015). In the field of human-robot collaboration physical contact between the human and the robot may even be desired. Therefore, the approach proposed by Magrini *et al.* (2015) locates the contact point between the human and the robot and regulates the contact forces. Generally, the application of lightweight robots is desirable in the field of human-robot collaboration as it leads to reduced severity of collisions (Bauer *et al.*, 2016). In addition, elastic actuators and compliant materials are developed to further increase safety (Yu *et al.*, 2015).

Restricting the workspace or velocity of the robot does only guarantee safety if the formulated constraints are enforced by control. Model predictive control (MPC) is a powerful constrained control method. But in the context of human-robot collaboration the human behavior is required to be predicted which may be considered to be unsafe. However, contributions in which MPC approaches are applied for human related tasks can be found. In Matschek *et al.* (2020) a MPC is applied to achieve constrained robot assisted surgery. The human behavior i. e. its breathing is predicted by Gaussian processes. Bipedal robots carrying objects together with humans are considered in Agravante *et al.* (2019). A MPC is applied to stabilize the robot. The distance between the foot center points of the robot

and the contact point of the resulting ground contact forces is minimized. As a result the vertical stability of the robot is enhanced. In addition, constraints are enforced to keep the contact points of the ground contact forces in an admissible region. Forces resulting from the human-robot interaction are predicted using the model of an inverted pendulum. Constrained robot control approaches that do not rely on the prediction of the human behavior can also be found in a wide variety. In Kimmel and Hirche (2017) impedance control is applied as a compliant nominal controller to achieve reference tracking of the robot end effector. Geometrical constraints are formulated to avoid collisions with body parts of the human e. g. the hands. The constraints are enforced by means of invariance control. However, as the robot evades from the human the approach impedes contact which may be unfavorable in human-robot collaboration scenarios. An approach enforcing the end effector to remain in a bounding box so that it can be touched by the human from outside is proposed in Kimmel *et al.* (2012). Again invariance control is applied to enforce the constraints. A similar approach with bounding box constraints can be found in Rauscher *et al.* (2016). The constraints are enforced by means of control barrier functions. Control of a bipedal robot that evades from dynamic obstacles is considered in Agrawal and Sreenath (2017). The obstacles are described by ellipses and constraint satisfaction is achieved using control barrier functions. A three level robot control scheme is proposed in Solanes *et al.* (2018). The first level consists of a sliding mode controller that enforces the constraints. A possible constraint is e. g. to keep the orientation of an object admissible so that it can be transported together by human and robot. The second level is an admittance controller (see Landi *et al.*, 2017) which defines how the robot should move if it is pushed by the human. The third level can be applied if the robot is a so-called redundant robot. In this case the controller allows to bring the robot into a more safe configuration which is more distant from the obstacles. Only one of the three control levels can be applied at once. The active control law is selected based on a task prioritization scheme.

In the following a safe robot control concept is introduced. The approach is designed to handle safety critical situations in which humans and robots interact with each other. The proposed approach is exemplarily designed for a two-link robot with rotatory joints. It may be extended to different classes of robots. The human is described as a circular scalable obstacle in a two-dimensional plane. The safety concept is based on three geometrical zones: a stop zone, a safety disk, and an outer zone. The stop zone is a geometrical construction that moves with the robot. The borders of the stop zone are guaranteed to have a distance to the links, the joints, and the end effector of the robot that is greater than a user-defined value. If the obstacle enters the stop zone the controller aims to keep the robot at its current position to avoid severe collisions. The safety disk is a geometrical zone that is equal to the work space of the robot plus a safety margin. If the obstacle is within the safety disk then the absolute angular velocities of the robot are restricted to a minimum value. The outer zone lays outside of the safety disk. It is a zone in which the upper bounds of the absolute angular velocities are gradually increased or decreased. If the obstacle moves towards the robot the bounds are decreased if it moves away from the robot the bounds are increased. The constraints that are formulated based on the three introduced geometrical zones are enforced by applying the proposed constrained controller of Section 5.1.3 (Algorithm 3). For that controller the tracking error bounds and the required time for the tracking error convergence are studied in Section 5.1.4. Based on that results it can be guaranteed that the absolute velocity of any point on the robot does not exceed a user-defined value at the moment when the robot and the obstacle collide with

each other. Consequently, the proposed concept offers a strategy to design the maximum velocity of the robot during a collision.

The new aspect of the proposed safety concept with regards to the literature is the robustness that is provided by the applied constrained sliding mode controller. The proposed safety concept explicitly makes use of the developed Algorithm 3 of Section 5.1.3. Algorithm 3 provides capabilities to solve the desired control problem as it can handle model uncertainty and allows to consider constraints with time-varying bounds. In contrast to that most of the existing human-robot control concepts do not provide any robustness at all. For instance, the aforementioned concepts that are developed by Kimmel and Hirche (2017) and Kimmel *et al.* (2012) are not robust. In both approaches the invariance controller is applied which is a constrained control method but not a robust one as it requires exact model knowledge. Also the constrained robot control concepts proposed by Rauscher *et al.* (2016); Agrawal and Sreenath (2017) are not robust. The applied constrained controller that is formulated based on control barrier functions requires an exact model description.

The section is organized as follows. In Section 5.2.1 the proposed concept for safe human-robot collaboration is mathematically described. The geometrical zones are introduces, the control algorithm is stated, and the mathematical properties of the proposed method are studied. In Section 5.2.2 a specific scenario of human-robot interaction is simulated to test the developed safety concept.

5.2.1 Safety Concept

In this section the concept of safe human-robot interaction is introduced. The considered robot is assumed to be the two link robot known from the application example of Section 5.1.5. The concept is described with respect to a two-dimensional plane $(x, y) \in \mathcal{X} \subset \mathbb{R}^2$ with coordinates x and y. The coordinates are formulated with respect to the coordinate system that is visualized in Fig. 5.9 (a). The origin of the coordinate system is located at the center point of the first joint of the robot. The human is described by a circular obstacle

$$\mathcal{O} = \{(x, y) \in \mathbb{R}^2 \mid \sqrt{(x - x_{oc})^2 + (y - y_{oc})^2} \leq r_o\}, \tag{5.194}$$

with center point

$$p_{oc} = \begin{bmatrix} x_{oc} \\ y_{oc} \end{bmatrix}, \tag{5.195}$$

and scalable radius $r_o > 0$. Every point $(x_o, y_o) \in \mathcal{O}$ is considered to be part of the obstacle. The velocity of the obstacles center is assumed to be bounded according to

$$\dot{p}_{oc} = \begin{bmatrix} \dot{x}_{oc} \\ \dot{y}_{oc} \end{bmatrix}, \qquad v_{oc} = \sqrt{\dot{x}_{oc}^2 + \dot{y}_{oc}^2} \leq v_{oc,M}, \tag{5.196}$$

with the upper bound $v_{o,M}$ assumed as known. The geometrical zones of the safety concept are visualized in Fig. 5.9 (b). There are three zones: the outer zone, the safety disk, and the stop zone. The outer zone is a geometrical zone that is described by a circular contour graph. Within the outer zone the allowed absolute joint velocities gradually decrease if the

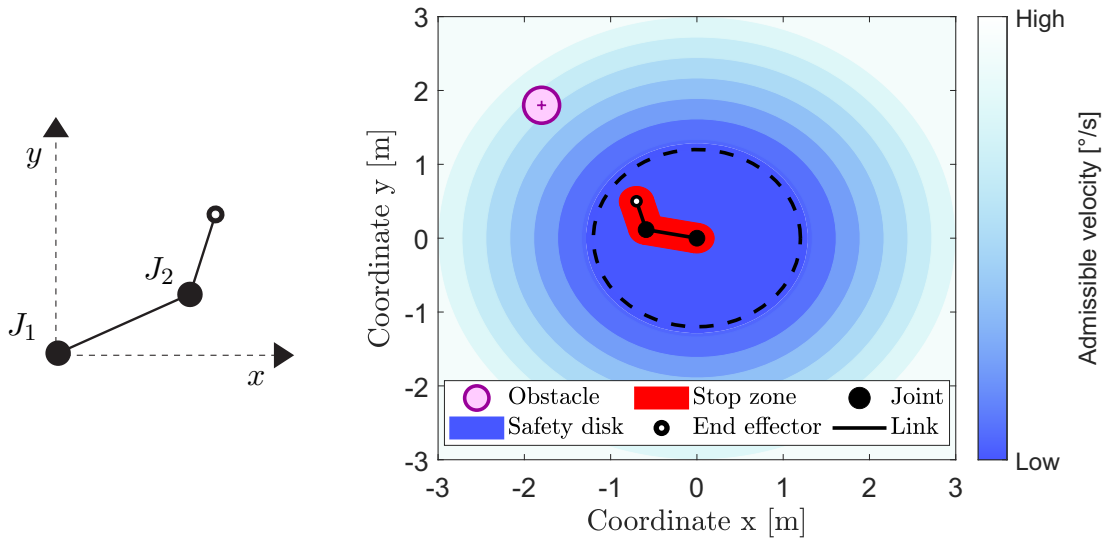

Figure 5.9: (a) Definition of coordinates x and y. The origin of the coordinate system is located at the first joint J_1 of the two-link robot. (b) Visualization of safety concept with contour graph, safety disk, and stop zone.

obstacle approaches the robot. The admissible absolute velocities decrease until a circular region denoted as safety disk is reached. The safety disk is defined as a circle

$$\mathcal{D} = \{(x, y) \in \mathbb{R}^2 \mid \sqrt{x^2 + y^2} \leq d_1 + d_2 + b\}, \qquad b > 0, \tag{5.197}$$

where d_1 and d_2 are the lengths of the first and second link of the robot and b is a tuning parameter. Consequently, the safety disk is comprised of the working area of the robot plus a safety distance. In accordance to (5.150) the time-varying bounds of the angular velocities of the robot are denoted by $l_{c_i,j}$. Dependent on the position of the obstacle in the two-dimensional plane the bound $l_{c_i,j}$ is given as

$$l_{c_i,j} = \begin{cases} l_{low}, & \text{if } p_{oc} \in \mathcal{D}, \\ \phi, & \text{if } p_{oc} \notin \mathcal{D} \wedge \phi \leq l_{high}, \\ l_{high}, & \text{if } p_{oc} \notin \mathcal{D} \wedge \phi > l_{high}, \end{cases} \tag{5.198}$$

$$\phi = l_{low} + m\left(\sqrt{x_{oc}^2 + y_{oc}^2} - d_1 - d_2 - b\right), \qquad m > 0, \quad l_{high} > 0, \quad l_{low} > 0.$$

In (5.198) quantity l_{high} denotes the maximum possible bound and quantity l_{low} denotes the minimal possible bound. From (5.198) it follows that within the safety disk $\mathcal{D}$ the bound of the allowed absolute joint velocities is always restricted to the minimal value l_{low}. In addition, it can be concluded from (5.198) that in the outer zone the allowed absolute velocities may gradually increase, but not beyond the value defined by l_{high}. The stop zone is a geometrical construction that moves with the robot. The structure of the stop zone is visualized in Fig. 5.10. Formally, the stop zone

$$\mathcal{S} = \mathcal{S}_1 \cup \mathcal{S}_2 \cup \mathcal{S}_3 \cup \mathcal{S}_4 \cup \mathcal{S}_5, \tag{5.199}$$

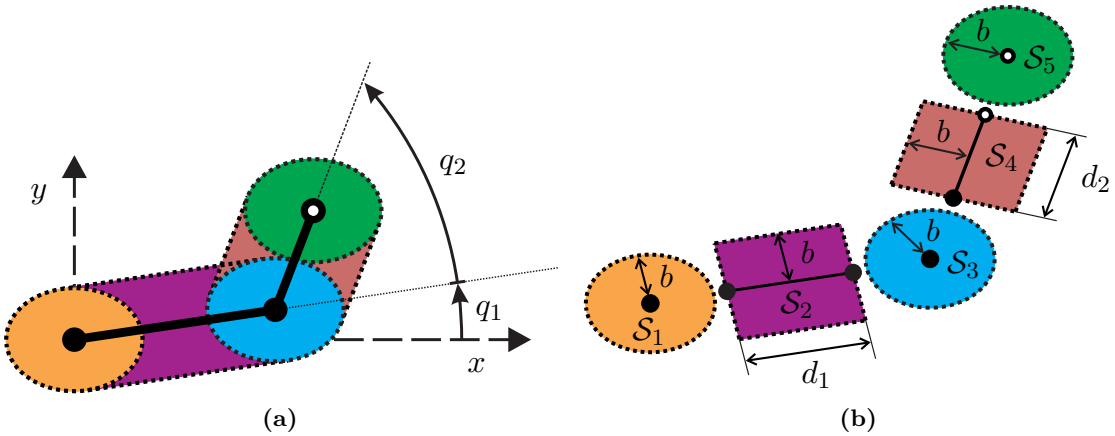

Figure 5.10: Definition of stop zone. The stop zone is the union of the shown geometric figures. The Euclidean distance between any point on the edge of the stop zone and any point on the robot is at least b.

is defined by the union of five geometric figures. The geometric figure

$$\mathcal{S}_1 = \{(x, y) \in \mathbb{R}^2 \mid \sqrt{x^2 + y^2} \leq b\}, \tag{5.200}$$

describes a circle around the first joint. The rectangle

$$\mathcal{S}_2 = \{(x, y) \in \mathbb{R}^2 \mid \mathsf{A}_1 \wedge \mathsf{A}_2\}, \tag{5.201}$$

$$\mathsf{A}_1\colon \quad \begin{bmatrix} x \\ y \end{bmatrix} = \alpha_1 \begin{bmatrix} \cos(q_1) \\ \sin(q_1) \end{bmatrix} + \beta \begin{bmatrix} -\sin(q_1) \\ \cos(q_1) \end{bmatrix}, \tag{5.202}$$

$$\mathsf{A}_2\colon \quad 0 \leq \alpha_1 \leq d_1, \qquad -b \leq \beta \leq b, \tag{5.203}$$

has its longitudinal axis aligned with the first link. The circle

$$\mathcal{S}_3 = \{(x, y) \in \mathbb{R}^2 \mid \sqrt{(x - d_1\cos(q_1))^2 + (y - d_1\sin(q_1))^2} \leq b\}, \tag{5.204}$$

is related to a circular area around the second joint. The rectangle

$$\mathcal{S}_4 = \{(x, y) \in \mathbb{R}^2 \mid \mathsf{A}_3 \wedge \mathsf{A}_4\}, \tag{5.205}$$

$$\mathsf{A}_3\colon \quad \begin{bmatrix} x \\ y \end{bmatrix} = d_1 \begin{bmatrix} \cos(q_1) \\ \sin(q_1) \end{bmatrix} + \alpha_2 \begin{bmatrix} \cos(q_1 + q_2) \\ \sin(q_1 + q_2) \end{bmatrix} + \beta \begin{bmatrix} -\sin(q_1 + q_2) \\ \cos(q_1 + q_2) \end{bmatrix}, \tag{5.206}$$

$$\mathsf{A}_4\colon \quad 0 \leq \alpha_2 \leq d_2, \qquad -b \leq \beta \leq b, \tag{5.207}$$

has its longitudinal axis aligned with the second link. The circle

$$\mathcal{S}_5 = \{(x, y) \in \mathbb{R}^2 \mid \mathsf{A}_5\}, \tag{5.208}$$

$$\mathsf{A}_5\colon \quad \sqrt{a} \leq b, \tag{5.209}$$

with

$$a = (x - d_1\cos(q_1) - d_2\cos(q_1 + q_2))^2 + (y - d_1\sin(q_1) - d_2\sin(q_1 + q_2))^2, \tag{5.210}$$

Algorithm 4 Stopping of robot

Inputs IsOutside.bool, $w_j^\star$, w_j

if IsOutside.bool $= 1$ **and** $p_{oc} \in \mathcal{S}$ **then**
IsOutside.bool $\leftarrow 0$
$w_j^\star \leftarrow w_j$
$w_j \leftarrow q_j$
end if
if IsOutside.bool $= 0$ **and** $p_{oc} \notin \mathcal{S}$ **then**
IsOutside.bool $\leftarrow 1$
$w_j \leftarrow w_j^\star$
end if

Output w_j

It is assumed that $p_o(t_0) \notin \mathcal{S}$ and IsOutside.bool$(t_0) = 1$ hold initially.

describes a circular area around the end effector. Within the stop zone the bounds of the constraints are set to the minimum value l_{low}. This follows from (5.198) as the stop zone is part of the safety disk $\mathcal{D}$. Consequently, the goal of the stop zone is not to alter the bounds of the constraints. Instead, the stop zone aims to keep the robot fixed at its current position. This is achieved by redefining the set points w_j of the joint angles. The strategy is described by Algorithm 4. If the obstacles center enters the stop zone the set points w_j are set to the current values q_j of the joint angles. The original set points are stored in a variable denoted as w_j^*. If the obstacles center leaves the stop zone the set points w_j are reset to the values w_j^* so that the robot can continue with the initial set point tracking task. The stop zone has a design parameter b. As shown by Fig. 5.10 the stop zone can be scaled up based on b. The borders of the stop zone are guaranteed to have a distance to the links, the joints, and the end effector of the robot that is greater than b. This allows to slow down the robot to a desired velocity when it collides with the obstacle. Finally, the robot is formally defined. The robot is composed of all points $\mathcal{R}$ given by

$$\mathcal{R} = \{(x, y) \in \mathbb{R}^2 \mid (\mathsf{A}_6 \wedge \mathsf{A}_7) \vee (\mathsf{A}_8 \wedge \mathsf{A}_9)\} \tag{5.211}$$

$$\mathsf{A}_6\colon \quad \begin{bmatrix} x \\ y \end{bmatrix} = \alpha_1 \begin{bmatrix} \cos(q_1) \\ \sin(q_1) \end{bmatrix}, \tag{5.212}$$

$$\mathsf{A}_7\colon \quad 0 \leq \alpha_1 \leq d_1, \tag{5.213}$$

$$\mathsf{A}_8\colon \quad \begin{bmatrix} x \\ y \end{bmatrix} = d_1 \begin{bmatrix} \cos(q_1) \\ \sin(q_1) \end{bmatrix} + \alpha_2 \begin{bmatrix} \cos(q_1 + q_2) \\ \sin(q_1 + q_2) \end{bmatrix}, \tag{5.214}$$

$$\mathsf{A}_9\colon \quad 0 \leq \alpha_2 \leq d_2, \tag{5.215}$$

that are located on link one or two.

From Section 5.1.5 it is known that the MIMO controller (5.152) can be applied to achieved constrained control of the considered robot. The auxiliary inputs ν_j of the MIMO controller are defined based on (5.164). The sliding surfaces $\sigma_{c_i,j} = 0$, $\sigma_{r,j} = 0$, the uncertainty bounds $\Psi_{M,j}$, $\Gamma_{M,j}$, $\Gamma_{m,j}$, the smoothing boundary layer widths $\epsilon_{r,j}$, $\epsilon_{c_i,j}$, the

controller parameters μ_{r_j}, $\mu_{c_i,j}$, α_j, β_j, γ_j and the tracking errors $e_{r,j}$ are all defined in accordance to Section 5.1.5. The auxiliary function $\eta_{c_i,j}$ and its describing quantities $\eta_{m,j}$ and $\dot{\eta}_{M,j}$ are defined as stated in (5.158)–(5.160). The auxiliary function $\eta_{c_i,j}$ is selected as

$$\eta_{c_i,j} = l_{c_i,j} - \epsilon_{c_i,j}, \qquad \epsilon_{c_i,j} > 0, \tag{5.216}$$

where the bound $l_{c_i,j}$ of the constraints is defined by (5.198). In the following the quantities $\eta_{m,j}$ and $\dot{\eta}_{M,j}$ are determined that are required to be known to selected the controller parameter α_j as stated by (5.163). Derivating (5.216) with respect to time and considering (5.198) yields

$$|\dot{\eta}_{c_i,j}| = |\dot{l}_{c_i,j}| = \begin{cases} |\dot{\phi}|, & \text{if } p_{oc} \notin \mathcal{D} \wedge \phi \leq l_{high}, \\ 0, & \text{else}, \end{cases} \tag{5.217}$$

with

$$|\dot{\phi}| = |\frac{\partial \phi}{\partial x_{oc}}\dot{x}_{oc} + \frac{\partial \phi}{\partial y_{oc}}\dot{y}_{oc}| = |\frac{m}{\sqrt{x_{oc}^2 + y_{oc}^2}}(\dot{x}_{oc}x_{oc} + \dot{y}_{oc}y_{oc})|, \tag{5.218}$$

$$\leq \frac{m}{\sqrt{x_{oc}^2 + y_{oc}^2}}\|p_{oc}\|\|\dot{p}_{oc}\| = m\|\dot{p}_{oc}\|. \tag{5.219}$$

Regarding (5.219) it is known that the obstacle velocity is bounded as $\|\dot{p}_{oc}\| = v_{oc} \leq v_{oc,M}$. Consequently, the controller parameter $\dot{\eta}_{M,j}$ is required to be selected as

$$\forall t, i \colon |\dot{\eta}_{c_i,j}(t)| \leq m v_{oc,M} < \dot{\eta}_{M,j}. \tag{5.220}$$

For the controller parameter $\eta_{m,j}$ it follows from (5.198) and (5.216) that $\eta_{m,j}$ has to be selected as

$$\forall t, i \colon 0 < \eta_{m,j} < l_{low} - \epsilon_{c_i,j} \leq \eta_{c_i,j}(t). \tag{5.221}$$

In the following the mathematical properties of the proposed safety concept are studied. The subsequently stated theorem guarantees the constraints to be always satisfied if the auxiliary function $\eta_{c_i,j}$ is chosen in accordance to (5.216).

Theorem 19 (Achievement of constrained robot control)**.**
Consider a two link robot as shown in Fig. 5.4 with dynamics described by (5.147). Let $\mathcal{O}$ define a circular obstacle as stated in (5.194). Assume the robotic system to be controlled by the MIMO controller (5.152) whose auxiliary inputs ν are defined based on Algorithm 3. Consider the bounds $l_{c_i,j}$ of the constraints to be defined by a circular contour graph as stated in (5.198). Assume the set point of the robot to be shifted as defined by Algorithm 4 if the obstacles center enters or leaves the stopping zone. Let the auxiliary function $\eta_{c_i,j}$ be selected as stated in (5.216) and assume

$$\forall i, j \colon \sigma_{c_i,j}(t_0) \leq \epsilon_{c_i,j}, \tag{5.222}$$

to hold initially. Then the constraints are always satisfied i. e.

$$-l_{c_2,j}(t) \leq \dot{q}_j(t) \leq l_{c_1,j}(t), \tag{5.223}$$

holds for $t \geq t_0$.

Proof.

Step 1: Consider a change of the set point to occur at some time instant $t^\star$. It will be shown that if the constraints are satisfied up until $t^\star$ they will remain satisfied after the change of the set point. From definition (5.197) it follows that the stop zone is a subset of the safety disk. Assuming the constraints to be satisfied up until $t^\star$ it follows $|\dot{q}_j(t^\star)| \leq l_{low}$ from the definition of the contour graph (5.198). Following (5.216), (5.198) the auxiliary function is

$$\eta_{c_i,j}(t^\star) = l_{low} - \epsilon_{c_i,j}, \tag{5.224}$$

at $t^\star$. Substituting (5.224) into the definition of $\sigma_{c_i,j}$ according to

$$\sigma_{c_i,j} = -\eta_{c_i,j} + s_{c_i,j}\dot{q}_j, \tag{5.225}$$

and considering $|\dot{q}_j(t^\star)| \leq l_{low}$ yields

$$\sigma_{c_i,j}(t^\star) = \epsilon_{c_i,j} - l_{low} + s_{c_i,j}\dot{q}_j \leq \epsilon_{c_i,j} - l_{low} + l_{low} = \epsilon_{c_i,j}. \tag{5.226}$$

It follows from Theorem 8 that the constraints remain satisfied after the change of the set point.

Step 2: By applying Theorem 8 it follows that the constraints are satisfied from beginning starting with the initial time instant t_0. So the constraints are indeed satisfied up until possible changes of the set points appear. □

The main result of the mathematical analysis is stated by the next theorem. It is shown that the maximum velocity of the robot during a possible collision with the obstacle can be designed based on the proposed safety concept. Therefore, the scaling parameter b of the stop zone has to be selected sufficiently large so that the inequality (5.228) is satisfied. The inequality is mainly affected by the time interval τ that describes how fast the tracking error convergence of the controller can be realized. In case of a collision the velocity of the robot is guaranteed to be upper bounded by the value that is stated in (5.229). If the obstacle leaves the stop zone without entering it again the tracking error converges in finite-time. In particular, the angle q_j is guaranteed to reach its initial set point w_j in finite-time with a precision that is described by equation (5.239).

Theorem 20 (Boundedness of robot velocity at time of collision and tracking error convergence)**.**
Consider a two link robot as shown in Fig. 5.4 with dynamics described by (5.147). Assume the robotic system to be controlled by the MIMO controller (5.152) whose auxiliary inputs ν are defined based on Algorithm 3. Consider the bounds of the constraints to be defined by a circular contour graph as stated in (5.198). Let $\eta_{c_i,j}$ be selected as stated in (5.216) and let the controller parameters satisfy (5.220) and (5.221). Assume μ_{c_i} to be chosen as $\mu_{c_i} \geq \mu_r$. Further assume

$$\forall i,j\colon \sigma_{c_i,j}(t_0) \leq \epsilon_{c_i,j}, \tag{5.227}$$

to hold initially. Let an obstacle $\mathcal{O}$ with radius r_o be defined based on (5.194) and let the velocity of the obstacles center be bounded as $v_{oc} \leq v_{oc,M}$ with $v_{oc,M}$ assumed as known. Consider the stopping zone $\mathcal{S}$ to be defined according to (5.199) and let $(x_r, y_r) \in \mathcal{R}$ define all points on the robot, where $\mathcal{R}$ is given by (5.211). Assume the set point of the robot to

be shifted as defined by Algorithm 4 if the obstacles center enters or leaves the stopping zone. If the scaling parameter b of the stopping zone satisfies

$$b \geq \left(v_{oc,M} + l_{low}(d_1 + 2d_2)\right)\tau + r_o, \tag{5.228}$$

then the velocity $v_r(x_r, y_r)$ of any point $(x_r, y_r) \in \mathcal{R}$ on the robot is bounded by

$$v_r(x_r, y_r) \leq \dot{q}_M(d_1 + 2d_2), \tag{5.229}$$

in the moment when (x_r, y_r) collides with the obstacle i. e. $(x_r, y_r) \in \mathcal{O}$. In (5.229) quantity $\dot{q}_M > 0$ is a design value that defines the controller parameters according to

$$2\epsilon_{r,j} + 2\epsilon_{c,M,j} + \frac{\mu_{e,j}}{\sqrt{2}} \leq \dot{q}_M, \qquad 0 < \mu_{e,j} \leq \eta_{m,j}\sqrt{2}, \tag{5.230}$$

$$\epsilon_{c,M,j} = \max_i\{\epsilon_{c_i,j}\}. \tag{5.231}$$

Time span

$$\tau = \max_j\{\tau_{1,j}\} + \max_j\{\tau_{2,j}\}, \tag{5.232}$$

is obtained from

$$\tau_{1,j} = \frac{l_{low} - (\epsilon_{r,j} + \epsilon_{c,M,j})}{\varrho_j}, \qquad \varrho_j = \min\left\{\frac{\mu_{r,j}}{\sqrt{2}}, \mu_{a,j}\eta_{m,j}\right\}, \tag{5.233}$$

and

$$\tau_{2,j} = (e_{r,M^\star,j} - e_{r,M,j})\frac{\sqrt{2}}{\mu_{e,j}}, \tag{5.234}$$

where $e_{r,M^\star,j}$ solves

$$\alpha_j e_{r,M^\star,j} + \beta_j e_{r,M^\star,j}^{\gamma_j} = \epsilon_{r,j} + \epsilon_{c,M,j} + l_{low}, \tag{5.235}$$

and $e_{r,M,j}$ solves

$$\alpha_j e_{r,M,j} + \beta_j e_{r,M,j}^{\gamma_j} = \epsilon_{r,j} + \epsilon_{c,M,j} + \frac{\mu_{e,j}}{\sqrt{2}}. \tag{5.236}$$

In addition the following holds. Let the obstacles center enter the stopping zone at time instant $t^\star$ and assume the center to remain in the stop zone at least until $t^\star + \tau$ then

$$v_r(x_r, y_r) \leq \dot{q}_M(d_1 + 2d_2), \tag{5.237}$$

and

$$|\dot{q}_j| \leq \dot{q}_M, \tag{5.238}$$

hold until the center leaves the stop zone again.

If it is known that the obstacle will leave the stop zone without entering it again then the convergence of the tracking error can be guaranteed. The angular velocity q_j reaches its initial reference value w_j after a a finite-time $t^\dagger$ with an accuracy of

$$|w_j(t) - q_j(t)| \leq e_{r,M,j}, \qquad t \geq t^\dagger. \tag{5.239}$$

The upper bound $e_{r,M,j}$ of (5.239) is obtained from (5.236).

Proof.

Outline: First, an outline of the proof is given. Consider the obstacles center to enter the stopping zone so that the set point of the robot is shifted according to Algorithm 4. At that moment the obstacles center is located at the edge of the stopping zone. The definition of the stopping zone guarantees that the distance between any point on the robot and the edge of the stopping zone is at least b. Based on Theorem 14 it is possible to determine the time span τ that is required to bound the angular velocities as $|\dot{q}_j| \leq \dot{q}_M$. During time span τ the points on the robot may move no more than the distance $l_{low}(d_1 + 2d_2)\tau$ in direction of the obstacle and the obstacle may move no more than $v_{oc,M}\tau$ towards the robot. The stopping zone can be scaled up based on parameter b. Consequently, choosing b as $b \geq (v_{oc,M} + l_{low}(d_1 + 2d_2))\tau + r_o$ guarantees that a collision of the obstacle with any point on the robot may only occur after τ when the angular velocities are guaranteed to be bounded by the desired value of $\dot{q}_M$. The proof is discussed in detail as follows.

Step 1: The time span τ after which the angular velocities are bounded by $\dot{q}_M$ is determined. From Theorem 19 it is known that the constraints are always satisfied. Consider the obstacles center to enter the stopping zone at some time instant $t^\star$. The obstacles center is located at the edge of the stopping zone at $t^\star$. According to Algorithm 4 the set point is shifted. The angular velocities are known to be bounded as $|\dot{q}_j| \leq l_{low}$ because the stopping zone is a subset of the safety disk which has the velocity bound l_{low}. It follows that

$$|\sigma_{r,j}(t^\star)| = |\dot{q}_j(t^\star) - \alpha_j e_{r,j}(t^\star) - \beta_j |e_{r,j}(t^\star)|^{\gamma_j} \mathrm{sgn}(e_{r,j}(t^\star))| = |\dot{q}_j(t^\star)| \leq l_{low}, \tag{5.240}$$

holds due to the shifted set point and the bounded angular velocity. Substituting (5.119) in (5.127) it follows from Theorem 14 that

$$|\dot{q}_j(t)| \leq \dot{q}_M, \qquad \dot{q}_M > 0, \tag{5.241}$$

can be achieved for $t \geq t^\star + \tau$ if

$$2\epsilon_{r,j} + 2\epsilon_{c,M,j} + \frac{\mu_{e,j}}{\sqrt{2}} \leq \dot{q}_M, \qquad 0 < \mu_{e,j} \leq \eta_{m,j}\sqrt{2}, \tag{5.242}$$

$$\epsilon_{c,M,j} = \max_i \{\epsilon_{c_i,j}\}, \tag{5.243}$$

holds. Following Theorem 14 time span τ can be calculated according to

$$\tau = \max_j \{\tau_{1,j} + \tau_{2,j}\}, \tag{5.244}$$

where $\tau_{1,j}$ is

$$\tau_{1,j} = \frac{l_{low} - (\epsilon_{r,j} + \epsilon_{c,M,j})}{\varrho_j}, \qquad \varrho_j = \min\left\{\frac{\mu_{r,j}}{\sqrt{2}}, \mu_{a,j}\eta_{m,j}\right\}, \tag{5.245}$$

due to the bound (5.240) and $\tau_{2,j}$ is

$$\tau_{2,j} = (e_{r,M^\star,j} - e_{r,M,j})\frac{\sqrt{2}}{\mu_{e,j}}. \tag{5.246}$$

Assume the obstacles center to remain in the stopping zone after time instant $t^\star$. Then it is

$$l_{c,j}(t^\star + \tau_{1,j}) = \max\left\{l_{c_1,j}(t^\star + \tau_{1,j}), l_{c_2,j}(t^\star + \tau_{1,j})\right\} \leq l_{low}, \tag{5.247}$$

and according to (5.124) it follows that $e_{r,M^\star,j}$ of (5.246) can be obtained from

$$\alpha_j e_{r,M^\star,j} + \beta_j e_{r,M^\star,j}^{\gamma_j} = \epsilon_{r,j} + \epsilon_{c,M,j} + l_{low}. \tag{5.248}$$

Quantity $e_{r,M,j}$ of (5.246) is the solution of

$$\alpha_j e_{r,M,j} + \beta_j e_{r,M,j}^{\gamma_j} = \epsilon_{r,j} + \epsilon_{c,M,j} + \frac{\mu_{e,j}}{\sqrt{2}}, \tag{5.249}$$

as stated in (5.119).

Step 2: The required size of the scaling parameter b of the stop zone is determined. Assume the angular velocities to be bounded as

$$|\dot{q}_j| \leq \Omega. \tag{5.250}$$

The velocity $v_r(x_{r,l_1}, y_{r,l_1})$ of any point (x_{r,l_1}, y_{r,l_1}) on link one of the robot is given by

$$v_r(x_{r,l_1}, y_{r,l_1}) = \sqrt{\dot{x}_{r,l_1}^2 + \dot{y}_{r,l_1}^2}, \tag{5.251}$$

with

$$\begin{bmatrix} x_{r,l_1} \\ y_{r,l_1} \end{bmatrix} = \alpha_1 \begin{bmatrix} \cos(q_1) \\ \sin(q_1) \end{bmatrix}, \qquad 0 \leq \alpha_1 \leq d_1. \tag{5.252}$$

Substituting

$$\dot{x}_{r,l_1} = -\alpha_1 \dot{q}_1 \sin(q_1), \tag{5.253}$$
$$\dot{y}_{r,l_1} = \alpha_1 \dot{q}_1 \cos(q_1), \tag{5.254}$$

in (5.251) and considering (5.250) yields

$$v_r(x_{r,l_1}, y_{r,l_1}) = \alpha_1 |\dot{q}_1| \leq \alpha_1 \Omega \leq d_1 \Omega. \tag{5.255}$$

The velocity $v_r(x_{r,l_2}, y_{r,l_2})$ of any point (x_{r,l_2}, y_{r,l_2}) on link two of the robot is given by

$$v_r(x_{r,l_2}, y_{r,l_2}) = \sqrt{\dot{x}_{r,l_2}^2 + \dot{y}_{r,l_2}^2}, \tag{5.256}$$

with

$$\begin{bmatrix} x_{r,l_2} \\ y_{r,l_2} \end{bmatrix} = d_1 \begin{bmatrix} \cos(q_1) \\ \sin(q_1) \end{bmatrix} + \alpha_2 \begin{bmatrix} \cos(q_1 + q_2) \\ \sin(q_1 + q_2) \end{bmatrix}, \qquad 0 \leq \alpha_2 \leq d_2. \tag{5.257}$$

From

$$\dot{x}_{r,l_2} = -d_1 \dot{q}_1 \sin(q_1) - \alpha_2 (\dot{q}_1 + \dot{q}_2) \sin(q_1 + q_2), \tag{5.258}$$
$$\dot{y}_{r,l_2} = d_1 \dot{q}_1 \cos(q_1) + \alpha_2 (\dot{q}_1 + \dot{q}_2) \cos(q_1 + q_2), \tag{5.259}$$

and the angle addition and subtraction theorems it follows

$$\dot{x}_r^2 + \dot{y}_r^2 = d_1^2 \dot{q}_1^2 + \alpha_2^2 (\dot{q}_1 + \dot{q}_2)^2 + 2 d_1 \alpha_2 \dot{q}_1 (\dot{q}_1 + \dot{q}_2) \cos(q_2), \tag{5.260}$$
$$\leq d_1^2 \dot{q}_1^2 + \alpha_2^2 (\dot{q}_1 + \dot{q}_2)^2 + 2 d_1 \alpha_2 (|\dot{q}_1|^2 + |\dot{q}_1||\dot{q}_2|), \tag{5.261}$$

which leads to

$$\dot{x}_r^2 + \dot{y}_r^2 \leq d_1^2\Omega^2 + 4\alpha_2^2\Omega^2 + 4d_1\alpha_2\Omega^2 = \Omega^2(d_1 + 2\alpha_2)^2 \leq \Omega^2(d_1 + 2d_2)^2, \tag{5.262}$$

if (5.250) is considered. Substituting (5.262) in (5.256) gives

$$v_r(x_{r,l_2}, y_{r,l_2}) = \sqrt{\dot{x}_{r,l_2}^2 + \dot{y}_{r,l_2}^2} \leq (d_1 + 2d_2)\Omega. \tag{5.263}$$

Consequently, from (5.255) and (5.263) it follows that the velocity $v_r(x_r, y_r)$ of any point $(x_r, y_r) \in \mathcal{R}$ on the robot is bounded as

$$v_r(x_r, y_r) \leq (d_1 + 2d_2)\Omega. \tag{5.264}$$

From the definition of the stop zone according to (5.199) and Fig. 5.10 it is known that the Euclidean distance between any point on the edge of the stop zone and any point $(x_r, y_r) \in \mathcal{R}$ on the robot is at least b. At time $t^\star$ the obstacles center appears at the edge of the stop zone and the angular velocities are bounded by $|\dot{q}_j| \leq l_{low}$ as long as the obstacles center remains in the stop zone. It follows from (5.264) that during the time span τ the maximum distance that any point (x_r, y_r) may move towards the obstacles center is $(d_1 + 2d_2)l_{low}\tau$. The maximum distance that the obstacles center may move towards a point on the robot is $v_{oc,M}\tau$ as the obstacles center velocity is known to be bounded as $v_{oc} \leq v_{oc,M}$. Consequently, if the scaling parameter satisfies (5.228) a collision between the obstacle and the robot can occur at time instant $t^\star + \tau$ at the earliest. As after the time span τ the angular velocities are bounded by $\dot{q}_M$ it follows from (5.264) that the velocity of the robot is bounded as stated in (5.229) if it collides with the obstacle.

Step 3: Achievement of tracking error convergence if the path of the robot is not blocked. In this case it follows from (5.118) and (5.119) of Theorem 14 that

$$|w_j(t) - q_j(t)| \leq e_{r,M,j}, \tag{5.265}$$

holds. The upper bound $e_{r,M,j}$ of (5.265) is obtained from (5.249). The convergence of the tracking error described by (5.265) is achieved in finite-time as stated by Theorem 14. □

5.2.2 Application Example

In this section the previously introduced safe robot control concept is applied. A scenario is considered in which human and robot interact with each other. The scenario is illustrated by Fig. 5.11. The end effector of the robot moves from a waypoint A (WP-A) to a waypoint B (WP-B). An obstacle is initially located in the outer zone. The obstacle moves towards the safety disk. When the obstacle has reached the safety disk the end effector of the robot is still on its movement from WP-A to WP-B. As the robot continues moving the obstacle will enter the stop zone. This forces the robot to stop. After a short period of time the obstacle continues its movement. It leaves the safety disk and clears the path of the robot. The robot continues its movement and finally reaches WP-B. To show that the proposed safety concept is robust against model uncertainties an unknown payload is applied to the end effector of the robot. The payload is active all along and it is described by the external force $F_y = 9.81\,[\mathrm{m/s^2}] \times 80\,[\mathrm{kg}]$. The circular obstacle is assumed to have a radius $r_o = 0.5\,[\mathrm{m}]$ and a velocity v_{oc} that is bounded as $v_{oc} \leq 1\,[\mathrm{m/s}]$. The values of the waypoints are defined in Table 5.4. The parameters of the contour graph (5.198) are given

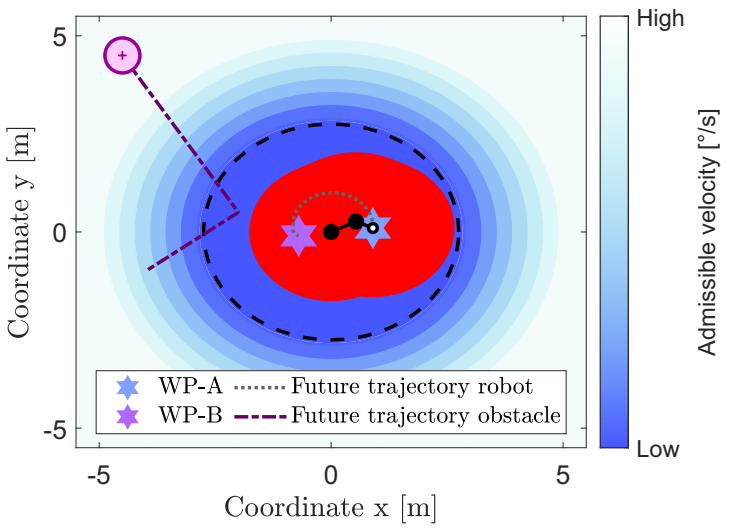

Figure 5.11: Visualization of considered scenario between obstacle and robot. The robot moves from WP-A to WP-B while the obstacle enters and leaves the safety disk.

as $l_{high} = 30\,[°/s]$, $l_{low} = 10\,[°/s]$, and $m = 0.15\,[\text{rad m/s}]$. The controller parameters are selected as follows. The auxiliary function η_{c_i} is chosen as stated in (5.216). According to (5.220) quantity $\dot{\eta}_{M,j}$ is obtained from

$$\forall t, i\colon |\dot{\eta}_{c_i,j}(t)| \leq m v_{oc,M} = 0.1500 < \dot{\eta}_{M,j}, \tag{5.266}$$

and according to (5.221) parameter $\eta_{m,j}$ is selected based on

$$\forall t, i\colon 0 < \eta_{m,j} < 0.1735 = l_{low} - \epsilon_{c_i,j} \leq \eta_{c_i,j}(t), \tag{5.267}$$

The boundary layer width $\epsilon_{c_i,j}$ in (5.267) is $\epsilon_{c_i,j} = 0.001$. The uncertainty bound $\hat{\Psi}_{M,j}$ is assumed to be 10 and it is confirmed by simulation that for $\hat{\Psi}_{M,j} = 10$ quantity $|\Psi_j|$ is indeed upper bounded by $\hat{\Psi}_{M,j}$. The scaling parameter of the stop zone is chosen as $b = 1.75\,[\text{m}]$. The selected controller parameters are summarized in Table 5.5.

Based on the controller parameters and the Theorems 19 and 20 a proposition is stated as follows. The proposition guarantees that the velocity constraints of the robot are always satisfied for the considered scenario. In addition, if the robot collides with the obstacle the velocity of the robot is restricted to 0.011 [m/s]. If the robot and the obstacle do not collide but the obstacle is at least for 1 [s] in the stop zone then the velocity of robot is also restricted to 0.011 [m/s] until the obstacle leaves the stop zone again. Regarding the tracking error convergence it can be guaranteed that WP-B is reached in finite-time with an accuracy in the range of $\pm 0.0024\,[°]$.

Table 5.4: Reference values in Cartesian coordinates (x_{ca}, y_{ca}) and joint angles (w_1, w_2)

	x_{ca} [m]	y_{ca} [m]	w_1 [°]	w_2 [°]
WP-A	0.900	0.100	26.511	−51.318
WP-B	−0.700	−0.100	153.714	92.388

Table 5.5: Controller parameters related to control input ν_j (parameterization of both controllers identical)

$\mu_{r,j}$	10	$\mu_{c_i,j}$	10	$\mu_{a,j}$	25	β_j	5	γ_j	0.7	$\epsilon_{r,j}$	0.001
$\epsilon_{c_i,j}$	0.001	$\dot{\eta}_{M,j}$	0.16	$\eta_{m,j}$	0.17	$\hat{\Psi}_{M,j}$	10	$\Gamma_{M,j}$	1	$\Gamma_{m,j}$	1

Proposition 21.
Consider a two link robot as shown in Fig. 5.4 with dynamics described by (5.147). Assume the robotic system to be controlled by the MIMO controller (5.152) whose auxiliary inputs ν are defined based on Algorithm 3. Consider the bounds of the constraints to be defined by a circular contour graph as stated in (5.198) with $l_{high} = 30\,[°/\mathrm{s}]$, $l_{low} = 10\,[°/\mathrm{s}]$, and $m = 0.15\,[\mathrm{rad\,m/s}]$. Let the auxiliary function $\eta_{c_i,j}$ be defined as stated in (5.216). Assume the controller parameters to be chosen as stated in Table 5.5 and assume Ψ_j to be bounded as $|\Psi_j| \leq \hat{\Psi}_{M,j}$. Further assume the initial angular velocities of the robot to be zero. Let the obstacle be defined as $\mathcal{O}$ based on (5.194) with radius $r_o = 0.5\,[\mathrm{m}]$ and let $(x_o, y_o) \in \mathcal{O}$ be a point lying within the bounds of the obstacle. Assume the velocity of the obstacles center to be bounded as $v_{oc} \leq 1\,[\mathrm{m/s}]$. Consider $(x_r, y_r) \in \mathcal{R}$ to be any point on the links of the robot and let $v_r(x_r, y_r)$ be the velocity of any of that points. Consider the stop zone $\mathcal{S}$ to be defined according to (5.199) with scaling parameter $b = 1.75\,[\mathrm{m}]$. Assume the set point of the robot to be shifted as defined by Algorithm 4 if the obstacles center enters or leaves the stopping zone. Then the following can be stated:

- *The constraints defined by contour graph (5.198) are never violated.*
- *If there exists a point (x_r, y_r) on the robot that coincides with the obstacle, i. e. $(x_r, y_r) \in \mathcal{O}$, then the robots velocity on that point is bounded as $v_r(x_r, y_r) \leq 0.011\,[\mathrm{m/s}]$ and the angular velocities are bounded as $|\dot{q}_j| \leq 0.43\,[°/\mathrm{s}]$.*
- *If the obstacle center enters the stop zone and remains in there for at least $1\,[\mathrm{s}]$ then the robots velocity on any point (x_r, y_r) is bounded as $v_r(x_r, y_r) \leq 0.011\,[\mathrm{m/s}]$ and the angular velocities are bounded as $|\dot{q}_j| \leq 0.43\,[°/\mathrm{s}]$ until the obstacles center leaves the stop zone again.*
- *The angular velocities q_j are guaranteed to converge to the initial set points w_j with an accuracy of $|w_j(t) - q_j(t)| < 0.0024\,[°]$ after $t \geq t^\dagger$ where $t^\dagger$ is finite.*

Proof. Theorem 19 can be applied as the auxiliary function $\eta_{c_i,j}$ is chosen according to (5.216) and due to

$$\forall i, j \colon \sigma_{c_i,j}(t_0) = -\eta_{c_i,j}(t_0) + s_{c_i}\dot{q}_j(t_0) < 0 \leq \epsilon_{c_i,j}, \qquad \epsilon_{c_i,j} > 0, \quad \eta_{c_i,j}(t_0) > 0,$$

which is satisfied as the initial angular velocities are zero. It follows from the theorem that the constraints are never violated.

The remaining statements are obtained from Theorem 20. Based on the controller parameters of Table 5.5 it follows from (5.230) that $\dot{q}_M$ may be selected as

$$2 \max_j\{\epsilon_{r,j}\} + 2 \max_j\{\epsilon_{c,j}\} + \frac{\mu_{e,j}}{\sqrt{2}} = \dot{q}_M = 0.424\,[°/\mathrm{s}], \tag{5.268}$$

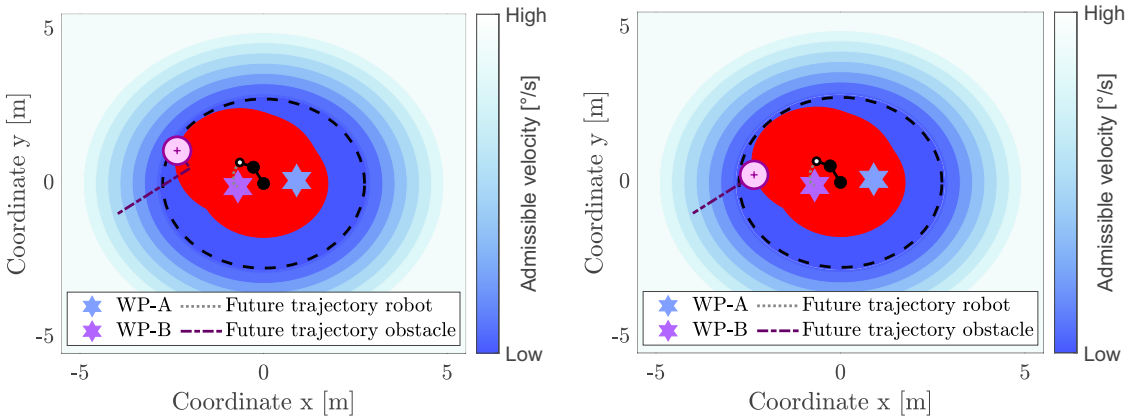

Figure 5.12: (a) Obstacles center enters stop zone. (b) Obstacles center leaves stop zone.

with $\mu_{e,j}$ chosen as $\mu_{e,j} = \eta_{m,j}\sqrt{2}/50$. Equation (5.229) gives

$$v_r(x_r, y_r) \leq \dot{q}_M(d_1 + 2d_2) = 0.0104\,[\mathrm{m/s}], \tag{5.269}$$

and (5.232) leads to

$$\tau = \max_j\{\tau_{1,j}\} + \max_j\{\tau_{2,j}\} = 0.9944\,[\mathrm{s}]. \tag{5.270}$$

The selection of the scaling parameter b is sufficient as (5.228) yields

$$b = 1.75\,[\mathrm{m}] \geq 1.7374\,[\mathrm{m}] = \left(v_{oc,M} + l_{low}(d_1 + 2d_2)\right)\tau + r_o. \tag{5.271}$$

The convergence of the tracking error is studied as follows. From the description of the considered scenario according to Fig. 5.11 it is known that the obstacle finally leaves the stop zone. As $e_{r,M,j}$ of (5.265) equals $0.0024\,[^\circ]$ it follows that the tracking error is bounded by

$$|w_j(t) - q_j(t)| < 0.0024\,[^\circ], \qquad t \geq t^\dagger, \tag{5.272}$$

after a finite-time $t^\dagger$. □

In the following the stated results of Proposition 21 are confirmed by simulation. The closed loop system is simulated using the Euler method with a sampling time of 0.05 [ms]. The robot is located at WP-A initially with zero angular velocities. The simulation terminates if the robot reaches the reference angles of WP-B with an error in the range of $\pm 0.0024\,^\circ$. The simulation results are discussed as follows. In Fig. 5.12 two specific situations are depicted namely when the obstacles center enters the stop zone and when the obstacles center leaves the stop zone. The figure shows that the robot is stopped while the obstacle moves across the stop zone. In Fig. 5.13 the joint angles q_1 and q_2 and their corresponding velocities $\dot{q}_1$ and $\dot{q}_2$ are visualized. It can be seen that the constraints are never violated. With regards to the tracking performance the figure shows that the set point changes to the current value of the joint angles when the obstacle enters the stop zone. As long as the obstacle remains in the stop zone the robot is kept fixed by the

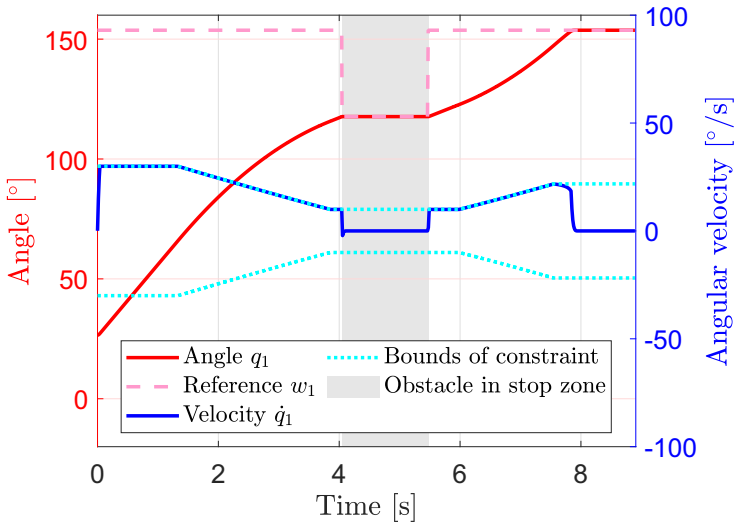

(a)

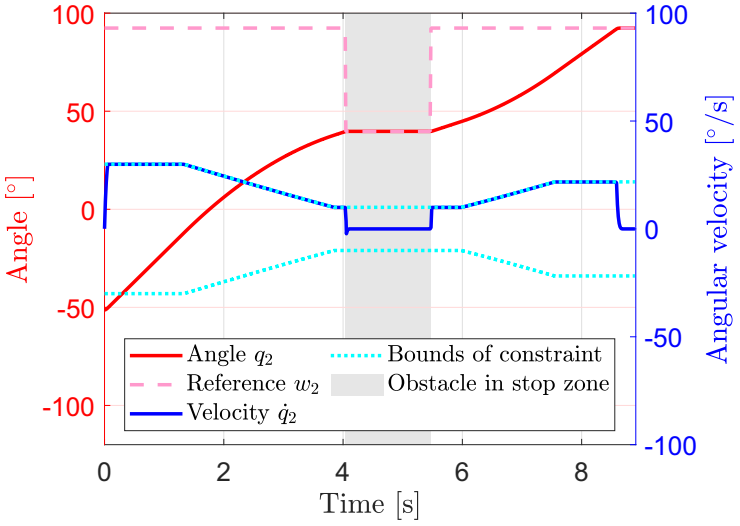

(b)

Figure 5.13: Visualization of bounds, constrained variables, set points, and control variables. (a) First joint. (b) Second joint.

controller. When the obstacle leaves the stop zone the set point switches back to its initial value and the robot continues moving. Finally, the end effector reaches WP-B. In Fig. 5.14 the maximum velocity of the robot is visualized. Formally, the maximum velocity of any point $(x_r, y_r) \in \mathcal{R}$ on the robot is given by

$$\max_{x_r, y_r} \{v_r(x_r, y_r)\}. \tag{5.273}$$

Based on (5.264) an upper bound $v_{r,M}(t)$ of (5.273) can be stated as

$$v_r(x_r(t), y_r(t)) \leq \max_{x_r(t), y_r(t)} \{v_r(x_r(t), y_r(t))\},$$

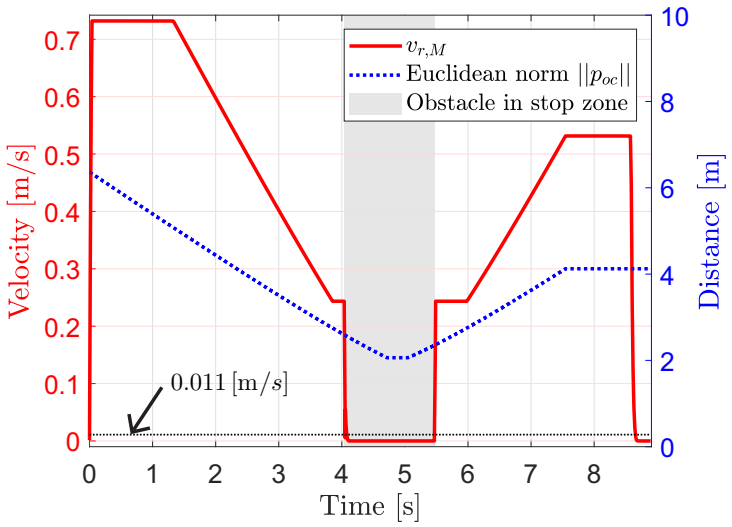

(a)

Figure 5.14: Maximum velocity $v_{r,M}(t)$ according to (5.274) guaranteed to be bounded by $0.011\,[\mathrm{m}/s]$ if obstacle remains at least $1\,[\mathrm{s}]$ in the stop zone.

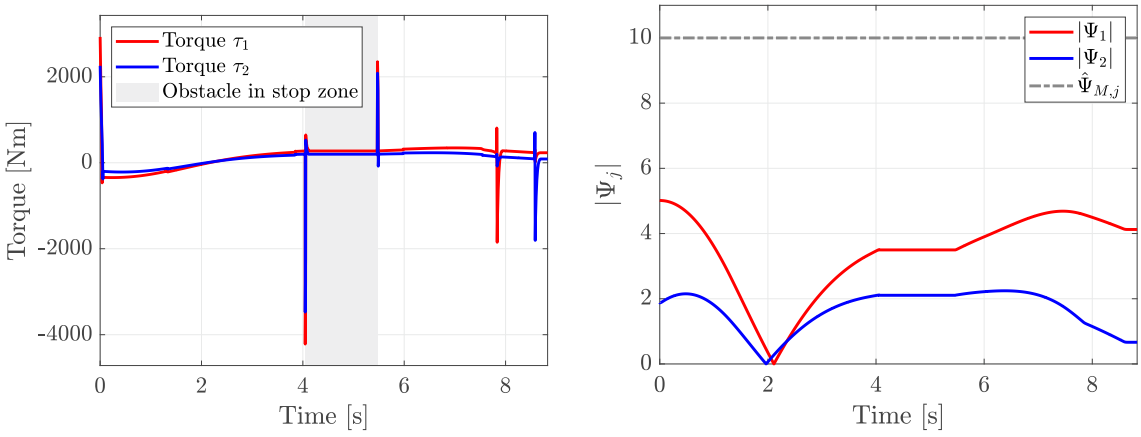

(a) **(b)**

Figure 5.15: (a) Input signals. (b) Proof that $\Psi_{M,j}$ is indeed an upper bound of $|\Psi_j|$.

$$\leq \max\{|\dot{q}_1(t)|, |\dot{q}_2(t)|\}(d_1 + 2d_2) \triangleq v_{r,M}(t). \tag{5.274}$$

The upper bound $v_{r,M}(t)$ of (5.274) is depicted in Fig. 5.14. It can be seen that the maximum velocity of the robot is below $0.011\,[\mathrm{m/s}]$ if the obstacle stays in the stop zone for at least $1\,[\mathrm{s}]$. The velocity remains bounded by $0.011\,[\mathrm{m/s}]$ until the obstacle leaves the stop zone again. In Fig. 5.15 (a) the control inputs are visualized. The chattering is well attenuated but the changes of the set points induce some peaks in the control signals. In Fig. 5.15 (b) the disturbance term $|\Psi_j|$ is shown to be indeed upper bounded by the assumed value $\hat{\Psi}_{M,j} = 10$ of the uncertainty bound. Finally, all statements of Proposition 21 are confirmed by the simulation results.

5.2.3 Summary

In the previous sections a safety concept for human-robot interaction is proposed. The concept is exemplarily designed for a two-link robot with rotary joints. The human is described by a scalable circular obstacle in a two-dimensional plane. The proposed strategy is based on three geometrical zones. These zones guarantee that the joint velocities decrease if the robot is approached by the obstacle. Within the working area of the robot the admissible velocities are restricted to a minimum value. Moreover, in the vicinity of the robot a stop zone is defined. If the obstacle is located within the stop zone the robot is forced to stop. The proposed concept can be applied to design the maximum velocity of the robot that occurs during a collision with the obstacle. The robot does not evade from the obstacle. Consequently, the developed strategy allows any kind of interaction between human and robot and guarantees that the appearing robot velocities are uncritical. The main advantage of the suggested method with regards to the literature is the ability to handle model uncertainty. The velocity constraints are guaranteed to be satisfied as long as the uncertainty bounds are chosen sufficiently large which can be achieved by experimental tuning. The proposed concept is tested on a specific scenario of human-robot interaction. Model uncertainty is simulated by a applying an unknown exogenous payload to the end effector. Based on the chosen controller parameters concrete bounds for the robot velocity can be determined. The simulation results confirm that the robot velocity is indeed bounded by the values that are provided through the theory.

6 Conclusions and Perspectives

This thesis considers three main contributions to sliding mode control and observation: An optimization of the smooth variable structure filter, a chattering mitigated adaptive sliding mode control approach, and a constrained sliding mode controller for nonlinear uncertain systems. The novelties of the three approaches are summarized as follows. The achievements in terms of the formulated goals of Section 1.1 are highlighted and a perspective on possible future works is given.

6.1 Summary and Conclusions

The smooth variable structure filter is a state estimation approach for discrete-time nonlinear systems. It follows the predictor corrector scheme of the Kalman filter and utilizes elements known from sliding mode control and observation. The smooth variable structure filter can handle model uncertainty but its performance highly depends on the width of the smoothing boundary layer which is a tuning parameter. In this thesis a novel reformulation of the SVSF approach is stated. The reformulation gives insights on how the smoothing boundary layer width affects the behavior of the filter. If the output estimation error exceeds the width of the boundary layer the filter ignores the a priori estimation. This behavior of the filter seems to be reasonable as the a priori estimation can be imprecise due to the uncertainty of the model. The SVSF does not minimize any estimation performance criterion like the Kalman filter does. To improve the estimation performance of the SVSF a new filter gain is derived that minimizes the MSE. Therefore, the a posteriori error covariance of the reformulated filter is determined. The original filter gain is replaced by a gain that minimizes the MSE. The filter with the optimized gain is shown to behave equally to the extended Kalman filter. To achieve a compromise between robustness and minimization of the MSE a combination of the smooth variable structure and the Kalman filter is proposed. In addition, a parameter optimization scheme is developed to optimize the tuning parameters of the original SVSF and the new combined estimation approach. The optimization scheme neither requires any data from the true system to be known nor does it require any knowledge about the true system description. In the optimization scheme a training process is considered. Within the training the parameters of the known nominal system description are varied to simulate model uncertainty. As the true states of the simulated system are known the estimation performance of the filter can be optimized under the influence of model uncertainty. This finally leads to a robustification of the filter. For the combined estimation approach it can be guaranteed that the performance in the training process is at least as good as the one of the original SVSF. The proposed combined estimation approach is tested on an uncertain nonlinear system. Its estimation performance is compared to the one of original SVSF. The parameters of the combined approach and the SVSF are optimized based on the proposed scheme. The results clearly

show that the state estimations of the combined approach are more precise than the ones of the SVSF. From the optimized parameters it can be concluded that at least for the considered example the SVSF gain does not contribute well to the robust estimation performance of the combined approach. Instead the combined approach behaves similar to a parameterized Kalman filter that is optimized to handle model uncertainty.

In adaptive sliding mode control the controller gain is adaptively adjusted to reduce the chattering effect. As pointed out in this thesis all adaptive SMC approaches suffer from the problem that the controller gain can not be effectively reduced on the sliding surface. This is the case because on the sliding surface the so-called equivalent control input is required to be applied to keep the system in sliding mode. As the controller gain can not be effectively reduced on the sliding surface a remaining chattering effect is present. To overcome the problem a data-driven adaptive SMC approach is developed in this thesis. The suggested approach is based on a model-free controller and an adaptive SMC. The model-free controller is active on the sliding surface to avoid the chattering and the adaptive SMC is active otherwise to guarantee boundedness of the tracking error. The model-free controller is a predictive controller that is formulated based on a local linear system description. The local system description is identified through a Kalman filter and describes the system behavior in the near future. Based on the incoming measurements of the system the Kalman filter keeps the local model up-to-date. To achieve a suitable prediction performance of the local model the true system is required to have sufficient slow dynamics. The predictive controller is obtained by solving a standard linear MPC problem. A nonlinear MIMO three tank water system is considered to test the predictive controller and the prediction capabilities of the local model. The dynamics of the system are assumed unknown. Set-point tracking as well as handling of constraints can be achieved by the proposed model-free controller. The new chattering mitigated sliding mode control approach is formulated by combining the model-free controller with an adaptive SMC. Weighting functions are introduced to achieve chattering mitigation and boundedness of the tracking error. The new data-driven adaptive SMC is tested on a nonlinear chemical plant. The approach is stationary accurate with no noticeable amount of chattering.

Constrained control approaches can be found in a wide variety of applications. Sliding mode based methods offer the ability to handle model uncertainty. The provided robustness is especially interesting for safety-critical systems that consider for example the interaction of humans and robots. The application field of the existing constrained SMCs is rather limited. Often the constrained control problem is only solved in theory but the stated controllers are infeasible in practice due to chattering. Most of the approaches only consider box-constraints so that the bounds of the constraints can not be updated online. In this thesis a new constrained sliding mode control approach for nonlinear relative degree two systems is developed. The first time derivative of the control variable is assumed to be constrained and the upper and lower bounds may explicitly depend on time. An accurate system description is not required only finite uncertainty bounds are assumed. The suggested approach is based on a combination of two SMC sub-controllers. The sub-controllers guarantee reaching of two sliding manifolds. One manifold is designed to achieve set point tracking the other manifold avoids constraint violation. Smooth transitions between the sub-controllers are guaranteed. Chattering mitigation can be achieved without violating the constraints. For the proposed controller it is analytically proven that the constrained control problem can be solved. Sufficient conditions related to the

controller parameters are derived to guarantee convergence of the tracking error and satisfaction of the constraints. Moreover, the tracking error bounds are stated and a maximum time is determined after which convergence with respect to the bounds is achieved. The developed approach is applied to a robotic systems. A point to point robot control problem subject to velocity constraints is considered. The robot is disturbed by an unknown payload that is applied to the end effector. Based on the developed theory and the selected controller parameters concrete values for the tracking error bounds are stated. A specific time interval is determined after which the considered control problem is guaranteed to be solved. The theoretical results are confirmed by simulation. Further, the developed constrained controller is applied within a proposed concept for safe human-robot interaction. The safety concept is exemplarily designed for a two-link robot with rotary joints. A scaleable circular obstacle in a two-dimensional plane is used to describe the human. Three geometrical zones are defined that restrict the velocity of the robot. Physical contact between the robot and the human is allowed by the concept. The maximum velocity of the robot that occurs during a possible collision with the obstacle is a design value. Consequently, the concept can be applied for any human-robot interaction and guarantees that the appearing velocities are uncritical. In contrast to existing safety concepts the proposed strategy is robust. As the developed constrained SMC is applied within the stated concept robustness against model uncertainty is achieved. This is of special interest in safety critical applications. A specific scenario of human-robot interaction is considered to validate the proposed concept. To simulate model uncertainty an unknown external payload is applied to the end effector. Based on the selected controller parameters a specific velocity can be determined that is not exceeded by the robot in case of a collision. The theoretical results are confirmed by simulation.

6.2 Perspectives

The smooth variable structure filter does not show general superiority when the system description is imprecise. The combined estimation approach that is formulated in this thesis achieves a better estimation performance although it primarily behaves like an optimized Kalman filter. In addition, the application field of the SVSF approach is limited as it requires full state measurements. As a consequence, it seems to be more promising to further improve the ability of the Kalman filter to handle model uncertainty. For linear systems many methods already exist like the robust Kalman filtering approach of Dong and You (2006). In case of linear observable systems it is even possible to estimate the whole state space description and the Kalman filter gain from input-output data (Qin, 2006). The challenge is to achieve a robustification of the Kalman filter in case of nonlinear uncertain systems. An optimal Kalman filter gain can be determined if the error covariance is known. The estimation of the error covariance that is described in this thesis is based on the assumption of full state measurements. However, the estimation strategy could be modified to handle systems for which the states are not measured entirely. The error covariance could be simply parameterized and the introduced parameters may be optimized based on the optimization scheme that is proposed in this thesis.

The developed data-driven adaptive SMC approach of this thesis can indeed mitigate the chattering effect. However, the formulated approach is only applicable to nonlinear systems with sufficient slow dynamics. In addition, no mathematical analysis of the model-free predictive controller which is part of the proposed control concept is provided. The

convergence of the model-free predictive controller is not guaranteed. To make the proposed approach applicable to a wider class of systems nonlinear neural networks could be used for the system identification. Nonlinear networks can provide enhance prediction capabilities but may lead to nonlinear non-convex optimization problems that are hard to solve. However, so-called input convex nonlinear networks exist (Amos *et al.*, 2017). This networks lead to convex optimization problems which facilitate the design of the model-free predictive controller.

Although the developed constrained sliding mode control approach is formulated with respect to single input relative degree two systems it can be applied to MIMO systems as well. This is the case if the system is fully actuated like it is for the robotic MIMO system that is considered in this thesis. Also other mechanical systems such as autonomous underwater vehicles are commonly fully actuated and have a relative degree of two related to position control. However, it may still be advantageous to reformulate the proposed constrained controller for nonlinear MIMO systems. This can be achieved by applying the sliding mode control concept of Slotine and Li (1991, Chap. 7.4) that is described in Section 2.1.2. The advantage of the reformulation of the controller would be that a further degree of model uncertainty could be considered.

Bibliography

Afshari, H.H., M. Attari, R. Ahmed, A. Delbari, S. Habibi and T. Shoa (2018). Reliable state of charge and state of health estimation using the smooth variable structure filter. *Control Engineering Practice* **77**, 1–14.

Agee, J., S. Kizir and Z. Bingul (2015). Intelligent proportional-integral (i-PI) control of a single link flexible joint manipulator. *Journal of Vibration and Control* **21**(11), 2273–2288.

Agravante, D.J., A. Cherubini, A. Sherikov, P.B. Wieber and A. Kheddar (2019). Human-humanoid collaborative carrying. *IEEE Transactions on Robotics* **35**(4), 833–846.

Agrawal, A. and K. Sreenath (2017). Discrete control barrier functions for safety-critical control of discrete systems with application to bipedal robot navigation.. In: *Robotics: Science and Systems*.

Ahmed, R., M. El Sayed, S.A. Gadsden, J. Tjong and S. Habibi (2016). Artificial neural network training utilizing the smooth variable structure filter estimation strategy. *Neural Computing and Applications* **27**(3), 537–548.

Ahmed, R.M., M.A. El Sayed, S.A. Gadsden and S.R. Habibi (2011). Fault detection of an engine using a neural network trained by the smooth variable structure filter. In: *IEEE International Conference on Control Applications (CCA)*. IEEE. pp. 1190–1196.

Al-Shabi, M. and S. Habibi (2011). Iterative smooth variable structure filter for parameter estimation. *International Scholarly Research Notices*.

Al-Shabi, M., S.A. Gadsden and S.R. Habibi (2013). Kalman filtering strategies utilizing the chattering effects of the smooth variable structure filter. *Signal Processing* **93**(2), 420–431.

Allam, A., M. Tadjine, A. Nemra and E. Kobzili (2017). Stereo vision as a sensor for SLAM based smooth variable structure filter with an adaptive boundary layer width. In: *6th International Conference on Systems and Control (ICSC)*. IEEE. pp. 14–20.

Ames, A.D., J.W. Grizzle and P. Tabuada (2014). Control barrier function based quadratic programs with application to adaptive cruise control. In: *53rd IEEE Conference on Decision and Control*. IEEE. pp. 6271–6278.

Amos, Brandon, Lei Xu and J. Z. Kolter (2017). Input convex neural networks. In: *International Conference on Machine Learning*. PMLR. pp. 146–155.

Anderson, B.D.O. and J.B. Moore (1979). *Optimal filtering*. Prentice-Hall.

Attari, M., S.A. Gadsden and S.R. Habibi (2013). Target tracking formulation of the SVSF as a probabilistic data association algorithm. In: *Proc. of the 2013 American Control Conference*. pp. 6328–6332.

Attari, M., Z. Luo and S. Habibi (2015). An SVSF-based generalized robust strategy for target tracking in clutter. *IEEE Trans. on Intelligent Transportation Systems* **17**(5), 1381–1392.

Barbot, J.P., M. Djemai and T. Boukhobza (2002). Sliding mode observers. *Sliding mode control in engineering* **11**, 33.

Barbot, J.P., T. Boukhobza and M. Djemai (1996). Sliding mode observer for triangular input form. In: *Proceedings of 35th IEEE conference on decision and control*. Vol. 2. IEEE. pp. 1489–1490.

Bartolini, G. and E. Punta (2010). Reduced-order observer in the sliding-mode control of nonlinear nonaffine systems. *IEEE transactions on automatic control* **55**(10), 2368–2373.

Bartolini, G. and E. Punta (2012). Sliding mode output-feedback stabilization of uncertain nonlinear nonaffine systems. *Automatica* **48**(12), 3106–3113.

Bartoszewicz, A. and A. Nowacka-Leverton (2010). ITAE optimal sliding modes for third-order systems with input signal and state constraints. *IEEE Transactions on Automatic Control* **55**(8), 1928–1932.

Bauer, W., M. Bender, M. Braun, P. Rally and O. Scholtz (2016). Lightweight robots in manual assembly—best to start simply. *Fraunhofer-Institut für Arbeitswirtschaft und Organisation IAO, Stuttgart*.

Bemporad, A. (1998). Reference governor for constrained nonlinear systems. *IEEE Transactions on Automatic Control* **43**(3), 415–419.

Bemporad, A., F. Borrelli and M. Morari (2003). Min-max control of constrained uncertain discrete-time linear systems. *IEEE Transactions on Automatic Control* **48**(9), 1600–1606.

Blom, H.A.P. and Y. Bar-Shalom (1988). The interacting multiple model algorithm for systems with Markovian switching coefficients. *IEEE Trans. on Automatic Control* **33**(8), 780–783.

Calafiore, G.C. and L. Fagiano (2012). Robust model predictive control via scenario optimization. *IEEE Transactions on Automatic Control* **58**(1), 219–224.

Campi, M., A. Lecchini and S. Savaresi (2002). Virtual reference feedback tuning: a direct method for the design of feedback controllers. *Automatica* **38**(8), 1337–1346.

Cannon, M., J. Buerger, B. Kouvaritakis and S. Rakovic (2011). Robust tubes in nonlinear model predictive control. *IEEE Transactions on Automatic Control* **56**(8), 1942–1947.

Cao, L., Y. Chen, Z. Zhang, H. Li and A.K. Misra (2017). Predictive smooth variable structure filter for attitude synchronization estimation during satellite formation flying. *IEEE Transactions on Aerospace and Electronic Systems* **53**(3), 1375–1383.

Ceriani, N.M., A.M. Zanchettin, P. Rocco, A. Stolt and A. Robertsson (2015). Reactive task adaptation based on hierarchical constraints classification for safe industrial robots. *IEEE/ASME Transactions on Mechatronics* **20**(6), 2935–2949.

Demim, F., A. Nemra and K. Louadj (2016). Robust SVSF-SLAM for unmanned vehicle in unknown environment. *IFAC-PapersOnLine* **49**(21), 386–394.

Demmel, J. (1997). *Applied numerical linear algebra*. Vol. 56. Siam.

Ding, B., T. Zhang and H. Fang (2020). On the equivalence between the unbiased minimum-variance estimation and the infinity augmented Kalman filter. *International Journal of Control* **93**(12), 2995–3002.

Ding, S., K. Mei and S. Li (2018). A new second-order sliding mode and its application to nonlinear constrained systems. *IEEE Transactions on Automatic Control* **64**(6), 2545–2552.

Dinuzzo, F. and A. Ferrara (2009). Higher order sliding mode controllers with optimal reaching. *IEEE Transactions on Automatic Control* **54**(9), 2126–2136.

Doherty, S., J. Gomm and D. Williams (1997). Experiment design considerations for non-linear system identification using neural networks. *Computers & chemical engineering* **21**(3), 327–346.

Dong, Z. and Z. You (2006). Finite-horizon robust Kalman filtering for uncertain discrete time-varying systems with uncertain-covariance white noises. *IEEE Signal Process. Letters* **13**(8), 493–496.

Edwards, C. and S. Spurgeon (1994). On the development of discontinuous observers. *International Journal of control* **59**(5), 1211–1229.

Edwards, C. and S. Spurgeon (1998). *Sliding mode control: theory and applications*. CRC Press.

Edwards, C. and Y. Shtessel (2016). Adaptive continuous higher order sliding mode control. *Automatica* **65**, 183–190.

Edwards, C., S. Spurgeon and R. Patton (2000). Sliding mode observers for fault detection and isolation. *Automatica* **36**(4), 541–553.

ElBsat, M.N. and E.E. Yaz (2013). Robust and resilient finite-time bounded control of discrete-time uncertain nonlinear systems. *Automatica* **49**(7), 2292–2296.

Esmaeili, B., M. Salim, M. Baradarannia and A. Farzamnia (2019). Data-driven observer-based model-free adaptive discrete-time terminal sliding mode control of rigid robot manipulators. In: *2019 7th international conference on robotics and mechatronics (ICRoM)*. IEEE. pp. 432–438.

Fallaha, C.J., M. Saad, H.Y. Kanaan and K. Al-Haddad (2010). Sliding-mode robot control with exponential reaching law. *IEEE Transactions on Industrial Electronics* **58**(2), 600–610.

Faroni, M., M. Beschi and N. Pedrocchi (2019). An MPC framework for online motion planning in human-robot collaborative tasks. In: *2019 24th IEEE International Conference on Emerging Technologies and Factory Automation (ETFA)*. IEEE. pp. 1555–1558.

Favoreel, W., B. De Moor, M. Gevers and P. Van Overschee (1999). Closed-loop model-free subspace-based LQG-design. In: *Proc. of the 7th ieee mediterranean conference on control and automation, june*. pp. 28–30.

Fei, J. and H. Ding (2012). Adaptive sliding mode control of dynamic system using RBF neural network. *Nonlinear Dynamics* **70**(2), 1563–1573.

Feng, Y., X. Yu and Z. Man (2002). Non-singular terminal sliding mode control of rigid manipulators. *Automatica* **38**(12), 2159–2167.

Filippov, A.F. (2013). *Differential equations with discontinuous righthand sides: control systems*. Vol. 18. Springer Science & Business Media.

Fliess, M. and C. Join (2008). Intelligent PID controllers. In: *2008 16th Mediterranean Conference on Control and Automation*. IEEE. pp. 326–331.

Gadsden, S.A. and S.R. Habibi (2010). A new form of the smooth variable structure filter with a covariance derivation. In: *49th IEEE Conference on Decision and Control (CDC)*. IEEE. pp. 7389–7394.

Gadsden, S.A., D. Dunne, S.R. Habibi and T. Kirubarajan (2011*a*). Combined particle and smooth variable structure filtering for nonlinear estimation problems. In: *14th International Conference on Information Fusion*. IEEE. pp. 1–8.

Gadsden, S.A., M. Al-Shabi, I. Arasaratnam and S.R. Habibi (2014*a*). Combined cubature Kalman and smooth variable structure filtering: A robust nonlinear estimation strategy. *Signal Processing* **96**, 290–299.

Gadsden, S.A., M. El Sayed and S.R. Habibi (2011*b*). Derivation of an optimal boundary layer width for the smooth variable structure filter. In: *Proc. of the 2011 American Control Conference*. IEEE. pp. 4922–4927.

Gadsden, S.A., S. Habibi and T. Kirubarajan (2014*b*). Kalman and smooth variable structure filters for robust estimation. *IEEE Transactions on Aerospace and Electronic Systems* **50**(2), 1038–1050.

Gadsden, S.A., S.R. Habibi and T. Kirubarajan (2010). A novel interacting multiple model method for nonlinear target tracking. In: *Proc. of the 13th Conference on Information Fusion (FUSION)*. IEEE. pp. 1–8.

Gadsden, S.A., Y. Song and S.R. Habibi (2013). Novel model-based estimators for the purposes of fault detection and diagnosis. *IEEE/ASME Transactions on Mechatronics* **18**(4), 1237–1249.

Gao, W. and J.C. Hung (1993). Variable structure control of nonlinear systems: a new approach. *IEEE Transactions on Industrial Electronics* **40**(1), 45–55.

Garcia-Gabin, W., D. Zambrano and E.F. Camacho (2009). Sliding mode predictive control of a solar air conditioning plant. *Control Engineering Practice* **17**(6), 652–663.

Garelli, F., R.J. Mantz and H. de Battista (2011). *Advanced control for constrained processes and systems*. The Institution of Engineering and Technology.

Garone, E., S. Di Cairano and I. Kolmanovsky (2017). Reference and command governors for systems with constraints: A survey on theory and applications. *Automatica* **75**, 306–328.

Gilbert, E.G. and K.T. Tan (1991). Linear systems with state and control constraints: The theory and application of maximal output admissible sets. *IEEE Transactions on Automatic control* **36**(9), 1008–1020.

Gillijns, S. and B. De Moor (2007). Unbiased minimum-variance input and state estimation for linear discrete-time systems. *Automatica* **43**(1), 111–116.

Habibi, S. (2007). The smooth variable structure filter. *Proc. of the IEEE* **95**(5), 1026–1059.

Hassibi, B., A.H. Sayed and T. Kailath (1999). *Indefinite quadratic estimation and control: a unified approach to H_2 and H_∞ theories*. Society for Industrial and Applied Mathematics.

Haykin, S. (2001). *Kalman filtering and neural networks*. Wiley Online Library.

Hide, C., T. Moore and M. Smith (2003). Adaptive Kalman filtering for low-cost INS/GPS. *The J. of Navigation* **56**(1), 143–152.

Hiriart-Urruty, J.B. and C. Lemaréchal (2013). *Convex analysis and minimization algorithms I: Fundamentals*. Vol. 305. Springer science & business media.

Hjalmarsson, H., S. Gunnarsson and M. Gevers (1994). A convergent iterative restricted complexity control design scheme. In: *Proceedings of 1994 33rd IEEE Conference on Decision and Control*. Vol. 2. IEEE. pp. 1735–1740.

Hmida, F.B., K. Khémiri, J. Ragot and M. Gossa (2012). Three-stage Kalman filter for state and fault estimation of linear stochastic systems with unknown inputs. *J. of the Franklin Institute* **349**(7), 2369–2388.

Hou, Z. and S. Jin (2011). Data-driven model-free adaptive control for a class of MIMO nonlinear discrete-time systems. *IEEE Transactions on Neural Networks* **22**(12), 2173–2188.

Hou, Z. and Y. Zhu (2013). Controller-dynamic-linearization-based model free adaptive control for discrete-time nonlinear systems. *IEEE Transactions on Industrial Informatics* **9**(4), 2301–2309.

Hou, Z. and Z. Wang (2013). From model-based control to data-driven control: Survey, classification and perspective. *Information Sciences* **235**, 3–35.

Hsu, S.C., X. Xu and A.D. Ames (2015). Control barrier function based quadratic programs with application to bipedal robotic walking. In: *2015 American Control Conference (ACC)*. IEEE. pp. 4542–4548.

Hu, Y., Y. Cao and S. Zhang (2013). Design of sliding mode control with disturbance observers for inertial platform. In: *2013 25th Chinese Control and Decision Conference (CCDC)*. IEEE. pp. 4652–4656.

Huang, Y.J., T.C. Kuo and S.H. Chang (2008). Adaptive sliding-mode control for nonlinear systems with uncertain parameters. *IEEE Transactions on Systems, Man, and Cybernetics, Part B (Cybernetics)* **38**(2), 534–539.

Incremona, G.P., M. Rubagotti and A. Ferrara (2016). Sliding mode control of constrained nonlinear systems. *IEEE Transactions on Automatic Control* **62**(6), 2965–2972.

Innocenti, M. and M. Falorni (1998). State constrained sliding mode controllers. In: *Proceedings of the 1998 American Control Conference*. Vol. 1. IEEE. pp. 104–108.

Iplikci, S. (2006). Support vector machines-based generalized predictive control. *International Journal of Robust and Nonlinear Control: IFAC-Affiliated Journal* **16**(17), 843–862.

Isermann, R. and M. Münchhof (2010). *Identification of dynamic systems: an introduction with applications*. Springer Science & Business Media.

Isidori, A., E.D. Sontag and M. Thoma (1995). *Nonlinear control systems*. Vol. 3. Springer.

Jaskuła, M. and P. Leśniewski (2020). Constraining state variables and control signal via sliding mode control approach. *IEEE Access* **8**, 111475–111481.

Kailath, T., A. Sayed and B. Hassibi (2000). *Linear estimation*. Prentice Hall.

Kerrigan, E.C. and J.M. Maciejowski (2000). Soft constraints and exact penalty functions in model predictive control. In: *UKACC International Conference on Control (Control 2000)*. The institution of engineering and technology.

Khalil, H.K. (2002). *Nonlinear systems*. Vol. 3. Prentice Hall.

Khatib, O. (1986). Real-time obstacle avoidance for manipulators and mobile robots. In: *Autonomous robot vehicles*. pp. 396–404. Springer.

Kim, T., Y. Wang, H. Fang, Z. Sahinoglu, T. Wada, S. Hara and W. Qiao (2015). Model-based condition monitoring for lithium-ion batteries. *J. of Power Sources* **295**, 16–27.

Kimmel, M. and S. Hirche (2014). Invariance control with chattering reduction. In: *53rd IEEE Conference on Decision and Control*. IEEE. pp. 68–74.

Kimmel, M. and S. Hirche (2017). Invariance control for safe human–robot interaction in dynamic environments. *IEEE Transactions on Robotics* **33**(6), 1327–1342.

Kimmel, M., M. Lawitzky and S. Hirche (2012). 6D workspace constraints for physical human-robot interaction using invariance control with chattering reduction. In: *2012 IEEE/RSJ International Conference on Intelligent Robots and Systems*. IEEE. pp. 3377–3383.

Kitanidis, P.K. (1987). Unbiased minimum-variance linear state estimation. *Automatica* **23**(6), 775–778.

Landi, C.T., F. Ferraguti, L. Sabattini, C. Secchi and C. Fantuzzi (2017). Admittance control parameter adaptation for physical human-robot interaction. In: *2017 IEEE international conference on robotics and automation (ICRA)*. IEEE. pp. 2911–2916.

Langson, W., I. Chryssochoos, S.V. Raković and D.Q. Mayne (2004). Robust model predictive control using tubes. *Automatica* **40**(1), 125–133.

Levant, A. (1993). Sliding order and sliding accuracy in sliding mode control. *International journal of control* **58**(6), 1247–1263.

Levant, A. (2003). Higher-order sliding modes, differentiation and output-feedback control. *International Journal of Control* **76**(9-10), 924–941.

Levant, A. (2009). Non-homogeneous finite-time-convergent differentiator. In: *Proceedings of the 48h IEEE Conference on Decision and Control (CDC) held jointly with 2009 28th Chinese Control Conference*. IEEE. pp. 8399–8404.

Levant, A. and X. Yu (2018). Sliding-mode-based differentiation and filtering. *IEEE Transactions on Automatic Control* **63**(9), 3061–3067.

Litt, J., D. Frederick and T.H. Guo (2009). The case for intelligent propulsion control for fast engine response. *AIAA Infotech@Aerospace Conference* pp. AIAA2009–1876.

Liu, D. and G.H. Yang (2017). Data-driven adaptive sliding mode control of nonlinear discrete-time systems with prescribed performance. *IEEE Transactions on Systems, Man, and Cybernetics: Systems* **49**(12), 2598–2604.

Liu, Y. and C. Wang (2018). A FastSLAM based on the smooth variable structure filter for UAVs. In: *15th International Conference on Ubiquitous Robots (UR)*. IEEE. pp. 591–596.

Longbin, M., S. Xiaoquan, Z. Yiyu, S.Z. Kang and Y. Bar-Shalom (1998). Unbiased converted measurements for tracking. *IEEE Trans. on Aerospace and Electronic Systems* **34**(3), 1023–1027.

Longman, R. (2000). Iterative learning control and repetitive control for engineering practice. *International journal of control* **73**(10), 930–954.

Luo, Z., M. Attari, S. Habibi and M. Von Mohrenschildt (2019). Online multiple maneuvering vehicle tracking system based on multi-model smooth variable structure filter. *IEEE Transactions on Intelligent Transportation Systems* **21**(2), 603–616.

Magni, L., G. De Nicolao, L. Magnani and R. Scattolini (2001). A stabilizing model-based predictive control algorithm for nonlinear systems. *Automatica* **37**(9), 1351–1362.

Magrini, E., F. Flacco and A. De Luca (2015). Control of generalized contact motion and force in physical human-robot interaction. In: *2015 IEEE international conference on robotics and automation (ICRA)*. IEEE. pp. 2298–2304.

Mainprice, J. and D. Berenson (2013). Human-robot collaborative manipulation planning using early prediction of human motion. In: *2013 IEEE/RSJ International Conference on Intelligent Robots and Systems*. IEEE. pp. 299–306.

Martino, L., J. Read, V. Elvira and F. Louzada (2017). Cooperative parallel particle filters for online model selection and applications to urban mobility. *Digital Signal Process.* **60**, 172–185.

Matschek, J., T. Gonschorek, M. Hanses, N. Elkmann, F. Ortmeier and R. Findeisen (2020). Learning references with Gaussian processes in model predictive control applied to robot assisted surgery. In: *2020 European Control Conference (ECC)*. IEEE. pp. 362–367.

Mikuláš, O. (2013). Quadratic programming algorithms for fast model-based predictive control. Bachelor's thesis. Czech Technical University in Prague.

Mitić, D., M. Spasić, M. Hovd and D. Antić (2013). An approach to design of sliding mode based generalized predictive control. In: *2013 IEEE 8th International Symposium on Applied Computational Intelligence and Informatics (SACI)*. IEEE. pp. 347–351.

Obeid, H., L.M. Fridman, S. Laghrouche and M. Harmouche (2018). Barrier function-based adaptive sliding mode control. *Automatica* **93**, 540–544.

Pietrala, M. and M. Jaskuła (2019). IAE minimization in sliding mode control for second order systems with velocity constraint. In: *2019 20th International Carpathian Control Conference (ICCC)*. IEEE. pp. 1–6.

Pietrala, M., M. Jaskula and A. Bartoszewicz (2018). Terminal sliding mode control of second order systems with velocity constraint. In: *2018 19th International Carpathian Control Conference (ICCC)*. IEEE. pp. 223–227.

Piga, D., S. Formentin and A. Bemporad (2017). Direct data-driven control of constrained systems. *IEEE Transactions on Control Systems Technology* **26**(4), 1422–1429.

Plestan, F., Y. Shtessel, V. Bregeault and A. Poznyak (2010). New methodologies for adaptive sliding mode control. *International Journal of Control* **83**(9), 1907–1919.

Qin, S. J. (2006). An overview of subspace identification. *Computers & chemical engineering* **30**(10-12), 1502–1513.

Raimondo, D.M., D. Limon, M. Lazar, L. Magni and E.F. Camacho (2009). Min-max model predictive control of nonlinear systems: A unifying overview on stability. *European Journal of Control* **15**(1), 5–21.

Rauscher, M., M. Kimmel and S. Hirche (2016). Constrained robot control using control barrier functions. In: *2016 IEEE/RSJ International Conference on Intelligent Robots and Systems (IROS)*. IEEE. pp. 279–285.

Rawlings, J.B. and D.Q. Mayne (2009). *Model predictive control: Theory and design*. Nob Hill Pub.

Ren, J.C., D. Liu, Z. Wang and Y. Wan (2019). Data-driven model-free adaptive sliding mode control for melt surface temperature of Czochralski silicon monocrystal growth process. In: *2019 Chinese Automation Congress (CAC)*. IEEE. pp. 4047–4051.

Richter, H. (2011). A multi-regulator sliding mode control strategy for output-constrained systems. *Automatica* **47**(10), 2251–2259.

Richter, H., B.D. O'Dell and E.A. Misawa (2007). Robust positively invariant cylinders in constrained variable structure control. *IEEE Transactions on Automatic Control* **52**(11), 2058–2069.

Robla-Gómez, S., V.M. Becerra, J.R. Llata, E. Gonzalez-Sarabia, C. Torre-Ferrero and J. Perez-Oria (2017). Working together: A review on safe human-robot collaboration in industrial environments. *IEEE Access* **5**, 26754–26773.

Rubagotti, M., D.M. Raimondo, A. Ferrara and L. Magni (2010). Robust model predictive control with integral sliding mode in continuous-time sampled-data nonlinear systems. *IEEE Transactions on Automatic Control* **56**(3), 556–570.

Ryan, E.P. and M. Corless (1984). Ultimate boundedness and asymptotic stability of a class of uncertain dynamical systems via continuous and discontinuous feedback control. *IMA journal of mathematical control and information* **1**(3), 223–242.

Saranrittichai, P., N. Niparnan and A. Sudsang (2013). Robust local obstacle avoidance for mobile robot based on dynamic window approach. In: *2013 10th International Conference on Electrical Engineering/Electronics, Computer, Telecommunications and Information Technology*. IEEE. pp. 1–4.

Schildbach, G., L. Fagiano, C. Frei and M. Morari (2014). The scenario approach for stochastic model predictive control with bounds on closed-loop constraint violations. *Automatica* **50**(12), 3009–3018.

Seborg, D.E., D. Mellichamp, T. Edgar and F. Doyle III (2010). *Process dynamics and control*. John Wiley & Sons.

Shin, J., H. Kim, S. Park and Y. Kim (2010). Model predictive flight control using adaptive support vector regression. *Neurocomputing* **73**(4-6), 1031–1037.

Shtessel, Y., C. Edwards, L. Fridman and A. Levant (2014). *Sliding mode control and observation*. Springer.

Shtessel, Y., M. Taleb and F. Plestan (2012). A novel adaptive-gain supertwisting sliding mode controller: Methodology and application. *Automatica* **48**(5), 759–769.

Siciliano, B., L. Sciavicco, L. Villani and G. Oriolo (2010). *Robotics: modelling, planning and control*. Springer Science & Business Media.

Slotine, J.J. (1984). Sliding controller design for non-linear systems. *International Journal of Control* **40**(2), 421–434.

Slotine, J.J. and W. Li (1991). *Applied Nonlinear Control*. Prentice hall Englewood Cliffs, N.J.

Söffker, D., T.J. Yu and P. Müller (1995). State estimation of dynamical systems with nonlinearities by using proportional-integral observer. *International Journal of Systems Science* **26**(9), 1571–1582.

Solanes, J.E., L. Gracia, P. Munoz-Benavent, J.V. Miro, M.G. Carmichael and J. Tornero (2018). Human–robot collaboration for safe object transportation using force feedback. *Robotics and Autonomous Systems* **107**, 196–208.

Song, J., Y. Niu and Y. Zou (2016). Finite-time sliding mode control synthesis under explicit output constraint. *Automatica* **65**, 111–114.

Sorenson, H. (1970). Least-squares estimation: from Gauss to Kalman. *IEEE spectrum* **7**(7), 63–68.

Spiller, M. and D. Söffker (2021). Robust control of relative degree two systems subject to output constraints with time-varying bounds. In: *2021 IEEE Conference on Decision and Control (CDC)*. IEEE. accepted.

Spiller, M. and D. Söffker (2020*a*). Chattering mitigated sliding mode control of uncertain nonlinear systems. In: *Proceedings of IFAC World Congress 2020*. International Federation of Automatic Control.

Spiller, M. and D. Söffker (2020*b*). On the relation between smooth variable structure and adaptive Kalman filter. *Front. Appl. Math. Stat. 6: 585439. doi: 10.3389/fams.*

Spiller, M., F. Bakhshande and D. Söffker (2018). The uncertainty learning filter: a revised smooth variable structure filter. *Signal Processing* **152**, 217–226.

Spiller, M., F. Bakhshande and D. Söffker (2020). Adaptive neural network based predictive control of nonlinear systems with slow dynamics. In: *International Design Engineering Technical Conferences and Computers and Information in Engineering Conference*. Vol. 83914. American Society of Mechanical Engineers. p. V002T02A029a.

Su, H., J. Sandoval, M. Makhdoomi, G. Ferrigno and E. De Momi (2018). Safety-enhanced human-robot interaction control of redundant robot for teleoperated minimally invasive surgery. In: *2018 IEEE International Conference on Robotics and Automation (ICRA)*. IEEE. pp. 6611–6616.

Tanaskovic, M., L. Fagiano, C. Novara and M. Morari (2017). Data-driven control of nonlinear systems: An on-line direct approach. *Automatica* **75**, 1–10.

Tian, Y., H. Suwoyo, W. Wang and L. Li (2019). An ASVSF-SLAM algorithm with time-varying noise statistics based on MAP creation and weighted exponent. *Mathematical Problems in Engineering* **2019**, Article ID 2765731.

Utkin, V.I. (1992). Sliding modes in control and optimization. In: *Communications and Control Engineering Series*. Springer-Verlag Berlin Heidelberg.

Utkin, V.I. (2011). Chattering problem. *IFAC Proceedings Volumes* **44**(1), 13374–13379.

Utkin, V.I. and A.S. Poznyak (2013*a*). Adaptive sliding mode control. In: *Advances in sliding mode control*. pp. 21–53. Springer.

Utkin, V.I. and A.S. Poznyak (2013*b*). Adaptive sliding mode control with application to super-twist algorithm: Equivalent control method. *Automatica* **49**(1), 39–47.

Utkin, V.I. and J. Shi (1996). Integral sliding mode in systems operating under uncertainty conditions. In: *Proceedings of 35th IEEE conference on decision and control*. Vol. 4. IEEE. pp. 4591–4596.

Venkataraman, S.T. and S. Gulati (1992). Control of nonlinear systems using terminal sliding modes. In: *1992 American Control Conference*. pp. 891–893.

Villagra, J., B. Vinagre and I. Tejado (2012). Data-driven fractional PID control: application to DC motors in flexible joints. *IFAC Proceedings Volumes* **45**(3), 709–714.

Wang, H., X. Ye, Y. Tian, G. Zheng and N. Christov (2016). Model-free–based terminal SMC of quadrotor attitude and position. *IEEE Transactions on Aerospace and Electronic Systems* **52**(5), 2519–2528.

Wang, L. (2009). *Model predictive control system design and implementation using MATLAB®*. Springer Science & Business Media.

Weng, Y. and X. Gao (2017). Adaptive sliding mode decoupling control with data-driven sliding surface for unknown MIMO nonlinear discrete systems. *Circuits, Systems, and Signal Processing* **36**(3), 969–997.

Wilkie, D., J. Van Den Berg and D. Manocha (2009). Generalized velocity obstacles. In: *2009 IEEE/RSJ International Conference on Intelligent Robots and Systems*. IEEE. pp. 5573–5578.

Wolff, J. and M. Buss (2004). Invariance control design for nonlinear control affine systems under hard state constraints. *IFAC Proceedings Volumes* **37**(13), 555–560.

Xu, Q. and Y. Li (2011). Model predictive discrete-time sliding mode control of a nanopositioning piezostage without modeling hysteresis. *IEEE Trans. on Control Systems Technology* **20**(4), 983–994.

Yang, Y. and W. Gao (2006). An optimal adaptive Kalman filter. *J. of Geodesy* **80**(4), 177–183.

Yu, H., S. Huang, G. Chen, Y. Pan and Z. Guo (2015). Human–robot interaction control of rehabilitation robots with series elastic actuators. *IEEE Transactions on Robotics* **31**(5), 1089–1100.

Yu, S., X. Yu, B. Shirinzadeh and Z. Man (2005). Continuous finite-time control for robotic manipulators with terminal sliding mode. *Automatica* **41**(11), 1957–1964.

Yu, X. and M. Zhihong (2002). Fast terminal sliding-mode control design for nonlinear dynamical systems. *IEEE Transactions on Circuits and Systems I: Fundamental Theory and Applications* **49**(2), 261–264.

Zanchettin, A.M., N.M. Ceriani, P. Rocco, H. Ding and B. Matthias (2015). Safety in human-robot collaborative manufacturing environments: Metrics and control. *IEEE Transactions on Automation Science and Engineering* **13**(2), 882–893.

Zhihong, M., A.P. Paplinski and H.R. Wu (1994). A robust MIMO terminal sliding mode control scheme for rigid robotic manipulators. *IEEE transactions on automatic control* **39**(12), 2464–2469.

This thesis is based on the results and development steps presented in the following previous publications.

Journal Articles

Spiller, M. and D. Söffker (2020). 'On the Relation Between Smooth Variable Structure and Adaptive Kalman Filter.' *Frontiers in Applied Mathematics and Statistics* **6**, 61.

Spiller, M., F. Bakhshande and D. Söffker (2018). 'The Uncertainty Learning Filter: A Revised Smooth Variable Structure Filter.' *Signal Processing* **152**, 217-226.

Conference Papers

Spiller, M. and D. Söffker (2021). 'Robust Control of Relative Degree Two Systems Subject to Output Constraints with Time-Varying Bounds.' *60th IEEE Conference on Decision and Control* - accepted.

Spiller, M. and D. Söffker (2020). 'Chattering mitigated sliding mode control of uncertain nonlinear systems.' *IFAC-PapersOnLine* **53**(2), 6244-6249.

Spiller, M. and D. Söffker (2020). 'Output Constrained Sliding Mode Control: A Variable Gain Approach.' *IFAC-PapersOnLine* **53**(2), 6201-6206.

Spiller, M., F. Bakhshande and D. Söffker (2020). 'Adaptive Neural Network Based Predictive Control of Nonlinear Systems With Slow Dynamics.' *International Design Engineering Technical Conferences and Computers and Information in Engineering Conference* **83914**, V002T02A029a.

During the time of research the subsequently listed papers were published in addition. However, the content of this contributions is not or not directly related to the content of this thesis.

Journal Articles

Spiller, M. and D. Söffker (2020). 'Stator-Rotor Contact Force Estimation of Rotating Machine.' *Automation* **2**(3), 83-97.

Conference Papers

Spiller, M. and D. Söffker (2020). 'Automated Target Interception Based on Multiple Object Tracking.' *2020 European Control Conference (ECC)* IEEE, 1763-1768.

Bakhshande, F., M. Spiller and D. Söffker (2020). 'Computationally Efficient Model Predictive Control for Real Time Implementation experimentally applied on a Hydraulic Differential Cylinder.' *IFAC-PapersOnLine* **53**(2), 8979-8984.

In the context of research projects at the Chair of Dynamics and Control, the following student thesis have been supervised by Mark Spiller and Univ.-Prof. Dr.-Ing. Dirk Söffker. Development steps and results of the research projects and the student theses are integrated with each other and hence are also part of this thesis.

Seal, S. 'Destination estimation from partially observed tracked object trajectories.' Master Thesis, 2021.

Adhisaputra, S. 'Neural Network-based Model Predictive Control for a MIMO System using a Structured Control Strategy.' Bachelor Thesis, 2020.

Ali, O. 'Implementation and control of a three tank system using model predictive control.' Master Thesis, 2020.

Lau, C.Z. 'Real time implementation of NN-based model predictive control on a hydraulic differential cylinder.' Bachelor Thesis, 2020.

Diwadkar, A. 'Data-driven position control of autonomous vehicle based on SLAM estimations.' Master Thesis, 2020.

Ranjan, R. 'Analysis and extension of Simultaneous Localization and Mapping (SLAM) algorithm.' Master Thesis, 2020.

King, Y.L. 'Real time implementation of model predictive control using hydraulic cylinder.' Bachelor Thesis, 2019.

Hering, J. 'Model predictive control of a nonlinear MIMO system.' Bachelor Thesis, 2019.

Darwish, M. 'Identification and control of a MIMO nonlinear system using neural network-based model predictive control.' Bachelor Thesis, 2019.

Liu, B. 'Acquisition and processing of eye-tracker sensor data.' Bachelor Thesis, 2019.

Mohd Fadil, M. 'Construction of elastic multi-storey structure.' Bachelor Thesis, 2019.

Lu, X. 'Identification and control of MIMO nonlinear systems using artificial intelligence approach.' Bachelor Thesis, 2018.

Huang, Q. 'Object Detection in Video Data Based on Adaptive Background Gaussian-Mixture Models.' Bachelor Thesis, 2018.

Huang, J. 'Application and optimization of a filtering approach for multiple object tracking in video data.' Master Thesis, 2018.

A Simulation Study of Section 3.5

A.1 Jacobian of Discrete-time CSTR System

The Jacobian of the time-continuous system

$$\begin{bmatrix}\dot{x}_1\\ \dot{x}_2\end{bmatrix} = \begin{bmatrix}f_1(x,u)\\ f_2(x,u)\end{bmatrix} = f(x,u), \tag{A.1}$$

$$f_1(x,u) = \frac{q}{V}(C_{Af} - x_1) - k_0 x_1 \exp\left(-\frac{E}{Rx_2}\right),$$

$$f_2(x,u) = \frac{q}{V}(T_f - x_2) + \frac{(-\Delta H)k_0 x_1}{\rho C_p}\exp\left(-\frac{E}{Rx_2}\right) + \frac{UA}{V\rho C_p}(u + T_{eq,c} - x_2),$$

is given by

$$J(x) = \begin{bmatrix}\frac{\partial f_1}{\partial x_1} & \frac{\partial f_1}{\partial x_2}\\ \frac{\partial f_2}{\partial x_1} & \frac{\partial f_2}{\partial x_2}\end{bmatrix} = \begin{bmatrix}-\frac{q}{V} - k_0\exp\left(-\frac{E}{Rx_2}\right) & -k_0 x_1 \frac{E}{Rx_2^2}\exp\left(-\frac{E}{Rx_2}\right)\\ \frac{(-\Delta H)k_0}{\rho C_p}\exp\left(-\frac{E}{Rx_2}\right) & \frac{(-\Delta H)k_0 x_1 E}{\rho C_p x_2^2 R}\exp\left(-\frac{E}{Rx_2}\right) - \frac{q}{V} - \frac{UA}{V\rho C_p}\end{bmatrix},$$

so that the Jacobian of the discrete-time system

$$x_{k+1} = \underbrace{f(x_k,u_k)\times T_s + x_k}_{f_d(x_k,u_k)}, \tag{A.2}$$

with sampling time T_s is obtained as

$$J_d(x_k) = \frac{\partial f_d}{\partial x_k} = J(x_k)\times T_s + I_2. \tag{A.3}$$

A.2 Optimized Parameters of EKF and SVSF

The optimized parameters of the extended Kalman filter and the smooth variable structure filter are shown in Table A.1. The parameters correspond to the training process described by Table 3.2.

Table A.1: Optimized parameters of EKF and SVSF

		Training I	Training II	Training III	Training IV	Training V
EKF	q_{11}	0.4857705	0.4896970	18.365799	0.1054488	18.410656
	q_{12}	-0.000100	0.0000347	0.0000360	0.0000460	0.0000472
	q_{22}	0.0112983	777.61160	143.88359	369.08842	246.75960
SVSF	ψ_1	4.0112549	4.0348145	0.0635671	6.0151829	0.0635484
	ψ_2	6.4780212	6.1078125	1.2476379	3.2376635	1.2476431
	ϕ_1	0.9999891	0.9999695	0	0.9999843	0
	ϕ_2	0.9999389	0.7109375	0.0002407	0.9999542	0

B Quadratic Program with Soft-Constraints

In the following the hard constraints of a quadratic program are reformulated as soft-constraints. This is a well-known procedure. Explanation can be found in e. g. Mikuláš (2013). Consider the quadratic program

$$\arg\min_{u} \frac{1}{2} u^T G u + d^T u, \tag{B.1}$$

with hard constraints

$$A_c u \leq b_c, \tag{B.2}$$

and $0 \preceq G \in \mathbb{R}^{m \times m}$, $A_c \in \mathbb{R}^{p \times m}$, $d \in \mathbb{R}^m$, $u \in \mathbb{R}^m$, $b_c \in \mathbb{R}^p$. The constraints are rewritten as soft-constraints

$$A_c u \leq b_c + \nu, \tag{B.3}$$

based on a vector of slack variables $(\nu_i) = \nu \in \mathbb{R}^p$. To enforce the constraints minimization of the slack variables $|\nu_i|$ with $i = 1, \ldots, p$ is desired. Therefore, the cost function is modified as

$$\arg\min_{u,\nu} \frac{1}{2} u^T G u + d^T u + \frac{1}{2} \nu^T W \nu, \tag{B.4}$$

with the additional weighting matrix $0 \preceq W \in \mathbb{R}^{p \times p}$. The modified cost function can be rewritten as a quadratic program

$$\arg\min_{\tilde{u}} \frac{1}{2} \tilde{u}^T \tilde{G} \tilde{u} + \tilde{d}^T \tilde{u}, \tag{B.5}$$

subject to

$$\tilde{A}_c \tilde{u} \leq b_c, \tag{B.6}$$

with

$$\tilde{u} = \begin{bmatrix} u \\ \nu \end{bmatrix}, \qquad \tilde{G} = \begin{bmatrix} G & 0 \\ 0 & W \end{bmatrix}, \qquad \tilde{d} = \begin{bmatrix} d \\ 0 \end{bmatrix}, \qquad \tilde{A}_c = \begin{bmatrix} A_c & -I_n \end{bmatrix}, \tag{B.7}$$

Then the constraints defined by (B.2) are almost satisfied for increasing weights of W.

C Adaptive Sliding Mode Controller of Plestan

In Plestan *et al.* (2010) an adaptive SMC is proposed that has the ability to decrease the controller gain in the near of the sliding surface. The controller is described by Algorithm 5. Outside the boundary layer the SMC gain is continuously increased to guarantee finite-time convergence of the sliding variable. Inside the boundary layer the gain is reset. This resetting is based on an estimation of the equivalent control input i. e. an estimation of the input that is required to keep σ on the sliding surface. The estimation of the equivalent control input is achieved based on a low-pass filtering of the switching term $\text{sgn}(\sigma)$. The filtered signal γ_1 is multiplied with $\bar{k}_2$. The equivalent control input is given by the statement $\bar{k}_2\gamma_1 + \bar{k}_3$.

In Section 4.2.3 the A-SMC approach is compared with the model-free predictive controller (PC) and the chattering mitigated sliding mode controller (CM-SMC). The controller parameters of A-SMC are tuned by visual inspection of the chattering effect and the tracking performance. The following values are chosen: $\epsilon_1 = 1$, $\bar{k}_1 = 10$, $\bar{k}_3 = 2$, $\tau_1 = 100$, $k_{A-SMC}(t_0) = 20$, and $\gamma_1(t_0) = 0$.

Algorithm 5 Adaptive SMC (A-SMC) of Plestan *et al.* (2010)

Input $\sigma(t)$, $\epsilon_1 > 0$, $\tau_1 > 0$, $\bar{k}_1 > 0$, $\bar{k}_3 > 0$, $k_{A-SMC}(t_0) > 0$, $\gamma_1(t_0)$

  if $|\sigma| \leq \epsilon_1$ **then** ▷ If σ is inside the boundary layer ...

    $k_{A-SMC}(t) \leftarrow \bar{k}_2|\gamma_1| + \bar{k}_3$ ▷ Reset SMC gain

    with

    $\bar{k}_2 \leftarrow k_{A-SMC}(t^*)$

    t^* directly after t^{*-} so that $|\sigma(t^*)| \leq \epsilon_1$ and $|\sigma(t^{*-})| > \epsilon_1$

    $\tau_1\dot{\gamma}_1 + \gamma_1 \leftarrow \text{sgn}(\sigma)$

  else if $|\sigma| > \epsilon_1$ **then** ▷ If σ is outside the boundary layer ...

    $\dot{k}_{A-SMC} \leftarrow \bar{k}_1|\sigma|$ ▷ Increase SMC gain

  end if

  $u \leftarrow -k_{A-SMC} \times \text{sgn}(\sigma)$

Output $u(t)$

D Proof of Lemma 10

Proof. It will be shown that for the possible control inputs $u = u_r^*$, $u = u_{c_1}^*$, and $u = u_{c_2}^*$ the sliding variable $\sigma_r \leq -\epsilon_r$ increases to $-\epsilon_r < 0$ in finite-time.

Step 1: Consideration of control input $u = u_r^*$ according to (5.56). From the reachability condition (5.44) and the definition of the smooth approximation (5.55) it follows that

$$\dot{\sigma}_r \geq \frac{\mu_r}{\sqrt{2}}, \tag{D.1}$$

holds in case of $\sigma_r \leq -\epsilon_r$.

Step 2: Consideration of control input

$$u = u_{c_2}^* = u_r^* + \text{sat}\left(\frac{\sigma_{c_2}}{\epsilon_{c_2}}\right) \times k_{c_2}^*, \tag{D.2}$$

with

$$k_{c_2}^* = \left(\frac{\mu_{c_2} + \Psi_M\sqrt{2}}{\Gamma_m\sqrt{2}} + \frac{|\dot{\eta}_{c_2}|}{\Gamma_m} - \text{sat}\left(\frac{\sigma_{c_2}}{\epsilon_{c_2}}\right) u_r^* + \frac{\alpha + \beta\gamma|e_r|^{\gamma-1}}{\Gamma_m}|\dot{y}_r|\right), \tag{D.3}$$

according to (5.57). The saturation function is bounded as

$$0 \leq \text{sat}\left(\frac{\sigma_{c_2}}{\epsilon_{c_2}}\right) \leq 1, \tag{D.4}$$

because $\sigma_{c_2} > 0$ holds if $u = u_{c_2}^*$ is applied. Input u_r^* is part of (D.2) and (D.3). As $u = u_{c_2}^*$ is only applied if $\sigma_{c_2} = -\eta_{c_1} - \dot{y}_r > 0$ holds it follows that $\dot{y}_r < 0$ holds and u_r^* is

$$u_r^* = \frac{\mu_r + \Psi_M\sqrt{2}}{\Gamma_m\sqrt{2}} + \frac{\alpha + \beta\gamma|e_r|^{\gamma-1}}{\Gamma_m}|\dot{y}_r| > 0, \tag{D.5}$$

in case of $\sigma_r \leq -\epsilon_r$. Substituting (D.5) in (D.3) and considering (D.4) yields

$$0 \leq \frac{\mu_{c_2} - \mu_r}{\Gamma_m\sqrt{2}} + \frac{|\dot{\eta}_{c_2}|}{\Gamma_m} \leq k_{c_2}^*, \tag{D.6}$$

in case of $\mu_{c_2} \geq \mu_r$. From (D.2) it follows $u_{c_2}^* \geq u_r^*$. The reachability condition

$$\dot{\sigma}_r = \Psi + \Gamma u + \alpha\dot{y}_r + \beta\gamma\dot{y}_r|e_r|^{\gamma-1} \geq \frac{\mu_r}{\sqrt{2}}, \qquad \mu_r > 0, \tag{D.7}$$

known from (5.44) is satisfied if inequality

$$u \geq \frac{\mu_r + \Psi_M\sqrt{2}}{\Gamma_m\sqrt{2}} - \frac{\alpha + \beta\gamma|e_r|^{\gamma-1}}{\Gamma}\dot{y}_r, \tag{D.8}$$

holds. As stated in Step 1 the reachability condition is satisfied for $u = u_r^*$ if $\sigma_r \leq -\epsilon_r$ holds. As $u_{c_2}^* \geq u_r^*$ holds it is

$$u_{c_2}^* \geq u_r^* \geq \frac{\mu_r + \Psi_M\sqrt{2}}{\Gamma_m\sqrt{2}} - \frac{\alpha + \beta\gamma|e_r|^{\gamma-1}}{\Gamma}\dot{y}_r, \tag{D.9}$$

and the reachability condition is also satisfied for $u = u_{c_2}^*$. Consequently,

$$\dot{\sigma}_r \geq \frac{\mu_r}{\sqrt{2}}, \tag{D.10}$$

holds.

Step 3: Consider application of control input $u = u_{c_1}^*$ according to (5.57).
Case I:

It is first studied the behavior of σ_r if input $u(t) = u_{c_1}^*(t)$ is applied on some time interval $t \in [t_1, t_2)$ but not at instant t_2. As $u(t) = u_{c_1}^*(t)$ is applied at time instants t but not at instant t_2 it follows that $\sigma_{c_1}(t) > 0$ and $\sigma_{c_1}(t_2) = 0$ hold. Consequently, $\sigma_{c_1}(t^\star) \geq 0$ with $t^\star \in [t_1, t_2]$ holds. According to (5.39) it is

$$\sigma_r(t^\star) = \dot{y}_r(t^\star) - \alpha e_r(t^\star) - \beta|e_r(t^\star)|^\gamma \mathrm{sgn}(e_r(t^\star)), \tag{D.11}$$

for $t^\star \in [t_1, t_2]$. As $\sigma_{c_1}(t^\star) = -\eta_{c_1}(t^\star) + \dot{y}_r(t^\star) \geq 0$ holds it follows from (5.35), (5.36) and (5.37) that

$$\dot{y}_r(t^\star) \geq \eta_{c_1}(t^\star) > \eta_m > 0, \qquad \eta_m > 0, \tag{D.12}$$

holds. As $\sigma_r(t^\star) < 0$ and $\dot{y}_r(t^\star) > 0$ hold it can be seen from (D.11) that $e_r(t^\star) > 0$ holds. Consequently, equation (D.11) can be simplified as

$$\sigma_r(t^\star) = \dot{y}_r(t^\star) - \alpha e_r(t^\star) - \beta|e_r(t^\star)|^\gamma. \tag{D.13}$$

From (D.13), (D.12), and $e_r = w - y_r$ it follows that

$$\begin{aligned}\sigma_r(t^\star) \geq \eta_{c_1}(t^\star) - \alpha w + \alpha y_r(t_1) - \beta|e_r(t_1)|^\gamma \\ + \int_{t_1}^{t^\star} \alpha\dot{y}_r(\tau)d\tau + \int_{t_1}^{t^\star} \gamma\beta\dot{y}_r(\tau)|e_r(\tau)|^{\gamma-1}d\tau,\end{aligned} \tag{D.14}$$

holds for any time $t^\star \in [t_1, t_2]$. Substituting

$$\alpha = \frac{\dot{\eta}_M}{\eta_m} + \mu_\alpha \geq -\frac{\dot{\eta}_{c_1}(t)}{\dot{y}_r(t)} + \mu_\alpha, \qquad \mu_\alpha > 0, \tag{D.15}$$

in (D.14) and considering $\dot{y}_r(t^\star) \geq \eta_m > 0$ as well as $\beta > 0$, $\gamma > 0$ leads to

$$\sigma_r(t^\star) \geq -\alpha w + \alpha y_r(t_1) - \beta|e_r(t_1)|^\gamma + \eta_{c_1}(t_1) + \mu_\alpha\eta_m(t^\star - t_1). \tag{D.16}$$

Adding $\dot{y}_r(t_1) - \dot{y}_r(t_1)$ to (D.16) and considering the definition of σ_r according to (5.39) yields

$$\begin{aligned}\sigma_r(t^\star) &\geq \dot{y}_r(t_1) - \alpha e_r(t_1) - \beta|e_r(t_1)|^\gamma - \dot{y}_r(t_1) + \eta_{c_1}(t_1) + \mu_\alpha \eta_m(t^\star - t_1), \\ &= \sigma_r(t_1) - \dot{y}_r(t_1) + \eta_{c_1}(t_1) + \mu_a \eta_m(t^\star - t_1), \qquad \mu_a \eta_m > 0, \end{aligned} \tag{D.17}$$

for $t^\star \in [t_1, t_2]$.
Case II:

It is now studied the behavior of σ_r if input $u(t) = u^*_{c_1}(t)$ is applied on some time interval $t \in (t_1, t_2)$ but not at time instants t_1 and t_2. It follows that $\sigma_{c_1}(t) > 0$, $\sigma_{c_1}(t_1) = 0$, $\sigma_{c_1}(t_2) = 0$, and $\sigma_{c_1}(t^\star) \geq 0$ with $t^\star \in [t_1, t_2]$ hold. According to (5.39) it is

$$\sigma_r(t^\star) = \dot{y}_r(t^\star) - \alpha e_r(t^\star) - \beta|e_r(t^\star)|^\gamma \mathrm{sgn}(e_r(t^\star)), \tag{D.18}$$

for $t^\star \in [t_1, t_2]$. As $\sigma_{c_1}(t^\star) = -\eta_{c_1}(t^\star) + \dot{y}_r(t^\star) \geq 0$ holds it follows from (5.35), (5.36), and (5.37) that

$$\dot{y}_r(t^\star) \geq \eta_{c_1}(t^\star) > \eta_m > 0, \qquad \eta_m > 0, \tag{D.19}$$

holds. Considering $\dot{y}_r(t^\star) > 0$ and $\sigma_r(t^\star) < 0$ it can be seen from (D.18) that $e_r(t^\star) > 0$ holds which leads to

$$\sigma_r(t^\star) = \dot{y}_r(t^\star) - \alpha e_r(t^\star) - \beta|e_r(t^\star)|^\gamma. \tag{D.20}$$

From (D.19), (D.20), and $e_r = w - y_r$ it follows that

$$\begin{aligned}\sigma_r(t^\star) \geq \eta_{c_1}(t^\star) - \alpha w + \alpha y_r(t_1) - \beta|e_r(t_1)|^\gamma \\ + \int_{t_1}^{t^\star} \alpha \dot{y}_r(\tau) d\tau + \int_{t_1}^{t^\star} \gamma\beta \dot{y}_r(\tau)|e_r(\tau)|^{\gamma-1} d\tau,\end{aligned} \tag{D.21}$$

holds for any time $t^\star \in [t_1, t_2]$. Substituting

$$\alpha = \frac{\dot{\eta}_M}{\eta_m} + \mu_\alpha \geq -\frac{\dot{\eta}_{c_1}(t)}{\dot{y}_r(t)} + \mu_\alpha, \qquad \mu_\alpha > 0, \tag{D.22}$$

in (D.21) and considering $\dot{y}_r(t^\star) \geq \eta_m > 0$ as well as $\beta > 0$, $\gamma > 0$ leads to

$$\sigma_r(t^\star) \geq -\alpha w + \alpha y_r(t_1) - \beta|e_r(t_1)|^\gamma + \eta_{c_1}(t_1) + \mu_\alpha \eta_m(t^\star - t_1). \tag{D.23}$$

As $\sigma_{c_1}(t_1) = -\eta_{c_1}(t_1) + \dot{y}_r(t_1) = 0$ holds it follows $\eta_{c_1}(t_1) = \dot{y}_r(t_1)$. Replacing $\eta_{c_1}(t_1) = \dot{y}_r(t_1)$ in (D.23) and considering the definition of σ_r from (5.39) yields

$$\sigma_r(t^\star) \geq \sigma_r(t_1) + \mu_a \eta_m(t^\star - t_1), \qquad \mu_a \eta_m > 0, \tag{D.24}$$

for $t^\star \in [t_1, t_2]$.

Step 4: Occurrence of Case I and Case II of Step 3. It will be shown that Case I of Step 3 can only occur if $u = u^*_{c_1}$ is applied first, meaning that once input $u = u^*_r$ or $u = u^*_{c_2}$ has been applied Case I of Step 3 can not occur anymore.

According to Algorithm 3 input $u = u^*_r$ or $u = u^*_{c_2}$ are only applied if $\sigma_{c_1} = -\eta_{c_1} + \dot{y}_r \leq 0$ holds. Consider $u = u^*_r$ or $u = u^*_{c_2}$ to be applied before the input switches to $u = u^*_{c_1}$. That means that there exists a time instant t_1 with $\sigma_{c_1}(t_1) = -\eta_{c_1}(t_1) + \dot{y}_r(t_1) = 0$ just

before σ_{c_1} switches to a positive number inducing the switch of the input to $u = u^*_{c_1}$. As $\sigma_{c_1}(t_1) = 0$ holds it follows $\eta_{c_1}(t_1) = \dot{y}_r(t_1)$ (Case II) and not $\eta_{c_1}(t_1) < \dot{y}_r(t_1)$ (Case I).

Step 5: Rate of decrease. Let $\mu_{c_2} \geq \mu_r$ and $\sigma_r(t) \leq -\epsilon_r$ hold for some interval $t \in [t_1, t_2]$. From (D.1), (D.10), (D.17), (D.24), and Step 4 it follows that $\sigma_r(t)$ increases to $-\epsilon_r < 0$ in finite time according to

$$\begin{aligned} \sigma_r(t) &\leq \kappa + \varrho(t - t_1), \qquad \text{(D.25)} \\ \kappa &= \min\Big\{\sigma_r(t_1), \sigma_r(t_1) - \dot{y}_r(t_1) + \eta_{c_1}(t_1)\Big\}, \\ \varrho &= \min\left\{\frac{\mu_r}{\sqrt{2}}, \mu_a \eta_m\right\}, \end{aligned}$$

with $t \in [t_1, t_2]$. □

DOI: 10.17185/duepublico/76530
URN: urn:nbn:de:hbz:465-20220822-113832-3